frontiers | Research Topics

Exploration of the human brain using magnetic resonance imaging and spectroscopy with transcranial direct current stimulation

Edited by
Chang-Hoon Choi, Jon Shah and Ferdinand Binkofski

Published in
Frontiers in Neuroscience
Frontiers in Human Neuroscience

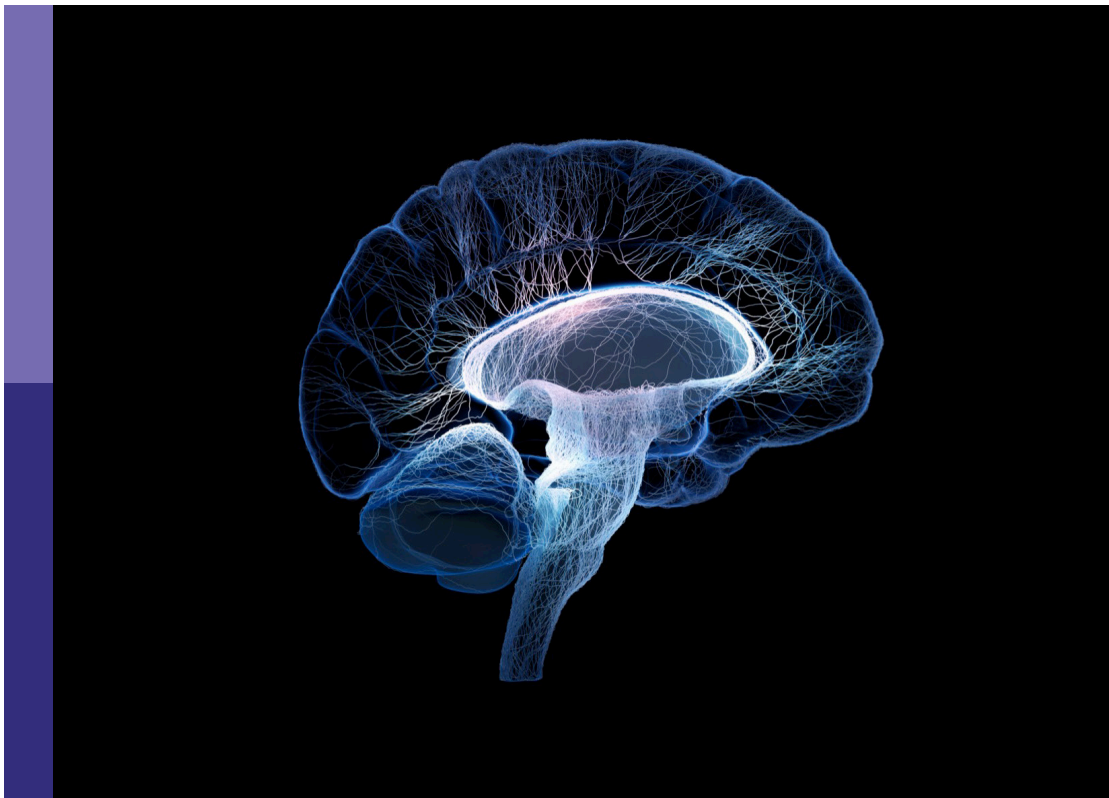

ISSN 1664-8714
ISBN 978-2-8325-5860-7
DOI 10.3389/978-2-8325-5860-7

About Frontiers

Frontiers is more than just an open access publisher of scholarly articles: it is a pioneering approach to the world of academia, radically improving the way scholarly research is managed. The grand vision of Frontiers is a world where all people have an equal opportunity to seek, share and generate knowledge. Frontiers provides immediate and permanent online open access to all its publications, but this alone is not enough to realize our grand goals.

Frontiers journal series

The Frontiers journal series is a multi-tier and interdisciplinary set of open-access, online journals, promising a paradigm shift from the current review, selection and dissemination processes in academic publishing. All Frontiers journals are driven by researchers for researchers; therefore, they constitute a service to the scholarly community. At the same time, the *Frontiers journal series* operates on a revolutionary invention, the tiered publishing system, initially addressing specific communities of scholars, and gradually climbing up to broader public understanding, thus serving the interests of the lay society, too.

Dedication to quality

Each Frontiers article is a landmark of the highest quality, thanks to genuinely collaborative interactions between authors and review editors, who include some of the world's best academicians. Research must be certified by peers before entering a stream of knowledge that may eventually reach the public - and shape society; therefore, Frontiers only applies the most rigorous and unbiased reviews. Frontiers revolutionizes research publishing by freely delivering the most outstanding research, evaluated with no bias from both the academic and social point of view. By applying the most advanced information technologies, Frontiers is catapulting scholarly publishing into a new generation.

What are Frontiers Research Topics?

Frontiers Research Topics are very popular trademarks of the *Frontiers journals series*: they are collections of at least ten articles, all centered on a particular subject. With their unique mix of varied contributions from Original Research to Review Articles, Frontiers Research Topics unify the most influential researchers, the latest key findings and historical advances in a hot research area.

Find out more on how to host your own Frontiers Research Topic or contribute to one as an author by contacting the Frontiers editorial office: frontiersin.org/about/contact

Exploration of the human brain using magnetic resonance imaging and spectroscopy with transcranial direct current stimulation

Topic editors

Chang-Hoon Choi — Physics of Medical Imaging (INM-4), Institute of Neuroscience and Medicine, Julich Research Center, Helmholtz Association of German Research Centres (HZ), Germany

Jon Shah — Institute of Neuroscience and Medicine – 4, Forschungszentrum Jülich GmbH, Germany

Ferdinand Binkofski — RWTH Aachen University, Germany

Citation

Choi, C.-H., Shah, J., Binkofski, F., eds. (2025). *Exploration of the human brain using magnetic resonance imaging and spectroscopy with transcranial direct current stimulation*. Lausanne: Frontiers Media SA. doi: 10.3389/978-2-8325-5860-7

Table of contents

frontiers | Frontiers in Neuroscience

TYPE Editorial
PUBLISHED 17 December 2024
DOI 10.3389/fnins.2024.1538414

OPEN ACCESS

EDITED AND REVIEWED BY
Vince D. Calhoun,
Georgia State University, United States

*CORRESPONDENCE
Chang-Hoon Choi
✉ c.choi@fz-juelich.de

RECEIVED 02 December 2024
ACCEPTED 05 December 2024
PUBLISHED 17 December 2024

CITATION
Choi C-H, Shah NJ and Binkofski F (2024) Editorial: Exploration of the human brain using magnetic resonance imaging and spectroscopy with transcranial direct current stimulation. *Front. Neurosci.* 18:1538414. doi: 10.3389/fnins.2024.1538414

Editorial: Exploration of the human brain using magnetic resonance imaging and spectroscopy with transcranial direct current stimulation

Chang-Hoon Choi[1]*, N. Jon Shah[1,2,3,4] and Ferdinand Binkofski[1,5]

[1]Institute of Neuroscience and Medicine - 4, Forschungszentrum Jülich, Jülich, Germany, [2]Institute of Neuroscience and Medicine - 11, Forschungszentrum Jülich, Jülich, Germany, [3]JARA - BRAIN - Translational Medicine, Aachen, Germany, [4]Department of Neurology, RWTH Aachen University, Aachen, Germany, [5]Division of Clinical Cognitive Sciences, Department of Neurology, RWTH Aachen University Hospital, Aachen, Germany

KEYWORDS

tDCS, MRI, MRS, brain, magnetic resonance spectroscopy, transcranial direct current stimulation

Editorial on the Research Topic
Exploration of the human brain using magnetic resonance imaging and spectroscopy with transcranial direct current stimulation

The enormous progress made in brain stimulation and neuroimaging approaches in recent decades has dramatically supported the exploration and understanding of the human brain. These approaches have cast light on various brain functions and diseases and also have provided clinically and therapeutically relevant information.

Transcranial electrical stimulation (tES) encompasses a range of non-invasive brain stimulation tools, including transcranial direct current stimulation (tDCS) and transcranial alternating current stimulation (tACS). Furthermore, transcranial magnetic stimulation (TMS) is a widely used method that employs magnetic fields to induce electrical currents in the brain, modulating neuronal activity. These brain stimulation techniques influence brain function and facilitate research into neural processes and potential therapeutic applications by applying weak electrical or magnetic currents to the scalp. tDCS, a specific type of tES, has gained prominence since its introduction (Priori et al., 1998; Nitsche and Paulus, 2000), and is the primary focus of this Research Topic. This technique modulates neuronal excitability by inducing hyper- or hypo-polarization of membranes and altering energy levels in the brain. The acute effects of tDCS are observed during stimulation, while the after-effects can be monitored long after the stimulation has ceased (Bikson et al., 2019; Patel et al., 2019). The impact of tDCS on the brain is influenced by various parameters, including polarity, duration, current intensity and target area, with the choice of montages being particularly crucial (Choi et al., 2021).

Complementing tES, magnetic resonance imaging (MRI) and spectroscopy (MRS) are well-established techniques extensively utilized in clinical practice and neuroscience research. These methods allow for the *in vivo* examination of the human brain, providing excellent soft tissue contrast and detailed metabolic and functional information. MRS is particularly valuable for quantifying the concentrations of various brain metabolites,

such as γ-aminobutyric acid (GABA), glutamine, glutamate, and high-energy phosphates, with high sensitivity. Positron emission tomography (PET) further supplements these imaging and spectroscopic techniques by enabling the study of metabolic processes and neuroreceptor activity.

This Research Topic includes valuable studies focusing on cutting-edge methods or advancements in using novel tDCS in conjunction with/without imaging and spectroscopic tools for the human brain. Given the potential these modalities have for illuminating various brain structures and functions, Research Topic will certainly be of great interest in the neuroscience community.

The study led by Binkofski (Patel et al.) investigated changes in GABA levels and energy metabolites in the primary motor cortex (M1) following anodal tDCS using proton (^{1}H) and phosphorus (^{31}P) MRS techniques. The results demonstrated the feasibility of measuring both ^{1}H and ^{31}P components in a single measurement, appeared to show an increase in GABA concentration, ATP/Pi and PCR/Pi ratios after stimulation.

Cohen et al. used tDCS and tACS with functional MRI (fMRI) to investigate genetic generalized epilepsy in M1, focusing on sensorimotor network alterations. Their initial findings indicated no dependency on stimulation polarity, suggesting further research with larger cohorts to understand current distribution and brain structures. Sun et al. examined refractory epilepsy patients using tES, resting-state and event-related fMRI, revealing a reduction in the small-world property of brain networks and a shift toward random configurations. This structural change could impair neural stability and cognitive functions, highlighting the complex interplay between network architecture and neurological disorders.

Kern et al. investigated the somatotopic organization and functional role of the supplementary motor area (SMA) using repetitive navigated TMS and MRI. Their study refined and validated a protocol for precise SMA mapping, including the non-dominant hemisphere and lower extremities, contributing to understanding the role of SMA in motor language function.

Sato et al.'s study assessed the effects of tDCS current direction on motor performance and cortical excitability, targeting M1 and SMA regions relevant to leg function. They found that precise electrode positioning enhanced motor performance, with A-P tDCS improving sit-to-stand repetitions and P-A tDCS increasing knee flexor strength and reducing intracortical inhibition.

Chang et al. explored auditory-motor integration in vocal pitch regulation using tDCS targeting the left dorsolateral prefrontal cortex (DLPFC). Anodal tDCS reduced peak magnitudes and prolonged peak times of vocal adjustments to pitch perturbations compared to sham stimulation, supporting the idea that the left DLPFC exerts inhibitory control over vocal feedback mechanisms through a top-down process.

Shaikh et al. used TMS, ^{18}F-desmethoxyfallypride PET and MRI to study the DLPFC. They found that repeated intermittent theta burst stimulation enhanced regional prefrontal excitation and modulated the fronto-striatal network in a dose-dependent manner. Their approach monitored changes in radioligand binding, offering insights into cortical control over dopamine release mechanisms and striatal mapping.

Honda et al. examined the correlation between music rhythm processing and glutamatergic levels in the caudate using ^{1}H MRS. They discovered that higher neurometabolite levels were associated with improved rhythm and meter production abilities, suggesting the importance of measuring these levels to understand the neurochemical mechanisms underlying musical rhythm processing.

Meinzer et al. reviewed the effects of tDCS on neural mechanisms underlying human cognition, addressing gaps in understanding its impact on cognitive functions in health and disease. They discussed factors contributing to variability in tDCS studies, design considerations for tDCS-fMRI research, and emphasized rigorous experimental control. The review also explored how tDCS effects vary across the lifespan and proposed establishing large-scale, multidisciplinary consortia to enhance tDCS research.

Author contributions

C-HC: Writing – original draft, Writing – review & editing. NJS: Writing – review & editing. FB: Writing – review & editing.

Acknowledgments

We thank Ms. Claire Rick for English proofreading.

Conflict of interest

The authors declare that the research was conducted in the absence of any commercial or financial relationships that could be construed as a potential conflict of interest.

The author(s) declared that they were an editorial board member of Frontiers, at the time of submission. This had no impact on the peer review process and the final decision.

Publisher's note

References

Bikson, M., Esmaeilpour, Z., Adair, D., Kronberg, G., Tyler, W. J., Antal, A., et al. (2019). Transcranial electrical stimulation nomenclature. *Brain Stimul.* 12, 1349–1366. doi: 10.1016/j.brs.2019.07.010

Choi, C.-H., Iordanishvili, E., Shah, N. J., and Binkofski, F. (2021). Magnetic resonance spectroscopy with transcranial direct current stimulation to explore the underlying biochemical and physiological mechanism of the human brain:

a systematic review. *Hum. Brain Mapp.* 42, 2642–2671. doi: 10.1002/hbm.25388

Nitsche, M. A., and Paulus, W. (2000). Excitability changes induced in the human motor cortex by weak transcranial direct current stimulation. *J. Physiol.* 527, 633–639. doi: 10.1111/j.1469-7793.2000.t01-1-00633.x

Patel, H. J., Romanzetti, S., Pellicano, A., Nitsche, M. A., Reetz, K., and Binkofski, F. (2019). Proton Magnetic Resonance Spectroscopy of the motor cortex reveals long term GABA change following anodal transcranial direct current stimulation. *Sci. Rep.* 9:2807. doi: 10.1038/s41598-019-39262-7

Priori, A., Berardelli, A., Rona, S., Accornero, N., and Manfredi, M. (1998). Polarization of the human motor cortex through the scalp. *NeuroReport* 9:2257.

frontiers | Frontiers in Neuroscience

TYPE Original Research
PUBLISHED 30 June 2023
DOI 10.3389/fnins.2023.1208581

OPEN ACCESS

EDITED BY
Allison Hilger,
University of Colorado Boulder, United States

REVIEWED BY
Saul Frankford,
Boston University, United States
Henry Railo,
University of Turku, Finland

*CORRESPONDENCE
Hanjun Liu
✉ lhanjun@mail.sysu.edu.cn
Peng Liu
✉ liupeng2@mail.sysu.edu.cn
Xiuqin Wu
✉ wuxq36@mail.sysu.edu.cn

†These authors have contributed equally to this work

RECEIVED 19 April 2023
ACCEPTED 16 June 2023
PUBLISHED 30 June 2023

CITATION
Chang Y, Peng D, Zhao Y, Chen X, Li J, Wu X, Liu P and Liu H (2023) Transcranial direct current stimulation over left dorsolateral prefrontal cortex facilitates auditory-motor integration for vocal pitch regulation. *Front. Neurosci.* 17:1208581. doi: 10.3389/fnins.2023.1208581

Transcranial direct current stimulation over left dorsolateral prefrontal cortex facilitates auditory-motor integration for vocal pitch regulation

Yichen Chang[1†], Danhua Peng[1†], Yan Zhao[1], Xi Chen[1], Jingting Li[1], Xiuqin Wu[1*], Peng Liu[1*] and Hanjun Liu[1,2*]

[1]Department of Rehabilitation Medicine, The First Affiliated Hospital, Sun Yat-sen University, Guangzhou, China, [2]Guangdong Provincial Key Laboratory of Brain Function and Disease, Zhongshan School of Medicine, Sun Yat-sen University, Guangzhou, China

Background: A growing body of literature has implicated the left dorsolateral prefrontal cortex (DLPFC) in the online monitoring of vocal production through auditory feedback. Specifically, disruption of or damage to the left DLPFC leads to exaggerated compensatory vocal responses to altered auditory feedback. It is conceivable that enhancing the cortical excitability of the left DLPFC may produce inhibitory influences on vocal feedback control by reducing vocal compensations.

Methods: We used anodal transcranial direct current stimulation (a-tDCS) to modulate cortical excitability of the left DLPFC and examined its effects on auditory-motor integration for vocal pitch regulation. Seventeen healthy young adults vocalized vowel sounds while hearing their voice pseudo-randomly pitch-shifted by ±50 or ±200 cents, either during (online) or after (offline) receiving active or sham a-tDCS over the left DLPFC.

Results: Active a-tDCS over the left DLPFC led to significantly smaller peak magnitudes and shorter peak times of vocal compensations for pitch perturbations than sham stimulation. In addition, this effect was consistent regardless of the timing of a-tDCS (online or offline stimulation) and the size and direction of the pitch perturbation.

Conclusion: These findings provide the first causal evidence that a-tDCS over the left DLPFC can facilitate auditory-motor integration for compensatory adjustment to errors in vocal output. Reduced and accelerated vocal compensations caused by a-tDCS over left DLPFC support the hypothesis of a top–down neural mechanism that exerts inhibitory control over vocal motor behavior through auditory feedback.

KEYWORDS

auditory feedback, speech motor control, left dorsolateral prefrontal cortex, transcranial direct current stimulation, top–down modulation

Introduction

Auditory feedback is an essential part of speech motor control, providing sensory information that allows spakers to monitor and adjust their vocal out to produce their intended speech goals (Smotherman, 2007). This control process is known as auditory-motor integration for speech production, typically manifested as compensatory adjustment of vocal motor behavior in response to any mismatches between expected and actual auditory feedback in voice fundamental frequency (f_o), intensity, or formant frequency (F_1) (Burnett et al., 1998; Houde and Jordan, 1998; Bauer et al., 2006). Using various neuromaging techqnies including functional magnetic resonance imaging (fMRI), magnetoencephalography (MEG), electroencephalography (ECoG), and event-realted potential (ERP), a growing body of literature has revealed a complex, widely distributed network located in the frontal, parietal and temporal regions as well as subcortical areas (Houde and Nagarajan, 2011; Behroozmand et al., 2015; Guenther and Hickok, 2015; Behroozmand et al., 2018). These regions are thought to detect auditory feedback errors and generate corrective motor commands to control speech production. The precise roles of these brain regions in auditory-vocal integration, however, remain far from clear.

The prefrontal cortex, particularly the inferior frontal gyrus (IFG), has been considered to be an essential region that supports vocal feedback control. For instance, the directions into velocity of articulators (DIVA) model proposes that the left IFG contains a speech sound map that initiates the feedback and feedforward control of speech production (Golfinopoulos et al., 2010). Similarly, the dual stream model posits that the left IFG serves as a core component of a dorsal stream responsible for mapping acoustic speech signals onto articulatory representations (Hickok and Poeppel, 2007). In line with these models, empirical evidence has identified activation of the IFG and its connectivity with temporal and parietal regions in producing vocal adjustments to auditory feedback errors (Flagmeier et al., 2014; Behroozmand et al., 2015; Kort et al., 2016).

In contrast, little attention has been paid to the dorsolateral prefrontal cortex (DLPFC) in the context of auditory-vocal integration. The DLPFC encompasses a large brain region characterized by considerable structural heterogeneity, spanning over Brodmann areas 9, 8a, 8b, and the dorsal part of 46 (Glasser et al., 2016). This structural complexity of the DLPFC positions it as a key brain region for involvement in a variety of cognitive functions, including working memory (Edin et al., 2009), attentional control (Brosnan and Wiegand, 2017), and executive functions (Mansouri et al., 2009). Notably, these cognitive functions have been implicated in auditory-vocal integration. For example, focused attention led to enhanced vocal compensations for pitch perturbations and/or ERP P2 response while divided attention reduced them (Tumber et al., 2014; Liu et al., 2015). As well, engagement of working memory during vocal pitch regulation led to increased vocal compensations and ERP N1 amplitudes but decreased ERP P2 amplitudes in response to pitch perturbations (Guo et al., 2017). Moreover, patients with Alzheimer's disease (AD) exhibited abnormally enhanced magnitudes and reduced durations of vocal compensations for pitch perturbations that were significantly correlated with their executive and memory dysfunctions (Ranasinghe et al., 2017). These findings suggest that the DLPFC may contribute to auditory-motor integration for vocal production in a top-down manner.

A few neuroimaging studies have provided direct evidence supporting the involvement of the DLPFC in vocal feedback control. For example, Zarate and Zatorre (2008) reported activation of the left DLPFC in non-singers who were instructed to ignore or compensate for perceived pitch perturbations during singing. Ranasinghe et al. (2019) found that patients with AD exhibited significantly larger vocal compensations for pitch perturbations and lower left DLPFC activity than healthy controls, with lower left DLPFC activity predicting larger vocal compensations across both groups. One possible explanation for these abnormalities in vocal feedback control associated with AD is the impairment of prefrontal mediated inhibition (Ranasinghe et al., 2017). More recently, Liu et al. (2020) found that inhibiting the left DLPFC with continuous theta burst stimulation (cTBS), a non-invasive brain stimulation (NIBS) technique that induces inhibitory effects on cortical excitability (Huang et al., 2005), led to enhanced vocal compensations and reduced ERP P2 amplitudes in response to pitch perturbations. This finding establishes a causal link between the left DLPFC and auditory-motor integration for vocal production.

Building upon the essential role of the left DLPFC in suppressing reflex-like or inappropriate behavioral responses (Loftus et al., 2015; Angius et al., 2019) and modulating auditory processing (Knight et al., 1989; Mitchell et al., 2005), Liu et al. (2020) proposed that the left DLPFC may exert top-down control over the interaction between auditory and motor representations of vocal sounds to inhibit compensatory adjustment for feedback perturbations, thereby preventing vocal motor control from being excessively influenced by auditory feedback. This top-down mechiansm mediated by the left DLPFC generates an inhibitory influence on auditory feedback control of vocal production. Dysfunction of this mechanism may account for abnormally ehnaced vocal compensations for feedback errors when the left DLPFC was impaired (Ranasinghe et al., 2017, 2019) or inhibited (Liu et al., 2020). Conversely, it is reasonable that enhancing activity in the left DLPFC may produce inhibitory influences on vocal feedback control. This hypothesis is supported by the findings of Guo et al. (2017), showing that extensive training of working memory that is primarily subserved by the DLPFC decreased vocal compensations and increased ERP P2 amplitudes in response to pitch perturbations. However, direct causal evidence in support of this hypothesis is still lacking.

Therefore, the present study aimed to fill this gap by using transcranial direction current stimulation (tDCS), another NIBS technique that modulates cortical excitability by delivering an electric current to the scalp through electrodes (Nitsche and Paulus, 2000), to increase left DLPFC activity and investigate whether it can produce inhibitory effects on vocal feedback control. Generally, anodal tDCS (a-tDCS) increases cortical excitability whereas cathodal tDCS (c-tDCS) decreases it (Stagg and Nitsche, 2011). Previous studies have shown that a-tDCS over the left DLPFC increases its cortical excitability, as indicated by increased EEG power or fMRI activation in the frontal regions (Keeser et al., 2011; Zaehle et al., 2011). A large body of literature has shown that tDCS over brain regions can influence cognitive or motor functions in healthy and clinical populations (Mancuso et al., 2016; Lefaucheur et al., 2017; Manor et al., 2021; Tedla et al., 2023). Recently, tDCS has been used to investigate the neural mechanisms of auditory-motor integration for vocal production from a causal perspective. For example, Behroozmand et al. (2020) found that a-tDCS and c-tDCS over the

left ventral motor cortex led to decreased vocal compensations for downward pitch perturbations compared to sham stimulation, with stronger effects associated with c-tDCS. In contrast, a-tDCS over the left sensorimotor cortex led to increased adaptive responses to F_1 perturbations during speech production (Scott et al., 2020). In addition, vocal compensations for pitch perturbations became significantly larger when a-tDCS was applied over the right cerebellum relative to sham stimulation (Peng et al., 2021).

The frequency-altered feedback (FAF) paradigm was used to assess the effects of a-tDCS on vocal feedback control in the present study, during which participants produced sustained vocalizations while hearing their voice pitch-shifted unexpectedly. Participants received either active or sham a-tDCS over the left DLPFC during (online stimulation) or before (offline stimulation) the FAF task. The timing of tDCS was manipulated in the present study, as previous studies have reported inconsistent results regarding the optimal timing of tDCS for congitive performance or motor learning (Stagg et al., 2011; Mancuso et al., 2016; Buchwald et al., 2019). Additionally, Peng et al. (2021) found both online and offline a-tDCS over the right cerebellum led to enhacemed vocal compensations for pitch perturbations. Buidling upon the findings of abnormally enhanced vocal compensations for pitch perturbations when activity of the left DLPFC was disrupted by inhibitory c-TBS (Liu et al., 2020) or impaired due to AD (Ranasinghe et al., 2019), we hypothesized that increasing cortical exicitability of the left DLPFC with a-tDCS would result in reduced vocal compensations comapred to sham stimulation. Consistent with this hypothesis, our results showed smaller vocal responses to pitch perturbations following a-tDCS over the left DLPFC, providing further evidence for its invovlment in top-down inhibitory control over vocal motor behavior.

Materials and methods

Subjects

Twenty students [11 females and 9 males; age (mean ± SD): 21.8 ± 2.2 years] from Sun Yat-sen University were enrolled in this study. All participants met the following criteria: right-handed; native Mandarin speaker; no hearing or speech impairment; no history of neurological diseases; no use of neuropsychiatric drugs; no implanted medical devices such as pacemakers; not pregnant; and no claustrophobia. Three participants were excluded from the statistical analysis because they did not produce sustained vocalizations in a steady manner as required, resulting in the failure of extracting reliable voice f_0 contours from their voice signals. Therefore, their data had to be excluded from the present study, and the final data pool contained the data from 17 participants [9 females and 8 males; age (mean ± SD): 21.4 ± 2.1 years]. All participants provided written informed consent and the research protocol was approved by the Institutional Review Board of The First Affiliated Hospital of Sun Yat-sen University in accordance with the Code of Ethics of the World Medical Association (Declaration of Helsinki).

Transcranial direct current stimulation

Direct current stimulation was administered by a battery-driven, constant current-stimulator (model EM8060, E&M Medical Tech., China). The present study consisted of two stimulation conditions: anodal stimulation and sham stimulation. In both conditions, a 6 cm × 4 cm electrode was placed over the F3 position on the scalp according to the 10–20 International System of EEG electrode placement to target the left DLPFC (Herwig et al., 2003) and a reference electrode with the same size was placed on the right deltoid muscle. During the anodal stimulation, a constant current of 1 mA was administered for 20 min with a 30 s ramp up/down phase at the beginning and end (Nitsche and Paulus, 2000). During the sham stimulation, the current was turned off after 30 s when it reached 1 mA.

Experimental procedure

This was a randomized, crossover study with four sessions: online active a-tDCS, online sham a-tDCS, offline active a-tDCS, and offline sham a-tDCS. Each session was conducted at least 48 h apart to eliminate the possible carry-over effects. Participants received active or sham a-tDCS over left DLPFC (i.e., online stimulation) while vocalizing the /u/ sound for 6 s following a blue light cue on the computer screen. During each vocalization, participants heard their voice pitch-shifted upwards or downwards by 50 or 200 cents (200 ms duration) in a pseudo-randomized manner. The direction and size of pitch perturbations were varied because previous studies have shown their effects on vocal compensation behavior (Chen et al., 2007; Liu et al., 2011; Scheerer et al., 2013). Additionally, Behroozmand et al. (2020) found that tDCS over left ventral motor cortex reduced vocal compensations only for downward pitch perturbations. A number of five pitch perturbations were pseudo-randomly presented within each vocalization, with the first pitch perturbation occurring 1,000–1,500 ms after the utterance onset and the subsequent ones at 700–900 ms inter-stimulus intervals. To avoid vocal fatigue, participants were required to take a break of 6 s prior to initiating the next vocalization. For the offline stimulation sessions, participants received active or sham a-tDCS over left DLPFC for 20 min before performing the vocalization task with the same parameters as the online stimulation sessions. Within each stimulation session, participants produced 40 consecutive vocalizations that led to a total of 200 trials, with 50 trials for each of the four perturbations (+50, −50, +200, and −200 cents). Notably, sponge electrodes were placed on the scalp during the online active a-tDCS session but were removed from the scalp in the offline active a-tDCS session. To control for the potential confounding effects of subject expectation or motivation between the online and offline stimulation conditions, two different sham conditions were implemented in this study: sponge electrodes were kept on the scalp during the online sham session, but removed during the offline sham session.

Data acquisition

All participants performed the FAF-based vocal production experiment in a sound-attenuated booth. A dynamic microphone (DM2200, Takstar Inc.) was used to pick up the voice signals, which were amplified by a MOTU Ultralite Mk3 Firewire audio interface to 10 dB SPL above the participants' voice level to reduce the masking effects of the air-and bone-conducted feedback. The voice signals were then pitch-shifted by an Eventide Eclipse Harmonizer controlled by a custom-developed MIDI software program (Max/MSP, v5.0 by Cycling 74). This program also generated the transistor-transistor logic (TTL) control pulse that marked the onset of the pitch shift and the visual cues that instructed the participants to start and stop the vocalizations. The pitch-shifted voice signals were delivered back to

the participants through insert earphones (ER-1, Etymotic Research Inc.) after amplification by an ICON NeoAmp headphone amplifier. A PowerLab A/D converter (ML880, AD Instruments) digitized the original and feedback voice signals and TTL control pulses at 10 kHz, and LabChart software (v7.0, AD Instruments) recorded them on an iMAC computer.

Data analyses

As previously described in Peng et al. (2021), an IGOR PRO software program (v6.0, Wavemetrics Inc.) was developed to measure the magnitude and latency of vocal compensations for pitch perturbations across the conditions. In brief, the voice f_o contours in Hertz was extracted from the voice signals using Praat software (Boersma, 2001) and converted into cents scale according to the following formula: cents = $100 \times (12 \times \log_2(f_o/\text{reference}))$ [reference = 195.997 Hz (G3 note)]. Then they were segmented into epochs from 100 ms before to 700 ms after the onset of the pitch perturbation. All individual trials were visually inspected to reject bad trials that were contaminated by vocal interruptions or signal processing errors. Artifact-free trials were averaged to generate an overall vocal response to pitch perturbations for each condition, followed by a base-correction procedure that subtracts the mean f_o value in the baseline period (−100 ms to 0) from the f_o value after the perturbation onset. The peak f_o value in cents and the peak time in ms were considered as the magnitude and latency of a vocal response when the voice f_o contours reached their minimum or maximum value.

Statistics analyses

Repeated-measures analysis of variances (RM-ANOVAs) were used to analyze the values of vocal responses to pitch perturbations in SPSS (v.20.0). To investigate the online or offline effects of a-tDCS over left DLPFC, the magnitudes and latencies of vocal responses were subjected to three-way RM-ANOVAs with three factors: stimulation condition (a-tDCS vs. sham), perturbation magnitude (50 vs. 200 cents), and perturbation direction (upwards vs. downwards). In addition, four-way RM-ANOVAs were conducted to examine where the effects of a-tDCS varied as a function of the stimulation timing was delivered, including factors of stimulation timing (online vs. offline), stimulation condition, perturbation size and perturbation direction. Any significant higher-order interactions among these factors led to subsidiary RM-ANOVAs, and Bonferroni correction was used for *post hoc* multiple comparisons. Probability values for multiple degrees of freedom were corrected using Greenhouse–Geisser in the case of violation of the assumption of Mauchly' test of Sphericity. Partial η^2 (η_p^2) was calculated as an index of effect size to quantify the proportion of variance. p-values <0.05 were considered significant.

Results

Effects of online a-tDCS over left DLPFC

Figure 1 shows the grand-averaged voice f_o responses to perburations of ±50 and ±200 cents during active or sham a-tDCS over the left DLPFC. A three-way RM-ANOVA conducted on the peak magnitudes of vocal responses revealed a significant main effect of stimulation condition [$F(1, 16) = 24.473$, $p < 0.001$, $\eta_p^2 = 0.605$], indicating that online a-tDCS over the left DLPFC elicited smaller vocal responses than sham stimulation (see Figures 2A,B). However, the magnitudes of vocal responses did not vary as a function of perturbation size [$F(1, 19) = 0.451$, $p = 0.512$] or direction [$F(1, 16) = 1.080$, $p = 0.314$]. In addition, there were no significant interactions among the three factors ($p > 0.3$).

For the peak latencies of vocal responses, there was a significant main effect of stimulation condition [$F(1, 16) = 14.142$, $p = 0.002$, $\eta_p^2 = 0.469$], indicating that a shorter time was required to reach the peak magnitude of vocal response for online a-tDCS over the left DLPFC relative to sham stimulation (see Figures 2C,D). Also, upward perturbations elicited significantly longer peak latencies of vocal responses than downward perturbations [$F(1, 16) = 16.595$, $p = 0.001$, $\eta_p^2 = 0.509$], and 200 cents perturbations elicited significantly longer peak latencies of vocal responses than 50 cents perturbations [$F(1, 16) = 9.265$, $p = 0.008$, $\eta_p^2 = 0.367$]. The interactions among the three factors were not significant ($p > 0.1$).

Effects of offline a-tDCS over left DLPFC

Figure 3 shows the grand-averaged voice f_o responses to perturbations of ±50 and ±200 cents after active or sham a-tDCS over the left DLPFC. A three-way RM-ANOVA revealed significantly smaller magnitudes of vocal responses elicited by offline a-tDCS over the left DLPFC than sham condition [$F(1, 16) = 67.972$, $p < 0.001$, $\eta_p^2 = 0.809$] (see Figures 4A,B). However, there were no significant main effects of perturbation size [$F(1, 16) = 0.350$, $p = 0.562$] and direction [$F(1, 19) = 1.051$, $p = 0.321$]. The interactions among the three factors were also not significant ($p > 0.1$).

For the peak latencies of vocal responses, upward perturbations elicited significantly longer peak latencies of vocal responses than downward perturbations [$F(1, 16) = 5.459$, $p = 0.033$, $\eta_p^2 = 0.254$] (see Figures 4C,D). A marginally significant main effect of stimulation condition [$F(1, 16) = 4.309$, $p = 0.054$, $\eta_p^2 = 0.212$] was found, indicating a trend of shorter peak latencies of vocal responses for offline a-tDCS over the left DLPFC than for sham stimulation. The main effect of perturbation size [$F(1, 19) = 1.627$, $p = 0.220$] and interactions among the three factors ($p > 0.1$) were not significant.

Effects of online vs. offline a-tDCS over left DLPFC

A four-way RM-ANOVA conducted on the peak magnitudes of vocal responses revealed a significant main effect of stimulation condition [$F(1, 16) = 48.477$, $p < 0.001$, $\eta_p^2 = 0.752$]. The main effect of stimulation timing [$F(1, 16) = 3.786$, $p = 0.069$] as well as its interaction with stimulation condition [$F(1, 16) = 0.014$, $p = 0.907$] did not reach significance. In addition, the peak magnitudes of vocal responses did not vary as a function of perturbation size [$F(1, 16) = 0.764$, $p = 0.395$] or direction [$F(1, 19) = 0.001$, $p = 0.972$]. The interactions among the four variables were also not significant ($p > 0.1$). These results indicate that, regardless of the timing of a-tDCS and the physical features of pitch perturbations, a-tDCS over the left DLPFC led to significantly smaller vocal compensations for pitch perturbations than sham stimulation (see Figure 5A).

Regarding the peak latencies of vocal responses, there was a significant main effect of stimulation condition [$F(1, 16) = 16.901$, $p = 0.001$, $\eta_p^2 = 0.514$]. The main effect of stimulation timing [$F(1,$

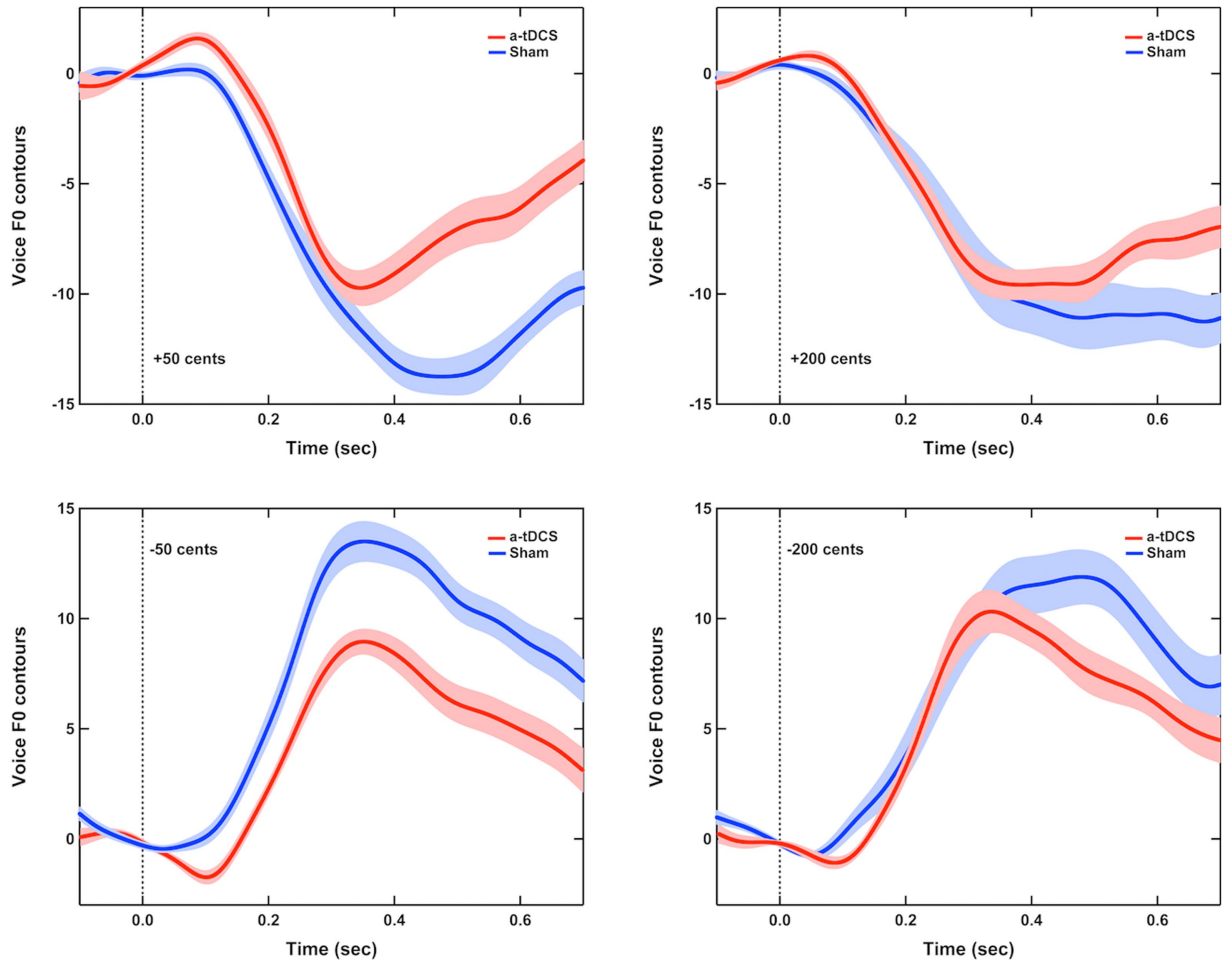

FIGURE 1
Grand-averaged voice f_0 responses to pitch perturbations of ±50 cents **(left panel)** and ±200 cents **(right panel)** when active (red solid lines) or sham (blue solid lines) a-tDCS over the left DLPFC was applied during the FAF task. Highlighted areas represent the standard errors of the mean vocal responses, while the vertical dash lines indicate the onset of pitch perturbations.

16) = 3.638, $p = 0.075$] as well as its interaction with stimulation condition [$F(1, 16) = 0.898$, $p = 0.357$] did not reach significance. The interactions among the four variables were also not significant ($p > 0.2$). That is, a-tDCS over the left DLPFC led to significantly shorter peak latencies of vocal compensations for pitch perturbations than sham stimulation, with no significant differences between online and offline stimulations (see Figure 5B). However, across the two stimulation timings, upward and 200 cents perturbations elicited longer peak latencies of vocal responses than downward [$F(1, 16) = 8.972$, $p = 0.009$, $\eta_p^2 = 0.359$] and 50 cents perturbations [$F(1, 16) = 31.741$, $p < 0.001$, $\eta_p^2 = 0.665$], respectively.

Discussion

The present study investigated the role of the left DLPFC in vocal feedback control by using a-tDCS during or prior to vocal pitch regulation through auditory feedback. The results showed that both online and offline a-tDCS over the left DLPFC led to smaller peak magnitudes and shorter peak times of vocal compensations for pitch perturbations regardless of their size or direction than sham stimulations. Importantly, there were no significant differences between online and offline stimulations, suggesting that the timing of a-tDCS does not significantly influence its effects on vocal feedback control. In conjunction with previous findings of enhanced vocal compensations for pitch perturbations following cTBS over the left DLPFC (Liu et al., 2020), these findings provide compelling causal evidence supporting the involvement of the left DLPFC in auditory-motor integration for vocal production, corroborating the hypothesis that the left DLPFC exerts top-down inhibitory control over vocal feedback control.

The present study confirms our hyothesis that a-tDCS over the left DLPFC led to reduced vocal compensations for pitch perturbations compared to sham stimulation. In light of the findings that cortical excitablity of the left DLPFC can be increased by a-tDCS (Keeser et al., 2011; Zaehle et al., 2011), this finding implies that enhancing left DLPFC activity with a-tDCS may produce inhibitory modulations of vocal pitch regulation through auditory feedback. Consistently, Liu et al. (2020) found increased vocal compensations for pitch perturbations as a consequence of disrupting activity in the left DLPFC with inhibitory cTBS. These studies collectively establish a causal link between the left DLPFC and vocal feedback control, suggesting that enhancing or inhibiting left DLPFC activity exerts modulatory effects on auditory-vocal integration.

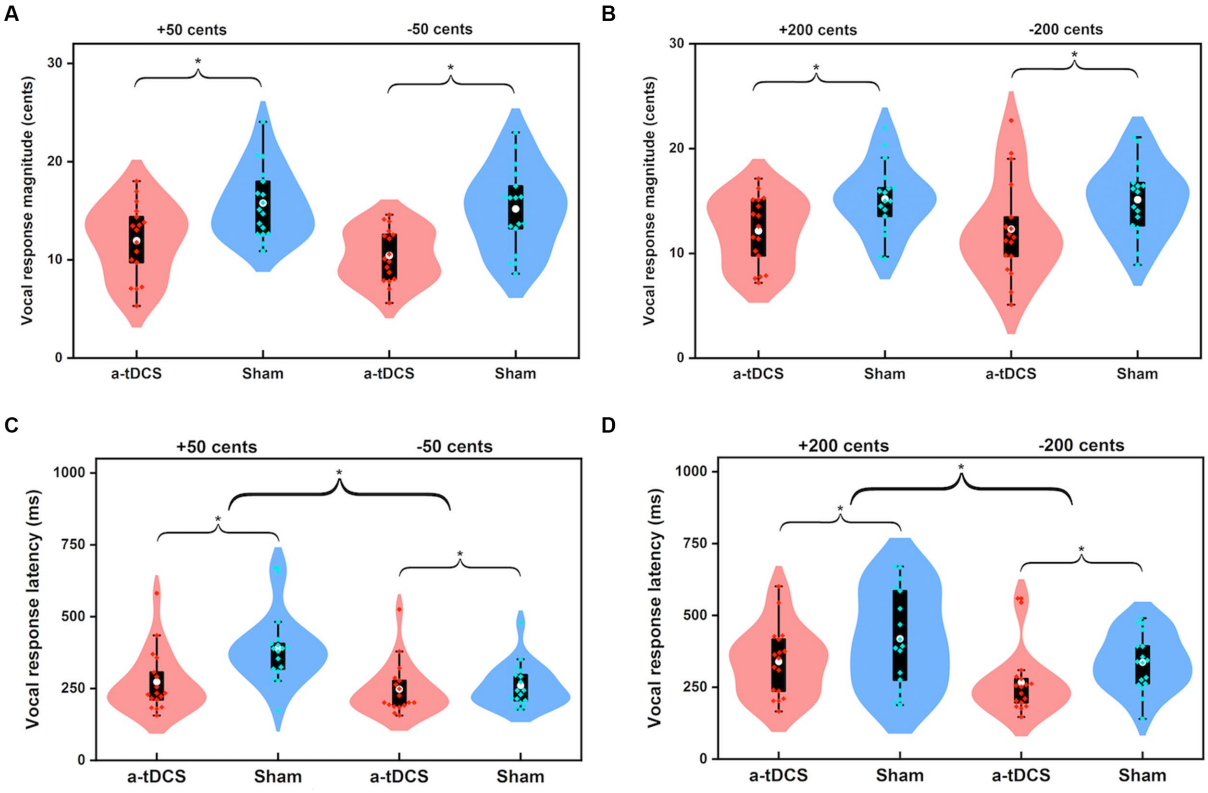

FIGURE 2
Violin plots illustrating the magnitudes **(A,B)** and latencies **(C,D)** of vocal responses to pitch perturbations of ±50 cents and ±200 cents when active (red) and sham (blue) a-tDCS over the left DLPFC was applied during the FAF task. The shape of the violin shows the kernel density estimate of the data. The white dots and box plots represent the medians and ranges from first to third quartiles of the data sets. The red and blue dots represent the individual vocal responses for active and sham a-tDCS over the left DLPFC. The asterisks indicate significant differences across the conditions.

Compensatory vocal adjustment in response to auditory feedback errors has been linked to sensorimotor control of vocal production. Previous studies have shown reduced vocal compensations for pitch perturbations in healthy individuals after speech-sound learning or working memory training (Chen et al., 2015; Guo et al., 2017) and in professional singers following intensive vocal training (Jones and Keough, 2008; Zarate and Zatorre, 2008; Wang et al., 2019). And enhanced vocal compensations for pitch perturbations have been observed in patients with neurological diseases such as AD (Ranasinghe et al., 2017), Parkinson's disease (PD) (Liu et al., 2012; Chen et al., 2013; Huang et al., 2016; Mollaei et al., 2016), and spinocerebellar ataxia (SCA) (Parrell et al., 2017; Houde et al., 2019; Li et al., 2019). Notably, treatment-induced normalization of this overcompensation behavior has been reported in patients with PD following intensive voice training (Li et al., 2021) or cTBS over the left supplementary motor area (SMA) (Dai et al., 2022), as well as in patients with SCA following cTBS over the right cerebellum (Lin et al., 2022). Therefore, reduced or enhanced compensatory vocal adjustment to perturbed auditory feedback may reflect improved or impaired auditory-motor integration for vocal production. Our results showed that a-tDCS over the left DLPFC led to reduced vocal compensations, suggesting that enhancing left DLPFC activity may facilitate vocal motor control through auditory feedback.

Our finding also showed that a-tDCS over the left DLPFC led to reduced peak times of vocal responses to pitch perturbations. In contrast, prolonged peak times of vocal responses were found when inhibitory cTBS was applied over the left DLPFC (Liu et al., 2020). Other NIBS studies targeting other brain regions have shown that a-tDCS over the right cerebellum prolonged the peak times of vocal responses to pitch perturbations (Peng et al., 2021), while cTBS over the right cerebellum (Lin et al., 2022) or the left or right SMG (Li et al., 2023) shortened them. Prolonged vocal responses to pitch perturbations have been observed in patients with PD (Kiran and Larson, 2001) or aphasia (Johnson et al., 2020), reflecting their impaired sensorimotor integration in speech processing. However, these prolonged vocal responses can be normalized by intensive voice training in patients with PD (Li et al., 2021). Accordingly, our observation of shortened peak times of vocal responses induced by a-tDCS over the left DLPFC leads further support to the idea that enhancing left DLPFC activity facilitates auditory feedback control of vocal production.

The present study found no significant differences between online and offline a-tDCS over the left DLPFC in modulating vocal pitch regulation. This pattern of results is consistent with one recent study that reported comparable effects on vocal pitch regulation of online or offline a-tDCS over the right cerebellum (Peng et al., 2021). These findings suggest that online and offline a-tDCS over the left DLPFC or right cerebellum may have equivalent effects on vocal feedback control. Nevertheless, whether online and offline tDCS have similar or distinct effects on cognitive or motor functions remains open and

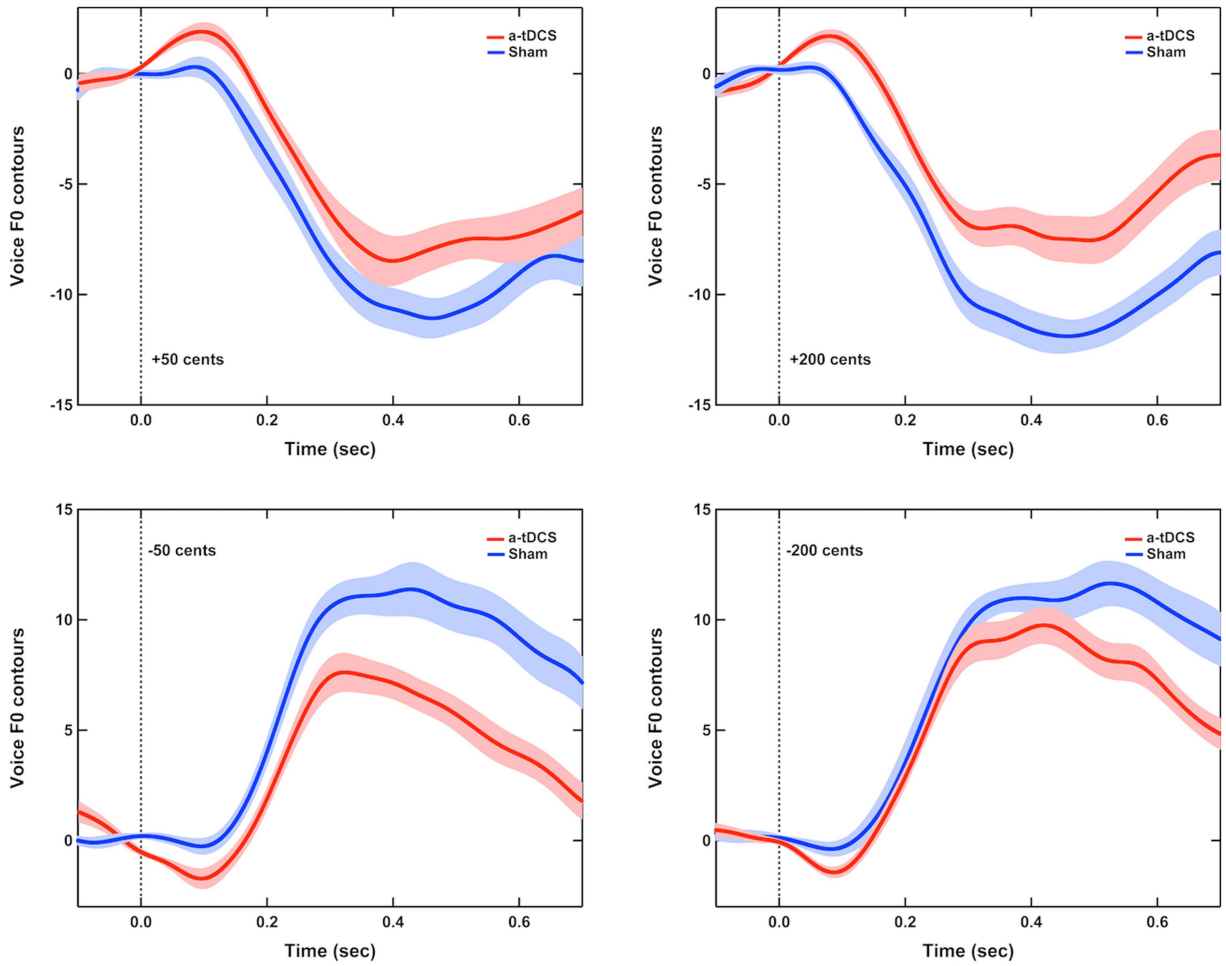

FIGURE 3
Grand-averaged voice f_0 contours in response to pitch perturbations of ±50 cents **(left panel)** and ±200 cents **(right panel)** when active (red solid lines) or sham (blue solid lines) a-tDCS was applied over the left DLPFC prior to the FAF task. Highlighted areas represent the standard errors of the mean vocal responses, while the vertical dash lines indicate the onset of pitch perturbations.

may be influenced by various factors, including the target site, polarity specificity, and task demands. A meta-analysis study reported similar positive effects of online and offline tDCS over the left DLPFC on cognitive and motor functions (Summers et al., 2016), but other studies found distinct effects of online and offline tDCS over the left DLPFC or the posterior parietal cortex (PPC) on verbal and spatial working memory tasks (Zivanovic et al., 2021), or over the cerebellum on motor learning tasks (Samaei et al., 2017). Therefore, further research is warranted to address the effects of online and offline tDCS over other brain regions on vocal motor control, which would not only elucidate the causality of the underlying neural mechanisms but also optimize the parameters and protocols of tDCS for potential therapeutic applications in motor speech disorders.

Our results, along with the findings of Liu et al. (2020), demonstrate that modulating left DLPFC activity affects vocal pitch regulation in a bidirectional manner: enhancing or inhibiting its activity decreased and increased vocal compensations for pitch perturbations, respectively. These findings can be accounted for a top-down inhibitory mechanism mediated by the left DLPFC (Liu et al., 2020), which relies on two key aspects: (1) the left DLPFC mediates cognitive functions such as attentional control, working memory, and inhibitory control, which have been demonstrated to be essentially involved in vocal feedback control (Tumber et al., 2014; Liu et al., 2015; Guo et al., 2017; Ranasinghe et al., 2017); (2) the DLPFC has reciprocal connections to auditory and motor regions (Selemon and Goldman-Rakic, 1988; Romanski et al., 1999). This mechanism suggests that the left DLPFC may exert top-down inhibitory control over the interaction between auditory and motor representations of speech sounds that prevents excessive compensatory vocal adjustment for feedback perturbations to ensure precise and stable speech production (Houde and Nagarajan, 2011). Similarly, Ranasinghe et al. (2017) proposed that the prefrontal cortex may generate an inhibiotry influence on vocal motor control that leads to incomplete compensations for feedback errors. Therefore, dysfucntions of this top-down inhibitory process would result in enhanced vocal compensations for feedback errors, as evidenced by patients with AD who showed enhanced vocal compensations and reduced left DLPFC activity (Ranasinghe et al., 2017, 2019). Conversely, improvement of this top–down inhibitory control process would result in reduced vocal compensation for feedback errors, as evidenced by patients with PD who showed improved vocal loudness following intensive voice training that was correlated with reduced

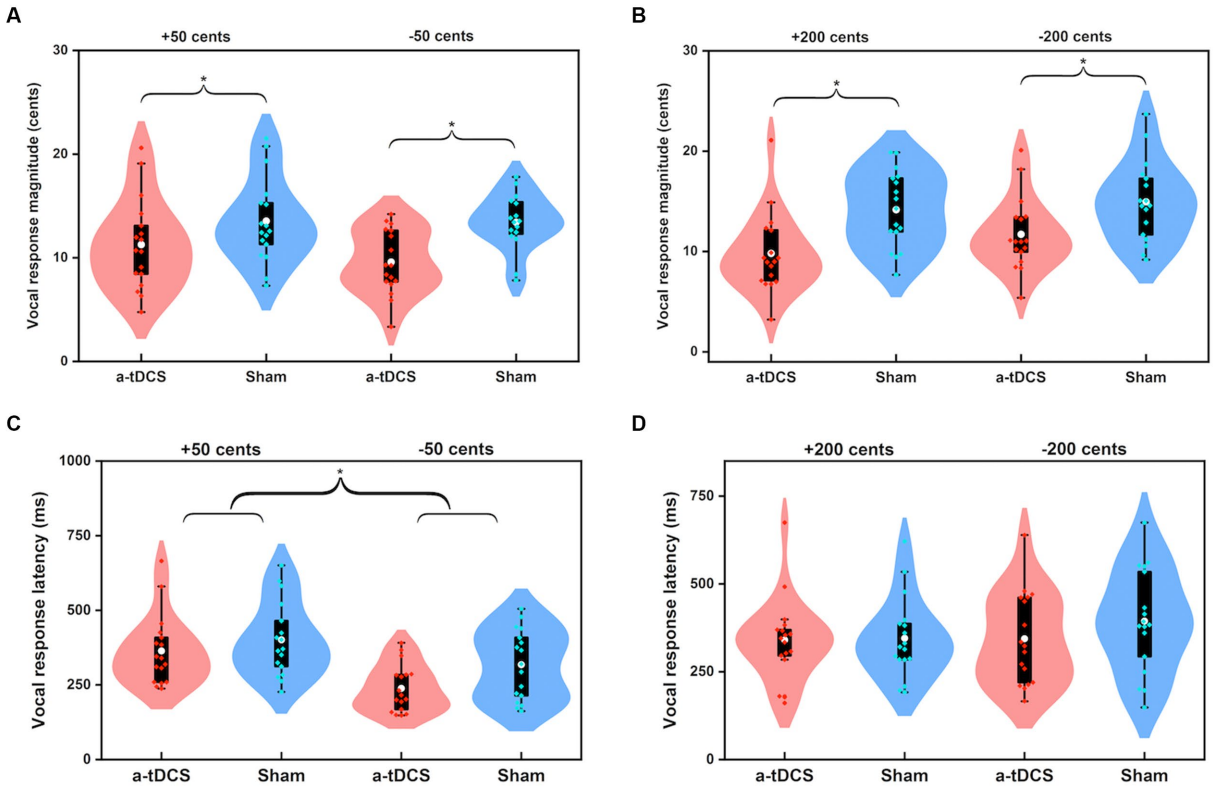

FIGURE 4
Violin plots illustrating the magnitudes **(A,B)** and latencies **(C,D)** of vocal responses to pitch perturbations of ±50 cents and ±200 cents when active (red) or sham (blue) a-tDCS was applied over the left DLPFC prior to the FAF task. The white dots and box plots represent the medians and ranges from first to third quartiles of the data sets. The red and blue dots represent the individual vocal responses for active and sham a-tDCS over the left DLPFC. The asterisks indicate significant differences across the conditions.

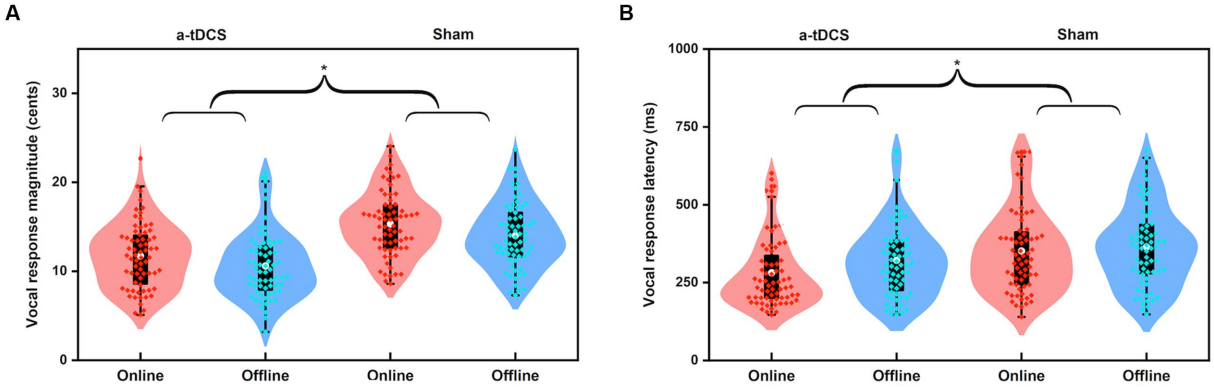

FIGURE 5
Violin plots illustrating the magnitudes **(A)** and latencies **(B)** of vocal responses to pitch perturbations when active or sham a-tDCS was applied over the left DLPFC prior to (offline) or during (online) the FAF task. The white dots and box plots represent the medians and ranges from first to third quartiles of the data sets. The red and blue dots represent the individual vocal responses for online and offline a-tDCS over the left DLPFC. The asterisks indicate significant differences across the conditions.

vocal compensations (Li et al., 2021) and increased activity in the DLPFC (Liotti et al., 2003; Narayana et al., 2010). This mechanism also helps explain why working memory training led to reduced vocal compensations for pitch perturbations (Guo et al., 2017). However, the precise neural mechanisms and pathways by which the left DLPFC exerts top-down control over vocal feedback control are largely unknown and warrant further investigation.

Several limitations of the present study should be acknowledged. First, the present study only used a single session of a-tDCS over the left DLPFC to evaluate their immediate effects on vocal pitch regulation. This design leaves open the long-term effects as well as the optimal parameters of a-tDCS for enhancing vocal feedback control. Second, the present study did not collect neuroimaging data such as ERP and fMRI concurrently with the acoustic data, limiting our ability

to elucidate the neural mechanisms underlying the causal role of the left DLPFC in vocal feedback control. Finally, the conventional tDCS protocol employed in the present study may induce widespread currents to other brain regions due to the limited focality of stimulation (de Berker et al., 2013). In subsequent studies, high-definition tDCS (HD-tDCS) that offers improved focality of brain stimulation should be considered to verify the present findings.

Conclusion

In summary, the present study showed that a-tDCS over the left DLPFC led to reduced peak magnitudes and prolonged peak times of vocal compensations for pitch perturbations relative to sham stimulation, regardless the size or direction of the pitch perturbation and the timing of the stimulation. These findings provide causal evidence that a-tDCS over the left DLPFC can facilitate auditory-motor integration for rapid and precise control of vocal production. The present study, together with Liu et al. (2020), lends support to the hypothesis of a top-down mechanism mediated by the left DLPFC that exerts inhibitory influences on vocal feedback control.

Data availability statement

The raw data supporting the conclusions of this article will be made available by the authors, without undue reservation.

Ethics statement

The studies involving human participants were reviewed and approved by Institutional Review Board of The First Affiliated Hospital of Sun Yat-sen University. The patients/participants provided their written informed consent to participate in this study.

Author contributions

YC, DP, and HL contributed to the design of the study. YC, DP, YZ, XC, XW, and JL contributed to the acquisition and analysis of data. YC, XW, PL, and HL contributed to drafting the manuscript and preparing the figures. All authors have reviewed and approved the contents of the paper.

Funding

This study was funded by grants from the National Natural Science Foundation of China (Nos. 82172528, 81772439, 81972147, 82102660, 82102648), Guangdong Basic and Applied Basic Research Foundation (No. 2022A1515011203, 2023A1515011758), Guangdong Province Science and Technology Planning Project (No. 2017A050501014), and Guangzhou Science and Technology Programme (No. 201604020115).

Conflict of interest

The authors declare that the research was conducted in the absence of any commercial or financial relationships that could be construed as a potential conflict of interest.

Publisher's note

All claims expressed in this article are solely those of the authors and do not necessarily represent those of their affiliated organizations, or those of the publisher, the editors and the reviewers. Any product that may be evaluated in this article, or claim that may be made by its manufacturer, is not guaranteed or endorsed by the publisher.

References

Angius, L., Santarnecchi, E., Pascual-Leone, A., and Marcora, S. M. (2019). Transcranial direct current stimulation over the left dorsolateral prefrontal cortex improves inhibitory control and endurance performance in healthy individuals. *Neuroscience* 419, 34–45. doi: 10.1016/j.neuroscience.2019.08.052

Bauer, J. J., Mittal, J., Larson, C. R., and Hain, T. C. (2006). Vocal responses to unanticipated perturbations in voice loudness feedback: an automatic mechanism for stabilizing voice amplitude. *J. Acoust. Soc. Am.* 119, 2363–2371. doi: 10.1121/1.2173513

Behroozmand, R., Johari, K., Bridwell, K., Hayden, C., Fahey, D., and den Ouden, D. B. (2020). Modulation of vocal pitch control through high-definition transcranial direct current stimulation of the left ventral motor cortex. *Exp. Brain Res.* 238, 1525–1535. doi: 10.1007/s00221-020-05832-9

Behroozmand, R., Phillip, L., Johari, K., Bonilha, L., Rorden, C., Hickok, G., et al. (2018). Sensorimotor impairment of speech auditory feedback processing in aphasia. *NeuroImage* 165, 102–111. doi: 10.1016/j.neuroimage.2017.10.014

Behroozmand, R., Shebek, R., Hansen, D. R., Oya, H., Robin, D. A., Howard, M. A. 3rd, et al. (2015). Sensory-motor networks involved in speech production and motor control: an fMRI study. *NeuroImage* 109, 418–428. doi: 10.1016/j.neuroimage.2015.01.040

Boersma, P. (2001). Praat, a system for doing phonetics by computer. *Glot Int.* 5, 341–345.

Brosnan, M. B., and Wiegand, I. (2017). The dorsolateral prefrontal cortex, a dynamic cortical area to enhance top-down attentional control. *J. Neurosci.* 37, 3445–3446. doi: 10.1523/JNEUROSCI.0136-17.2017

Buchwald, A., Calhoun, H., Rimikis, S., Lowe, M. S., Wellner, R., and Edwards, D. J. (2019). Using tDCS to facilitate motor learning in speech production: the role of timing. *Cortex* 111, 274–285. doi: 10.1016/j.cortex.2018.11.014

Burnett, T. A., Freedland, M. B., Larson, C. R., and Hain, T. C. (1998). Voice F0 responses to manipulations in pitch feedback. *J. Acoust. Soc. Am.* 103, 3153–3161. doi: 10.1121/1.423073

Chen, S. H., Liu, H., Xu, Y., and Larson, C. R. (2007). Voice F0 responses to pitch-shifted voice feedback during English speech. *J. Acoust. Soc. Am.* 121, 1157–1163. doi: 10.1121/1.2404624

Chen, Z., Wong, F. C., Jones, J. A., Li, W., Liu, P., Chen, X., et al. (2015). Transfer effect of speech-sound learning on auditory-motor processing of perceived vocal pitch errors. *Sci. Rep.* 5:13134. doi: 10.1038/srep13134

Chen, X., Zhu, X., Wang, E. Q., Chen, L., Li, W., Chen, Z., et al. (2013). Sensorimotor control of vocal pitch production in Parkinson's disease. *Brain Res.* 1527, 99–107. doi: 10.1016/j.brainres.2013.06.030

Dai, G., Chen, M., Chen, X., Guo, Z., Li, T., Jones, J. A., et al. (2022). A causal link between left supplementary motor area and auditory-motor control of vocal production: evidence by continuous theta burst stimulation. *NeuroImage* 264:119767. doi: 10.1016/j.neuroimage.2022.119767

de Berker, A. O., Bikson, M., and Bestmann, S. (2013). Predicting the behavioral impact of transcranial direct current stimulation: issues and limitations. *Front. Hum. Neurosci.* 7:613. doi: 10.3389/fnhum.2013.00613

Edin, F., Klingberg, T., Johansson, P., McNab, F., Tegner, J., and Compte, A. (2009). Mechanism for top-down control of working memory capacity. *Proc. Natl. Acad. Sci. U. S. A.* 106, 6802–6807. doi: 10.1073/pnas.0901894106

Flagmeier, S. G., Ray, K. L., Parkinson, A. L., Li, K., Vargas, R., Price, L. R., et al. (2014). The neural changes in connectivity of the voice network during voice pitch perturbation. *Brain Lang.* 132, 7–13. doi: 10.1016/j.bandl.2014.02.001

Glasser, M. F., Coalson, T. S., Robinson, E. C., Hacker, C. D., Harwell, J., Yacoub, E., et al. (2016). A multi-modal parcellation of human cerebral cortex. *Nature* 536, 171–178. doi: 10.1038/nature18933

Golfinopoulos, E., Tourville, J. A., and Guenther, F. H. (2010). The integration of large-scale neural network modeling and functional brain imaging in speech motor control. *NeuroImage* 52, 862–874. doi: 10.1016/j.neuroimage.2009.10.023

Guenther, F. H., and Hickok, G. (2015). Role of the auditory system in speech production. *Handb. Clin. Neurol.* 129, 161–175. doi: 10.1016/B978-0-444-62630-1.00009-3

Guo, Z., Wu, X., Li, W., Jones, J. A., Yan, N., Sheft, S., et al. (2017). Top-down modulation of auditory-motor integration during speech production: the role of working memory. *J. Neurosci.* 37, 10323–10333. doi: 10.1523/JNEUROSCI.1329-17.2017

Herwig, U., Satrapi, P., and Schonfeldt-Lecuona, C. (2003). Using the international 10-20 EEG system for positioning of transcranial magnetic stimulation. *Brain Topogr.* 16, 95–99. doi: 10.1023/B:BRAT.0000006333.93597.9d

Hickok, G., and Poeppel, D. (2007). The cortical organization of speech processing. *Nat. Rev. Neurosci.* 8, 393–402. doi: 10.1038/nrn2113

Houde, J. F., Gill, J. S., Agnew, Z., Kothare, H., Hickok, G., Parrell, B., et al. (2019). Abnormally increased vocal responses to pitch feedback perturbations in patients with cerebellar degeneration. *J. Acoust. Soc. Am.* 145, EL372–EL378. doi: 10.1121/1.5100910

Houde, J. F., and Jordan, M. I. (1998). Sensorimotor adaptation in speech production. *Science* 279, 1213–1216. doi: 10.1126/science.279.5354.1213

Houde, J. F., and Nagarajan, S. S. (2011). Speech production as state feedback control. *Front. Hum. Neurosci.* 5:82. doi: 10.3389/fnhum.2011.00082

Huang, X., Chen, X., Yan, N., Jones, J. A., Wang, E. Q., Chen, L., et al. (2016). The impact of Parkinson's disease on the cortical mechanisms that support auditory-motor integration for voice control. *Hum. Brain Mapp.* 37, 4248–4261. doi: 10.1002/hbm.23306

Huang, Y. Z., Edwards, M. J., Rounis, E., Bhatia, K. P., and Rothwell, J. C. (2005). Theta burst stimulation of the human motor cortex. *Neuron* 45, 201–206. doi: 10.1016/j.neuron.2004.12.033

Johnson, L. P., Sangtian, S., Johari, K., Behroozmand, R., and Fridriksson, J. (2020). Slowed compensation responses to altered auditory feedback in post-stroke aphasia: implications for speech sensorimotor integration. *J. Commun. Disord.* 88:106034. doi: 10.1016/j.jcomdis.2020.106034

Jones, J. A., and Keough, D. (2008). Auditory-motor mapping for pitch control in singers and nonsingers. *Exp. Brain Res.* 190, 279–287. doi: 10.1007/s00221-008-1473-y

Keeser, D., Meindl, T., Bor, J., Palm, U., Pogarell, O., Mulert, C., et al. (2011). Prefrontal transcranial direct current stimulation changes connectivity of resting-state networks during fMRI. *J. Neurosci.* 31, 15284–15293. doi: 10.1523/JNEUROSCI.0542-11.2011

Kiran, S., and Larson, C. R. (2001). Effect of duration of pitch-shifted feedback on vocal responses in Parkinson's disease patients and normal controls. *J. Speech Lang. Hear. Res.* 44, 975–987. doi: 10.1044/1092-4388(2001/076)

Knight, R. T., Scabini, D., and Woods, D. L. (1989). Prefrontal cortex gating of auditory transmission in humans. *Brain Res.* 504, 338–342. doi: 10.1016/0006-8993(89)91381-4

Kort, N. S., Cuesta, P., Houde, J. F., and Nagarajan, S. S. (2016). Bihemispheric network dynamics coordinating vocal feedback control. *Hum. Brain Mapp.* 37, 1474–1485. doi: 10.1002/hbm.23114

Lefaucheur, J. P., Antal, A., Ayache, S. S., Benninger, D. H., Brunelin, J., Cogiamanian, F., et al. (2017). Evidence-based guidelines on the therapeutic use of transcranial direct current stimulation (tDCS). *Clin. Neurophysiol.* 128, 56–92. doi: 10.1016/j.clinph.2016.10.087

Li, Y., Tan, M., Fan, H., Wang, E. Q., Chen, L., Li, J., et al. (2021). Neurobehavioral effects of LSVT® LOUD on auditory-vocal integration in Parkinson's disease: a preliminary study. *Front. Neurosci.* 15:624801. doi: 10.3389/fnins.2021.624801

Li, T., Zhu, X., Wu, X., Gong, Y., Jones, J. A., Liu, P., et al. (2023). Continuous theta burst stimulation over left and right supramarginal gyri demonstrates their involvement in auditory feedback control of vocal production. *Cereb. Cortex* 33, 11–22. doi: 10.1093/cercor/bhac049

Li, W., Zhuang, J., Guo, Z., Jones, J. A., Xu, Z., and Liu, H. (2019). Cerebellar contribution to auditory feedback control of speech production: evidence from patients with spinocerebellar ataxia. *Hum. Brain Mapp.* 40, 4748–4758. doi: 10.1002/hbm.24734

Lin, Q., Chang, Y., Liu, P., Jones, J. A., Chen, X., Peng, D., et al. (2022). Cerebellar continuous theta burst stimulation facilitates auditory-vocal integration in spinocerebellar ataxia. *Cereb. Cortex* 32, 455–466. doi: 10.1093/cercor/bhab222

Liotti, M., Ramig, L. O., Vogel, D., New, P., Cook, C. I., Ingham, R. J., et al. (2003). Hypophonia in Parkinson's disease: neural correlates of voice treatment revealed by PET. *Neurology* 60, 432–440. doi: 10.1212/WNL.60.3.432

Liu, D., Dai, G., Liu, C., Guo, Z., Xu, Z., Jones, J. A., et al. (2020). Top-down inhibitory mechanisms underlying auditory-motor integration for voice control: evidence by TMS. *Cereb. Cortex* 30, 4515–4527. doi: 10.1093/cercor/bhaa054

Liu, Y., Hu, H., Jones, J. A., Guo, Z., Li, W., Chen, X., et al. (2015). Selective and divided attention modulates auditory-vocal integration in the processing of pitch feedback errors. *Eur. J. Neurosci.* 42, 1895–1904. doi: 10.1111/ejn.12949

Liu, H., Meshman, M., Behroozmand, R., and Larson, C. R. (2011). Differential effects of perturbation direction and magnitude on the neural processing of voice pitch feedback. *Clin. Neurophysiol.* 122, 951–957. doi: 10.1016/j.clinph.2010.08.010

Liu, H., Wang, E. Q., Verhagen Metman, L., and Larson, C. R. (2012). Vocal responses to perturbations in voice auditory feedback in individuals with Parkinson's disease. *PLoS One* 7:e33629. doi: 10.1371/journal.pone.0033629

Loftus, A. M., Yalcin, O., Baughman, F. D., Vanman, E. J., and Hagger, M. S. (2015). The impact of transcranial direct current stimulation on inhibitory control in young adults. *Brain Behav.* 5:e00332. doi: 10.1002/brb3.332

Mancuso, L. E., Ilieva, I. P., Hamilton, R. H., and Farah, M. J. (2016). Does transcranial direct current stimulation improve healthy working memory?: a Meta-analytic review. *J. Cogn. Neurosci.* 28, 1063–1089. doi: 10.1162/jocn_a_00956

Manor, B., Dagan, M., Herman, T., Gouskova, N. A., Vanderhorst, V. G., Giladi, N., et al. (2021). Multitarget transcranial electrical stimulation for freezing of gait: a randomized controlled trial. *Mov. Disord.* 36, 2693–2698. doi: 10.1002/mds.28759

Mansouri, F. A., Tanaka, K., and Buckley, M. J. (2009). Conflict-induced behavioural adjustment: a clue to the executive functions of the prefrontal cortex. *Nat. Rev. Neurosci.* 10, 141–152. doi: 10.1038/nrn2538

Mitchell, T. V., Morey, R. A., Inan, S., and Belger, A. (2005). Functional magnetic resonance imaging measure of automatic and controlled auditory processing. *Neuroreport* 16, 457–461. doi: 10.1097/00001756-200504040-00008

Mollaei, F., Shiller, D. M., Baum, S. R., and Gracco, V. L. (2016). Sensorimotor control of vocal pitch and formant frequencies in Parkinson's disease. *Brain Res.* 1646, 269–277. doi: 10.1016/j.brainres.2016.06.013

Narayana, S., Fox, P. T., Zhang, W., Franklin, C., Robin, D. A., Vogel, D., et al. (2010). Neural correlates of efficacy of voice therapy in Parkinson's disease identified by performance-correlation analysis. *Hum. Brain Mapp.* 31, 222–236. doi: 10.1002/hbm.20859

Nitsche, M. A., and Paulus, W. (2000). Excitability changes induced in the human motor cortex by weak transcranial direct current stimulation. *J. Physiol.* 527, 633–639. doi: 10.1111/j.1469-7793.2000.t01-1-00633.x

Parrell, B., Agnew, Z., Nagarajan, S., Houde, J., and Ivry, R. B. (2017). Impaired feedforward control and enhanced feedback control of speech in patients with cerebellar degeneration. *J. Neurosci.* 37, 9249–9258. doi: 10.1523/JNEUROSCI.3363-16.2017

Peng, D., Lin, Q., Chang, Y., Jones, J. A., Jia, G., Chen, X., et al. (2021). A causal role of the cerebellum in auditory feedback control of vocal production. *Cerebellum* 20, 584–595. doi: 10.1007/s12311-021-01230-1

Ranasinghe, K. G., Gill, J. S., Kothare, H., Beagle, A. J., Mizuiri, D., Honma, S. M., et al. (2017). Abnormal vocal behavior predicts executive and memory deficits in Alzheimer's disease. *Neurobiol. Aging* 52, 71–80. doi: 10.1016/j.neurobiolaging.2016.12.020

Ranasinghe, K. G., Kothare, H., Kort, N., Hinkley, L. B., Beagle, A. J., Mizuiri, D., et al. (2019). Neural correlates of abnormal auditory feedback processing during speech production in Alzheimer's disease. *Sci. Rep.* 9:5686. doi: 10.1038/s41598-019-41794-x

Romanski, L. M., Tian, B., Fritz, J., Mishkin, M., Goldman-Rakic, P. S., and Rauschecker, J. P. (1999). Dual streams of auditory afferents target multiple domains in the primate prefrontal cortex. *Nat. Neurosci.* 2, 1131–1136. doi: 10.1038/16056

Samaei, A., Ehsani, F., Zoghi, M., Hafez Yosephi, M., and Jaberzadeh, S. (2017). Online and offline effects of cerebellar transcranial direct current stimulation on motor learning in healthy older adults: a randomized double-blind sham-controlled study. *Eur. J. Neurosci.* 45, 1177–1185. doi: 10.1111/ejn.13559

Scheerer, N. E., Behich, J., Liu, H., and Jones, J. A. (2013). ERP correlates of the magnitude of pitch errors detected in the human voice. *Neuroscience* 240, 176–185. doi: 10.1016/j.neuroscience.2013.02.054

Scott, T. L., Haenchen, L., Daliri, A., Chartove, J., Guenther, F. H., and Perrachione, T. K. (2020). Noninvasive neurostimulation of left ventral motor cortex enhances sensorimotor adaptation in speech production. *Brain Lang.* 209:104840. doi: 10.1016/j.bandl.2020.104840

Selemon, L. D., and Goldman-Rakic, P. S. (1988). Common cortical and subcortical targets of the dorsolateral prefrontal and posterior parietal cortices in the rhesus monkey: evidence for a distributed neural network subserving spatially guided behavior. *J. Neurosci.* 8, 4049–4068. doi: 10.1523/JNEUROSCI.08-11-04049.1988

Smotherman, M. S. (2007). Sensory feedback control of mammalian vocalizations. *Behav. Brain Res.* 182, 315–326. doi: 10.1016/j.bbr.2007.03.008

Stagg, C. J., Jayaram, G., Pastor, D., Kincses, Z. T., Matthews, P. M., and Johansen-Berg, H. (2011). Polarity and timing-dependent effects of transcranial direct current stimulation in explicit motor learning. *Neuropsychologia* 49, 800–804. doi: 10.1016/j.neuropsychologia.2011.02.009

Stagg, C. J., and Nitsche, M. A. (2011). Physiological basis of transcranial direct current stimulation. *Neuroscientist* 17, 37–53. doi: 10.1177/1073858410386614

Summers, J. J., Kang, N., and Cauraugh, J. H. (2016). Does transcranial direct current stimulation enhance cognitive and motor functions in the ageing brain? A systematic review and meta- analysis. *Ageing Res. Rev.* 25, 42–54. doi: 10.1016/j.arr.2015.11.004

Tedla, J. S., Sangadala, D. R., Reddy, R. S., Gular, K., and Dixit, S. (2023). High-definition trans cranial direct current stimulation and its effects on cognitive function: a systematic review. *Cereb. Cortex* 33, 6077–6089. doi: 10.1093/cercor/bhac485

Tumber, A. K., Scheerer, N. E., and Jones, J. A. (2014). Attentional demands influence vocal compensations to pitch errors heard in auditory feedback. *PLoS One* 9:e109968. doi: 10.1371/journal.pone.0109968

Wang, W., Wei, L., Chen, N., Jones, J. A., Gong, G., and Liu, H. (2019). Decreased gray-matter volume in insular cortex as a correlate of singers' enhanced sensorimotor control of vocal production. *Front. Neurosci.* 13:185. doi: 10.3389/fnins.2019.00815

Zaehle, T., Sandmann, P., Thorne, J. D., Jancke, L., and Herrmann, C. S. (2011). Transcranial direct current stimulation of the prefrontal cortex modulates working memory performance: combined behavioural and electrophysiological evidence. *BMC Neurosci.* 12:2. doi: 10.1186/1471-2202-12-2

Zarate, J. M., and Zatorre, R. J. (2008). Experience-dependent neural substrates involved in vocal pitch regulation during singing. *NeuroImage* 40, 1871–1887. doi: 10.1016/j.neuroimage.2008.01.026

Zivanovic, M., Paunovic, D., Konstantinovic, U., Vulic, K., Bjekic, J., and Filipovic, S. R. (2021). The effects of offline and online prefrontal vs parietal transcranial direct current stimulation (tDCS) on verbal and spatial working memory. *Neurobiol. Learn. Mem.* 179:107398. doi: 10.1016/j.nlm.2021.107398

frontiers | Frontiers in Neuroscience

TYPE Original Research
PUBLISHED 04 August 2023
DOI 10.3389/fnins.2023.1196805

OPEN ACCESS

EDITED BY
Chang-Hoon Choi,
Helmholtz Association of German Research Centres (HZ), Germany

REVIEWED BY
Yuhei Takado,
National Institutes for Quantum and Radiological Science and Technology, Japan
Anna E. Kirkland,
Medical University of South Carolina, United States

*CORRESPONDENCE
Shinichiro Nakajima
shinichiro_nakajima@hotmail.com
Yoshihiro Noda
yoshi-tms@keio.jp
Shinya Fujii
sfujii@sfc.keio.ac.jp

RECEIVED 30 March 2023
ACCEPTED 12 July 2023
PUBLISHED 04 August 2023

CITATION
Honda S, Noda Y, Matsushita K, Tarumi R, Nomiyama N, Tsugawa S, Tobari Y, Hondo N, Saito K, Mimura M, Fujii S and Nakajima S (2023) Glutamatergic neurometabolite levels in the caudate are associated with the ability of rhythm production.
Front. Neurosci. 17:1196805.
doi: 10.3389/fnins.2023.1196805

Glutamatergic neurometabolite levels in the caudate are associated with the ability of rhythm production

Shiori Honda[1], Yoshihiro Noda[1]*, Karin Matsushita[1], Ryosuke Tarumi[1,2], Natsumi Nomiyama[3], Sakiko Tsugawa[1], Yui Tobari[1], Nobuaki Hondo[1], Keisuke Saito[1], Masaru Mimura[1], Shinya Fujii[3]* and Shinichiro Nakajima[1,4]*

[1]Department of Neuropsychiatry, Keio University School of Medicine, Tokyo, Japan, [2]Seikeikai Komagino Hospital, Hachioji, Japan, [3]Faculty of Environment and Information Studies, Keio University, Kanagawa, Japan, [4]Multimodal Imaging Group, Research Imaging Centre, Centre for Addiction and Mental Health, Toronto, ON, Canada

Introduction: Glutamatergic neurometabolites play important roles in the basal ganglia, a hub of the brain networks involved in musical rhythm processing. We aimed to investigate the relationship between rhythm processing abilities and glutamatergic neurometabolites in the caudate.

Methods: We aquired Glutamatergic function in healthy individuals employing proton magnetic resonance spectroscopy. We targeted the right caudate and the dorsal anterior cingulate cortex (dACC) as a control region. Rhythm processing ability was assessed by the Harvard Beat Assessment Test (H-BAT).

Results: We found negative correlations between the production part of the Beat Saliency Test in the H-BAT and glutamate and glutamine levels in the caudate ($r = -0.693$, $p = 0.002$) whereas there was no such association in the dACC.

Conclusion: These results suggest that higher glutamatergic neurometabolite levels in the caudate may contribute to rhythm processing, especially the ability to produce meter in music precisely.

KEYWORDS

magnetic resonance spectroscopy, rhythm, glutamate, caudate, rhythm production

1. Introduction

Music contains rhythm, which configures patterns of time intervals. Previous studies noted that dopamine plays an important role in auditory rhythm processing (Grahn, 2009; Koshimori et al., 2019). According to a neuropharmacological study, the glutamatergic system may be involved in time perception by interacting with the dopaminergic system (Cheng et al., 2007). For example, an animal study reported that inhibiting glutamatergic function enhanced dopaminergic function, resulting in altered time perception (Cheng et al., 2007). These findings suggest that glutamatergic function may be related to music rhythm processing.

However, few animal studies reported the relationship between music and glutamatergic function. One study showed that exposing musical stimuli induced the expression of the glutamatergic AMPA receptor in mice (Xu et al., 2007). In addition, listening to music during childhood induced the expression of the glutamatergic NMDA receptor subunit NR2B protein in the auditory cortex, which enhanced the development of auditory functions (Xu et al., 2009). Another study reported that glutamatergic neurometabolite concentrations in the striatum were decreased with sad music called "Shange," which is one of the Chinese traditional

music therapy, and joyful and powerful music called "Zhi" and "Gong" increased its concentrations (Hao et al., 2020). However, these previous studies have the following limitations: (1) they were performed for only rodent models, and (2) they used musical stimuli which include changes not only in rhythm but also in melody, harmony, and timbre to assess the relationship between music and glutamatergic function. Therefore, the relationship between musical rhythm processing and glutamatergic neuro-systems remains unclear.

The striatum has been shown to be closely linked to the perception and production of musical rhythms (Grahn, 2009; Grahn and Rowe, 2013). Previous reports have demonstrated that the striato-thalamo-cortical network is particularly activated when processing beat-based rhythms in music (Grahn, 2009; Grahn and Brett, 2009; Teki et al., 2011a,b). Grahn and Rowe et al. have established that activity in the basal ganglia increases during the processing of musical rhythms (Grahn and Brett, 2009), and patients with Parkinson's disease who have dopamine dysfunction exhibit impairments in their rhythm perception (Grahn and Rowe, 2009). Additionally, the striatum has been identified as a central region where the dopamine and excitatory-inhibitory systems (glutamate – gamma-aminobutyric acid functions) interact (Agnoli et al., 2013).

Based on these findings, we hypothesized that glutamate levels in the striatum may be related to musical rhythm perception and production. Hence, the present study sought to investigate whether glutamatergic neurometabolite levels in the striatum relate to the rhythm processing ability in humans.

In this study, we quantified the concentrations of glutamatergic neurometabolites in the caudate as a region of interest employing proton magnetic resonance spectroscopy (^{1}H-MRS). As a control region, the dorsal anterior cingulate cortex (dACC) was selected from our previous study in an exploratory fashion (Tarumi et al., 2020). Tarumi et al. (2020) compared Glx levels in the caudate and dACC among patients with treatment-resistant schizophrenia, patients with treatment-responsive schizophrenia, and healthy controls. For the present study, we analyzed the data acquired from the same healthy subjects as in Tarumi et al. (2020). Given that the ACC plays an important role in global executive function, we hypothesized that we could not discern music-specific functions from this region. Thus, we set the dACC as a positive control ROI.

2. Methods

2.1. Participants

The study was approved by the ethics committees at Komagino Hospital, Keio University School of Medicine, and Keio University Shonan Fujisawa Campus. All methods were carried out in accordance with the relevant guidelines and regulations expressed in the Declaration of Helsinki. All participants provided written informed consent prior to enrollment. Thirty-three healthy individuals participated in this study via a private committee for recruitment (Table 1). All participants were screened by qualified psychiatrists (R.T., Y. N, and S.N.) based on the Diagnostic and Statistical Manual of Mental Disorders, Fifth Edition (DSM-5). The exclusion criteria of participants were a history of psychiatric disorders, neurological, or significant medical disorders. All experiments were performed at Komagino Hospital. All MRI images were shared with Tarumi et al. (2020).

TABLE 1 Demographic information.

Measures (mean ± SD)		
Number of participants		33
Number of participants for analyses	Caudate	22
	dACC	27
Age, years		43.233±11.849
Number of females		13
Duration of music training, years		5.032±7.468
Averages of H-BAT measures		
Beat Interval Test (BIT), $\log_2$ms	Perception	−1.568±1.501
	Production	−2.784±1.218
Beat Finding and Interval Test (BFIT), $\log_2$ms	Perception	−1.232±1.377
	Production	−2.029±1.903
Beat Saliency Test (BST), $\log_2$dB	Perception	0.823±1.128
	Production	1.615±1.488

The number of participants, Mean and standard deviation (SD) of age, number of females, and duration of musical training in years are shown.

2.2. Magnetic resonance imaging

All images were acquired by a 3T GE Signa HDxt scanner with an eight-channel head coil. We assessed a three-dimensional inversion recovery prepared T1-weighted magnetic resonance imaging (MRI) scan (Axial MRI 3D brain volume (BRAVO), echo time (TE) = 2.8, repetition time (TR) = 6.4, inversion time (TI) = 650 ms, flip angle = 8°, field of view (FOV) = 230 mm, 256 × 256 matrix, slice thickness = 0.9 mm). MR scanning as described in Tarumi et al. (2020).

2.3. Acquisition of glutamatergic levels and data processing

We acquired glutamatergic neurometabolite levels using ^{1}H-MRS. The scanning parameters were as follows: PRESS, TE = 35 ms, TR = 2000 ms, spectral width = 5000 Hz, 4096 data points, 128 water-suppressed, 16 water-unsuppressed averages, and 8 numbers of excitation. The locations of the ^{1}H-MRS voxels, and representative spectra are provided in Figures 1, 2. The voxels were placed on the right caudate (voxel size = 7.5 mL) and bilateral dACC (voxel size = 9.0 mL), based on the aims of another project (Tarumi et al., 2020). In this study, we used Glx levels, a combination of glutamate and glutamine. It is because the molecular structures and molecular weights of Glu and Gln are similar, and the spectrum peaks overlap, making it difficult to discriminate between them using 3T MRI. We employed the FID-Appliance for pre-processing of spectra, primarily for estimation and correction of frequency and phase drifts[1] (Simpson et al., 2017). Subsequently, we estimated neurometabolite levels utilizing a basis set, and extracted values that were normalized to the unsuppressed water signal from LCModel outputs with institutional units. The authors visually inspected all spectra exported from LCModel. Furthermore,

1 https://github.com/CIC-methods/FID-A

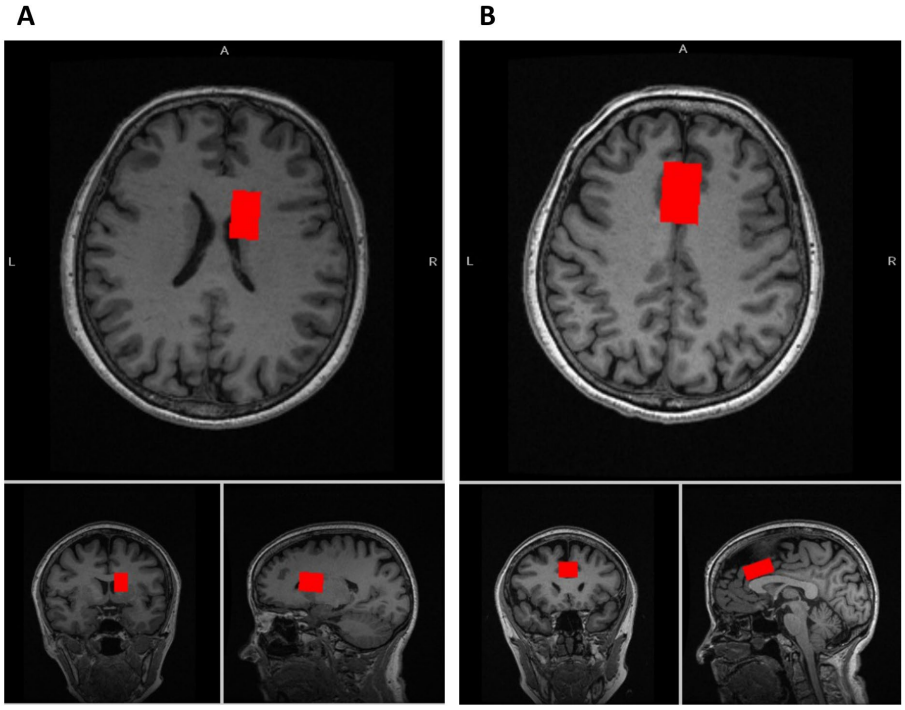

FIGURE 1
Voxel locations of MRS. **(A)** The voxel location of the caudate (voxel size: 7.5 mL [2.5 × 1.5 × 2.0 cm^3]). **(B)** The voxel location of the dorsal anterior cingulate cortex (dACC) (voxel size: 9.0 mL [3.0 × 2.0 × 1.5 cm^3]).

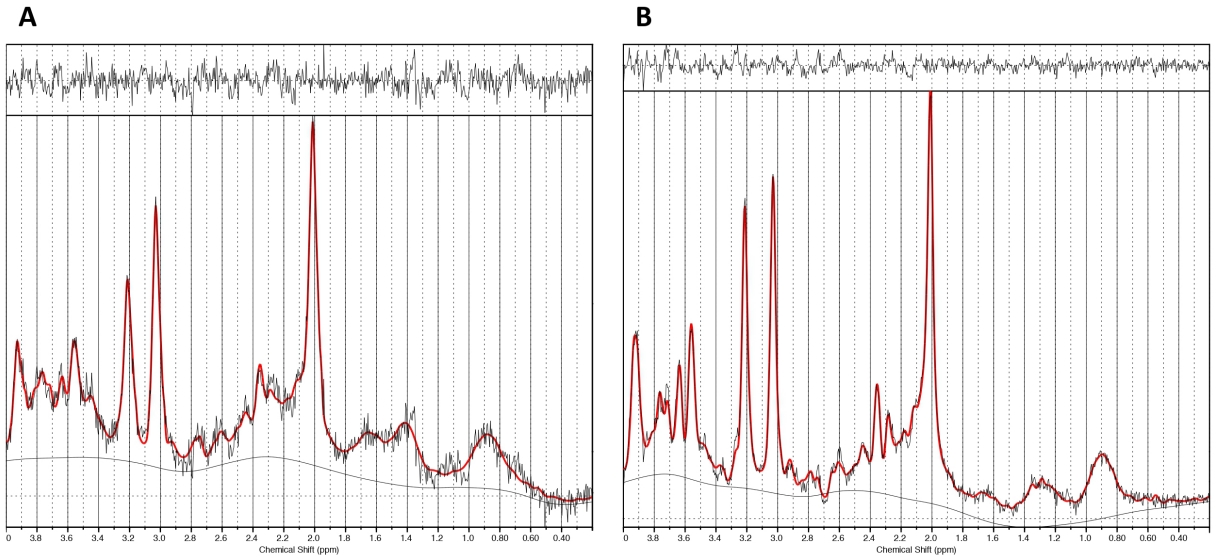

FIGURE 2
Representative spectra. **(A)** The caudate ^{1}H-MRS spectra. **(B)** The dACC ^{1}H-MRS spectra.

we established criteria for spectra quality and excluded spectra that failed to meet the following criteria: signal-to-noise ratios (SNR) ≤10, full-width at half maximum (FWHM) ≥10 Hz, or %SD values ≥20%. To correct for voxel tissue composition, we segmented the T1-weighted image into gray matter (GM), white matter (WM), and cerebrospinal fluid (CSF) using FSL (FMRIB Software Library v5.0, Oxford, UK). Subsequently, we generated individual masks that contained information about voxel size and location on the segmented T1-weighted images using GANNET.[2] To acquire the observed metabolite concentrations with respect to a relatively and fully relaxed

2 http://www.gabamrs.com

water peak from tissue [M], we took into account the effects of volume fractions, water relaxation times (T1, T2), and water concentrations for the three compartments (WM, GM, and CSF). We performed calculations that considered LCModel operations as follows:

$$[M] = [M]WS^{*}[(fCSF^{*}55556^{*}RCSF) + (fGM^{*}43300^{*}RGM) + (fWM^{*}35880^{*}RWM)] / (FLC^{*}(1 - fCSF))$$

Where [M] WS is water-scaled data from LCModel. And FLC is an LCModel factor that is used to undo the assumptions used by LCModel [i.e., FLC = WCONC*ATT20; WCONC = 35880 and ATT20 = 0.7 = exp(−30/80)].

$$RT = \left(1 - \exp\left(-TR./T1T\right) * \exp\left(-TE./T2T\right)\right)$$

where, fT and RT are the volume fraction and water relaxation parameters of tissue T (T = GM, WM, and CSF of the voxel), respectively. Relaxation times and relative water tissue content values are outlined in Supplementary Table 1. And, spectrum qualities and tissue heterogeneity values are shown in Supplementary Table 2.

2.4. Assessments for rhythm perception and production abilities

Rhythm perception and production abilities were assessed with the Harvard Beat Assessment Test (H-BAT) (16). The H-BAT consists of three subtests. (1) Beat Interval Test (BIT) in which the participants were discriminated if the tempo of a metronome was getting faster or slower (BIT perception), then tap in synchrony with the tempo-changing metronome without discrimination of temporal changes (BIT production). (2) Beat Finding and Interval Test (BFIT) in which the participants discriminated if the tempo of a rhythm pattern was getting faster or slower (BFIT perception), then tap the quarter-note beat with the tempo-changing rhythm pattern without discrimination of temporal changes (BFIT production). (3) Beat Saliency Test (BST) in which the participants discriminated if a sequence of accented quarter-notes was a duple or triple meter (BST perception), then produce the meter by changing the tap amplitudes without discrimination which meter they heard (BST production). In brief, BIT and BFIT assess the sensitivity to temporal change in non-isochronous tone sequences while BST assesses the sensitivity to amplitude change in isochronous tone sequences (Fujii and Schlaug, 2013). Each of the perception subtests assess the sensory process while that of production subtests assess the sensorimotor process.

The performance of BIT, BFIT, and BST in the H-BAT was quantified with perception and production thresholds. The lower the thresholds, the more precisely the participant perceives and produces the rhythms. The thresholds were normalized by log transformation with the base of two based on the previous study (Fujii and Schlaug, 2013; Paquette et al., 2017). For more details about the tests and analyses on the H-BAT, see the previous studies (Fujii and Schlaug, 2013; Paquette et al., 2017).

2.5. Statistical analysis

Statistical analyses were carried out using IBM SPSS Statistics version 26 (IBM Corporation, Armonk, NY). To account for the effect of music training, we calculated the standard division (SD) of the duration of music training for all participants. If the duration of music training exceeded ±2SD, the participant was excluded as an outlier from subsequent analyses. First, we performed partial correlation analyses by Pearson's method to examine the relationship between the H-BAT measures and glutamatergic levels in dACC and caudate using age and sex as covariates. Second, partial correlation analyses were performed to examine the effect of the duration of music training. All results of partial correlation analyses are also adjusted by the Bonferroni method. The significance level was $p < 0.004$ ($p < 0.05/n$ where n equals the number of ROIs and tests).

3. Results

Demographic information is shown in Table 1. Sixteen individuals have musical training imparted by professionals, excluding education in mandatory school. The breakdown of instruments is as follows: piano, 12; organ, 1; flute, 1; saxophone, 1; erhu, 1. A total of 22 and 27 participants' data were used for the analyses of the caudate and dACC, respectively. At the time of acquisition, we excluded 2 HCs who did not complete scans and 2 HCs with incidental brain anomalies. Further, the data of 2 participants were missing because of a technical issue with the H-BAT application. Regarding statistical analyses, 4 participants' data on the caudate were excluded due to low SNR values, and 1 participant was rejected through the preprocessing for the spectrum. If the duration of music training exceeded ±2SD, the participant was excluded as an outlier from subsequent analyses (see Supplementary Figure 1).

Partial correlation analyses using age and sex as covariates showed significant correlations between H-BAT subscores and Glx levels in the caudate or the dACC. Table 2 shows the correlation between the H-BAT measures and Glx levels in the caudate and dACC using age, sex, and the duration of musical training. There was a significant correlation between the BST production threshold and Glx levels in the caudate (Figure 3), while no association was found in the other H-BAT measures. We conducted the correlation analyses including the outlier data as a sensitivity analysis. We still had a significant correlation between BST perception and Glx levels in the caudate. On the other hand, in the ACC, no significant relationship was found between Glx levels and any of the H-BAT measures.

4. Discussion

This is the first ^{1}H-MRS study to examine the relationship between rhythm perception and production abilities measured with the H-BAT and glutamatergic levels in the caudate of healthy individuals. We found a negative relationship between BST production thresholds and Glx levels in the caudate in healthy individuals. On the other hand, no association was detected between the other H-BAT measures and Glx levels in the caudate, or between any H-BAT measures and Glx levels in the dACC (a control region). These results suggest that higher Glx levels in the caudate may specifically reflect the ability to produce a more precise isochronous meter.

TABLE 2 Results of correlation between H-BAT scores and Glx levels in the caudate and the dACC.

			Caudate	dACC
Beat Interval Test	Perception	Coefficient	−0.285	−0.003
		p value	0.268	0.989
	Production	Coefficient	−0.533	0.238
		p value	0.028	0.299
Beat Finding and Interval Test	Perception	Coefficient	−0.556	0.121
		p value	0.020	0.602
	Production	Coefficient	0.231	0.465
		p value	0.373	0.034
Beat Saliency Test	Perception	Coefficient	0.157	0.055
		p value	0.548	0.814
	Production	Coefficient	−0.693	0.301
		p value	0.002*	0.184

* significant correlations (Bonferroni corrected, $p < 0.004$).

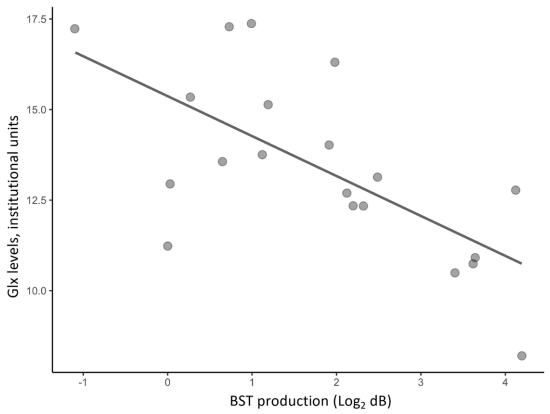

FIGURE 3
A scatter plot of a correlation between Glx levels in the caudate and BST production scores.

What is the role of glutamatergic function in time processing? The dopaminergic function in the striatum has been shown to play an important role in time processing while the glutamatergic function in time processing remains unclear. Cheng et al. (2007) performed a pharmacological study in rats using cocaine, a dopamine transporter blocker, and ketamine, a glutamate receptor antagonist. They showed that cocaine disrupted time perception and ketamine augmented the time disruption modulated by cocaine. This animal study suggests that the dopamine and glutamate pathways may interact with each other to process time (Cheng et al., 2007). In humans, it was noted that time perception was distorted in patients with schizophrenia where the dopamine and glutamate systems are impaired (Carroll et al., 2008). The dopamine dysfunction in the dorsal striatum, one of the pathological hypotheses for schizophrenia, may be caused by glutamatergic dysfunction in patients with schizophrenia (Flagstad et al., 2004; Wada et al., 2022). This study adds evidence to support the relationship between striatal glutamate levels and rhythm processing mechanisms in humans *in vivo*.

Why was the correlation found only in BST production but not in the other H-BAT measures? This correlation may be attributed to the specific characteristics of BST stimuli. Unlike BIT and BFIT, which use non-isochronous time intervals in their stimuli, BST uses isochronous time intervals. Specifically, the sound stimulus in BST consisted of a tone sequence of 500-msec isochronous time intervals with accented and unaccented tones (Fujii and Schlaug, 2013). To perform BST, participants had to encode the relative-intensity difference between the accented and unaccented tones precisely overtime to process the duple or triple meter precisely. Namely, it is crucial to encode the meter or an organization of sound intensity over time in isochronous intervals in BST. On the other hand, BIT and BFIT use non-isochronous time intervals without any accents. Both BIT and BFIT include gradual changes in time intervals to create a faster or slower tempo (Fujii and Schlaug, 2013). In BIT and BFIT, each interval in the stimuli is different, and therefore, encoding of the absolute duration of time intervals is considered to be important. A previous study noted that there was a difference in neural circuits in the brain when we process absolute and relative time intervals (Grube et al., 2010a,b; Teki et al., 2011a,b). The absolute, duration-based time intervals are considered to be processed in the olivocerebellar network, while the relative, beat-based time intervals are considered to be processed in the striato-thalamo-cortical network (Teki et al., 2011a,b). Considering the results of this study and these separated mechanisms of rhythm processing in the brain, we assume that BIT and BFIT may assess relatively olivocerebellar-based rhythm ability, while BST may assess striato-thalamo-cortical-based rhythm ability. In fact, our previous study showed that the gray-matter volume in the cerebellum was correlated with the BIT and BFIT scores but not with the BST score in the H-BAT in healthy individuals (Paquette et al., 2017). Therefore, these findings suggest that glutamatergic neurometabolite levels in the striatum may contribute to the processing of meter or temporal organization in isochronous time intervals.

Why does this effect appear in the production test but not in the perception test? This discrepancy may be attributed to the role of the striatum in motor output and auditory-motor interaction. Mounting evidence suggests that the cortico-striatal network has an important role in encoding and retrieving motor information; and also see a review by Miyachi et al. (1997), Matsumoto (1999), and Kotz et al. (2009). To perform BST production, participants are required to encode the pattern of accented and unaccented tones precisely as well as produce the meter as motor output by modulating their tapping amplitudes. Conversely, the perception test does not require the same level of motor output, such as the physical articulation of rhythm sequences. Hence, our results suggest that Glx levels in the caudate contribute to the encoding of auditory meter information, the auditory-motor transformation of the meter, and the significant role of motor output. On the other hand, in light of the statistical power of this study, we may not rule out the potential of other rhythm components which relate to glutamatergic function in the caudate. We need to consider differences in the relationship between various types of rhythm components and glutamatergic function in future studies.

We did not find any significant relationship between the H-BAT measures and glutamatergic neurometabolite levels in the dACC. Previous studies reported that both regions play important roles in cognitive monitoring, motor control, and association of perception-production (Bush et al., 2002; Maes et al., 2014; Brockett et al., 2020) and there are structural and functional connectivities between the dACC and striatum (Beckmann et al., 2009). However, our findings suggest

that Glx levels in the striatum are more directly related to rhythm or meter processing compared to those in the dACC. Further research is needed to examine the interaction between glutamatergic functions in the dACC and caudate and its relationship to rhythm processing.

There are several limitations to this study. Firstly, our acquisition was solely based on a resting-state quantitative ^{1}H MRS, averaged over time rather than functional MRS employing beat processing tasks Secondly, our research did not measure the voxel in another basal ganglia region. Previous reports have suggested distinct roles of the putamen and caudate in rhythm processing (Coull et al., 2011; Grahn and Rowe, 2013). Consequently, our study was unable to determine whether glutamate levels in each striatal subregion are different or the same in their relation to rhythm processing. Thirdly, we were unable to discern the precise origin of the glutamatergic signal, i.e., whether it was inside or outside the cells. The limitation of MRS only allowed for identifying an averaged glutamatergic signal from all receptors within the placed voxel, given the absence of pharmacological tracers.

5. Conclusion

In conclusion, we found that glutamatergic neurometabolite levels in the caudate were associated with the ability to produce rhythm or meter in healthy individuals. This result suggests that the neurometabilite levels measured with ^{1}H-MRS contribute to further understanding of musical rhythm processing. We propose that a multimodal measurement approach would be efficacious in furthering our understanding of the neurometabolite mechanisms underlying musical rhythm processing in humans.

Data availability statement

The raw data supporting the conclusions of this article will be made available by the authors, without undue reservation.

Ethics statement

The studies involving human participants were reviewed and approved by the Ethics Committees at Komagino Hospital, Keio University School of Medicine, and Keio University Shonan Fujisawa Campus. The patients/participants provided their written informed consent to participate in this study.

Author contributions

SH recruited healthy participants, collected the data, analyzed the dataset, and wrote the manuscript. YN, SF, and SN contributed to the study design, wrote the manuscript, and supervised this study. KM and NN collected the data and contributed to writing the manuscript. RT recruited patients and collected the data. ST analyzed the dataset and contributed to writing the manuscript. YT, NH, and KS contributed to writing the manuscript. MM supervised this study. All authors contributed to the article and approved the submitted version.

Funding

SH had received a Taikichiro Mori Memorial Research Grants, and Research Encouragement Scholarship for Graduate Students of Keio University, the Graduate School of Media and Governance Research Fund, and Keio SFC academic society grants. SH has received the JSPS Research Fellowship for Young Scientists (DC1), The Keio University Doctorate Student Grant-in-Aid Program from Ushioda Memorial Fund. YN has received a Grant-in-Aid for Scientific Research (B) (21H02813) from the Japan Society for the Promotion of Science (JSPS), research grants from Japan Agency for Medical Research and Development (AMED), investigator-initiated clinical study grants from Teijin Pharma Ltd. and Inter Reha Co., Ltd. He has also received research grants from Japan Health Foundation, Meiji Yasuda Mental Health Foundation, Mitsui Life Social Welfare Foundation, Takeda Science Foundation, SENSHIN Medical Research Foundation, Health Science Center Foundation, Mochida Memorial Foundation for Medical and Pharmaceutical Research, Taiju Life Social Welfare Foundation, and Daiichi Sankyo Scholarship Donation Program. He has received speaker's honoraria from Dainippon Sumitomo Pharma, Mochida Pharmaceutical Co., Ltd., Yoshitomiyakuhin Corporation, Qol Co., Ltd., Teijin Pharma Ltd., Takeda Pharmaceutical Co., Ltd., and Lundbeck Japan Co. Ltd. within the past 5 years outside the submitted work. He also receives equipment-in-kind support for an investigator-initiated study from Magventure Inc., Inter Reha Co., Ltd., Brainbox Ltd., and Miyuki Giken Co., Ltd. SN has received grants from Japan Society for the Promotion of Science (18H02755, 22H03002), Japan Agency for Medical Research and development (AMED), Japan Research Foundation for Clinical Pharmacology, Naito Foundation, Takeda Science Foundation, Watanabe Foundation, Uehara Memorial Foundation, and Daiichi Sankyo Scholarship Donation Program within the past 3 years. He has also received research support, manuscript fees or speaker's honoraria from Dainippon Sumitomo Pharma, Meiji-Seika Pharma, Otsuka Pharmaceutical, Shionogi, and Yoshitomi Yakuhin within the past 3 years. MM has received speaker's honoraria from Byer Pharmaceutical, Daiichi Sankyo, Dainippon-Sumitomo Pharma, Eisai, Eli Lilly, Fuji Film RI Pharma, Hisamitsu Pharmaceutical, Janssen Pharmaceutical, Kyowa Pharmaceutical, Mochida Pharmaceutical, MSD, Mylan EPD, Nihon Medi-physics, Nippon Chemipher, Novartis Pharma, Ono Yakuhin, Otsuka Pharmaceutical, Pfizer, Santen Pharmaceutical, Shire Japan, Takeda Yakuhin, Tsumura, and Yoshitomi Yakuhin within the past 3 years. Also, he received grants from Daiichi Sankyo, Eisai, Pfizer, Shionogi, Takeda, Tanabe Mitsubishi, and Tsumura within the past 3 years outside the submitted work. SF has received Grants-in-Aid from JSPS (20H04092 and 21K19734), JST COI-NEXT grant (JPMJPF2203), and research grants from Keio University Academic Development Funds.

Acknowledgments

The authors thank participants for their cooperation in this research.

Conflict of interest

The authors declare that the research was conducted in the absence of any commercial or financial relationships that could be construed as a potential conflict of interest.

Publisher's note

All claims expressed in this article are solely those of the authors and do not necessarily represent those of their affiliated organizations, or those of the publisher, the editors and the reviewers. Any product that may be evaluated in this article, or claim that may be made by its manufacturer, is not guaranteed or endorsed by the publisher.

Supplementary material

The Supplementary material for this article can be found online at: https://www.frontiersin.org/articles/10.3389/fnins.2023.1196805/full#supplementary-material

References

Agnoli, L., Mainolfi, P., Invernizzi, R. W., and Carli, M. (2013). Dopamine D1-like and D2-like receptors in the dorsal striatum control different aspects of attentional performance in the five-choice serial reaction time task under a condition of increased activity of corticostriatal inputs. *Neuropsychopharmacology* 38, 701–714. doi: 10.1038/npp.2012.236

Beckmann, M., Johansen-Berg, H., and Rushworth, M. F. S. (2009). Connectivity-based parcellation of human cingulate cortex and its relation to functional specialization. *J. Neurosci.* 29, 1175–1190. doi: 10.1523/JNEUROSCI.3328-08.2009

Brockett, A. T., Tennyson, S. S., de Bettencourt, C. A., Gaye, F., and Roesch, M. R. (2020). Anterior cingulate cortex is necessary for adaptation of action plans. *Proc. Natl. Acad. Sci.* 117, 6196–6204. doi: 10.1073/pnas.1919303117

Bush, G., Vogt, B. A., Holmes, J., Dale, A. M., Greve, D., Jenike, M. A., et al. (2002). Dorsal anterior cingulate cortex: a role in reward-based decision making. *Proc. Natl. Acad. Sci. U. S. A.* 99, 523–528. doi: 10.1073/pnas.012470999

Carroll, C. A., Boggs, J., O'Donnell, B. F., Shekhar, A., and Hetrick, W. P. (2008). Temporal processing dysfunction in schizophrenia. *Brain Cogn.* 67, 150–161. doi: 10.1016/j.bandc.2007.12.005

Cheng, R.-K., Ali, Y. M., and Meck, W. H. (2007). Ketamine "unlocks" the reduced clock-speed effects of cocaine following extended training: evidence for dopamine–glutamate interactions in timing and time perception. *Neurobiol. Learn. Mem.* 88, 149–159. doi: 10.1016/j.nlm.2007.04.005

Coull, J. T., Cheng, R.-K., and Meck, W. H. (2011). Neuroanatomical and neurochemical substrates of timing. *Neuropsychopharmacology* 36, 3–25. doi: 10.1038/npp.2010.113

Flagstad, P., Mørk, A., Glenthøj, B. Y., van Beek, J., Michael-Titus, A. T., and Didriksen, M. (2004). Disruption of neurogenesis on gestational day 17 in the rat causes behavioral changes relevant to positive and negative schizophrenia symptoms and alters amphetamine-induced dopamine release in nucleus accumbens. *Neuropsychopharmacology* 29, 2052–2064. doi: 10.1038/sj.npp.1300516

Fujii, S., and Schlaug, G. (2013). The Harvard beat assessment test (H-BAT): a battery for assessing beat perception and production and their dissociation. *Front. Hum. Neurosci.* 7:771. doi: 10.3389/fnhum.2013.00771

Grahn, J. A. (2009). The role of the basal ganglia in beat perception: neuroimaging and neuropsychological investigations. *Ann. N. Y. Acad. Sci.* 1169, 35–45. doi: 10.1111/j.1749-6632.2009.04553.x

Grahn, J. A., and Brett, M. (2009). Impairment of beat-based rhythm discrimination in Parkinson's disease. *Cortex* 45, 54–61. doi: 10.1016/j.cortex.2008.01.005

Grahn, J. A., and Rowe, J. B. (2009). Feeling the beat: premotor and striatal interactions in musicians and nonmusicians during beat perception. *J. Neurosci.* 29, 7540–7548. doi: 10.1523/JNEUROSCI.2018-08.2009

Grahn, J. A., and Rowe, J. B. (2013). Finding and feeling the musical beat: striatal dissociations between detection and prediction of regularity. *Cereb. Cortex* 23, 913–921. doi: 10.1093/cercor/bhs083

Grube, M., Cooper, F. E., Chinnery, P. F., and Griffiths, T. D. (2010a). Dissociation of duration-based and beat-based auditory timing in cerebellar degeneration. *Proc. Natl. Acad. Sci. U. S. A.* 107, 11597–11601. doi: 10.1073/pnas.0910473107

Grube, M., Lee, K.-H., Griffiths, T. D., Barker, A. T., and Woodruff, P. W. (2010b). Transcranial magnetic theta-burst stimulation of the human cerebellum distinguishes absolute, duration-based from relative, beat-based perception of subsecond time intervals. *Front. Psychol.* 1:171. doi: 10.3389/fpsyg.2010.00171

Hao, J., Jiang, K., Wu, M., Yu, J., and Zhang, X. (2020). The effects of music therapy on amino acid neurotransmitters: insights from an animal study. *Physiol. Behav.* 224:113024. doi: 10.1016/j.physbeh.2020.113024

Koshimori, Y., Strafella, A. P., Valli, M., Sharma, V., Cho, S.-S., Houle, S., et al. (2019). Motor synchronization to rhythmic auditory stimulation (RAS) attenuates dopaminergic responses in ventral striatum in young healthy adults: [11C]-(+)-PHNO PET study. *Front. Neurosci.* 13:106. doi: 10.3389/fnins.2019.00106

Kotz, S. A., Schwartze, M., and Schmidt-Kassow, M. (2009). Non-motor basal ganglia functions: a review and proposal for a model of sensory predictability in auditory language perception. *Cortex* 45, 982–990. doi: 10.1016/j.cortex.2009.02.010

Maes, P.-J., Leman, M., Palmer, C., and Wanderley, M. M. (2014). Action-based effects on music perception. *Front. Psychol.* 4:1008. doi: 10.3389/fpsyg.2013.01008

Matsumoto, D. (1999). American-Japanese cultural differences in judgements of expression intensity and subjective experience. *Cognit. Emot.* 13, 201–218. doi: 10.1080/026999399379339

Miyachi, S., Hikosaka, O., Miyashita, K., Kárádi, Z., and Rand, M. K. (1997). Differential roles of monkey striatum in learning of sequential hand movement. *Exp. Brain Res.* 115, 1–5. doi: 10.1007/PL00005669

Paquette, S., Fujii, S., Li, H. C., and Schlaug, G. (2017). The cerebellum's contribution to beat interval discrimination. *Neuroimage* 163, 177–182. doi: 10.1016/j.neuroimage.2017.09.017

Simpson, R., Devenyi, G. A., Jezzard, P., Hennessy, T. J., and Near, J. (2017). Advanced processing and simulation of MRS data using the FID appliance (FID-A)-an open source, MATLAB-based toolkit. *Magn. Reson. Med.* 77, 23–33. doi: 10.1002/mrm.26091

Tarumi, R., Tsugawa, S., Noda, Y., Plitman, E., Honda, S., Matsushita, K., et al. (2020). Levels of glutamatergic neurometabolites in patients with severe treatment-resistant schizophrenia: a proton magnetic resonance spectroscopy study. *Neuropsychopharmacology* 45, 632–640. doi: 10.1038/s41386-019-0589-z

Teki, S., Grube, M., and Griffiths, T. D. (2011a). A unified model of time perception accounts for duration-based and beat-based timing mechanisms. *Front. Integr. Neurosci.* 5:90. doi: 10.3389/fnint.2011.00090

Teki, S., Grube, M., Kumar, S., and Griffiths, T. D. (2011b). Distinct neural substrates of duration-based and beat-based auditory timing. *J. Neurosci.* 31, 3805–3812. doi: 10.1523/JNEUROSCI.5561-10.2011

Wada, M., Noda, Y., Iwata, Y., Tsugawa, S., Yoshida, K., Tani, H., et al. (2022). Dopaminergic dysfunction and excitatory/inhibitory imbalance in treatment-resistant schizophrenia and novel neuromodulatory treatment. *Mol. Psychiatry* 27, 2950–2967. doi: 10.1038/s41380-022-01572-0

Xu, F., Cai, R., Xu, J., Zhang, J., and Sun, X. (2007). Early music exposure modifies GluR2 protein expression in rat auditory cortex and anterior cingulate cortex. *Neurosci. Lett.* 420, 179–183. doi: 10.1016/j.neulet.2007.05.005

Xu, J., Yu, L., Cai, R., Zhang, J., and Sun, X. (2009). Early auditory enrichment with music enhances auditory discrimination learning and alters NR2B protein expression in rat auditory cortex. *Behav. Brain Res.* 196, 49–54. doi: 10.1016/j.bbr.2008.07.018

frontiers | Frontiers in Neuroscience

TYPE Brief Research Report
PUBLISHED 04 October 2023
DOI 10.3389/fnins.2023.1255209

OPEN ACCESS

EDITED BY
Laura Marzetti,
University of Studies G. d'Annunzio Chieti and Pescara, Italy

REVIEWED BY
Vittorio Pizzella,
University of Studies G. d'Annunzio Chieti and Pescara, Italy
Jyrki Mäkelä,
Hospital District of Helsinki and Uusimaa, Finland

*CORRESPONDENCE
Giulia Kern
giulia.kern@charite.de

RECEIVED 08 July 2023
ACCEPTED 18 September 2023
PUBLISHED 04 October 2023

CITATION
Kern G, Kempter M, Picht T and Engelhardt M (2023) Mapping of the supplementary motor area using repetitive navigated transcranial magnetic stimulation. *Front. Neurosci.* 17:1255209. doi: 10.3389/fnins.2023.1255209

Mapping of the supplementary motor area using repetitive navigated transcranial magnetic stimulation

Giulia Kern[1]*, Miriam Kempter[1], Thomas Picht[1,2,3] and Melina Engelhardt[1,2,4]

[1]Department of Neurosurgery, Charité - Universitätsmedizin, Corporate Member of Freie Universität Berlin and Humboldt-Universität zu Berlin, Berlin, Germany, [2]Einstein Center for Neurosciences, Charité – Universitätsmedizin, Corporate Member of Freie Universität Berlin and Humboldt-Universität zu Berlin, Berlin, Germany, [3]Cluster of Excellence Matters of Activity, Image Space Material, Humboldt-Universität zu Berlin, Berlin, Germany, [4]International Graduate Program Medical Neurosciences, Charité – Universitätsmedizin, Corporate Member of Freie Universität Berlin and Humboldt-Universität zu Berlin, Berlin, Germany

Background: The supplementary motor area (SMA) is important for motor and language function. Damage to the SMA may harm these functions, yet tools for a preoperative assessment of the area are still sparse.

Objective: The aim of this study was to validate a mapping protocol using repetitive navigated transcranial magnetic stimulation (rnTMS) and extend this protocol for both hemispheres and lower extremities.

Methods: To this purpose, the SMA of both hemispheres were mapped based on a finger tapping task for 30 healthy subjects (35.97 ± 15.11, range 21–67 years; 14 females) using rnTMS at 20 Hz (120% resting motor threshold (RMT)) while controlling for primary motor cortex activation. Points with induced errors were marked on the corresponding MRI. Next, on the identified SMA hotspot a bimanual finger tapping task and the Nine-Hole Peg Test (NHPT) were performed. Further, the lower extremity was mapped at 20 Hz (140%RMT) using a toe tapping task.

Results: Mean finger tapping scores decreased significantly during stimulation (25.70taps) compared to baseline (30.48; $p < 0.01$). Bimanual finger tapping led to a significant increase in taps during stimulation (28.43taps) compared to unimanual tapping ($p < 0.01$). Compared to baseline, completion time for the NHPT increased significantly during stimulation (baseline: 13.6 s, stimulation: 16.4 s; $p < 0.01$). No differences between hemispheres were observed.

Conclusion: The current study validated and extended a rnTMS based protocol for the mapping of the SMA regarding motor function of upper and lower extremity. This protocol could be beneficial to better understand functional SMA organisation and improve preoperative planning in patients with SMA lesions.

KEYWORDS

supplementary motor area, TMS, brain mapping, motor function, preoperative diagnostic

1. Introduction

The involvement of the supplementary motor area (SMA) in motor and language function has made this cortical area an interest of current research. Damage to this region due to lesion growth or surgical procedures can lead to a characteristic combination of symptoms called the SMA syndrome. This involves various degrees of contralateral akinesia and mutism (Laplane et al., 1977; Zentner et al., 1996; Nachev et al., 2008; Pinson et al., 2022). Depending on the location of the lesion, a characteristic pattern of facial, upper limb or lower limb motor impairment is more likely to occur. This anterior to posterior shift in the type of deficit suggests a somatotopic organisation of the SMA, thus highlighting the necessity for a holistic functional assessment. In addition, language deficits seem to only evolve specifically when the anterior part of the left hemispheric SMA is affected (Bannur and Rajshekhar, 2000; Fontaine et al., 2002; Zeharia et al., 2012). Examinations regarding the importance of the hemispheric dominance in motor function are lacking. Although the SMA syndrome is known to occur mostly temporarily, time of recovery differs between days to months. However, in some patients even persisting long-term deficits of fine motor function have been observed (Zentner et al., 1996; Krainik et al., 2004). The mechanisms of recovery are not yet fully understood. A common hypothesis proposes an increased interhemispheric connectivity especially towards the healthy SMA as underlying process (Krainik et al., 2004; Vassal et al., 2017; Oda et al., 2018; Tuncer et al., 2022).

The SMA is located within Brodmann area 6 in the superior frontal gyrus, however it is not segregated by strict anatomical boundaries (Nachev et al., 2008). So far research concerning preoperative risk assessment and exact determination of the SMA location to improve surgical planning is very limited. While most studies have focused on fMRI to map SMA function in the cortex, these results are too spatially unspecific for a detailed preoperative planning (Kokkonen et al., 2009; Wongsripuemtet et al., 2018). Recently, navigated transcranial magnetic stimulation (nTMS) over the SMA has been found effective to induce errors in executing fine motor skills using the upper extremity (Schramm et al., 2019, 2020). Furthermore, a protocol for mapping of the SMA with a higher spatial resolution compared to fMRI using repetitive nTMS (rnTMS) has been proposed. This protocol used a finger tapping task to localise upper extremity motor function in the SMA of the dominant hemisphere in healthy subjects (Engelhardt et al., 2023).

The aim of this study was to validate and extend the suggested protocol, while focusing on the involvement of the SMA in motor function especially. Specifically, both hemispheres were measured and a protocol extension for the mapping of the lower extremity has been developed. In the long run, this could be used to acquire a better understanding of the functional organisation of the SMA and to establish a non-invasive SMA mapping protocol within the clinical setting to improve risk assessment and preoperative diagnostics.

2. Methods

2.1. Ethics

This study was approved by the Ethics Committee of the Charité Universitätsmedizin Berlin and conducted in accordance with the Declaration of Helsinki. Written informed consent was provided by each participant.

2.2. Participants

30 healthy subjects (35.97 ± 15.11, range 21–67 years; 14 females) above the age of 18 were recruited for this prospective study. They all had no history of neurological or psychological diseases and met the criteria for receiving an nTMS and MRI. This includes no history of epilepsy or seizures also within the family, migraine, tinnitus, pregnancy, metallic implants (e.g., pacemaker, cochlear implants, intrauterine devices), intake of prescription drugs within the past 14 days and permanent makeup. One additional subject (55 years, female) was excluded from the study due to a high RMT (resting motor threshold) which precluded that required stimulation intensities could be reached.

2.3. MRI

Each participant received a T1-weighted structural MRI (MPRAGE, TR = 2.530 ms, TE = 4.94 ms, TI = 1.100 ms, flip angle = 7, voxel size = 1 mm × 1 mm × 1 mm, 176 slices) measured on a Siemens 3-T Magnetom Trio MRI scanner (Siemens AG, Erlangen, Germany) as individual navigational data for the nTMS.

2.4. Neuronavigated TMS

Using the navigated brain stimulation system (NBS 5, Nexstim, Helsinki, Finland) with a biphasic figure-of-eight coil (outer diameter: 70 mm) each subject underwent a nTMS session divided into two major components. For each hemisphere, assessment of the primary motor cortex was followed by the SMA mapping always examining the contralateral limb. The starting hemisphere was alternated between participants to avoid confounding of any hemispheric differences due to effects of stimulation order.

2.5. Motor mapping

The primary motor cortex was assessed using single pulse nTMS. To examine muscle activity, surface electrodes (Neuroline 720; Ambu, Ballerup, Denmark) connected to the systems's integrated EMG were attached to the first dorsal interosseus muscle of the corresponding hand. The ground electrode was placed on the left palmar wrist. To keep the muscle output below the threshold of 10 μV all participants were instructed to relax their hand. Subsequently the M1 hotspot was determined as the location, rotation and tilt where reliably the highest muscle responses could be evoked. Afterwards the RMT was assessed using the system's integrated algorithm (Engelhardt et al., 2019). Furthermore, cortical representation of the target muscle was assessed at 105% of the RMT (Engelhardt and Picht, 2020). This area mapping was performed to delineate motor areas from consequently determined SMA areas.

2.6. SMA mapping

Starting with the upper extremity the SMA was mapped using repetitive nTMS (20 Hz, 120% RMT, 5 s bursts, ITI 5 s) with the stimulation coil positioned perpendicular to the interhemispheric cleft (Engelhardt et al., 2023). Subjects were instructed to perform a finger tapping task for 5 s by tapping the index finger as fast as possible (Hiroshima et al., 2014; Schramm et al., 2019; Engelhardt et al., 2023). The number of taps was recorded by the Apple iPad App Counter +. Firstly, a baseline tapping score was acquired as an average of two rounds without stimulation. If a considerable increase in taps occurred over time due to practice effects the baseline was renewed at a later timepoint within the same session. Secondly, the same task was conducted with stimulation for 15 to 21 stimulation points depending on the individual anatomy. The covered SMA area was estimated as posterior part of the superior frontal gyrus rostral to M1 up to the cortical crossing point of a perpendicular line through the anterior commissure (Vorobiev et al., 1998). Subjects started finger tapping with the onset of SMA stimulation. To avoid muscle fatigue, the participants rested their hand for a few minutes after a maximum of seven stimulations. After covering the suspected SMA area, stimulation of each point was repeated in the same order. Afterwards a SMA hotspot was determined as stimulation point with the largest errors and hence the least amount of finger taps on average. To this purpose the two or three stimulation points with the least taps were stimulated again to decide on the final hotspot with the lowest tapping score as an average of three rounds. Further, only points that were unlikely to activate M1 based on RMT and proximity to M1, were considered as SMA hotspot (Table 1).

For this hotspot, the participants performed a bimanual finger tapping task to investigate bimanual coordination as part of the SMA function. This included tapping with the index fingers of both hands in parallel. This task was repeated three times. Taps of the stimulated hand were recorded to quantify a facilitation of tapping performance (reduction of the reduced error) compared to unimanual tapping. Further, subjects performed a shortened version of the Nine-Hole-Peg Test (NHPT), where they only had to insert pegs into the pegboard to examine the role of the SMA in dexterity. A shortened version was chosen to ensure task completion was feasible within the maximum possible stimulation duration. The time to insert all pegs was recorded for analysis. After two rounds as baseline, stimulation was applied three times for a maximum of 20 s to cover the full task performance.

Next, the lower extremity was mapped using repetitive nTMS (20 Hz, 140% RMT, 10s bursts, ITI 10s) while the subjects performed a toe tapping task. Two rounds of baseline were followed by stimulating 5 to 10 points in the posterior part of the SMA. This region was chosen according to the proposed somatotopy of the SMA (Bannur and Rajshekhar, 2000; Fontaine et al., 2002; Zeharia et al., 2012). Again, each point was stimulated twice. For analysis visually detected movement disruptions in tapping performance were recorded.

2.7. Data analysis

All sessions were recorded on video using the nTMS system's inbuilt camera. For each SMA stimulation point of the upper extremity the induced electric field at the M1 hotspot was compared with the RMT. This was achieved by placing the Nexstim software integrated crosshair on the M1 hotspot during SMA stimulation. The system is then automatically able to show the induced electric field in V/m for both the point of stimulation and the crosshair. If the RMT value was exceeded, the SMA stimulation point was excluded from further analysis. For the remaining points, errors were classified into three categories indicating the reduction in finger taps compared to baseline. A reduction of <10% accounted for no error, 10–20% for minor error and ≥ 20% for major error. A fourth category was used to mark M1 affected stimulation points.

For the lower extremity, potential functional SMA points were stimulated again at rest while EMG activity of the abductor hallucis brevis muscle was recorded. In case of strong muscle responses, this stimulation point was excluded from analysis. Errors were categorised into two groups depending on occurrence or absence of visually detected movement effects compared to baseline by two independent observers. Again, an additional category was used to mark M1 affected stimulation points.

Subsequently error classifications were imported into the NBS software to attain coloured SMA maps on the individual MRIs.

2.8. Statistical analysis

The median number of errors and error incidence with their respective interquartile range were calculated for the separate error categories to examine task disruption during stimulation. The focus was on replicable errors only, defined as points with a similar tapping score reduction according to the defined error categories in at least 2 stimulation rounds. In contrast, stimulation points with a tapping score reduction of ≥10% in at least 2 stimulation rounds but within different error categories were defined as limited replicable errors. Furthermore, the effect of SMA stimulation during unimanual and bimanual finger tapping to baseline finger tapping

TABLE 1 SMA mapping results of the upper extremity for 30 healthy subjects with a median of 19 (IQR 18–20) unique stimulation points per hemisphere.

Category	Number of subjects with errors (% of total sample)	Number of stimulation points with errors Median (IQR)	Error incidence in % Median (IQR)
Replicable major errors	11 (37%)	2 (1–3)	10.88 (5.34–15.79)
Replicable minor errors	23 (77%)	1 (1–2)	5.88 (5.13–10.53)
Limited replicable errors	13 (43%)	1 (1–1)	5.26 (5.00–5.72)

Number of stimulation points with errors and error incidences for different subgroups depending on the different error categories: major errors (≥15%), minor errors (10–20%), replicable (same error category in two stimulation rounds), limited replicable (different error category in two stimulation rounds). Median and IQR were calculated for the corresponding subgroups. Subjects are not unique to one category.

was compared using linear mixed models. Similarly, the impact of SMA stimulation on NHPT performance was assessed. To investigate the impact of hemispheric dominance 3 ambidextrous subjects were excluded leaving a population size of n = 27. Handedness was determined using Edinburgh Handedness Inventory (Oldfield, 1971). The importance of hemispheric dominance on incidence of finger and toe tapping errors during SMA stimulation was evaluated using two-sided Wilcoxon signed-rank test. Specifically, median finger and toe tapping error incidence and interquartile range for each error category was compared between both hemispheres. The level of statistical significance was set to $p < 0.05$. All analyses were performed using R Studio (version 2022.07.2 + 576) with the packages dplyr (Wickham et al., 2023a), car (Fox and Weisberg, 2019), ggplot2 (Wickham, 2016), reshape (Wickham, 2007), tidyverse (Wickham et al., 2019), MASS (Venables and Ripley, 2002), nlme (Pinheiro et al., 2023) and svglite (Wickham et al., 2023b).

3. Results

3.1. Mapping of the upper extremity

A median of 19 (IQR 18–20) unique points was stimulated across all participants. Replicable errors during the finger tapping task could be induced in 24 out of 30 healthy subjects for at least one hemisphere. Among those, 13 exhibited replicable errors for both hemispheres. In 11 subjects, stimulation led to replicable major errors over a median of 2 (IQR 1–3) points across all hemispheres. Hence, the median error incidence for these subjects was 10.88% (IQR 5.34–15.79%). 23 subjects showed replicable minor errors with a median of 1 (1–2) replicable minor error and a median error incidence of 5.88% (5.13–10.53%) accordingly. Limited replicable errors occurred in 13 subjects over a median of 1 (1–1) stimulation points. The median error incidence for these participants was 5.26% (5.00–5.72%). These results are summarized in Table 1. Overall, there were strong interindividual differences between the occurrence of errors as well as size and distribution of error maps. Some examples of SMA error maps are presented in Figure 1.

3.2. Additional tasks

A significant reduction of finger taps occurred during stimulation (25.70 ± 4.00 taps) compared to baseline (30.48 ± 2.94 taps; $p < 0.01$). This effect was not impacted by subjects' age ($p = 0.2604$). Bimanual finger tapping increased the number of taps (28.43 ± 3.74 taps) compared to unilateral tapping during stimulation significantly ($p < 0.01$). However, the number of finger taps in the bimanual condition still remained below baseline ($p < 0.01$; Figure 2A). An example of the different finger tapping task conditions for two subjects can be found in Supplementary Videos. Completion time for the NHPT increased significantly during stimulation (16.4 ± 4.2 s) compared to baseline (13.6 ± 2.7 s; $p < 0.01$; Figure 2B) as demonstrated for one subject in Supplementary Videos. In 11 cases (14 hemispheres), the intensity for the NHPT had to be reduced in 5% steps due to system inbuilt safety restrictions forbidding longer stimulation for the necessary completion time. The intensity was 110% for 9 hemispheres and 105% for 3 hemispheres. The lowest applied stimulation intensity was 100% for 2 hemispheres. One subject specifically described a built-up of stimulation effect on the finger tapping task over time.

3.3. Mapping of the lower extremity

For the lower extremity, a median of 10 (9–10) unique stimulation points was set per hemisphere across all participants. Replicable visually detected movement errors could be induced in 28 out of 30 subjects (20 bi-hemispherically, 28 uni-hemispherically) for a median of 2 (1–3). Hence, the median error incidence for the lower extremity in these subjects was 20.00% (11.11–33.33%). The exact type of visually detected movement errors varied between subjects. Increased arrhythmicity and reduced fluency in toe tapping was common (Supplementary Videos. Subject 1). In addition, some subjects showed sudden complete arrest of tapping or proceeded with the task even after the stimulation had stopped (Supplementary Videos. Subject 2). For 3 subjects the stimulation intensity was reduced to 130% (2 left-hemispherically, 1 right-hemispherically) due to a very high RMT.

3.4. Impact of hemispheric dominance

Data of 22 right-handed and 5 left-handed participants was included in this analysis. A median of 19 unique points was stimulated for both dominant (IQR 18–20) and non-dominant (IQR 19–20) hemisphere for the upper extremity across subjects. For participants with major errors the median error incidence was 11.76% (5.56–16.67%) for the dominant and 10.12% (5.20–15.20%) for the non-dominant hemisphere accordingly ($p = 0.075$). For minor errors the median error incidence was 5.88% (5.00–10.53%) for the dominant and 5.56% (5.26–10.39%) for the non-dominant hemisphere ($p = 0.672$). Subjects with limited replicable errors showed a median error incidence of 5.26% (5.00–5.88%) for the dominant and 5.00% (5.00–5.26%) for the non-dominant hemisphere ($p = 0.154$). For the lower extremity a median of 10 unique points (9–10) was stimulated across participants for the dominant hemisphere. The non-dominant hemisphere received the same amount of unique stimulation points. A median error incidence of 20.00% (20.00–33.33%) was evaluated for the dominant hemisphere across subjects with visually detected movement errors. For the non-dominant hemisphere, it was 18.33% (10.28–30.00%) respectively ($p = 0.204$). Overall, differences in error incidences between the dominant and non-dominant hemisphere did not reach the level of significance.

4. Discussion

This study validated a non-invasive rnTMS based protocol for SMA mapping in healthy subjects. The current findings underline the feasibility of an extension of the proposed protocol to the non-dominant hemisphere and lower extremity. Further, refined instructions for mapping procedures and error classifications were provided. Finally, the present study gives insights into the somatotopic organisation of the SMA.

Following the virtual lesion paradigm, the current results are in line with previous studies showing that rnTMS applied to the SMA can induce a reduction of finger taps (Schramm et al., 2019; Engelhardt et al., 2023). Mapping of both hemispheres was possible

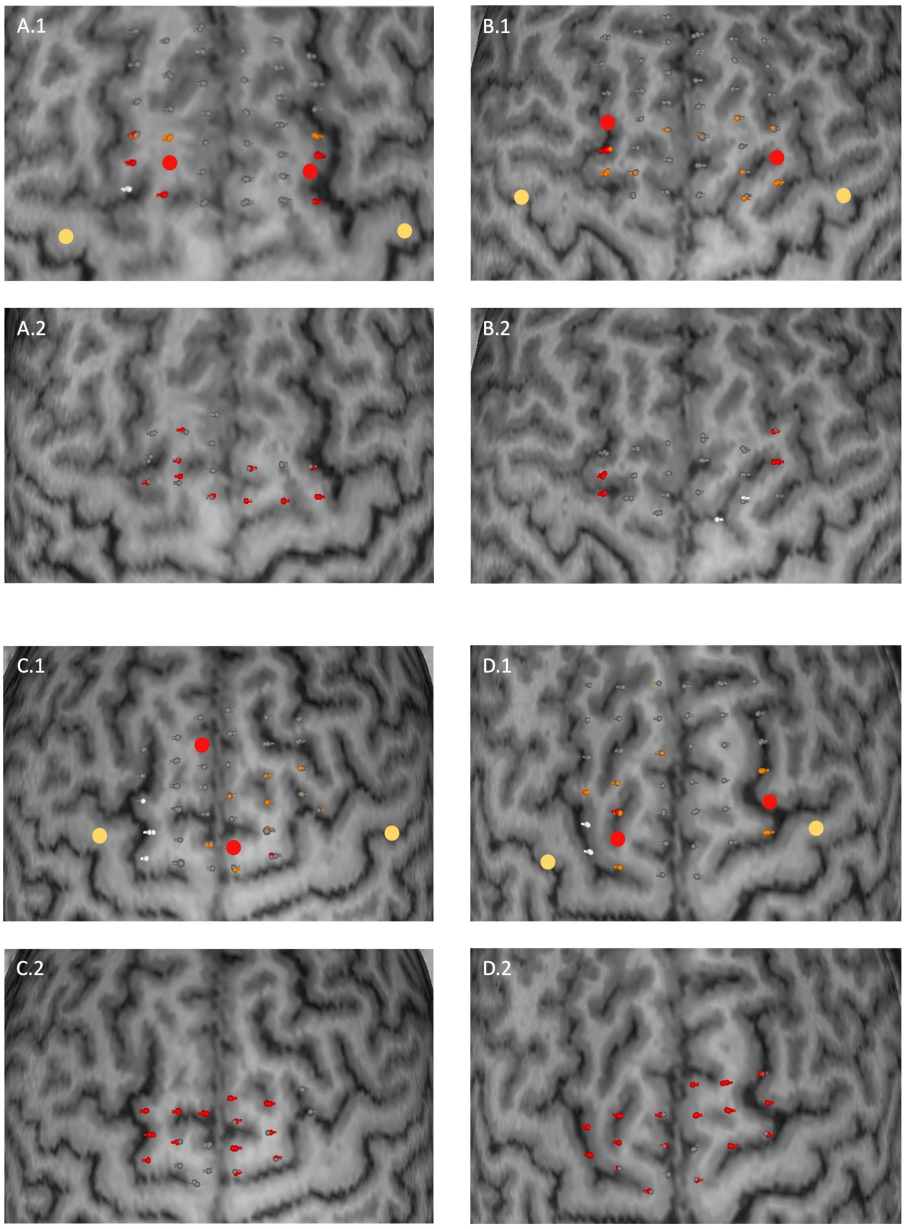

FIGURE 1
Examples of SMA error maps for four subjects **(A–D)**. Two subplots correspond to one subject for the upper extremity (0.1) and for the lower extremity (0.2). Stimulation points are coloured in their corresponding error category. Upper extremity: grey (no error), orange (minor error), red (major error); lower extremity: grey (no visually detected movement error) and red (visually detected movement error) respectively. White coloured points represent stimulation points for which the residual electrical field at the M1 hotspot field was above the RMT. Larger dots correspond to M1 (yellow) and SMA (red) hotspots. The distance between two stimulation points was 4 to 5 mm on average.

similarly to preceding studies which used the Jebsen-Taylor hand function test (Schramm et al., 2019, 2020). However, the importance of hemispheric dominance regarding SMA function is not yet fully understood. The mentioned studies report a stronger effect during stimulation of the right hemisphere when looking at right-handed subjects while the current results suggest no significant differences. Other studies linked the occurrence of language deficits to the resection of the dominant hemisphere (Bannur and Rajshekhar, 2000; Dalacorte et al., 2012). In this study, only the SMA involvement in motor function was investigated. Overall, the relevance of hemispheric dominance should be investigated by future studies.

The current study refined and standardised the protocol description and error classification of the previously proposed protocol (Engelhardt et al., 2023). According to this new protocol a minimum of 15 points was stimulated twice per hemisphere and subject. In this context error categories for the finger tapping reduction have been lowered from ≥30% to ≥20% for major errors and ≥ 15% to ≥10% for minor errors. Overall, protocol changes were made specifically with the focus on ensuring replicability of errors.

The previously observed built up of stimulation effects (Engelhardt et al., 2023) was only observed in one subject in the present study. This raises the question whether the effect was indeed related to stimulation or rather a characteristic of subject dependent muscle fatigue. In

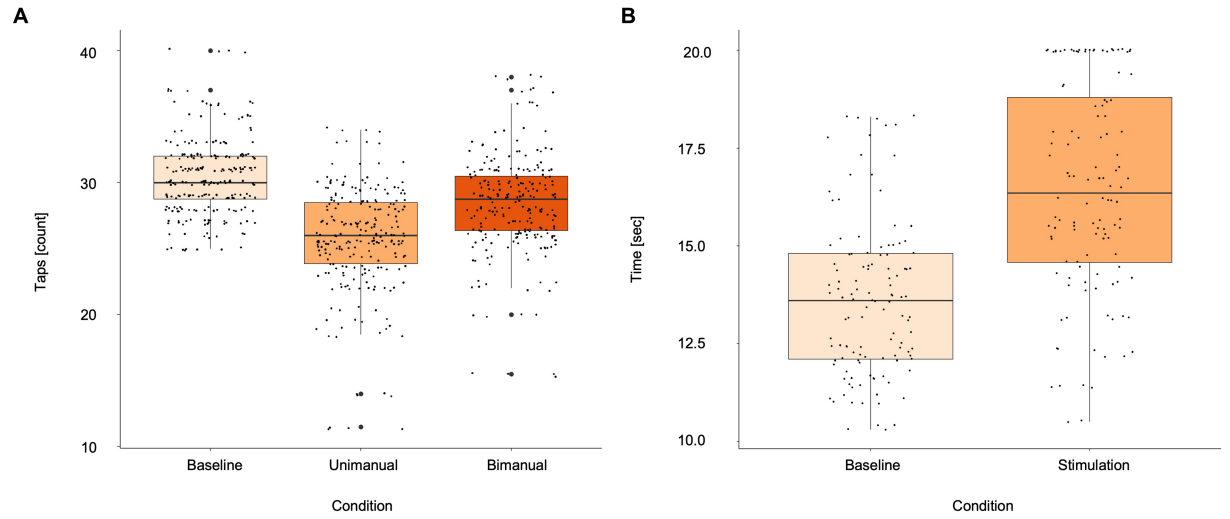

FIGURE 2
Boxplots for **(A)** finger tapping scores during baseline, unimanual and bimanual tapping during stimulation, **(B)** Nine-Hole Peg Test during baseline and stimulation. Asterisks indicate statistically different effects ($p < 0.05$; linear mixed models). Small black dots represent single subject values.

support of an actual stimulation induced effect, Emanuel et al. (2021) report an increased stuck-in-the-middle phenomenon meaning a sharper decrease in effort towards the middle of a task compared to beginning and end after inhibitory SMA stimulation.

The current results suggest an improvement of finger tapping performance due to bimanual instead of unimanual tapping during stimulation. It has been shown that SMA activation can drive also contralateral executive motor function in case of contralateral SMA failure through transcallosal connections. This is supported by the notion that a strong interhemispheric connectivity facilitates rehabilitation after SMA lesions (Krainik et al., 2004; Vassal et al., 2017). Previous studies have shown the involvement of the SMA in coordinating bimanual movements by altering the interhemispheric connectivity (Serrien et al., 2002; Welniarz et al., 2019). Therefore, a possible explanation might be that bimanual tapping compensates for stimulation induced disruptions. Further, it could be hypothesised that a short delay in tapping normalisation might occur due to the time needed for interhemispheric transmission.

Overall, the present study suggests stimulation effects smaller than reported by Engelhardt et al. (2023). Responsiveness could be increased with higher stimulation intensities while controlling for activation of M1yet at the cost of spatial specificity. The importance of ensuring proper SMA responses by controlling for the residual electric field over M1 was reinforced in the current study. A high interindividual difference regarding size and location of the area susceptible to stimulation was found similarly to the preceding study (Engelhardt et al., 2023). This could be partially explained by functio-anatomical differences or variable effects of methodology. Therefore, we suggest caution when interpreting the absence of errors as this could be due to the absence of function or due to the lack of a sufficiently intense simulation. In contrast, induced errors could be more reliable. However, these hypotheses need to be investigated in a clinical sample, where the relation between presence or absence of errors, a potential resection and postoperative deficits can be clearly established.

Previous studies highlight an underlying somatotopy of the SMA mostly based on the clinical outcome after SMA resection. These findings indicate a structural organisation of face, upper and lower extremity from anterior to posterior (Zentner et al., 1996; Fontaine et al., 2002; Krainik et al., 2004). The current results support this hypothesis as errors in upper extremity function occurred mostly in the medial part of the SMA and errors in lower extremity function in the posterior part. However, due to time constraints of the measurement not all SMA portions were examined for lower extremity errors, thus limiting these conclusions. Nevertheless, the present study demonstrates that a somatotopic map could be created using more tasks and testing upper and lower extremities.

As a next step, this refined protocol could be applied to patients to validate whether rnTMS positive stimulation points are functionally essential and therefore rnTMS based SMA mapping could deliver valuable clinical information. In this context, the protocol could be implemented within the clinical setting to aid risk assessment in addition to preoperative diagnostics and planning. Further, it could be used to assess SMA reorganisation due to surgery or other brain lesions by comparing SMA maps of different timepoints.

4.1. Limitations

The present study focused on the number of finger taps as a simple and easy to assess outcome. The toe tapping has been analysed regarding visually detected movement errors by two independent assessors. Future studies could use more detailed and objective measures by applying a sensor to measure timing of taps, inter-tap intervals or movement kinematics. In addition, these measures could be used to investigate a potential built-up of the SMA stimulation effect over time. Further, these analyses could aid to identify mechanisms behind bimanual movement coordination including whether the contralesional SMA takes over function of the lesioned side. Electric field estimates were based on the multi spherical head model integrated in the Nexstim system to enable fast and easy online assessment. However, more realistic head models might lead to slightly deviating results of the electric field estimates (Nieminen et al., 2022). These differences might become relevant when stimulating

close to M1 or with residual intensities close to the RMT. Especially for the lower extremity activation of the contralateral SMA cannot be completely excluded due to the high stimulation intensities used and proximity of both areas. Even though the strongest stimulation effects were observed a bit more distant from the midline, a potential confounding activation of the contralateral SMA should be carefully monitored. The current study focused on anatomical landmarks to identify the stimulation area, however SMA boundaries are not strictly defined (Nachev et al., 2008). Sites inducing foot movement disruptions also encompassed sites which produced major disruptions in finger tapping. This suggests that given the existence of a somatotopy, boundaries between hand and foot areas might not be sharp. Future studies could stimulate more frontal or lateral regions such as the pre-SMA to further investigate spatial delineation and somatotopic organisation of the SMA. This could also aid to additionally validate SMA specificity of stimulation effects.

4.2. Conclusion

The present study refined and validated a protocol for the non-invasive rnTMS based mapping of the SMA considering both hemispheres and somatotopy of the SMA. As a next step, this protocol will be tested in a clinical setting to test its ability to aid preoperative diagnostics, risk assessment for the occurrence of the SMA syndrome and assessment of postoperative reorganisation in brain tumor patients.

Data availability statement

The original contributions presented in the study are included in the article/Supplementary Material, further inquiries can be directed to the corresponding author.

Ethics statement

The studies involving humans were approved by Ethics Committee of the Charité Universitätsmedizin Berlin. The studies were conducted in accordance with the local legislation and institutional requirements. The participants provided their written informed consent to participate in this study.

Author contributions

GK: Conceptualization, Data curation, Formal analysis, Investigation, Methodology, Project administration, Visualization, Writing – original draft. MK: Conceptualization, Methodology, Writing – review & editing. TP: Conceptualization, Methodology, Supervision, Writing – review & editing. ME: Conceptualization, Data curation, Formal analysis, Methodology, Project administration, Supervision, Writing – review & editing.

Funding

The author(s) declare financial support was received for the research, authorship, and/or publication of this article. The authors acknowledge the support of the Cluster of Excellence Matters of Activity. Image Space Material funded by the Deutsche Forschungsgemeinschaft (DFG, German Research Foundation) under Germany's Excellence Strategy – EXC 2025-390648296. We acknowledge financial support from the Open Access Publication Fund of Charité – Universitätsmedizin Berlin and the German Research Foundation (DFG).

Acknowledgments

MRI scans for this study took place at the Berlin Center for Advanced Neuroimaging (BCAN).

Conflict of interest

The authors declare that the research was conducted in the absence of any commercial or financial relationships that could be construed as a potential conflict of interest.

Publisher's note

Supplementary material

The Supplementary material for this article can be found online at: https://www.frontiersin.org/articles/10.3389/fnins.2023.1255209/full#supplementary-material

References

Bannur, U., and Rajshekhar, V. (2000). Post operative supplementary motor area syndrome: clinical features and outcome. *Br. J. Neurosurg.* 14, 204–210.

Dalacorte, A., Portuguez, M. W., Maurer das Neves, C. M., Anes, M., and DaCosta, J. C. (2012). Functional Mri evaluation of supplementary motor area language dominance in right- and left-handed subjects. *Somatosens. Mot. Res.* 29, 52–61. doi: 10.3109/08990220.2012.662418

Emanuel, A., Herszage, J., Sharon, H., Liberman, N., and Censor, N. (2021). Inhibition of the supplementary motor area affects distribution of effort over time. *Cortex* 134, 134–144. doi: 10.1016/j.cortex.2020.10.018

Engelhardt, M., Kern, G., Karhu, J., and Picht, T. (2023). Protocol for mapping of the supplementary motor area using repetitive navigated transcranial magnetic stimulation. *Front. Neurosci.* 17:1185483. doi: 10.3389/fnins.2023.1185483

Engelhardt, M., and Picht, T. (2020). 1 Hz repetitive transcranial magnetic stimulation of the primary motor cortex: impact on excitability and task performance in healthy subjects. *J. Neurol. Surg. A Cent. Eur. Neurosurg.* 81, 147–154. doi: 10.1055/s-0040-1701624

Engelhardt, M., Schneider, H., Gast, T., and Picht, T. (2019). Estimation of the resting motor threshold (Rmt) in transcranial magnetic stimulation using relative-frequency and threshold-hunting methods in brain tumor patients. *Acta Neurochir.* 161, 1845–1851. doi: 10.1007/s00701-019-03997-z

Fontaine, D., Capelle, L., and Duffau, H. (2002). Somatotopy of the supplementary motor area: evidence from correlation of the extent of surgical resection with the clinical patterns of deficit. *Neurosurgery* 50, 297–303.

Fox, J., and Weisberg, S. (2019). *An R companion to applied regression*. Thousand Oaks CA: Sage. Available at: https://socialsciences.mcmaster.ca/jfox/Books/Companion/

Hiroshima, S., Anei, R., Murakami, N., and Kamada, K. (2014). Functional localization of the supplementary motor area. *Neurol. Med. Chir. (Tokyo)* 54, 511–520. doi: 10.2176/nmc.oa2012-0321

Kokkonen, S. M., Nikkinen, J., Remes, J., Kantola, J., Starck, T., Haapea, M., et al. (2009). Preoperative localization of the sensorimotor area using independent component analysis of resting-state fmri. *Magn. Reson. Imaging* 27, 733–740. doi: 10.1016/j.mri.2008.11.002

Krainik, A., Duffau, H., Capelle, L., Cornu, P., Boch, A. L., Mangin, J. F., et al. (2004). Role of the healthy hemisphere in recovery after resection of the supplementary motor area. *Neurology* 62, 1323–1332. doi: 10.1212/01.WNL.0000120547.83482.B1

Laplane, D., Talairach, J., Meininger, V., Bancaud, J., and Orgogozo, J. M. (1977). Clinical consequences of corticectomies involving the supplementary motor area in man. *J. Neurol. Sci.* 34, 301–314. doi: 10.1016/0022-510X(77)90148-4

Nachev, P., Kennard, C., and Husain, M. (2008). Functional role of the supplementary and pre-supplementary motor areas. *Nat. Rev. Neurosci.* 9, 856–869. doi: 10.1038/nrn2478

Nieminen, A. E., Nieminen, J. O., Stenroos, M., Novikov, P., Nazarova, M., Vaalto, S., et al. (2022). Accuracy and precision of navigated transcranial magnetic stimulation. *J. Neural Eng.* 19:066037. doi: 10.1088/1741-2552/aca71a

Oda, K., Yamaguchi, F., Enomoto, H., Higuchi, T., and Morita, A. (2018). Prediction of recovery from supplementary motor area syndrome after brain tumor surgery: preoperative diffusion tensor tractography analysis and postoperative neurological clinical course. *Neurosurg. Focus.* 44:E3. doi: 10.3171/2017.12.FOCUS17564

Oldfield, R. C. (1971). The assessment and analysis of handedness: the Edinburgh inventory. *Neuropsychologia* 9, 97–113. doi: 10.1016/0028-3932(71)90067-4

Pinheiro, J., Bates, D., and Team, R. C. (2023). nlme: Linear and nonlinear mixed effects models [online]. Available at: https://Cran.R-project.org/package=nlme (Accessed May 21, 2023).

Pinson, H., Van Lerbeirghe, J., Vanhauwaert, D., Van Damme, O., Hallaert, G., and Kalala, J. P. (2022). The supplementary motor area syndrome: a neurosurgical review. *Neurosurg. Rev.* 45, 81–90. doi: 10.1007/s10143-021-01566-6

Schramm, S., Albers, L., Ille, S., Schroder, A., Meyer, B., Sollmann, N., et al. (2019). Navigated transcranial magnetic stimulation of the supplementary motor cortex disrupts fine motor skills in healthy adults. *Sci. Rep.* 9:17744. doi: 10.1038/s41598-019-54302-y

Schramm, S., Sollmann, N., Ille, S., Meyer, B., and Krieg, S. M. (2020). Application of navigated transcranial magnetic stimulation to map the supplementary motor area in healthy subjects. *J. Clin. Neurophysiol.* 37, 140–149. doi: 10.1097/WNP.0000000000000530

Serrien, D. J., Strens, L. H., Oliviero, A., and Brown, P. (2002). Repetitive transcranial magnetic stimulation of the supplementary motor area (Sma) degrades bimanual movement control in humans. *Neurosci. Lett.* 328, 89–92. doi: 10.1016/S0304-3940(02)00499-8

Tuncer, M., Fekonja, L., Ott, S., Pfnür, A., Karbe, A.-G., Engelhardt, M., et al. (2022). Role of interhemispheric connectivity in recovery from postoperative supplementary motor area syndrome in glioma patients. *J. Neurosurg.* 139, 1–10. doi: 10.3171/2022.10.JNS221303

Vassal, M., Charroud, C., Deverdun, J., Le Bars, E., Molino, F., Bonnetblanc, F., et al. (2017). Recovery of functional connectivity of the sensorimotor network after surgery for diffuse low-grade gliomas involving the supplementary motor area. *J. Neurosurg.* 126, 1181–1190. doi: 10.3171/2016.4.JNS152484

Venables, W. N., and Ripley, B. D. (2002). *Modern applied statistics with S*, Springer, New York.

Vorobiev, V., Govoni, P., Rizzolatti, G., Matelli, M., and Luppino, G. (1998). Parcellation of human mesial area 6: cytoarchitectonic evidence for three separate areas. *Eur. J. Neurosci.* 10, 2199–2203. doi: 10.1046/j.1460-9568.1998.00236.x

Welniarz, Q., Gallea, C., Lamy, J. C., Méneret, A., Popa, T., Valabregue, R., et al. (2019). The supplementary motor area modulates interhemispheric interactions during movement preparation. *Hum. Brain Mapp.* 40, 2125–2142. doi: 10.1002/hbm.24512

Wickham, H. (2007). Reshaping data with the reshape package. *J. Stat. Softw.* 21, 1–20. doi: 10.18637/jss.v021.i12

Wickham, H. (2016). *ggplot2: Elegant graphics for data analysis*, Springer-Verlag New York.

Wickham, H., Averick, M., Bryan, J., Chang, W., Mcgowan, L. D., François, R., et al. (2019). Welcome to the tidyverse. *J. Open Source Softw.* 4:1686. doi: 10.21105/joss.01686

Wickham, H., François, R., Henry, L., Müller, K., and Vaughan, D. (2023a). Dplyr: A grammar of data manipulation [online]. Available at: https://dplyr.tidyverse.org, https://github.com/tidyverse/dplyr (Accessed May 21, 2023).

Wickham, H., Henry, L., Pedersen, T. L., Luciani, T. J., Decorde, M., Lise, V., et al. (2023b). Svglite: An 'svg' graphics device [online]. Available at: https://svglite.r-lib.org, https://github.com/r-lib/svglite (Accessed May 21, 2023).

Wongsripuemtet, J., Tyan, A. E., Carass, A., Agarwal, S., Gujar, S. K., Pillai, J. J., et al. (2018). Preoperative mapping of the supplementary motor area in patients with brain tumor using resting-state fmri with seed-based analysis. *AJNR Am. J. Neuroradiol.* 39, 1493–1498. doi: 10.3174/ajnr.A5709

Zeharia, N., Hertz, U., Flash, T., and Amedi, A. (2012). Negative blood oxygenation level dependent homunculus and somatotopic information in primary motor cortex and supplementary motor area. *Proc. Natl. Acad. Sci. U. S. A.* 109, 18565–18570. doi: 10.1073/pnas.1119125109

Zentner, J., Hufnagel, A., Pechstein, U., Wolf, H. K., and Schramm, J. (1996). Functional results after resective procedures involving the supplementary motor area. *J. Neurosurg.* 85, 542–549. doi: 10.3171/jns.1996.85.4.0542

frontiers | Frontiers in Neuroscience

TYPE Original Research
PUBLISHED 23 November 2023
DOI 10.3389/fnins.2023.1282232

OPEN ACCESS

EDITED BY
Chang-Hoon Choi,
Helmholtz Association of German Research Centres (HZ), Germany

REVIEWED BY
Zhengcao Cao,
Beijing Normal University, China
Christina Maher,
The University of Sydney, Australia

*CORRESPONDENCE
Yulei Sun
✉ sunyulei1224@163.com
Ailiang Miao
✉ ailiangmiao1986@163.com

†These authors have contributed equally to this work and share first authorship

RECEIVED 23 August 2023
ACCEPTED 07 November 2023
PUBLISHED 23 November 2023

CITATION
Sun Y, Shi Q, Ye M and Miao A (2023) Topological properties and connectivity patterns in brain networks of patients with refractory epilepsy combined with intracranial electrical stimulation.
Front. Neurosci. 17:1282232.
doi: 10.3389/fnins.2023.1282232

Topological properties and connectivity patterns in brain networks of patients with refractory epilepsy combined with intracranial electrical stimulation

Yulei Sun[1,2*†], Qi Shi[3†], Min Ye[1] and Ailiang Miao[2*]

[1]Department of Neurology, Nanjing BenQ Medical Center, The Affiliated BenQ Hospital of Nanjing Medical University, Nanjing, Jiangsu, China, [2]Department of Neurology, The Affiliated Brain Hospital of Nanjing Medical University, Nanjing, Jiangsu, China, [3]Department of Neurology, The Affiliated Wuxi People's Hospital of Nanjing Medical University, Wuxi, Jiangsu, China

Objective: Although intracranial electrical stimulation has emerged as a treatment option for various diseases, its impact on the properties of brain networks remains challenging due to its invasive nature. The combination of intracranial electrical stimulation and whole-brain functional magnetic resonance imaging (fMRI) in patients with refractory epilepsy (RE) makes it possible to study the network properties associated with electrical stimulation. Thus, our study aimed to investigate the brain network characteristics of RE patients with concurrent electrical stimulation and obtain possible clinical biomarkers.

Methods: Our study used the GRETNA toolbox, a graph theoretical network analysis toolbox for imaging connectomics, to calculate and analyze the network topological attributes including global measures (small-world parameters and network efficiency) and nodal characteristics. The resting-state fMRI (rs-fMRI) and the fMRI concurrent electrical stimulation (es-fMRI) of RE patients were utilized to make group comparisons with healthy controls to identify the differences in network topology properties. Network properties comparisons before and after electrode implantation in the same patient were used to further analyze stimulus-related changes in network properties. Modular analysis was used to examine connectivity and distribution characteristics in the brain networks of all participants in study.

Results: Compared to healthy controls, the rs-fMRI and the es-fMRI of RE patients exhibited impaired small-world property and reduced network efficiency. Nodal properties, such as nodal clustering coefficient (NCp), betweenness centrality (Bc), and degree centrality (Dc), exhibited differences between RE patients (including rs-fMRI and es-fMRI) and healthy controls. The network connectivity of RE patients (including rs-fMRI and es-fMRI) showed reduced intra-modular connections in subcortical areas and the occipital lobe, as well as decreased inter-modular connections between frontal and subcortical regions, and parieto-occipital regions compared to healthy controls. The brain networks of es-fMRI showed a relatively weaker small-world structure compared to rs-fMRI.

Conclusion: The brain networks of RE patients exhibited a reduced small-world property, with a tendency toward random networks. The network connectivity patterns in RE patients exhibited reduced connections between cortical and subcortical regions and enhanced connections among parieto-occipital regions.

Electrical stimulation can modulate brain network activity, leading to changes in network connectivity patterns and properties.

KEYWORDS

refractory epilepsy, functional magnetic resonance imaging, intracranial electrical stimulation, network connectivity patterns, small-world property

1 Introduction

Epilepsy is a neurological disorder characterized by recurrent and unprovoked seizures resulting from the intrinsic predisposition of the brain to generate unregulated electrical activity within its neural networks (Fisher et al., 2014). Although most epileptic patients show good responses to anti-seizure medications (ASMs), few patients continue to experience uncontrolled seizures despite receiving two ASMs (Schuele and Luders, 2008); this subgroup of epilepsy is called refractory epilepsy (RE) (Kwan et al., 2009). Frequent uncontrollable seizures can damage the developing cortical networks of the brain, leading to poor cognitive prognosis (Helmstaedter and Witt, 2017). It is essential to understand the pathogenesis underlying the electrical activity within brain networks to enable targeted interventions during the condition. Notably, functional imaging technology has been used frequently in neuropsychiatry (Li et al., 2017; Leitgeb et al., 2020; Wang et al., 2020; Song et al., 2021; Guan et al., 2022), thereby contributing significantly to the advancement of research on brain network disorders. Functional magnetic resonance imaging (fMRI), a non-invasive modality, can detect spontaneous neuronal activity within human brain networks at resting-state (Biswal et al., 1995). This technique has become increasingly essential for investigating healthy and dysfunctional brain function, facilitating a more comprehensive understanding of the mechanisms underlying seizure generation and propagation and the alterations within the framework of brain networks in epilepsy (Ogawa et al., 1992; Jiang et al., 2018).

Regarding brain networks, a brain region is defined as a node within the network. The direct topological connections or functional coupling correlations between these brain regions form the edges of the network (Guan et al., 2022). The rs-fMRI brain network approach has been used to identify significant topological characteristics in human brain functional networks through graph theory analysis; these features include small-world property and modular attributes (Wang et al., 2020). Furthermore, this method enables the investigation of functional connectivity between the entire brain and specific local brain regions (Guan et al., 2022). A brain network that exhibits the small-world property is referred to as a small-world network; this type of network is distinguished by a high degree of clustering coefficients (Cp) and a short average path length (Lp) (Watts and Strogatz, 1998; Bassett and Bullmore, 2017). It lies between random and regular networks, balancing the segregation and integration of information processing (Bassett and Bullmore, 2017). This organizational structure appears optimal for functioning in various complex systems, including brain networks (Bullmore and Sporns, 2009). Brain networks can be divided into modules, formed by a subset of highly connected nodes with limited connections to nodes in other modules (Meunier et al., 2010). These modules reflect the major functional systems of the brain, such as motor, somatosensory or visual functions (Stam and van Straaten, 2012). Frequently, damage to relevant modules or networks is associated with brain dysfunction in distinct neural networks.

A growing body of evidence suggests that these properties are altered in certain disease states; furthermore, these alterations in brain network connectivity can serve as valuable novel biomarkers for understanding the underlying psychopathology of diseases (Greicius, 2008; Liu et al., 2008; Zhang and Raichle, 2010; Vlooswijk et al., 2011; Tao et al., 2013; Sethi et al., 2016; Zheng et al., 2018; Tavakol et al., 2019; Drenthen et al., 2020; Tian et al., 2020; Song et al., 2021). For instance, Liu et al. (2008) discovered significant alterations in the small-world attribute of the prefrontal, parietal, and temporal lobes in patients with schizophrenia, compared to healthy controls. These variations also correlate with illness duration in schizophrenia (Liu et al., 2008). A study on Optic neuritis (Song et al., 2021) revealed that a decrease in Cp could signify reduced functional connectivity in specific brain regions due to severe demyelination, often seen in cases of axonal injury. Recent studies suggested that modular-related properties may be sensitive in reflecting brain changes in patients with major depressive disorder (Tao et al., 2013; Zheng et al., 2018; Tian et al., 2020). Studies on the topological properties of brain networks in epilepsy have also been reported. The study conducted by Drenthen et al. (2020) discovered a reduction in small-world organization in the brain networks of children with childhood absence epilepsy (CAE) in comparison to the controls. Additionally, the study revealed a positive correlation between Lp and disease duration as well as seizure frequency in CAE children. Studies of functional networks in temporal lobe epilepsy (TLE) have often reported increases in Lp (Vlooswijk et al., 2011; Sethi et al., 2016; Tavakol et al., 2019), and changes in these attributes have been associated with cognitive deficits (Vlooswijk et al., 2011).

These days, intracranial electrical stimulation has seen extensive use in treating psychiatric and neurological conditions, as well as in the preoperative localization of epilepsy (Lozano and Lipsman, 2013; Forouzannezhad et al., 2019; Thompson et al., 2020). Therefore, the impact of electrical stimulation on brain networks or brain functions, such as on perception (Parvizi et al., 2012), cognition (Parvizi et al., 2013), and emotion (Fried et al., 1998), has garnered considerable attention. However, studies on the properties of brain networks in relation to electrical stimulation are lacking due to its invasive nature. Patients with RE require surgery to intervene in the abnormal discharging of nerve cells in the brain due to uncontrollable seizures. This compensates for the fact that electrodes cannot be implanted in the brains of healthy people to study the effects of electrical stimulation. A novel approach integrates intracranial electrical stimulation with whole-brain neuroimaging in RE patients, enabling the quantification of acute long-range and network-level effects of the stimulation (Thompson et al., 2020). The method, which complements

existing rs-fMRI network studies, can examine alterations in the functional connectivity of brain networks following electrode implantation, providing a more intuitive understanding of the impact of electrical stimulation on functional networks (Oya et al., 2017). Therefore, investigating the association between electrical stimulation and functional connectivity can provide insights into the precise impact of electrical stimulation on brain function; this includes its potential to facilitate or impede information transfer. Quantifiable indicators or evaluation criteria are needed to assess this stimulating effect. If there are network properties or phenotypes associated with electrical stimulation, this will provide useful information for the clinical treatment of RE.

Therefore, our study aimed to investigate the brain network characteristics of patients with RE concurrent electrical stimulation and obtain possible clinically significant biomarkers. To achieve this goal, the fMRI data of RE patients under combined electrical stimulation will undergo network connectivity analysis using graph theory topological properties. Firstly, we investigated the network properties in individuals with RE during resting-state and synchronous electrical stimulation in comparison to healthy controls to identify the main features of brain networks in RE patients. Then, we also compared the characteristics of brain networks before and after electrode implantation in the same patients, providing further evidence of the potential effects of electrical stimulation on network properties. This study is expected to provide more information for the diagnosis and intervention of RE.

2 Methods and materials

This study used the [Dataset] ds002799, available on the OpenNeuro data sharing platform.[1] This dataset comprised 26 RE patients who underwent fMRI before and after electrode implantation. Most of them have no structural abnormalities or lesions in brain. The University of Iowa Institutional Review Board, Stanford University, and Caltech approved the study protocol. Informed consent was obtained from all the participants.

2.1 Data collection

All patients underwent anatomical MRI [T1-weighted (T1w) images] and rs-fMRI before electrode implantation. The T1w images were obtained using a 3 T GE Discovery 750w MRI equipped with a 32-channel head coil. The BRAVO sequence was used, with the following parameters: echo time (TE) of 3.376 ms, repetition time (TR) of 8.588 ms, flip angle of 12°, and voxel size of 1.0 × 1.0 × 0.8 mm. Participants were instructed to keep their eyes open during the rs-fMRI session before electrode implantation. Each session lasted 4.8 min and was conducted using a 32-channel head coil. The scan parameters were as follows: TR of 2,260 ms, TE of 30 ms, flip angle of 80°, and voxel size of 3.4 × 3.4 × 4.0 mm. Notably, no gap was present and the bandwidth was set at 2003 Hz/Px. The functional images after electrode implantation were scanned with simultaneous electrical stimulation on two distinct scanners before the surgery (Oya et al., 2017). The earlier images were obtained using a Siemens 3 T Trio scanner. In contrast, the later images were obtained using a 3 T Skyra (Siemens) due to specific collection conditions. The scan parameters used were as follows: TR of 3,000 ms; a delay of 100 ms was introduced in TR to coincide with the administration of electrical stimulation; TE of 30 ms; voxel size of 3 × 3 × 3 mm; flip angle of 90°; and bandwidth of 1934 Hz/Px. Notably, the authors of the raw data (Thompson et al., 2020) recommend treating the data obtained on the two scanners as comparable for group analyzes.

To minimize stimulation-induced MRI artifacts and the potential interactions between external electrical stimuli and radiofrequency or gradient switching-induced potentials in the electrodes, the delivery of electrical stimuli was interleaved with echo-planar imaging (EPI) volume acquisition, occurring within a 100 ms blank period devoid of scanner radiofrequency or gradient switching. Stimulation was blocked and organized in (approximately 30 s ON and OFF) with a total run duration of about 10 min for each electrical stimulation (es)-fMRI run of patients, with specific details varying slightly among patients. No significant difference was observed in head motion between no stimulation and stimulation epochs (Thompson et al., 2020). Most patients underwent multiple es-fMRI runs involving the implantation of several electrodes. These es-fMRI runs were included in the fMRI data preprocessing steps. The brain stimulation used bi-phasic charge-balanced square pulses characterized by a length of 50–90 ms, 8–12 mA, and 5–9 pulses administered at a stimulation rate of 100 Hz. The stimulation parameters, including amplitude, duration, and electrode position standard coordinates corresponding to the MNI152 template, can be found in the ieeg subdirectory of [Dataset] ds002799 on the OpenNeuro platform (Thompson et al., 2020). Table 1 presents the stimulation points for each patient. More details about the data collection can be found in these articles (Oya et al., 2017; Thompson et al., 2020).

For comparative analysis of network connectivity with healthy controls, we used the [Dataset] Berlin_Margulies from the 1,000 Functional Connectomes Project.[2] This dataset comprised structural and functional images of 26 healthy controls (without neurological or psychiatric disorders) aged 23–44 years. All imaging scans were conducted using a Siemens 3 T Trio scanner. The T1w imaging parameters were as follows: voxel size of 1 × 1 × 1 mm, TR of 2.3 s, TE of 2.98 ms, inversion time (TI) of 900 ms, flip angle of 9°, and bandwidth of 240 Hz/Px. Regarding the fMRI data acquisition, the following parameters were used: 34 slices, voxel size of 3 × 3 × 4 mm, TR of 2.3 s, TE of 30 ms, flip angle of 90°, a total of 200 measurements were acquired in 7.45 min, no delay in TR, and a bandwidth of 2,232 Hz/Px.

The functional scans obtained before electrode implantation are resting-state BOLD fMRI data and were referred to as "rs-fMRI" in our study. The functional data obtained after electrode implantation, scanning with simultaneous electrical stimulation, was denoted as "es-fMRI" in our study. As no task was performed during the es-fMRI scans, and the electrical stimulation did not affect perception or behavior noticeably, the es-fMRI scans can be treated as "resting-state" fMRI (Thompson et al., 2020). When comparing patients with RE and healthy controls, the fMRI data collected from the healthy controls

1 https://openneuro.org/datasets/ds002799/versions/1.0.4

2 http://fcon_1000.projects.nitrc.org/fcpClassic/FcpTable.html

group was labeled as "HC-fMRI." High-quality T1w images were acquired before any neurosurgical intervention, as the original data researchers recommended and supported by experimental evidence (Thompson et al., 2020). Therefore, during fMRI data pre-processing and analysis, T1w images were used for registration with the images of rs-fMRI and es-fMRI. Consistent with the findings of the previous study (Thompson et al., 2020), we successfully registered es-fMRI images with the T1w images before electrode implantation.

2.2 fMRI data pre-processing

The fMRI data from all enrolled participants were pre-processed using the GRETNA toolbox[3] (Wang et al., 2015) in the MATLAB 2013b platform (Mathworks, Natick, MA, United States). The pre-processing protocols involved several steps, including the removal of the initial 10 volumes, correction of slice timing, correction of head motion, normalization of spatial data through T1 segmentation, elimination of linear trends, temporal band filtering (0.01–0.08 Hz), and regression of nuisance signals, including 24-parameter head motion profiles and cerebrospinal fluid and white matter signals. Participants exhibiting excessive head movement (translation >3.0 mm or rotation >3.0° in any direction) and those with framewise displacement (FD) > 0.5 mm were excluded. Upon completion of fMRI data pre-processing, 18 RE patients and 23 healthy controls were included.

2.3 Network connectivity construction and analysis

This study analyzed the differences in network connectivity between RE patients (including rs-fMRI and es-fMRI) and healthy controls. Furthermore, it assessed the effects of electrical stimulation on fMRI network connectivity. The AAL-90 atlas was used to construct 90 × 90 network connectivity matrices for each participant. The parcellation atlas provides essential information about the order, location, and names of each node stored in the toolbox (… \GRETNA\ Templates). The resulting network connectivity matrices from various participants were then converted into two types of networks: binary and weighted. This conversion was achieved using sparsity thresholding techniques. These networks were used in our study to describe the characteristics of functional network connectivity. A recent study has demonstrated detailed algorithms for generating binary and weighted networks (Wang et al., 2015). The difference between binary and weighted networks primarily depends on whether connectivity strength is considered (Wang et al., 2015). Figure 1 shows the process for constructing network connectivity. The concept of sparsity, defined as the ratio of actual connections (E) to the total number of potential connections [N(N-1)/2] (Zalesky et al., 2012), has received significant attention in the scientific literatures. It has been used to investigate small-world organization across various connection densities. Previous studies have examined densities as low as 1–5% (Achard et al., 2006; Kitzbichler et al., 2011) and as high as 50% (Lynall et al., 2010). To ascertain small-world organization, the minimum connection density is often determined by ensuring that k > log(N), where k represents the mean node degree (Achard et al., 2006). Applying this principle to a network of dimensions $N = 90$ results in a minimum connection density of 5% (Zalesky et al., 2012). To ensure meaningful network connectivity and facilitate the estimation of small-world organization, the sparsity threshold used in our study was set at 5–35%, with increments of 1%. For our network connectivity analysis, we used the rs-fMRI data and 50 runs of es-fMRI data from 17 RE patients and fMRI data from 22 healthy controls.

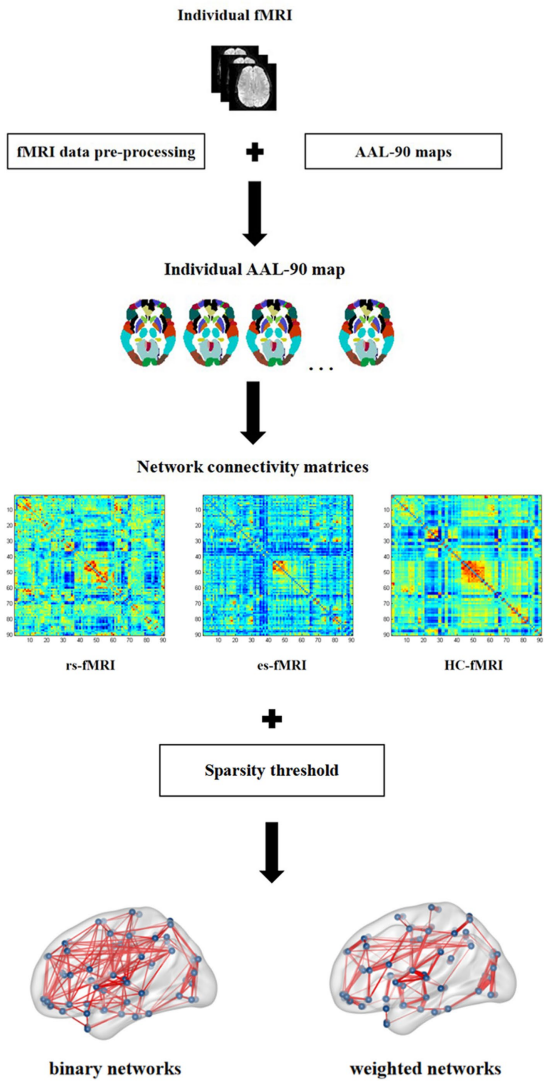

FIGURE 1
Network connectivity construction. In this figure, individual fMRI represents the fMRI image of each subject enrolled in present study, which is pre-processed on the standard AAL-90 atlas to construct the functional connectivity matrix for each subject. The three connectivity matrices in the figure show the example of one subject, respectively, selected from rs-fMRI, es-fMRI and HC-fMRI. Finally, the binary networks and weighted networks are constructed using sparsity threshold method. rs-fMRI, the resting-state fMRI of RE patients; es-fMRI, the fMRI concurrent electrical stimulation of RE patients; HC-fMRI, healthy controls' fMRI.

Our study analyzed various topological properties in brain networks, including global and nodal parameters. The global

3 http://www.nitrc.org/projects/gretna/

network properties included characteristics of small-world property and network efficiency, such as global network efficiency (Eg) and local network efficiency (Eloc). The small-world property was evaluated through these parameters, such as the Cp, Lp, normalized clustering coefficient (γ), normalized characteristic path length (λ), and small-worldness (σ). Notably, γ was calculated as the ratio of Cp to Cprand, whereas λ was computed as the ratio of Lp to Lprand. These reference values, Cprand and Lprand, were derived from randomized networks generated by using a Markov-chain algorithm (Maslov and Sneppen, 2002; Sporns and Zwi, 2004) within the GRETNA toolbox; this maintains an equivalent number of nodes and edges, as well as comparable degree distribution to the actual brain networks (Wang et al., 2015). Small-world networks exhibit a significantly elevated mean Cp akin to regular lattice networks ($\gamma > 1$), along with small Lp comparable to random networks ($\lambda \approx 1$) (Watts and Strogatz, 1998). Cp, defined as the proportion of connections established between a node's neighbors, provides insight into the extent of connections within a local cluster (Leitgeb et al., 2020). A pronounced Cp signifies efficient local information transfer and resilience against random attacks and subsequent node failures (Bullmore and Sporns, 2009; Rubinov and Sporns, 2010). In contrast, the Lp refers to the minimum number of edges necessary for traversing from one node to another (Van Straaten and Stam, 2013). The observed Lp within brain networks further emphasizes efficient parallel information transfer and effective global integration (Van Straaten and Stam, 2013).

Our study has also computed various nodal properties concerning network connectivity, including nodal clustering coefficient (NCp), nodal characteristic shortest path length (NLp), betweenness centrality (Bc), and degree centrality (Dc). Bc quantifies the impact of a node on the information flow in the graph, whereas Dc measures the number of direct connections a given node maintains with other nodes in the graph (Guan et al., 2022). To evaluate the global and nodal topological characteristics of the brain networks, the area under the curve (AUC) was computed for each parameter. This metric, calculated independently at the single threshold, is highly sensitive to the abnormal topological structure of brain diseases (Zhang et al., 2011). In the group analysis, AUC values of global and nodal network properties are used to compare the differences in network connectivity between rs-fMRI, es-fMRI and HC-fMRI.

To compare the distribution characteristics of fMRI network connectivity between RE patients (including rs-fMRI and es-fMRI) and healthy controls, network connectivity modules were constructed using a structural division of 90 regions of interest in AAL-90 atlas. These regions of interest were categorized into six sub-modules: frontal lobe, prefrontal lobe, subcortical areas, temporal lobe, occipital lobe, and parietal lobe. Our study computed the connectivity strength of intra-and inter-modules among rs-fMRI, es-fMRI, and HC-fMRI. In total, the connectivity strength from 15 inter-modular connections and 6 intra-modular connections were used to analyze modular connectivity patterns.

A comparative observation was performed using the fMRI data of same patients to conduct a more comprehensive analysis of brain networks pre-and post-electrode implantation. Multiple runs of es-fMRI images from the same patient were compared with their rs-fMRI images, using small-world parameters and network efficiency as comparable quantitative measures. These network properties values of es-fMRI runs were divided into two categories with the values greater than and less than rs-fMRI, and the differences between them were assessed to determine whether the parameters distribution originated from the same population.

All stages of image pre-processing, network construction, and analyses were performed using the GRETNA toolbox. The results about nodal properties and the network connectivity patterns were visualized using the BrainNet Viewer toolbox[4] (Xia et al., 2013).

2.4 Statistics

The connectivity topological properties, including global, nodal, and modular parameters, in brain networks of rs-fMRI, es-fMRI, and HC-fMRI were compared using a one-way analysis of variance (ANOVA) test; the analysis controlled for the covariates of mean FD and age of each participant. Non-parametric tests were used when data did not meet the criteria for normal distribution. p-values <0.05 were considered statistically significant. *Post hoc* tests were performed between any two groups in cases where the ANOVA test revealed significant differences. Bonferroni correction procedure was used to evaluate the multiple comparisons of nodal parameters and modular analysis. Fisher's exact test was used to determine the consistency of small-world parameters and network efficiency between es-fMRI runs and rs-fMRI data for individual comparisons. Statistical analyses were performed using SPSS version 20 (SPSS, Inc., Chicago, IL, United States).

3 Results

The network analysis finally included 17 patients with RE and 22 healthy controls in our study. No significant differences were observed between both groups with respect to age ($p = 0.171$) and sex ($p = 0.325$). The RE patients had an average age of 34.06 ± 11.85, among whom 5 were females and 12 were males. The healthy controls had an average age of 29.73 ± 4.86, including 12 females and 11 males. The demographics of all study participants are presented in Tables 1, 2.

3.1 Global network properties

The results revealed a consistent trend of change in network topological properties among RE patients and healthy controls as the sparsity threshold varied (Figure 2). As the network's sparsity threshold increased, σ, Lp, γ, and λ demonstrated a decrease in both binary and weighted networks. Conversely, Cp and network efficiency (Eg and Eloc) increased with varying sparsity thresholds in both network types. Upon comparing the global property parameters across three groups (rs-fMRI, es-fMRI and HC-fMRI), significant differences were observed in σ, γ, Eg, and Eloc among the three groups in both types of networks (Figure 3). Notably, significant differences were observed in Cp and Lp among the three groups in weighted networks (Figure 3). However, in binary networks, no significant

4 http://www.nitrc.org/projects/bnv/

TABLE 1 The RE patients' demographics information.

Subject	Sex	Age (y)	Electrode stimulation sites/es-fMRI runs
292	F	50	Left posterior medial frontal (3runs) Left heschls gyrus (2runs)
303	F	34	Right amygdala (2runs)
307	M	30	Left heschls gyrus (3runs)
316	F	31	Right heschls gyrus (2runs) Right amygdala (1run) Right posterior hippocampus (1run)
320	F	50	Right frontal lobe (1run) Left amygdala (2runs) Right heschls gyrus (1run)
330	M	43	right parietal lobe (1run) Right amygdala (1run) Right amygdala and planum temporal simultaneously (1run) Right superior posterior occipital lobe (1run)
331	M	35	Left amygdala (1run) Right frontal lobe (1run)
334	M	39	Right planum temporal (3runs) Left amygdala (4runs) Right posterior hippocampus (1run) Left and right amygdala (1run)
335	M	31	Right heschls gyrus (1run) Left anterior insula (1run)
352	M	31	Left heschls gyrus (1run)
357	M	36	Left posterior medial frontal lobe (1run)
372	M	34	Left heschls gyrus (1run)
395	M	13	Left amygdala (2runs)
399	F	22	Right anterior cingulate (2runs) Right amygdala (1run)
400	M	59	Left heschls gyrus (1run)
405	M	19	Right amygdala (1run) Left anterior insula orbitofrontal cortex (1run) Right hippocampus (1run)
413	M	22	Right frontal operculum ofc (1run) Right cingulate (1run) Right inferior posterior insula (1run)

The Table 1 documents the basic information of RE patients included in the network connectivity analysis, including age, sex, the brain regions of electrode stimulation and electrode stimulation corresponding to es-fMRI runs. RE, refractory epilepsy; y, years; F, female; M, male; es-fMRI, the fMRI concurrent electrical stimulation of RE patients.

differences were observed in Cp ($p = 0.174$) and Lp ($p = 0.101$) among the three groups. The binary networks of es-fMRI showed slightly elevated Cp values compared to those of rs-fMRI, although this difference was not statistically significant. The brain networks derived from the es-fMRI exhibited lower σ, γ, Eg, and Eloc and higher Lp values than those from the rs-fMRI and HC-fMRI (Figure 3). Although no statistically significant differences were observed in small-world parameters between the rs-fMRI and HC-fMRI, the rs-fMRI group demonstrated lower σ, Cp, γ and higher Lp values. The binary networks exhibited significant differences in Eg and Eloc between the rs-fMRI and HC-fMRI (Figure 3). The λ demonstrated no significant differences among the three groups, regardless of whether binary ($p = 0.429$) or weighted networks ($p = 0.578$) were considered.

3.2 Nodal network properties

Regarding nodal properties, Bc, Dc, and NCp exhibited differences among the three groups (rs-fMRI, es-fMRI and HC-fMRI) in binary and weighted networks (Figure 4). However, NLp displayed no significant differences among the three groups in either network type. In binary networks, specific nodes, such as the left fusiform gyrus (FFG.L), right putamen (PUT.R), left thalamus (THA.L), and right thalamus (THA.R), demonstrated distinct Bc values (Figure 4A). Similarly, in weighted networks, the Bc of PUT.R exhibited differences. Notably, healthy controls exhibited higher Bc values in the bilateral thalamus and FFG.L compared to RE patients (including rs-fMRI and es-fMRI) in binary networks. Conversely, the rs-fMRI and the es-fMRI of RE

TABLE 2 The healthy controls' demographics information.

Subject	Sex	Age (y)
06204	M	34
12855	M	33
18913	F	29
23506	F	27
27536	M	25
27711	F	26
27797	M	31
28092	F	26
33248	F	28
38279	M	29
47066	F	26
47791	M	31
49134	M	44
54976	M	37
57028	F	37
67166	F	32
75506	M	28
85681	F	26
86111	F	24
91966	F	27
95068	M	26
97162	M	28

The Table documents basic information of healthy controls included in the network connectivity analysis, including age and sex. y, years; F, female; M, male.

patients exhibited higher Bc values in PUT.R compared to healthy controls in both types of networks. The Dc of the right precuneus (PCUN.R), THA.L, and THA.R exhibited significant differences among the three groups in binary networks (Figure 4B), whereas the Dc of left rolandic operculum (ROL.L), left supramarginal gyrus (SMG.L), PCUN.R, left pallidum (PAL.L), right pallidum (PAL.R), THA.L and THA.R exhibited differences in weighted networks. Notably, the rs-fMRI and the es-fMRI of RE patients exhibited increased Dc values in PCUN.R compared to healthy controls in binary and weighted networks. Furthermore, the rs-fMRI exhibited higher Dc values in SMG.L compared to HC-fMRI and es-fMRI in weighted networks. Conversely, in binary networks, THA.L and THA.R demonstrated higher Dc values in healthy controls than RE patients (including rs-fMRI and es-fMRI). Moreover, in weighted networks, ROL.L, PAL.L, PAL.R, THA.L, and THA.R exhibited higher Dc values in healthy controls than RE patients (including rs-fMRI and es-fMRI). The left precentral gyrus (PreCG.L) exhibited higher NCp value in RE patients (including rs-fMRI and es-fMRI) compared to healthy controls in binary networks. By contrast, healthy controls demonstrated increased NCp in left parahippocampal gyrus (PHG.L), right superior occipital gyrus (SOG.R), left putamen (PUT.L), and left superior temporal gyrus (STG.L) compared to RE patients (including rs-fMRI and es-fMRI) in weighted networks (Figure 4C). The binary networks of rs-fMRI exhibited increased NCp in left insula (INS.L) compared to HC-fMRI, while the INS.L of es-fMRI showed the lowest NCp values in two types of networks.

3.3 Network connectivity patterns

The network connectivity distributions among brain modules of three groups (rs-fMRI, es-fMRi and HC-fMRI) were displayed in Figure 5A. The modular analysis revealed significant differences in inter-regional connectivity, such as the connections between frontal lobe module and subcortical regions, and the connections between parietal lobe module and occipital lobe module (Figure 5B). Internal connectivity differences were observed within subcortical areas and the occipital lobe module (Figure 5B). Compared to healthy controls, RE patients demonstrated reduced connectivity between the frontal and subcortical areas while exhibiting enhanced connectivity between the parietal and occipital areas. Notably, modular connectivity strength within the subcortical and occipital networks in RE patients was lower compared to healthy controls. In all modular differences, es-fMRI brain networks exhibited increased connectivity strength compared to those from rs-fMRI.

3.4 Individual network connectivity comparison between rs-fMRI and es-fMRI

The findings of sub334 were used to exemplify the differences in network connectivity between rs-fMRI and es-fMRI (Figure 6A). Notably, properties, such as σ, Cp, Lp, γ, Eg, and Eloc, exhibited differences, whereas λ showed no significant difference between rs-fMRI and es-fMRI. The rs-fMRI brain networks exhibited elevated σ and γ values, whereas the es-fMRI brain networks demonstrated relatively increased Lp values (Figure 6B) in both network types. Additionally, Eg in binary networks and Eloc in weighted networks of rs-fMRI were higher than those of es-fMRI. The Cp of es-fMRI demonstrated a relatively higher value in binary networks, consistent with group comparison results (Figure 3).

4 Discussion

4.1 Reduced small-world property and network efficiency

In our study, both RE patients and healthy controls exhibited consistent modifications in the network connectivity characteristics across both binary and weighted networks as the sparsity threshold varied, suggesting that the brain networks of RE patients maintained normal structural and functional properties. Notably, the brain networks of RE patients exhibited the characteristic small-world architecture, with $\gamma > 1$ and $\lambda \approx 1$. This persistence of small-world property suggests that information transfer within the brain during cognitive or motor activities continues to be facilitated in RE patients, consistent with a previous study (Song et al., 2021).

However, significant differences are observed in the small-world property between RE patients and healthy controls. In our findings, both rs-fMRI and es-fMRI exhibited lower σ, Cp, and γ and higher Lp values in brain networks compared to healthy controls. This implies that RE

patients possess a weaker small-world network than their healthy controls. The small-world property measures the equilibrium between global and local processing mechanisms (Guan et al., 2022). Elevated Cp and γ values signify functional segregation within brain networks, indicating a prevalence of localized interconnectivity (Guan et al., 2022). Conversely, reduced Lp and λ values may suggest functional integration within the brain, reflecting the ability to transmit global information (Guan et al., 2022). In our study, the decreased Cp and γ could suggest a weakening of the local brain networks, leading to decreased interconnections among neighboring brain regions and impeding effective communication. From a network topology perspective, this might result in diminished or severed functional connectivity between certain brain regions, effectively

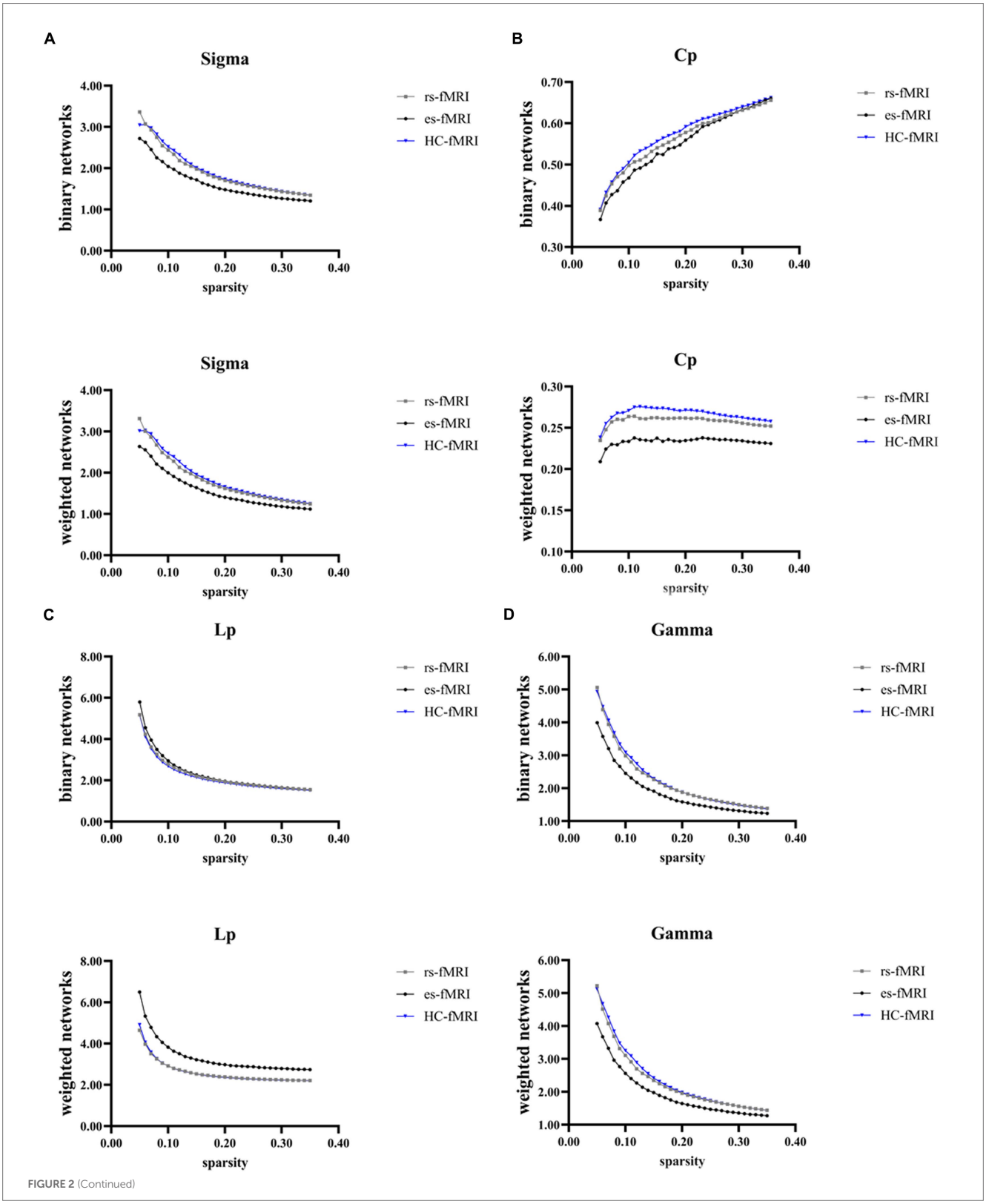

FIGURE 2 (Continued)

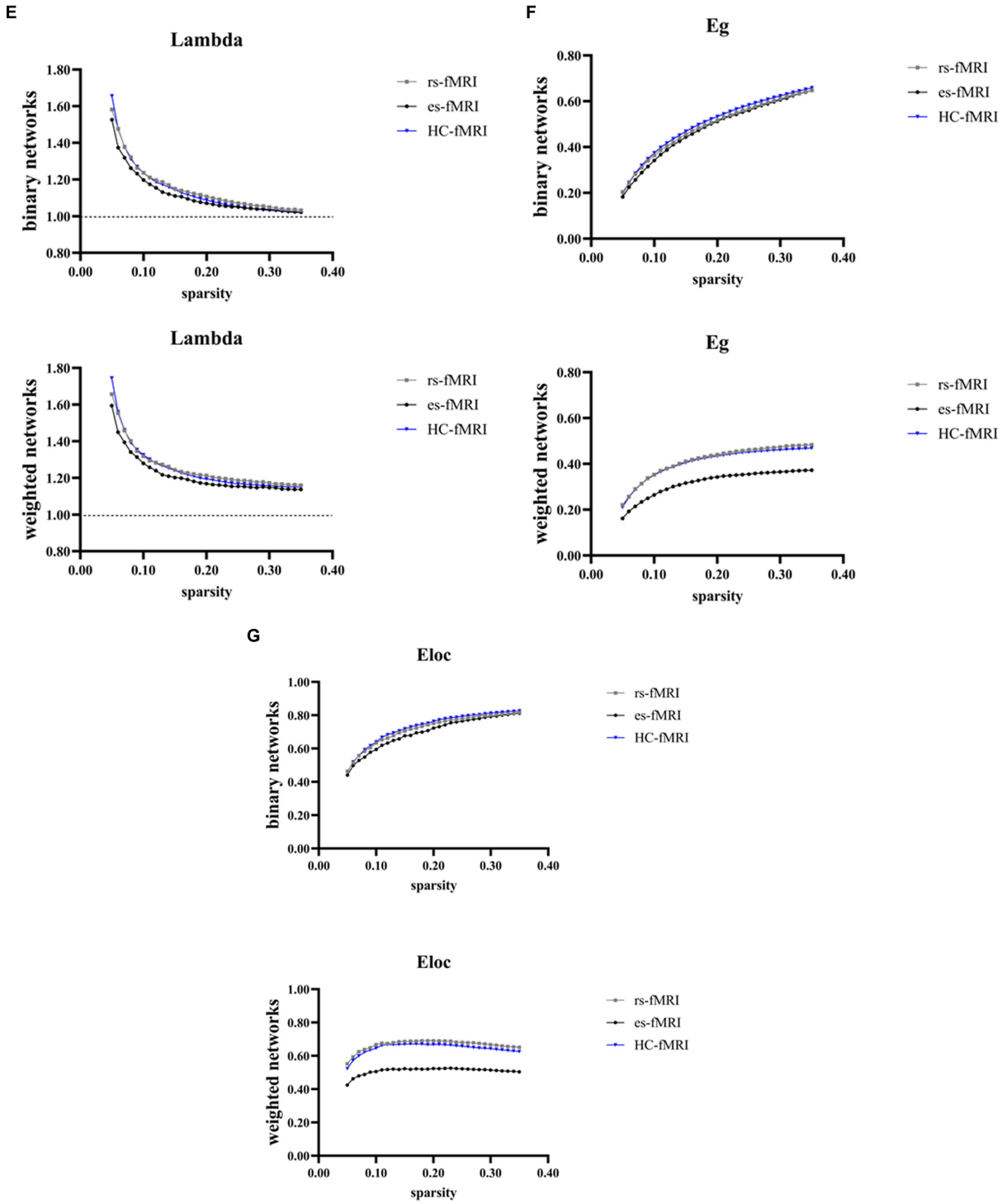

FIGURE 2
Global network properties varying with changes in sparsity. The figure illustrates the global network property parameters at different sparsity thresholds. The X-axis denotes the sparsity threshold, while the Y-axis represents the corresponding property values. The observed alterations in the line patterns indicate a consistent change in the network properties among the rs-fMRI, es-fMRI and HC-fMRI with varying sparsity levels. **(A–G)** The figures illustrate the variations in Sigma, Cp, Lp, Gamma, Lambda, Eg and Eloc values in response to changes in sparsity. Sigma (σ), small-worldness; Cp, clustering coefficient; Lp, characteristic path length; Gamma (γ), normalized clustering coefficient; Lambda (λ), normalized characteristic path length; Eg, global network efficiency; Eloc, local network efficiency; rs-fMRI, the resting-state fMRI of RE patients; es-fMRI, the fMRI concurrent electrical stimulation of RE patients; HC-fMRI, healthy controls' fMRI.

excluding them from processing pertinent brain activity. Simultaneously, the increased Lp could indicate a reduction in the communication efficiency of global networks, thereby inhibiting the comprehensive transmission of information during normal brain activity. This conclusion is further reinforced by the poorer network efficiency parameters (Eg and Eloc) in RE patients compared to healthy controls.

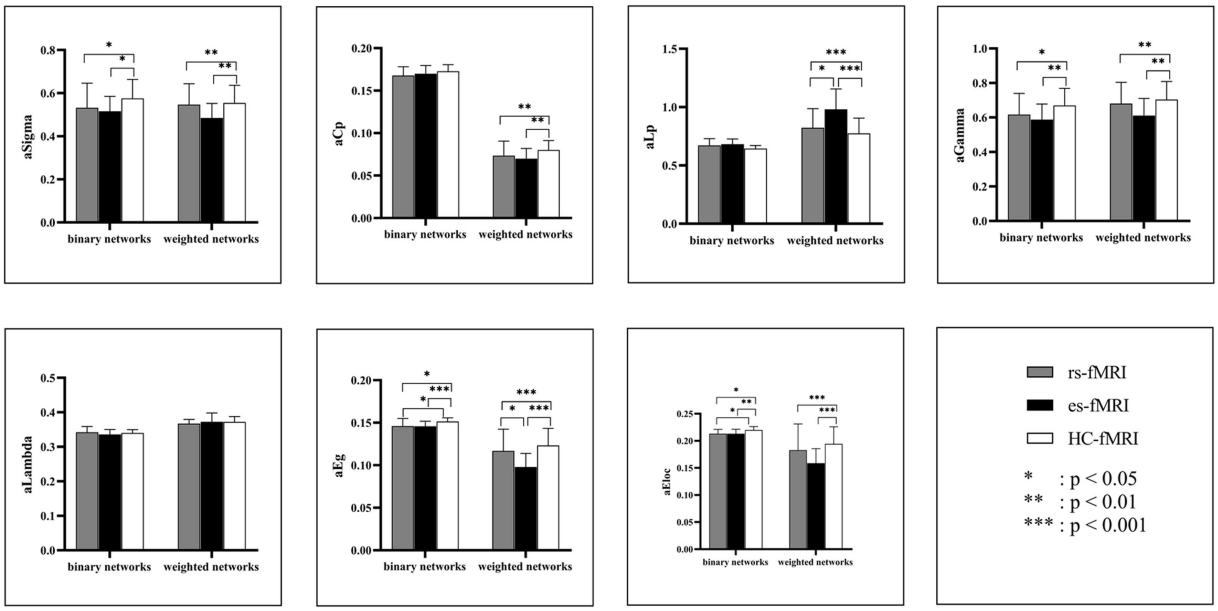

FIGURE 3
Comparisons of global network properties. The figure shows the AUC values comparison of global network properties of rs-fMRI, es-fMRI, and HC-fMRI in both binary and weighted networks under all sparsity thresholds. Network properties with statistical differences after multiple correlations are marked with black asterisks. The "a" refers to the AUC values of these network properties. AUC, area under the curve; Sigma (σ), small-worldness; Cp, clustering coefficient; Lp, characteristic path length; Gamma (γ), normalized clustering coefficient; Lambda (λ), normalized characteristic path length; Eg, global network efficiency; Eloc, local network efficiency; rs-fMRI, the resting-state fMRI of RE patients; es-fMRI, the fMRI concurrent electrical stimulation of RE patients; HC-fMRI, healthy controls' fMRI.

Whereas the findings of small-world property have not been consistent in previous similar studies. Consistent with our results, Jiang et al. (2017) found that the functional networks of right TLE tended to have more random attributes with reduced σ. During the interictal period, the neural network moved into a more randomly organized state with higher Lp and decreased Cp (Ponten et al., 2007). However, Wang J. et al. (2014) discovered that TLE patients exhibited statistically significant increases in Cp and Lp in comparison to the controls. Sethi et al. (2016) analyzed task-free fMRI data in polymicrogyria patients and found higher Cp and Lp in the affected area relative to the contralateral regions, indicating that the lesional anomalies may contribute disproportionately to global modifications. The reasons for the inconsistent findings remain unclear. They may be attributed to differences in sample sizes, patients' ages and epilepsy phenotype, methods of measuring the connection form, use of ASMs as well as different experimental techniques (Jiang et al., 2017). Network properties appear to correlate with epilepsy phenotypes, and brain network organization seem to be modulated by the specific lesional and histopathological subtype (Tavakol et al., 2019). The RE patients we studied were in a resting state, and we believe that the course of the disease and the state of the disease could also be the factors that influenced the results of the study. In summary, previous studies and our findings indicate elevated Lp with concomitant increases or decreases in Cp within the brain networks of patients with TLE or RE. This suggests that the efficiency of information transfer and integration within the brain networks of these individuals with epilepsy was impaired.

Our study demonstrated the potential decline in the small-world architecture of brain networks among RE patients, indicated by decreased Cp, σ and γ and increased Lp. The brain networks of RE patients may lean toward a more random network structure. Such a shift toward randomness could compromise the stability and coordination of network connectivity between different brain regions, leading to a potential lack of synchronized and systematic responses to external stimuli or spontaneous brain activity. This observation implies that certain brain functions may be compromised or impaired in RE patients. Similar studies have also reported the relationship between small-world parameters and brain dysfunction. For example, Wang X. B. et al. (2014) found that the γ and λ were increased in the patients with mild cognitive impairment, and these abnormalities were associated with the slow speed of information processing in brain networks. Bai et al. (2012) and Wang et al. (2013) demonstrated a positive correlation between higher Lp values and poorer cognitive performance, as evidenced by clinical manifestations such as emotional, cognitive, or language impairment. The authors (Hatlestad-Hall et al., 2021) investigated the correlation between σ and functional neurocognitive networks in focal epilepsy and found that the σ of the default mode network (DMN) was associated with memory performance in patients.

4.2 Decreased activity in certain brain regions affects relevant brain functions

Additionally, RE patients exhibited significant disparities in nodal attributes compared to healthy controls. Bc measures the ability of a node to efficiently transmit information in networks by assessing its contribution to the shortest path between all other pairs of points (Guan et al., 2022). Dc represents the sum of direct connections of a node in a network (Guan et al., 2022). An elevated Dc indicates more

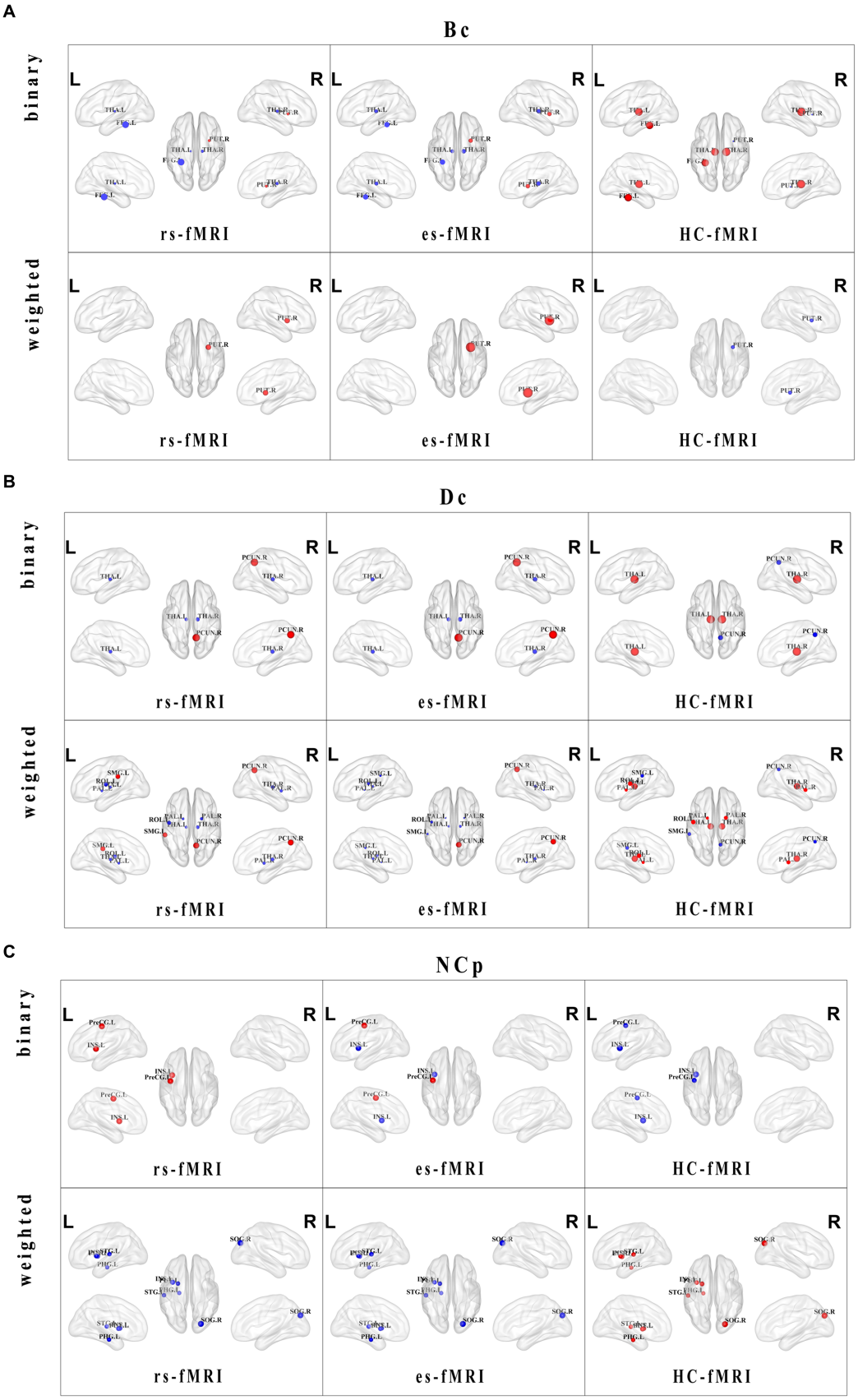

FIGURE 4
Distributions and comparisons of nodal network properties. The figure illustrates the distribution of nodal network properties within the brain, highlighting significant differences between RE patients (including rs-fMRI and es-fMRI) and healthy controls in both binary and weighted networks.

(Continued)

FIGURE 4 (Continued)
Specifically, the figures respectively display the comparisons of Bc **(A)**, Dc **(B)** and NCp **(C)** in the two types of networks across three groups of individuals. Nodes with distinct differences are exhibited in figures, and marked with their brain region abbreviations. The varying sizes of nodes reflect the different values of the nodal properties, where the red and blue dots, respectively, indicate the increased and decreased nodal property values in brain regions. Bc, betweenness centrality; Dc, degree centrality; NCp, nodal clustering coefficient; FFG.L, left fusiform gyrus; PUT.L, left putamen; PUT.R, right putamen; THA.L, left thalamus; THA.R, right thalamus; PAL.L, left pallidum; PAL.R, right pallidum; PCUN.R, right precuneus; ROL.L, left rolandic operculum; SMG.L, left supramarginal gyrus; SOG.R, right superior occipital gyrus; INS.L, left insula; PHG.L, left parahippocampal gyrus; PreCG.L, left precental gyrus; STG.L, left superior temporal gyrus.

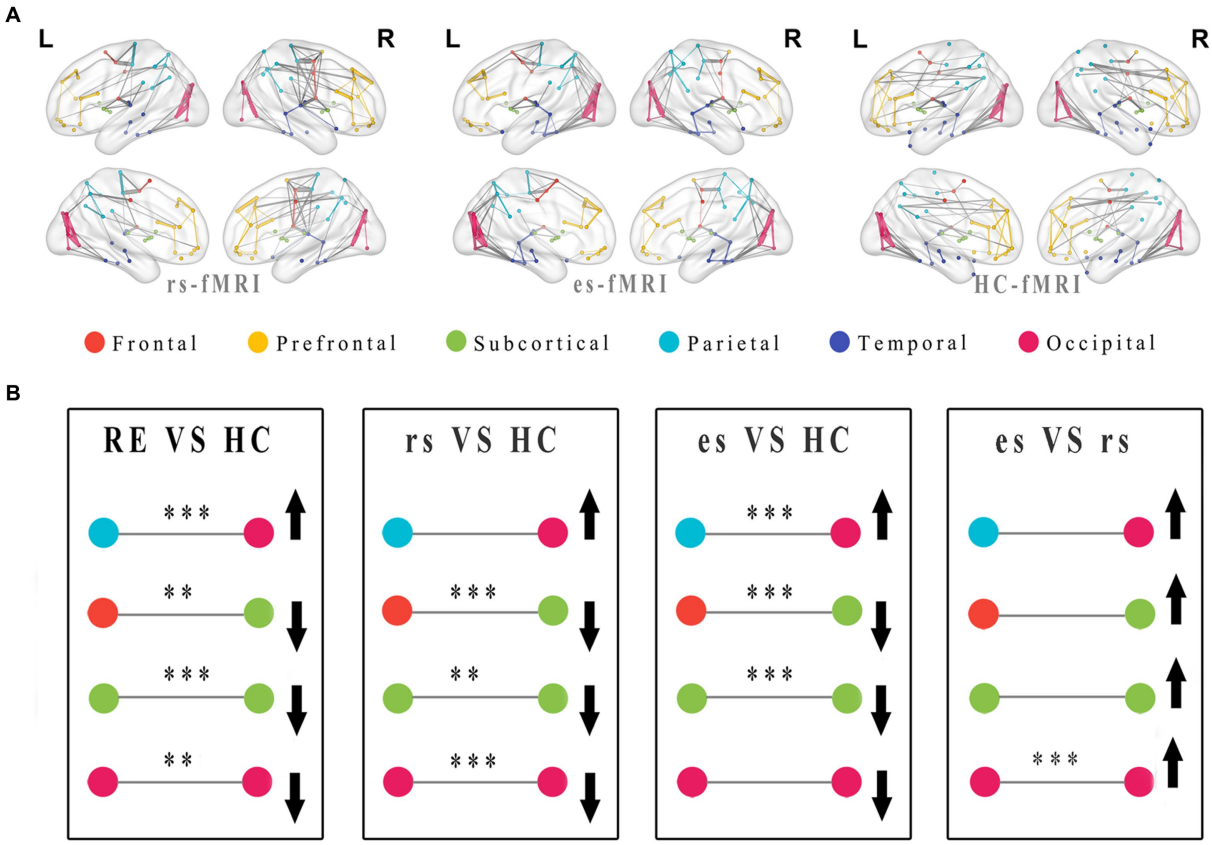

FIGURE 5
Modular distributions and comparisons of network connectivity patterns. The group average functional connectivity matrix of rs-fMRI, es-fMRI and HC-fMRI was used to construct group average connectivity map with modular division, and the connections greater than the sparsity threshold value of 0.05 were shown in this figure **(A)**. In this figure, the internal connections of the modules are connected with lines of the same color as the modules, and the connections between different modules are connected with gray lines. The thickness of the line indicates the connectivity strength of the connections between brain regions. **(B)** The figure shows the modularization analysis of RE patients and healthy controls. The black asterisks were used to exhibited significant differences after multiple comparisons, and the black arrows were utilized to indicate relative increase or decrease in module connectivity strength. Where the * means $p < 0.05$, ** means $p < 0.01$, *** means $p < 0.001$. RE, refractory epilepsy patients; HC, healthy controls; rs, the resting-state fMRI of RE patients; es, the fMRI concurrent electrical stimulation of RE patients.

connections (Rubinov and Sporns, 2010), implying a central hub status for the node. Variations in Bc and Dc within relevant brain regions indicate differences in transmission efficiency and connectivity strength. Notably, differences in Bc exhibited weakened transmission efficiency in the thalamus and fusiform gyrus among RE patients in our study. The thalamus is a relay station that receives sensory inputs from the ascending reticular activating system and transmits them to cortical areas (Sun et al., 2021), thereby maintaining heightened alertness and vigilance across the brain (Sun et al., 2021). The fusiform gyrus, located in the visual association cortex of the temporal lobe, is mainly responsible for face recognition. This result implies a potential impairment in information transmission ability and visual function among RE patients, affecting normal processing efficiency. Conversely, RE patients exhibited elevated Bc values in the right putamen, indicating the retention of motor control and postural coordination abilities. Additionally, an elevated Dc in the precuneus and supramarginal gyrus signifies increased connections with other brain areas, suggesting that the parietal lobe can serve as a highly connected hub in the brain networks of RE patients. By contrast, decreased Dc values in ROL.L, pallidum, and thalamus suggest reduced activity or connections within and around these brain areas. Notably, the precuneus, a part of the DMN, is activated during periods of rest and

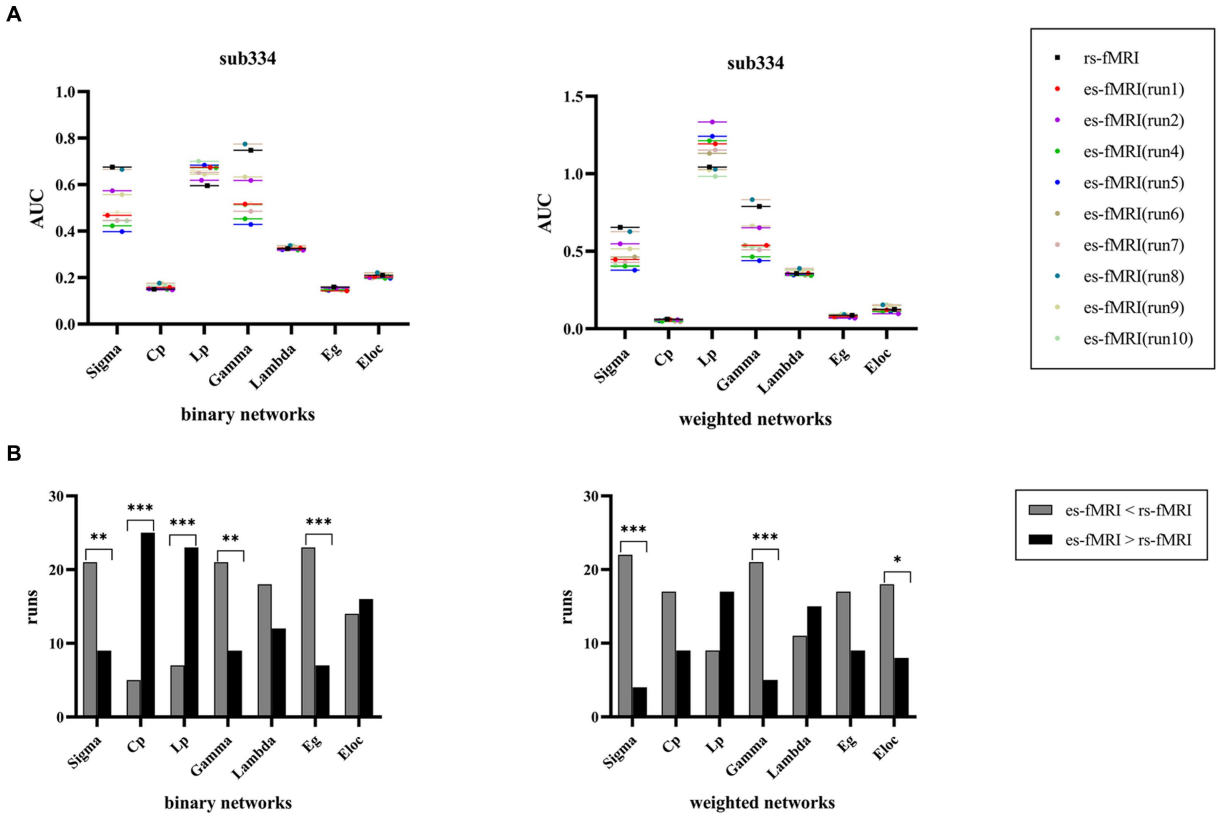

FIGURE 6
Comparisons of individual network properties between rs-fMRI and es-fMRI. **(A)** The figure shows the distribution of AUC values of global network properties between rs-fMRI and es-fMRI in two types of networks using sub334 as an example. **(B)** The figure shows the comparison of network connectivity properties between rs-fMRI and es-fMRI, and black asterisks mark significant differences in brain networks between the two states. AUC, area under the curve; Sigma (σ), small-worldness; Cp, clustering coefficient; Lp, characteristic path length; Gamma (γ), normalized clustering coefficient; Lambda (λ), normalized characteristic path length; Eg, global network efficiency; Eloc, local network efficiency; rs-fMRI, the resting-state fMRI of RE patients; es-fMRI, the fMRI concurrent electrical stimulation of RE patients.

relatively inactivated during external stimulus tasks, thereby maintaining the equilibrium of brain networks (Raichle et al., 2001; Luo et al., 2011). Its activation enables the continuous acquisition of information from the environment and the body (Raichle et al., 2001). Meanwhile, the supramarginal gyrus plays a role in complex movements. The enhanced connectivity observed in the precuneus and supramarginal gyrus might compensate for impaired efficiency of information, allowing basic information processing and activity capability maintenance.

NCp serves as an indicator of a local network connectivity strength or capacity of a node. Notably, RE patients exhibited increased NCp in the precentral gyrus and relatively diminished NCp in regions, such as the parahippocampus, occipital lobe, putamen, and temporal lobe, indicating that the local connectivity strength of brain networks in RE patients is lower compared to healthy controls. The precentral gyrus, located in the frontal lobe, is associated with somatomotor functions. The frontal lobe plays a crucial role in various higher-order cognitive functions, behavioral control, and somatomotor and somatosensory functions, which are actively engaged in the sustained consciousness of epilepsy (Caplan et al., 2008). This emphasizes the significance of the frontal lobe in information processing in the brain networks among RE patients. The parahippocampus, forming a part of the hippocampal circuit, is involved in higher neural functions, such as emotion, learning, and memory. The occipital lobe, primarily responsible for visual processing, is intricately connected to cognitive and behavioral control pathways, particularly about visuospatial ability. The superior temporal gyrus plays a vital role in sound processing. These observed findings suggest that the brain functions related to memory, learning, emotion, visuospatial, and sound may be impaired among RE patients. Compared to healthy controls, the discrepancy of NCp in INS.L between rs-fMRI and es-fMRI, suggesting the possible impact of electrical stimulation.

Our study demonstrates that both types of networks yield similar outcomes, indicating that the characteristics of network topological properties are prevalent in the brain networks of RE patients. Conducting a comprehensive analysis of both network types enhances the credibility of our findings. In our study, the results obtained from analyzing global and nodal network properties in RE patients are consistent and mutually reinforcing. The observed disruption of the small-world structure indicates a decline in local connections between different brain network regions, leading to a corresponding decrease in network transmission efficiency. Additionally, the nodal network properties exhibited decreased activity in the brain regions, such as

the thalamus, temporal lobe, occipital lobe, basal ganglia, and parahippocampus, whereas increased activity in the frontal lobe and precuneus among RE patients compared to healthy controls. This suggests disrupted connectivity within the brain networks of RE patients, potentially impairing the efficiency of information transmission and network functionality. Notably, these alterations impact brain functions related to consciousness, movement, somatosensory, visual, and auditory processes, emphasizing the mechanisms underlying the observed abnormal brain functions in RE patients.

4.3 Reduced network connectivity among intra-modules and inter-modules

Compared to healthy controls, network connectivity patterns in RE patients exhibited relatively diminished connections and weakened connectivity strength across the entire brain (Figures 5A,B). This observation implies potential reduced activity and impaired functions within areas, such as the occipital network areas and subcortical areas. The reduced connections between the frontal lobe and subcortical areas and the nodal property results suggest a potential weakening or disruption in synchronized activity between the cortex and the subcortical areas (particularly the thalamus), in RE patients. A previous animal study suggested that the cortex and thalamus are oscillatory structures responsible for generating sleep spindles (Steriade et al., 1985). Thus, our results indicate that reduced cortical-thalamic connectivity may affect normal brain activity. The es-fMRI brain networks exhibited a modular feature, with enhanced connections in the brain regions, such as the parieto-occipital lobe (Figure 5A). Nodal properties showed that the Dc values of parietal lobe were higher in RE patients than those in healthy subjects, supporting this finding. Enhanced parieto-occipital connectivity may be a remedy to offset the general reduced connections within inter-modules and intra-modules, allowing RE patients to maintain the basic functions of brain networks. These alterations in network connectivity among RE patients, even during resting-state, could serve as a compensatory mechanism before structural and functional damage ensues. This theory emphasizes the significance of functional connectivity changes before structural changes in certain conditions (Xu et al., 2019; Guan et al., 2022). The increased modular connectivity strength in the es-fMRI brain networks following electrical stimulation can be attributed to the activation of activity between specific brain regions through electrical stimulation, resulting in enhanced connectivity.

4.4 Electrical stimulation can regulate brain activity through network systems

Compared to rs-fMRI, es-fMRI showed comparatively lower σ and γ, as well as increased Lp in two network types and Cp in binary networks. The comparison of network property results among three groups offers additional support for these results. In general, the brain networks of es-fMRI displayed a weaker small-world property and a lower overall efficiency of information transmission. This increased local network connectivity (increased Cp) can be attributed to the effect of electrical stimulation, which causes certain regions of the brain to become more active. It indicates that electrical stimulation may play a significant role in influencing or modulating network activity or connectivity within the brain. Nodal properties suggest that electrical stimulation can contribute to the observed increases or decreases in the activity of certain brain regions compared to their pre-electrode implantation states. This modulation of brain network activity subsequently leads to changes in connectivity patterns, thereby affecting network properties, such as the small-world property.

Our present findings suggest that electrical stimulation may result in less efficient neuronal networks (a weaken small-world network), leading to decreased synchronized connectivity throughout the brain. We attribute the reasons for this outcome to several factors. First, there is a slight signal attenuation resulting from electrode implantation (Thompson et al., 2020). Though the impact is negligible after undergoing quality control and data preprocessing, it cannot be disregarded entirely. Second, various stimulation sites could produce distinctive effects on the characteristics of brain network, because each targeted stimulus might have a different function in brain network pathways. For example, the amygdala is a part of the limbic system and is associated with emotions. The frontal lobe is responsible for many higher cognitive functions, such as language and motor functions. Therefore, their regulation of brain activity might be different, which can lead to different network phenotypic characteristics. Based on the data conditions of our study, the effect of electrical stimulation with the amygdala as the main stimulus target may produce lower network efficiency results (Supplementary Table 1). Of course, more researches are needed to support this hypothesis, which will be improved in future study. Third, electrical stimulation does not solely activate the brain activity surrounding the stimulus point, but produces particular effects by regulating the activity of brain regions through a network system (Fox et al., 2014; Thompson et al., 2020; Vetkas et al., 2022b). Stimulation delivered through implanted electrodes can trigger activation in specific brain regions and enhance activity. By contrast, other regions of the brain may exhibit decreased activity or remain relatively inactive. Consequently, the interconnectivity between brain regions may undergo modification, thereby regulating the flow of information within the original network pathway. It is possible that brain networks as a whole may exhibit a reduction in network efficiency even if enhanced activity in certain brain regions. Combined with the increased Cp, nodal attributes and modular results of es-fMRI, we support the possibility of the latter two hypotheses.

However, the usefulness of this regulatory effect (activation or inhibition) for disease-specific brain networks varies in different circumstances. In other words, whether the electrical stimulation can achieve the desired therapeutic effect is dependent on the pathogenesis, severity of lesions (Fox et al., 2014), and network mechanism of particular diseases. RE, for instance, is primarily caused by recurrent and uncontrollable abnormal synchronous discharges from brain neurons. The treatment approach is to inhibit or terminate these discharges instead of activating them. If the stimulation in a particular area of the brain can regulate the interconnectivity of regions along the neural network pathway, resulting in reduced connectivity strength and efficiency, and ultimately inhibit aberrant synchronous neuronal activity, then this could advance the research

and clinical implementation of electrical stimulation for the treatment of RE. Therefore, there is a need for further experimental research to investigate the regulatory effects of electrical stimulation on the brain network systems in the treatment of specific diseases like RE. Several important issues need to be addressed, such as determining the optimal placement of implanted electrodes and effectively managing the regulatory effects. Various brain targets have been explored for deep brain stimulation (DBS) in RE. Targets that have been investigated in randomized controlled trials and are currently used clinically include the anterior nucleus of the thalamus (ANT), the centromedian nucleus of the thalamus (CMT), and the hippocampus (Zangiabadi et al., 2019). The impact of identical target stimulation on distinct epilepsy phenotypes varies. A systematic review analysis suggests more efficient DBS of ANT for focal seizures, wider use of CMT for generalized seizures, and hippocampal DBS for temporal lobe seizures (Vetkas et al., 2022a). In our study, the electrical stimulation sites were predominantly situated in the amygdala and heschls gyrus. However, given the limited findings currently available, it would be premature to conclude if the electrical stimulation at these targets can lead to more effective therapeutic outcomes. To achieve therapeutic benefits, it is advisable to target brain regions that have the potential to induce significant modulation of brain activity while simultaneously inhibiting or disrupting disease-related activities or connections. Future research will identify specific network connectivity models and corresponding network attributes from diverse stimulation sites of individuals with RE. Experimental verification is essential to investigate the changes in brain activity resulting from electrical stimulation. We propose that this study represents an essential initial step toward the comprehensive exploration of network alterations at the individual level following intracranial brain stimulation, which could potentially enhance clinical decision-making in the context of refractory neurological disorders.

5 Limitations

Our study had several limitations. First, it should be recognized that changes to the MRI scanner and parameters were introduced in the laboratory settings before and after electrode implantation, potentially influencing certain fMRI data. However, the authors of raw data conducted quality assessment and made a comparison with a larger sample of healthy individuals, to address this concern. Although the resulting es-fMRI data exhibited some noise and signal loss, these effects did not significantly impact the overall findings. As recommended by the authors (Thompson et al., 2020), data processing was primarily controlled to mitigate motion artifacts and noise, leading to the exclusion of relevant subjects and data. Second, the study faced limitations in establishing a correlation between patients' clinical characteristics and network connectivity due to constraints in available data. Third, due to relatively small sample size and unbalanced scanning conditions and parameters of this dataset, it is not sufficient for us to draw firm conclusions about the causal effects of electrical stimulation. However, we used two types of networks in the study to improve the scientific quality of the results. And the results of global attributes, nodal attributes and modular analysis supported and complemented each other, which increased the credibility and repeatability of the results of this study. To further substantiate the effects of electrical stimulation, we performed a comparative analysis of the global network properties of the different stimulation points (Supplementary Table 1; Figure 1). Due to the small sample size of the data, only the global network properties in amygdala and heschls gyrus were compared, and there are currently no obvious differences other than network efficiency. In conclusion, our study still provides a lot of information to support the study for the characteristics of brain networks and possible effects of electrical stimulation in patients with RE.

6 Conclusion

Our findings emphasize a reduction in small-world property among RE patients, indicating a shift toward random networks. This alteration in network architecture, characterized by reduced connectivity between network regions, potentially undermines network stability and information transmission efficiency. The revised inter-brain network connectivity pattern observed in RE patients may implicate cognitive and behavioral regulation. Electrical stimulation is a promising avenue for regulating specific brain regions or broader network systems. This approach offers a valuable means to investigate the effects of electrical stimulation on brain network connectivity and may supplement existing methodologies. This provides a foundation for studying the mechanisms of brain networks in RE and developing interventions. In future studies, larger sample sizes and monitoring dynamic changes in functional images following electrode implantation in RE patients will significantly enhance research in this field.

Data availability statement

Publicly available datasets were analyzed in this study. This data can be found at: https://openneuro.org/datasets/ds002799/versions/1.0.4.

Ethics statement

The studies involving humans were approved by The University of Iowa Institutional Review Board, Stanford University, and Caltech. The studies were conducted in accordance with the local legislation and institutional requirements. Written informed consent for participation in this study was provided by the participants' legal guardians/next of kin.

Author contributions

YS: Formal analysis, Funding acquisition, Investigation, Methodology, Project administration, Supervision, Writing – original draft, Writing – review & editing. QS: Writing – original draft, Writing – review & editing. MY: Supervision, Writing – review & editing. AM: Project administration, Supervision, Writing – review & editing, Formal analysis, Investigation, Methodology.

Funding

The author(s) declare financial support was received for the research, authorship, and/or publication of this article. This study work is supported by Science and Technology Development General Project of Nanjing Health Commission [Grant No. YKK22251] and Nanjing Medical University Fund Project [Grant No. NMUB20210177]. The [Dataset] ds002799 is funded by NIH grant U01NS103780 (RP, RA, and MH) The Simons Foundation Collaboration on the Global Brain (RA) Knut and Alice Wallenberg Foundation grant 2016.0473 (WHT) United Kingdom Wellcome Trust (CIP) and European Research Council (CIP) The OpenNeuro repository is funded by NIH Grant R24MH117179 (RP).

Acknowledgments

We express our gratitude to the authors of the [Dataset] ds002799 and the researchers of 1000 functional connectomes project for their efforts in procuring and making these datasets available without charge.

Conflict of interest

The authors declare that the research was conducted in the absence of any commercial or financial relationships that could be construed as a potential conflict of interest.

Publisher's note

All claims expressed in this article are solely those of the authors and do not necessarily represent those of their affiliated organizations, or those of the publisher, the editors and the reviewers. Any product that may be evaluated in this article, or claim that may be made by its manufacturer, is not guaranteed or endorsed by the publisher.

Supplementary material

The Supplementary material for this article can be found online at: https://www.frontiersin.org/articles/10.3389/fnins.2023.1282232/full#supplementary-material

References

Achard, S., Salvador, R., Whitcher, B., Suckling, J., and Bullmore, E. (2006). A resilient, low-frequency, small-world human brain functional network with highly connected association cortical hubs. *J. Neurosci.* 26, 63–72. doi: 10.1523/JNEUROSCI.3874-05.2006

Bai, F., Shu, N., Yuan, Y., Shi, Y., Yu, H., Wu, D., et al. (2012). Topologically convergent and divergent structural connectivity patterns between patients with remitted geriatric depression and amnestic mild cognitive impairment. *J. Neurosci.* 32, 4307–4318. doi: 10.1523/JNEUROSCI.5061-11.2012

Bassett, D. S., and Bullmore, E. T. (2017). Small-world brain networks revisited. *Neuroscientist* 23, 499–516. doi: 10.1177/1073858416667720

Biswal, B., Yetkin, F. Z., Haughton, V. M., and Hyde, J. S. (1995). Functional connectivity in the motor cortex of resting human brain using echo-planar MRI. *Magn. Reson. Med.* 34, 537–541. doi: 10.1002/mrm.1910340409

Bullmore, E., and Sporns, O. (2009). Complex brain networks: graph theoretical analysis of structural and functional systems. *Nat. Rev. Neurosci.* 10, 186–198. doi: 10.1038/nrn2575

Caplan, R., Siddarth, P., Stahl, L., Lanphier, E., Vona, P., Gurbani, S., et al. (2008). Childhood absence epilepsy: behavioral, cognitive, and linguistic comorbidities. *Epilepsia* 49, 1838–1846. doi: 10.1111/j.1528-1167.2008.01680.x

Drenthen, G. S., Fasen, F., Fonseca Wald, E. L. A., Backes, W. H., Aldenkamp, A. P., Vermeulen, R. J., et al. (2020). Functional brain network characteristics are associated with epilepsy severity in childhood absence epilepsy. *Neuroimage Clin.* 27:102264. doi: 10.1016/j.nicl.2020.102264

Fisher, R. S., Acevedo, C., Arzimanoglou, A., Bogacz, A., Cross, J. H., Elger, C. E., et al. (2014). ILAE official report: a practical clinical definition of epilepsy. *Epilepsia* 55, 475–482. doi: 10.1111/epi.12550

Forouzannezhad, P., Abbaspour, A., Fang, C., Cabrerizo, M., Loewenstein, D., Duara, R., et al. (2019). A survey on applications and analysis methods of functional magnetic resonance imaging for Alzheimer's disease. *J. Neurosci. Methods* 317, 121–140. doi: 10.1016/j.jneumeth.2018.12.012

Fox, M. D., Buckner, R. L., Liu, H., Chakravarty, M. M., Lozano, A. M., and Pascual-Leone, A. (2014). Resting-state networks link invasive and noninvasive brain stimulation across diverse psychiatric and neurological diseases. *Proc. Natl. Acad. Sci. U. S. A.* 111, E4367–E4375. doi: 10.1073/pnas.1405003111

Fried, I., Wilson, C. L., MacDonald, K. A., and Behnke, E. J. (1998). Electric current stimulates laughter. *Nature* 391:650. doi: 10.1038/35536

Greicius, M. (2008). Resting-state functional connectivity in neuropsychiatric disorders. *Curr. Opin. Neurol.* 21, 424–430. doi: 10.1097/WCO.0b013e328306f2c5

Guan, B., Xu, Y., Chen, Y. C., Xing, C., Xu, L., Shang, S., et al. (2022). Reorganized brain functional network topology in Presbycusis. *Front. Aging Neurosci.* 14:905487. doi: 10.3389/fnagi.2022.905487

Hatlestad-Hall, C., Bruna, R., Erichsen, A., Andersson, V., Syvertsen, M. R., Skogan, A. H., et al. (2021). The organization of functional neurocognitive networks in focal epilepsy correlates with domain-specific cognitive performance. *J. Neurosci. Res.* 99, 2669–2687. doi: 10.1002/jnr.24896

Helmstaedter, C., and Witt, J. A. (2017). Epilepsy and cognition - a bidirectional relationship? *Seizure* 49, 83–89. doi: 10.1016/j.seizure.2017.02.017

Jiang, W., Li, J., Chen, X., Ye, W., and Zheng, J. (2017). Disrupted structural and functional networks and their correlation with alertness in right temporal lobe epilepsy: a graph theory study. *Front. Neurol.* 8:179. doi: 10.3389/fneur.2017.00179

Jiang, L. W., Qian, R. B., Fu, X. M., Zhang, D., Peng, N., Niu, C. S., et al. (2018). Altered attention networks and DMN in refractory epilepsy: a resting-state functional and causal connectivity study. *Epilepsy Behav.* 88, 81–86. doi: 10.1016/j.yebeh.2018.06.045

Kitzbichler, M. G., Henson, R. N., Smith, M. L., Nathan, P. J., and Bullmore, E. T. (2011). Cognitive effort drives workspace configuration of human brain functional networks. *J. Neurosci.* 31, 8259–8270. doi: 10.1523/JNEUROSCI.0440-11.2011

Kwan, P., Arzimanoglou, A., Berg, A. T., Brodie, M. J., Allen Hauser, W., Mathern, G., et al. (2009). Definition of drug resistant epilepsy: consensus proposal by the ad hoc task force of the ILAE commission on therapeutic strategies. *Epilepsia* 51, 1069–1077. doi: 10.1111/j.1528-1167.2009.02397.x

Leitgeb, E. P., Sterk, M., Petrijan, T., Gradisnik, P., and Gosak, M. (2020). The brain as a complex network: assessment of EEG-based functional connectivity patterns in patients with childhood absence epilepsy. *Epileptic Disord.* 22, 519–530. doi: 10.1684/epd.2020.1203

Li, C., Huang, B., Zhang, R., Ma, Q., Yang, W., Wang, L., et al. (2017). Impaired topological architecture of brain structural networks in idiopathic Parkinson's disease: a DTI study. *Brain Imaging Behav.* 11, 113–128. doi: 10.1007/s11682-015-9501-6

Liu, Y., Liang, M., Zhou, Y., He, Y., Hao, Y., Song, M., et al. (2008). Disrupted small-world networks in schizophrenia. *Brain* 131, 945–961. doi: 10.1093/brain/awn018

Lozano, A. M., and Lipsman, N. (2013). Probing and regulating dysfunctional circuits using deep brain stimulation. *Neuron* 77, 406–424. doi: 10.1016/j.neuron.2013.01.020

Luo, C., Li, Q., Lai, Y., Xia, Y., Qin, Y., Liao, W., et al. (2011). Altered functional connectivity in default mode network in absence epilepsy: a resting-state fMRI study. *Hum. Brain Mapp.* 32, 438–449. doi: 10.1002/hbm.21034

Lynall, M. E., Bassett, D. S., Kerwin, R., McKenna, P. J., Kitzbichler, M., Muller, U., et al. (2010). Functional connectivity and brain networks in schizophrenia. *J. Neurosci.* 30, 9477–9487. doi: 10.1523/JNEUROSCI.0333-10.2010

Maslov, S., and Sneppen, K. (2002). Specificity and stability in topology of protein networks. *Science* 296, 910–913. doi: 10.1126/science.1065103

Meunier, D., Lambiotte, R., and Bullmore, E. T. (2010). Modular and hierarchically modular organization of brain networks. *Front. Neurosci.* 4:200. doi: 10.3389/fnins.2010.00200

Ogawa, S., Tank, D. W., Menon, R., Ellermann, J. M., Kim, S. G., Merkle, H., et al. (1992). Intrinsic signal changes accompanying sensory stimulation: functional brain

mapping with magnetic resonance imaging. *Proc. Natl. Acad. Sci. U. S. A.* 89, 5951–5955. doi: 10.1073/pnas.89.13.5951

Oya, H., Howard, M. A., Magnotta, V. A., Kruger, A., Griffiths, T. D., Lemieux, L., et al. (2017). Mapping effective connectivity in the human brain with concurrent intracranial electrical stimulation and BOLD-fMRI. *J. Neurosci. Methods* 277, 101–112. doi: 10.1016/j.jneumeth.2016.12.014

Parvizi, J., Jacques, C., Foster, B. L., Witthoft, N., Rangarajan, V., Weiner, K. S., et al. (2012). Electrical stimulation of human fusiform face-selective regions distorts face perception. *J. Neurosci.* 32, 14915–14920. doi: 10.1523/JNEUROSCI.2609-12.2012

Parvizi, J., Rangarajan, V., Shirer, W. R., Desai, N., and Greicius, M. D. (2013). The will to persevere induced by electrical stimulation of the human cingulate gyrus. *Neuron* 80, 1359–1367. doi: 10.1016/j.neuron.2013.10.057

Ponten, S. C., Bartolomei, F., and Stam, C. J. (2007). Small-world networks and epilepsy: graph theoretical analysis of intracerebrally recorded mesial temporal lobe seizures. *Clin. Neurophysiol.* 118, 918–927. doi: 10.1016/j.clinph.2006.12.002

Raichle, M. E., MacLeod, A. M., Snyder, A. Z., Powers, W. J., Gusnard, D. A., and Shulman, G. L. (2001). A default mode of brain function. *Proc. Natl. Acad. Sci. U. S. A.* 98, 676–682. doi: 10.1073/pnas.98.2.676

Rubinov, M., and Sporns, O. (2010). Complex network measures of brain connectivity: uses and interpretations. *NeuroImage* 52, 1059–1069. doi: 10.1016/j.neuroimage.2009.10.003

Schuele, S. U., and Luders, H. O. (2008). Intractable epilepsy: management and therapeutic alternatives. *Lancet Neurol.* 7, 514–524. doi: 10.1016/S1474-4422(08)70108-X

Sethi, M., Pedersen, M., and Jackson, G. D. (2016). Polymicrogyric cortex may predispose to seizures via abnormal network topology: an fMRI Connectomics study. *Epilepsia* 57, e64–e68. doi: 10.1111/epi.13304

Song, K., Li, J., Zhu, Y., Ren, F., Cao, L., and Huang, Z. G. (2021). Altered small-world functional network topology in patients with optic neuritis: a resting-state fMRI study. *Dis. Markers* 2021, 9948751–9948759. doi: 10.1155/2021/9948751

Sporns, O., and Zwi, J. D. (2004). The small world of the cerebral cortex. *Neuroinformatics* 2, 145–162. doi: 10.1385/NI:2:2:145

Stam, C. J., and Van Straaten, E. C. (2012). The organization of physiological brain networks. *Clin. Neurophysiol.* 123, 1067–1087. doi: 10.1016/j.clinph.2012.01.011

Steriade, M., Deschenes, M., Domich, L., and Mulle, C. (1985). Abolition of spindle oscillations in thalamic neurons disconnected from nucleus reticularis thalami. *J. Neurophysiol.* 54, 1473–1497. doi: 10.1152/jn.1985.54.6.1473

Sun, Y., Li, Y., Sun, J., Zhang, K., Tang, L., Wu, C., et al. (2021). Functional reorganization of brain regions into a network in childhood absence epilepsy: a magnetoencephalography study. *Epilepsy Behav.* 122:108117. doi: 10.1016/j.yebeh.2021.108117

Tao, H., Guo, S., Ge, T., Kendrick, K. M., Xue, Z., Liu, Z., et al. (2013). Depression uncouples brain hate circuit. *Mol. Psychiatry* 18, 101–111. doi: 10.1038/mp.2011.127

Tavakol, S., Royer, J., Lowe, A. J., Bonilha, L., Tracy, J. I., Jackson, G. D., et al. (2019). Neuroimaging and connectomics of drug-resistant epilepsy at multiple scales: from focal lesions to macroscale networks. *Epilepsia* 60, 593–604. doi: 10.1111/epi.14688

Thompson, W. H., Nair, R., Oya, H., Esteban, O., Shine, J. M., Petkov, C. I., et al. (2020). A data resource from concurrent intracranial stimulation and functional MRI of the human brain. *Sci. Data* 7:258. doi: 10.1038/s41597-020-00595-y

Tian, S., Sun, Y., Shao, J., Zhang, S., Mo, Z., Liu, X., et al. (2020). Predicting escitalopram monotherapy response in depression: the role of anterior cingulate cortex. *Hum. Brain Mapp.* 41, 1249–1260. doi: 10.1002/hbm.24872

Van Straaten, E. C., and Stam, C. J. (2013). Structure out of chaos: functional brain network analysis with EEG, MEG, and functional MRI. *Eur. Neuropsychopharmacol.* 23, 7–18. doi: 10.1016/j.euroneuro.2012.10.010

Vetkas, A., Fomenko, A., Germann, J., Sarica, C., Iorio-Morin, C., Samuel, N., et al. (2022a). Deep brain stimulation targets in epilepsy: systematic review and meta-analysis of anterior and centromedian thalamic nuclei and hippocampus. *Epilepsia* 63, 513–524. doi: 10.1111/epi.17157

Vetkas, A., Germann, J., Elias, G., Loh, A., Boutet, A., Yamamoto, K., et al. (2022b). Identifying the neural network for neuromodulation in epilepsy through connectomics and graphs. *Brain Commun.* 4:92. doi: 10.1093/braincomms/fcac092

Vlooswijk, M. C., Vaessen, M. J., Jansen, J. F., de Krom, M. C., Majoie, H. J., Hofman, P. A., et al. (2011). Loss of network efficiency associated with cognitive decline in chronic epilepsy. *Neurology* 77, 938–944. doi: 10.1212/WNL.0b013e31822cfc2f

Wang, R., Lin, J., Sun, C., Hu, B., Liu, X., Geng, D., et al. (2020). Topological reorganization of brain functional networks in patients with mitochondrial encephalomyopathy with lactic acidosis and stroke-like episodes. *Neuroimage Clin.* 28:102480. doi: 10.1016/j.nicl.2020.102480

Wang, J., Qiu, S., Xu, Y., Liu, Z., Wen, X., Hu, X., et al. (2014). Graph theoretical analysis reveals disrupted topological properties of whole brain functional networks in temporal lobe epilepsy. *Clin. Neurophysiol.* 125, 1744–1756. doi: 10.1016/j.clinph.2013.12.120

Wang, J., Wang, X., Xia, M., Liao, X., Evans, A., and He, Y. (2015). GRETNA: a graph theoretical network analysis toolbox for imaging connectomics. *Front. Hum. Neurosci.* 9:386. doi: 10.3389/fnhum.2015.00386

Wang, X. B., Zhao, X. H., Jiang, H., Qian, X. I., and Wang, P. J. (2014). Small-worldness of brain fMRI network in patients with mild cognitive impairment. *Chin. J. Med. Imaging Technol.* 30, 791–793. doi: 10.13929/j.1003-3289.2014.05.040

Wang, J., Zuo, X., Dai, Z., Xia, M., Zhao, Z., Zhao, X., et al. (2013). Disrupted functional brain connectome in individuals at risk for Alzheimer's disease. *Biol. Psychiatry* 73, 472–481. doi: 10.1016/j.biopsych.2012.03.026

Watts, D. J., and Strogatz, S. H. (1998). Collective dynamics of 'small-world' networks. *Nature* 393, 440–442. doi: 10.1038/30918

Xia, M., Wang, J., and He, Y. (2013). BrainNet viewer: a network visualization tool for human brain connectomics. *PLoS One* 8:e68910. doi: 10.1371/journal.pone.0068910

Xu, J., Chen, F., Liu, T., Wang, T., Zhang, J., Yuan, H., et al. (2019). Brain functional networks in type 2 diabetes mellitus patients: a resting-state functional MRI study. *Front. Neurosci.* 13:239. doi: 10.3389/fnins.2019.00239

Zalesky, A., Fornito, A., and Bullmore, E. (2012). On the use of correlation as a measure of network connectivity. *NeuroImage* 60, 2096–2106. doi: 10.1016/j.neuroimage.2012.02.001

Zangiabadi, N., Ladino, L. D., Sina, F., Orozco-Hernandez, J. P., Carter, A., and Tellez-Zenteno, J. F. (2019). Deep brain stimulation and drug-resistant epilepsy: a review of the literature. *Front. Neurol.* 10:601. doi: 10.3389/fneur.2019.00601

Zhang, D., and Raichle, M. E. (2010). Disease and the brain's dark energy. *Nat. Rev. Neurol.* 6, 15–28. doi: 10.1038/nrneurol.2009.198

Zhang, J., Wang, J., Wu, Q., Kuang, W., Huang, X., He, Y., et al. (2011). Disrupted brain connectivity networks in drug-naive, first-episode major depressive disorder. *Biol. Psychiatry* 70, 334–342. doi: 10.1016/j.biopsych.2011.05.018

Zheng, H., Li, F., Bo, Q., Li, X., Yao, L., Yao, Z., et al. (2018). The dynamic characteristics of the anterior cingulate cortex in resting-state fMRI of patients with depression. *J. Affect. Disord.* 227, 391–397. doi: 10.1016/j.jad.2017.11.026

Glossary

RE	Refractory epilepsy
fMRI	Functional magnetic resonance imaging
rs-fMRI	The resting-state fMRI of RE patients
es-fMRI	The fMRI concurrent electrical stimulation of RE patients
HC-fMRI	Healthy controls' fMRI
GRETNA	A graph theoretical network analysis toolbox for imaging connectomics
ASMs	Anti-seizure medications
CAE	Childhood absence epilepsy
TLE	Temporal lobe epilepsy
EPI	Echo-planar imaging
TR	Repetition time
TE	Echo time
TI	Inversion time
AUC	Area under the curve
FD	Framewise displacement
DMN	Default mode network
Sigma (σ)	Small-worldness
Cp	Clustering coefficient
Lp	Characteristic path length
Gamma (γ)	Normalized clustering coefficient`
Lambda (λ)	Normalized characteristic path length
Eg	Global network efficiency
Eloc	Local network efficiency
NCp	Nodal clustering coefficient
NLp	Nodal characteristic shortest path length
Bc	Betweenness centrality
Dc	Degree centrality
AUC	Area under the curve
FFG.L	Left fusiform gyrus
PUT.L	Left putamen
PUT.R	Right putamen
THA.L	Left thalamus
THA.R	Right thalamus
PAL.L	Left pallidum
PAL.R	Right pallidum
PCUN.R	Right precuneus
ROL.L	Left rolandic operculum
SMG.L	Left supramarginal gyrus
SOG. R	Right superior occipital gyrus
INS. L	Left insula
PHG. L	Left parahippocampal gyrus
PreCG. L	Left precental gyrus
STG. L	Left superior temporal gyrus
DBS	Deep brain stimulation
ANT	Anterior thalamic nucleus
CMT	Centromedian thalamic nucleus

frontiers | Frontiers in Neuroscience

TYPE Original Research
PUBLISHED 18 January 2024
DOI 10.3389/fnins.2023.1295151

OPEN ACCESS

EDITED BY
Yilong Ma,
Feinstein Institute for Medical Research,
United States

REVIEWED BY
Craig David Workman,
University of Iowa Hospitals and Clinics,
United States
Martin Lotze,
University of Greifswald, Germany

*CORRESPONDENCE
Usman Jawed Shaikh
ushaik@ukaachen.de
Ferdinand Binkofski
f.binkofski@fz-juelich.de

†These authors share first authorship

RECEIVED 15 September 2023
ACCEPTED 20 November 2023
PUBLISHED 18 January 2024

CITATION
Shaikh UJ, Pellicano A, Schüppen A, Heinzel A, Winz OH, Herzog H, Mottaghy FM and Binkofski F (2024) Increasing striatal dopamine release through repeated bouts of theta burst transcranial magnetic stimulation of the left dorsolateral prefrontal cortex. A 18F-desmethoxyfallypride positron emission tomography study.
Front. Neurosci. 17:1295151.
doi: 10.3389/fnins.2023.1295151

Increasing striatal dopamine release through repeated bouts of theta burst transcranial magnetic stimulation of the left dorsolateral prefrontal cortex. A 18F-desmethoxyfallypride positron emission tomography study

Usman Jawed Shaikh[1*†], Antonello Pellicano[2†], Andre Schüppen[1,3], Alexander Heinzel[4,5], Oliver H. Winz[4], Hans Herzog[5], Felix M. Mottaghy[4,6,7] and Ferdinand Binkofski[5,1,7*]

[1]Section Clinical Cognitive Sciences, Department of Neurology, Faculty of Medicine, RWTH Aachen University, Aachen, Germany, [2]Department of Educational Sciences, University of Catania, Catania, Italy, [3]Interdisciplinary Center for Clinical Research – Brain Imaging Facility, University Hospital Aachen, Aachen, Germany, [4]Department of Nuclear Medicine, Faculty of Medicine, RWTH Aachen University, Aachen, Germany, [5]Research Centre Juelich, Institute of Neuroscience and Medicine (INM-4), Juelich, Germany, [6]Department of Radiology and Nuclear Medicine, Maastricht University Medical Center (MUMC+), Maastricht, Netherlands, [7]Juelich Aachen Research Alliance (JARA)—BRAIN, Juelich, Germany

Introduction: Transcranial Magnetic Stimulation (TMS) can modulate fronto-striatal connectivity in the human brain. Here Positron Emission Tomography (PET) and neuro-navigated TMS were combined to investigate the dynamics of the fronto-striatal connectivity in the human brain. Employing 18F-DesmethoxyFallypride (DMFP) – a Dopamine receptor-antagonist – the release of endogenous dopamine in the striatum in response to time-spaced repeated bouts of excitatory, intermittent theta burst stimulation (iTBS) of the Left-Dorsolateral Prefrontal Cortex (L-DLPFC) was measured.

Methods: 23 healthy participants underwent two PET sessions, each one with four blocks of iTBS separated by 30 minutes: sham (control) and verum (90% of individual resting motor threshold). Receptor Binding Ratios were collected for sham and verum sessions across 37 time frames (about 130 minutes) in striatal sub-regions (Caudate nucleus and Putamen).

Results: Verum iTBS increased the dopamine release in striatal sub-regions, relative to sham iTBS. Dopamine levels in the verum session increased progressively across the time frames until frame number 28 (approximately 85 minutes after the start of the session and after three iTBS bouts) and then essentially remained unchanged until the end of the session.

Conclusion: Results suggest that the short-timed iTBS protocol performed in time-spaced blocks can effectively induce a dynamic dose dependent increase in dopaminergic fronto-striatal connectivity. This scheme could provide an alternative to unpleasant and distressing, long stimulation protocols in experimental and therapeutic settings. Specifically, it was demonstrated that three repeated bouts of iTBS, spaced by short intervals, achieve larger effects than one single stimulation. This finding has implications for the planning of therapeutic interventions, for example, treatment of major depression.

KEYWORDS

positron emission tomography (PET), transcranial magnetic stimulation (TMS), intermittent theta burst stimulation (iTBS), prefrontal cortex (PFC), dorso-lateral prefrontal cortex (DLPFC), resting motor threshold (rMT), ANOVA, repeated-measure analysis of variance

1 Introduction

The fronto-striatal networks share a well-established association between the frontal cortex and sub-cortical areas (striatum) and are responsible for a wide range of motor and cognitive functions that includes emotion regulation, movement, and attention (Beste et al., 2012). Dopamine plays a vital role in maintaining the normal function in the cortico-subcortical system (Carlsson and Carlsson, 1990; Cachope and Cheer, 2014; Kaiser et al., 2018) over the lifespan (Klostermann et al., 2012; Parr et al., 2021). Earlier animal studies have shown evidence of frontal cortex control over striatal dopamine release (Murase et al., 1993; Karreman and Moghaddam, 2002). Furthermore, animal and human experiments demonstrated that transcranial brain stimulation is able to induce significant release of dopamine and measurable changes in dopaminergic function in cortico-striatal networks (Bean et al., 1989; Strafella et al., 2001; Keck et al., 2002; Kanno et al., 2004). However, up to date little is known about the dose dependent effects of frontal stimulation on the striatal dopamine release in humans.

Neuroimaging techniques such as positron emission tomography (PET) provide the opportunity to quantify dopaminergic activity in the human brain (Badgaiyan, 2010; Kaiser et al., 2018). Neuroimaging studies employed multimodal combination of PET and non-invasive, repetitive transcranial magnetic stimulation (rTMS) (Paus et al., 1997, 2001; Chouinard et al., 2003; Ko et al., 2008; Cho and Strafella, 2009; Hallett et al., 2017). In their seminal study, Strafella et al. (2001) provided evidence of cortico-striatal control of dopamine release in the human brain, by applying rTMS on the left dorsolateral prefrontal cortex (DLPFC) and measuring the dopamine release in striatum using 11C-Raclopride. Their results displayed a significant dopamine release in the ipsilateral caudate. Later, they targeted the primary motor cortex with the same rTMS protocol and found evidence for induction of dopamine release in the ipsilateral putamen (Strafella, 2003).

Abnormalities in the fronto-striatal dopaminergic system are observed in movement disorders, such as Parkinson's disease (Kish et al., 1988; Zgaljardic et al., 2003; Cropley et al., 2008), in schizophrenia (Grace, 1991; Lotze et al., 2009; Haber and Knutson, 2010; Lin et al., 2018) and in depression (Willner, 1983; Paus and Barrett, 2004; Furman et al., 2011; Li et al., 2015). Non-invasive brain stimulation is a potential tool for the treatment of neuropsychiatric disorders (Tremblay et al., 2020; Fried et al., 2021; Rossi et al., 2021). Therapeutical effects of rTMS are based on its capability to modulate brain activity and neurotransmitter release (Philip et al., 2019; Cole et al., 2020; Cristancho et al., 2020; Ishida et al., 2020; Zrenner et al., 2020). The DLPFC is one of the most frequently stimulated regions for therapeutic purposes, while it is highly interconnected with cortical and sub-cortical areas (Sibon et al., 2007; Cho and Strafella, 2009; Tik et al., 2017; Dowdle et al., 2018; Masina et al., 2019). Studies have shown, that the left DLPFC and right DLPFC possess an imbalance in activity, therefore providing high freuqency TMS on the left DLPFC accelerates the lower acitivity in the region (Johnson et al., 2013; Janicak and Dokucu, 2015). Considering the literature on the role of the DLPFC in depression, different DLPFC-rTMS protocols have been explored regarding their therapeutic potentials to improve depression symptoms (Bulteau et al., 2019; Mendlowitz et al., 2019; Ishida et al., 2020). Among them, the intermittent theta burst represents a reliable approach for its relatively short duration of application and its positive effects on adults with treatment-resistant depression (Li et al., 2014; Duprat et al., 2016). Indeed, iTBS can be delivered within 3 min (instead of the 37 min needed for a conventional 10 Hz rTMS treatment session) and demonstrated clinical effectiveness and safety at the same time (Huang et al., 2005; Blumberger et al., 2018; McGirr et al., 2021).

Stimulation intensity plays an important part in the effectiveness of iTBS protocols. By employing resting state functional Magnetic Resonance Imaging (rsfMRI) and different intensities of iTBS to the left DLPFC, our group demonstrated the threshold dependent modulation of fronto-striatal functional connectivity (Alkhasli et al., 2019). In particular, we applied iTBS at sub-threshold (90% rMT) and supra-threshold (120% rMT) intensities. Interestingly, the sub-threshold intensity was associated with a more reliable increase in functional connectivity between the DLPFC and bilateral Caudate Nucleus, as compared to supra-threshold intensity.

One important aspect of the present study is the choice of 18F-Desmethoxyfallypride (DMFP) which is a selective dopamine D2/D3 receptor radioligand (Mukherjee et al., 1996). The sensitivity of the radiotracer towards competition with dopamine allows the detection of changes in the levels of endogenous dopamine after the intervention of TMS. The binding of such a radiotracer has been shown to be inversely proportional to levels of dopamine concentration (Endres et al., 1997; Laruelle, 1997). This radioligand fulfils the demand of pharmacologic challenging studies because of its longer physical half-life of 110 min and its availability also at sites without a local cyclotron unit (Mukherjee et al., 2002; Gründer et al., 2003). During such long DMFP-PET measurements repeated iTBS became possible. Indeed, this is a crucial advantage over the 11C-Raclopride, that allows for shorter measurements given its much shorter half-life of 20 min (Schreckenberger et al., 2004; Li et al., 2014; Nettekoven et al., 2014; Hanlon et al., 2017). For example, Strafella in their two seminal studies (Strafella et al., 2001; Strafella, 2003) performed the TMS before the start of the 11C-Raclopride PET measurements.

In sum, the aim of the present study was to test the dose dependent effects of repeated bouts of iTBS over the left DLPFC on the dopamine

Abbreviations: PET, positron emission tomography; TMS, transcranial magnetic stimulation; iTBS, intermittent theta burst stimulation; PFC, prefrontal cortex; DLPFC, dorso-lateral prefrontal cortex; 18F-DMFP, 18 Flouride- Desmethoxy Fallypride; rMT, resting motor threshold; ANOVA, repeated-measure analysis of variance.

release in the striatum. Therefore the analysis were restricted within the brain mask of the striatum. The repeated iTBS was delivered in intervals of 30 min. Stimulations inside the PET scanner were performed using neuro-navigation. We used DMFP as tracer, which allowed us to perform measurements lasting 130 min.

2 Materials and methods

2.1 Participants

A total number of 26 healthy participants were recruited; three of them were excluded from the analyses because they did not conclude their scans: one participant complained of back pain while laying in the PET scanner, two participants completed the first session but did not show-up for the second session. Analyses were conducted on data from 23 participants (nine females and fourteen males) with an age range of 18–65 years (mean age = 27.82, SD = 12.08), mean height of 174.60 cm (SD = 8.64) and mean weight of 74.78 kg (SD = 11.69). All of them were right-handed having a mean score of 95.77 (SD = 0.21) (quantified with the Edinburgh Handedness Inventory, Oldfield, 1971) and had no record of psychiatric or neurological disorder. Exclusion criteria were: contraindications for MRI (metals in the body such as magnetic dental implants, implantable neurostimulation systems, cathetors with metallic components, stents, piercings. etc), TMS (metal implants in the head such as cochlear implants, Implanted Cardioverter Defibrillator, Deep brain stimulator) and/or PET imaging: Claustrophobia; pregnancy, a test was performed on the day of each scan. All participants gave written informed consent after receiving full information on the study. They received a compensation of 350 € for participating in the study.

The study was in accordance with the Declaration of Helsinki and approved by the ethic committee (Protocol number: 003/15) of the Aachen University Hospital, RWTH Aachen University (Germany). Furthermore, the PET protocol was approved by the German authority for radiation protection in humans [Bundesamt für Strahlenschutz (BfS)].

2.2 Experimental procedure

In order to get the subjects familiar with the TMS protocol and to check their tolerability of the procedure a pre-screening session for each volunteer was performed. This included the application of the excitatory iTBS protocol to the prefrontal cortex with stimulation intensity equal to 90% of the individual resting motor threshold (rMT; procedure described below).

The experiment was conducted on three separate days for each participant. On day one, the screening for exclusion criteria, the informed written consent, and an MRI scan of the brain anatomy was acquired.

The verum and the sham stimulation sessions were administered on day two and day three, with their order counterbalanced between the participants.

2.3 Transcranial magnetic stimulation

The anatomical scan was integrated with a 3D model of the participant's head obtained through an infrared neuro-navigation system (TMS navigator, Localite GmbH, Sankt Augustin, Germany). For the TMS equipment, a figure-of-eight coil (model: C-B60) was connected to a X100 MagPro simulator (MagVenture, Farum, Denmark). The Hotspot (M1 hand area) was determined visually by identifying anatomical landmarks in the primary morter cortex of each participant before delivering biphasic single pulses. The individual rMT was obtained through the collection of at least 5 motor evoked potentials (MEPs) over 10 stimulations with a peak greater than 50 uV. The stimulation intensity at the TMS machine was first increased in 2% steps until the determination of hotspot (M1 hand area), and then reduced stepwise to find out the lowest TMS intensity still inducing the supra threshold MEPs (greater than 50 uV). MEPs were recorded from the contralateral first dorsal interosseus (FDI) muscle of the right hand with pre-gelled surface electrodes. This procedure enabled us to determine the stimulation strength from M1 hand area, which is an important parameter and also a prerequisite for the stimulation at the brain target area.

The exact positioning of the TMS coil on the target site (iTBS over the DLPFC) of participant's head was guided in real-time by the same previously described infrared neuro-navigational system. From behind the PET scanner, the TMS coil was fixed on the participant's head with the help of a mechanical arm, whereas infrared cameras were placed in front of the PET scanner. Individual anatomical images were transformed into the Talairach system using the neuronavigation system (Localite TMS navigator), with the stimulation target (i.e., Dorsolateral Prefrontal Cortex) identified by the following Talairach coordinates (x, y, z): −45,45,35 (Fitzgerald et al., 2009). For the PET image analysis in SPM the MNI system was used.

The sham and verum stimulation session, consisted of 4 excitatory iTBS (Huang et al., 2005) delivered to the left-DLPFC at 30 min interval (Figure 1). Excitatory iTBS protocol was comprised of 600 pulses, delivered in a sequence of 20 trains and 10 theta-bursts in a total duration of 190 s. Each 2 s long train consisted of a burst of 3 stimuli at 50 Hz, repeated in 5 Hz frequency and having inter-train interval of 8 s. In the verum condition, the stimulation intensities were set to 90% of the individual rMT (mean score = 38.65 ± 9.33). In the sham condition, the stimulation intensities were set at 30%, and the placebo coil was placed at the same target site as verum.

2.4 Magnetic resonance imaging

MRI scans were performed on a Magnetom Prisma 3.0 Tesla scanner (Siemens Medical Solutions, Erlangen, Germany). Anatomical data were acquired using a 3D magnetization-prepared, rapid acquisition gradient echo sequence (MPRAGE) with the following parameter: TR = 2,300 ms, TE = 2.98 ms, FOV = 256 mm, 176 sagital slices, slice thickness = 1 mm, in-plane resolution = 1 × 1 × 1 mm and matrix size of 256 × 256 × 128. The obtained T1 anatomical image from the MRI scanner was utilized for the imaging analysis including the setup for neuro navigation system and also for PET co-registration.

2.5 Positron emision tomography

The images were acquired on a Siemens ECAT EXACT HR+ scanner (Siemens-CTI, Knoxville, TN, USA). During the PET measurement, a 1-cm thick lead neck shield was used to limit scatter

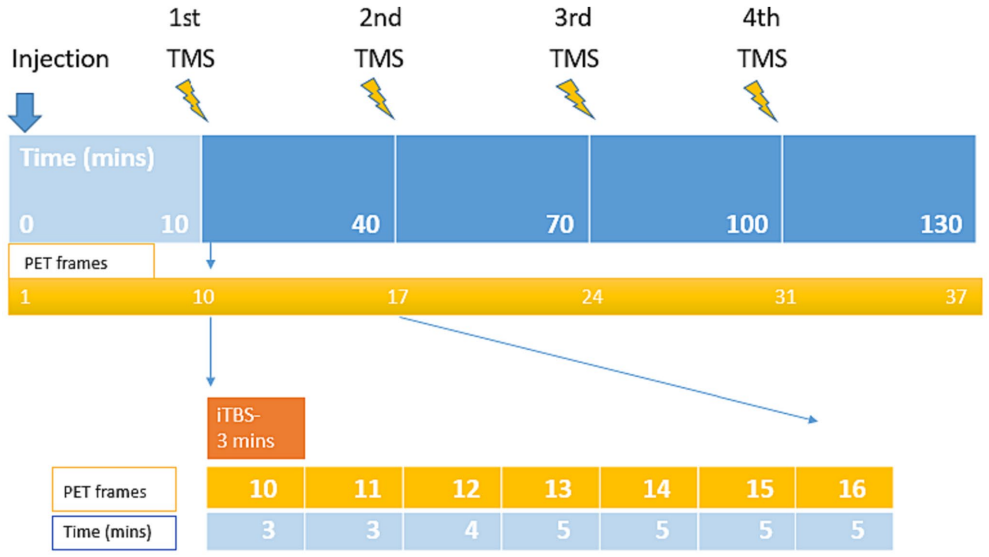

FIGURE 1
Visualization of the experimental design and durations of the combined TMS and PET measurement. The PET scan lasted 130 min, consisting of 4 iTBS, each delivered in 3 min stimulations delivered to the left-DLPFC at 30 min interval.

radiation arising from outside the field of view. PET data acquisition was initiated simultaneously with the bolus infusion of the radioligand (followed by a saline flush). A 18F-DMFP dose of approx. 200 MBq was administered to each of the participants per session. The doses (mean ± SD) were: 198.38 ± 7.66 at Day 1, and 201.42 ± 7.53 at Day 2 (total: 389.96 ± 10.02). PET data acquisition protocol comprised of a series of 37 time frames with a progressively increasing duration [3 × 20 s, 3 × 60 s, 3 × 120 s (2 min), 8 × 180 s (3 min), 4 × 240 s (4 min) and 16 × 300 s (5 min)].

PET scan was initiated simultaneously with the radiotracer injection. The first iTBS was delivered 10 min after the injection (i.e., into the uptake time of the radiotracer). In total, PET scan included 37 frames: the initial 9 frames (frame 1–9, total 10 min) were reserved for radiotracer uptake, and the remaining 28 frames (frame 10–37, total 120 min) were allocated for the experiment. For each block of Short iTBS (3 min), 7 gradually increasing PET frames were recorded.

18F-DMFP demonstrates as a highly reliable tracer for PET imaging of D2, D3 striatal dopamine receptors, which also acts as an efficient substitute for 11C-Raclopride, with the major advantage of carrying 18F-label, allowing the possibility for the transportation to PET facilitities (Mukherjee et al., 1996; Gründer et al., 2003). It also adds the benefit of using non-invasive reference methods without arterial blood sampling providing valid receptor quantities in human striatum region (procedure described below). 18F-DMFP shares the same intermediate affinity as 11C-Raclopride, but has a slight advantage for the binding in the extrastriatal regions like cortices (Mukherjee et al., 1996).

The dynamic molecular imaging technique used in this study detects the competition between the injected radiotracer and the endogenous dopamine for the occupancy of the same receptor binding sites. This competition results in the displacement of the radioligand from the receptor sites by the endogenous dopamine released by the TMS. Therefore, lower receptor bindings indicates the result of a higher dopamine concentration in the synaptic cleft (Badgaiyan et al., 2009; Badgaiyan, 2010).

2.6 Image pre-processing

The individual emission datasets were reconstructed per time frame by three-dimensional filtered back projection (Hamming filter, cut-off at 4 mm) algorithm resulting in 63 slices (2.425 mm thickness) using a128 × 128 image matrix (pixel size 2×2 mm). Datasets were fully corrected for photon attenuation, random coincidences, scatter radiation, and dead time. All image pre-processing procedures were performed using a dedicated software package (PMOD, version 3.8, PMOD Technologies, Zurich, Switzerland).

For each subject, the dynamic PET images were first automatically (mutual information algorithm) realigned to correct for potential effects of head movement. All PET processing were then performed according to an automatic protocol using the PMOD Fusion Tool (PFUS). Re-aligned PET images were first rigidly co-registered to individual Anatomical MRI scan. Then the individual MR images were spatially normalized and nonlinearly co-registered to the MNI space and the resulting transformation parameters were subsequently applied to each PET frame. All normalized co-registered images were visually checked for accuracy, and if necessary, manually adjusted.

For the region-based group comparison analysis of sham-verum stimulations, predefined masks were generated for each subject according to the WFU pick ATLAS. The predefined masks included the region of interest for caudate nucleus, putamen and cerebellum. Volume of Interests drawn on the normalized images were used to extract dynamic Time Activity Curves from the striatum and cerebellum region.

The standard methods including simplified reference tissue approach for the calculation of the binding of the radiotracer has an important prerequisite, stating that the condition of the system to

be investigated is not amended. The application of the online-rTMS during the acquisition disturbs the system and creates an unstable condition. This violates the case and the valid outcome parameters such as Binding Potential and Relative Distribution Volume are not applicable here.

In order to describe the receptor behaviour in our TMS study, simple ratio method is implemented as an alternative approach which extracts the indices pointing to the receptor binding.

Receptor Binding Ratios were calculated from the simple ratio of specifically bound radioactivity in a receptor-rich (RC) and a receptor-free (RF) region, (RC/RF). The cerebellum (including the cerebellar hemispheres without the vermis) was used as the reference region, because of its lack of D2/3 receptors as described earlier (Siessmeier et al., 2005). Hence, simple ratios of striatal and cerebellar activities [S/C(t)] at different time points were derived for both sham and verum conditions, providing instantaneous values with changing over time.

Receptor Binding Ratios of the radiolabelled receptor ligands is inversely proportional to the concentration of dopamine. Therefore a reduction in the Receptor Binding Ratios in the striatum region after the TMS to the DLPFC suggest's an increase in the amount of striatal dopamine.

As an alternative approach to the simplified reference tissue model, PET images were normalized to the cerebellum by dividing them with there corresponding cerebellar acitivties. Difference between the PET images (sham and verum condition) were calculated for the different time points. The resulting outcome is interpreted as indices of the neuroreceptor behaviour as a function of the rTMS.

For the voxel-based analysis on the images of binding ratios at each time point, paired t-test model was implemented in SPM 12 (Welcome Department of Imaging Neuroscience, London). The images were masked with a small search region (striatum). Direct contrast analysis (difference) between TMS condition (Sham vs. Verum) was calculated. *A-priori* striatal areas were defined using the masks from WFU_Pick-Atlas (SPM extension toolbox).

2.7 Statistical analysis

A within-participants repeated-measure analysis of variance (ANOVA) was performed on mean Receptor Bindings with *Area* (Caudate Nucleus vs. Putamen), *Hemisphere* (left vs. right), *Time Frame* (frame 10 to 37), and *TMS* (sham vs. verum) as within-subjects factors. A probability value of $p = 0.05$ was set as the significance threshold. Partial eta-squared (η^2_p) was calculated within the ANOVA as a measure of effect size.

All statistical tests were performed in SPSS (IBM, USA). When necessary, paired samples *t*-tests were performed as post-hoc comparisons with Bonferroni-corrected *p* value, as well as explorative difference (reverse Helmert) contrasts. An open-source tool was used to compute Cohen's d_z effect size for the *t*-tests.[1]

1 https://memory.psych.mun.ca/models/stats/effect_size.shtml

3 Results

3.1 Analysis of variance

Crucial for our hypothesis, the main effect of *TMS* resulted significant [$F(1, 22) = 6.282$, $p = 0.020$, $\eta^2_p = 0.22$]: the Receptor Binding was reduced in the verum stimulation (mean Receptor Binding = 2.21) relative to the sham stimulation condition (mean Receptor Binding = 2.45) (Figure 2) and Table 1.

The main effect of *Time Frame* was significant [$F(27, 594) = 239.124$, $p < 0.001$, $\eta^2_p = 0.92$], displaying an increasing pattern of receptor binding over the time frame sequence (i.e., from frame 10 to 37). Importantly, the interaction between TMS and Time Frame was also significant [$F(27, 594) = 2.731$, $p < 0.001$, $\eta^2_p = 0.11$] (see Figure 3). Difference contrasts (reverse Helmert contrasts) were applied to explore changes of the effect size (i.e., the receptor binding difference between sham and verum conditions) across the time frames. The effect size increased significantly at time frame 11 relative to time frame 10 [$F(1, 22) = 5.210$, $p = 0.032$, $\eta^2_p = 0.19$], at time frame 14 [$F(1, 22) = 5.107$, $p = 0.034$, $\eta^2_p = 0.19$], at time frame 16–20 [$Fs(1, 22) <= 7.229$, $p <= 0.044$, $\eta^2_p <= 0.25$], 24 and 25 [$Fs(1, 22) <= 7.062$, $p <= 0.043$, $\eta^2_p <= 0.24$], and 27 and 28 [$Fs(1, 22) <= 5.937$, $p <= 0.031$, $\eta^2_p <= 0.21$], relative to the mean of previous frames. In other terms, compared to the sham condition, receptor bindings in the verum condition showed a progressive decrease from time frame 10 to time frame 28 and then stabilized until frame 37. No other interactions involved TMS.

ANOVA also revealed a significant main effect of *Area* [$F(1, 22) = 181.323$, $p < 0.001$, $\eta^2_p = 0.89$], indicating that the Receptor Binding in the Putamen (mean Receptor Binding = 2.77) was higher than in the Caudate Nucleus (mean Receptor Binding = 1.89). The main effect of *Hemisphere* was not significant [$F(1, 22) = 0.316$, $p = 0.584$, $\eta^2_p = 0.01$]. The interaction between Area and Hemisphere [$F(1, 22) = 16.582$, $p < 0.001$, $\eta^2_p = 0.43$] was significant: Receptor Bindings were lower in the left Putamen (mean Receptor Binding = 2.72) relative to the right Putamen (mean Receptor Binding = 2.82) [$t(22) = 3.261$, $p = 0.004$, $d_z = 0.67$]. No difference was observed between the left Caudate Nucleus (mean Receptor Binding = 1.91) and the right Caudate Nucleus (mean Receptor Binding = 1.80) [$t(22) = 1.617$, $p = 0.120$, $d_z = 0.34$] (Bonferroni-corrected alpha level = 0.025).

Among other interactions, Time Frame interacted with Area [$F(27, 594) = 18.828$, $p < 0.001$, $\eta^2_p = 0.46$] and with Area and Hemisphere [$F(27, 594) = 7.134$, $p < 0.001$, $\eta^2_p = 0.24$]. These interactions are not crucial to test our experimental hypothesis, since they pooled together data from real (verum) and "fake" (sham) TMS. *Post-hoc*/pairwise comparisons are reported from these interactions for the sake of completeness. In the Area and Time Frame interaction, Putamen compared with Time Frames 10 to 27 results in significance [$t(22) <= 18.170$, $p <= 0.016$] and Time Frames 28 to 37 non-significance [$t(22) <= 2.062$, $p >= 0.05$], Caudate Nucleus compared with Time Frame 10 to 21 [$t(22) <= 17.701$, $p <= 0.001$] and Time Frames 22 to 37 non-significance [$t(22) <= 1.571$, $p >= 0.05$]. In the Interaction from Area, Hemisphere and Time frame, Putamen with left Hemisphere from Time Frame 10 to 21 shows significance [$t(22) <= 22.012$, $p <= 0.001$] and the Time Frames 22 to 37 non-significance [$t(22) <= 8.011$, $p >= 0.05$], Putamen with right Hemisphere Time Frames 10 to 21 shows significance [$t(22) <=$

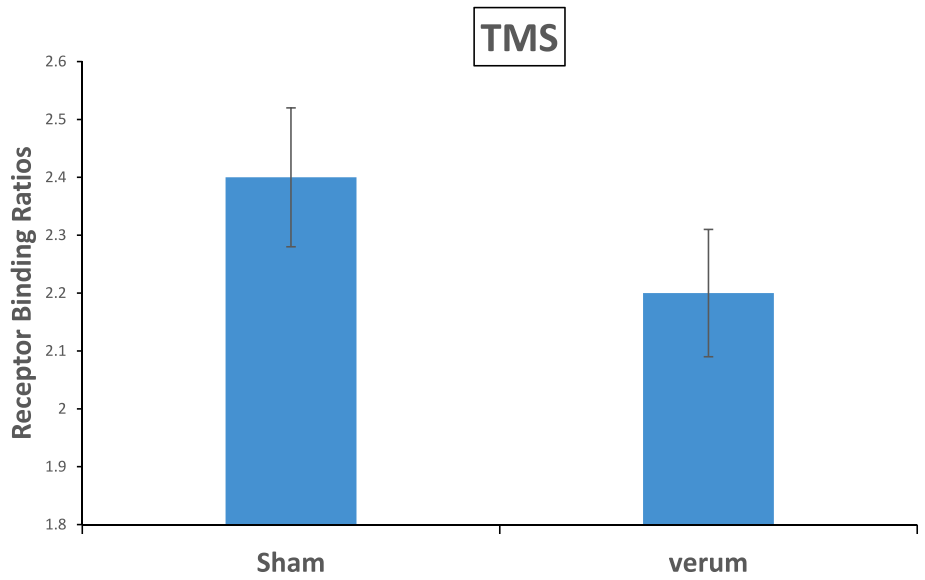

FIGURE 2
The main effect of TMS results in significance with a value of p = 0.02 on the Receptor Binding in the striatum. The verum stimulation showed a reduction of 8.6% 18F-DMFP Receptor Binding as compared to the sham stimulation. Error bars represents the standard errors.

TABLE 1 Statistically significant repeated measures of ANOVA results.

Measure	Effect	SS	*df*	MD	*F*	*p*	η^2_p
TMS	Main effect	70.16	(1,22)	70.16	6.28	0.020	0.22
Time Frame	Main effect	783.01	(27,594)	29.00	239.12	0.000	0.22
TMS, Time Frame	Interaction	7.09	(27,594)	0.26	2.73	0.000	0.11
Area	Main effect	993.88	(1,22)	993.88	181.32	0.000	0.89
Area, Hemisphere	Interaction	25.36	(1,22)	25.36	16.58	0.000	0.43
Time Frame, Area	Interaction	33.88	(27,594)	1.25	18.82	0.000	0.46
Time Frame, Area Hemisphere	Interaction	4.24	(27,594)	0.15	7.134	0.000	0.24

Repeated measures analysis of variance results in significant main effects and interaction effects. Significance levels were computed using value of $p < 0.05$. SS, sum of squares; df, degrees of freedom; MS, mean squares; MD, mean difference; F, *F*-ratio; *p*, value of *p*; n^2p, partial eta square.

22.024, $p <= 0.001$] and the Time Frames 22 to 37 non-significance [$t(22) <= 9.043$, $p >= 0.05$], also Caudate Nucleus with left Hemisphere from Time Frame 10 to 21 shows significance [$t(22) <= 9.011$, $p <= 0.001$] and the Time Frames 22 to 37 non-significance [$t(22) <= 7.002$, $p >= 0.05$], Caudate Nucleus with right Hemisphere Time Frames 10 to 28 shows significance [$t(22) <= 9.023$, $p <= 0.001$] and the Time Frames 29 to 37 non-significance [$t(22) <= 7.033$, $p >= 0.05$].

3.2 SPM analyses

Analyses were restricted to data from time frames 17–37, that is after the second, third and fourth iTBS, where the Receptor Binding effect size was maximum and essentially stabilized across the time frames. The results showed a contralateral dopamine release in the basal ganglia region with one separate cluster, the largest one having its peak at the $x = 4$, $y = 14$, $z = 6$ coordinates (Nucleus Caudate). The peak *t* was 8.85 and the cluster size was 46 voxels (see Figure 4).

4 Discussion

The primary goal of the present study was to evaluate the dose dependent effects of iTBS to the L-DLPFC on dopamine release in the striatum using more advanced radiotracer and stimulation protocol than in earlier studies (Strafella et al., 2001). We wanted to disentangle the iTBS aftereffects on fronto-striatal connectivity by implementing neuro-navigated repeated bouts of iTBS, with 30 min interval, in a sham-controlled study. On the basis of the results we also wanted to find implications for the planning of therapeutic interventions with iTBS on L-DLPFC.

In line with our hypotheses, we found that the application of repetitive blocks of iTBS over L-DLPFC (verum stimulation) resulted in a significant increase of dopaminergic levels in the striatum (as reflected by decreased Receptor Bindings) compared to sham stimulation (Figure 2). Specifically, increased releases of dopamine were localized in the contralateral caudate nucleus (Figure 4). Importantly, dopamine levels in the verum condition increased progressively across the time frames until time frame 28

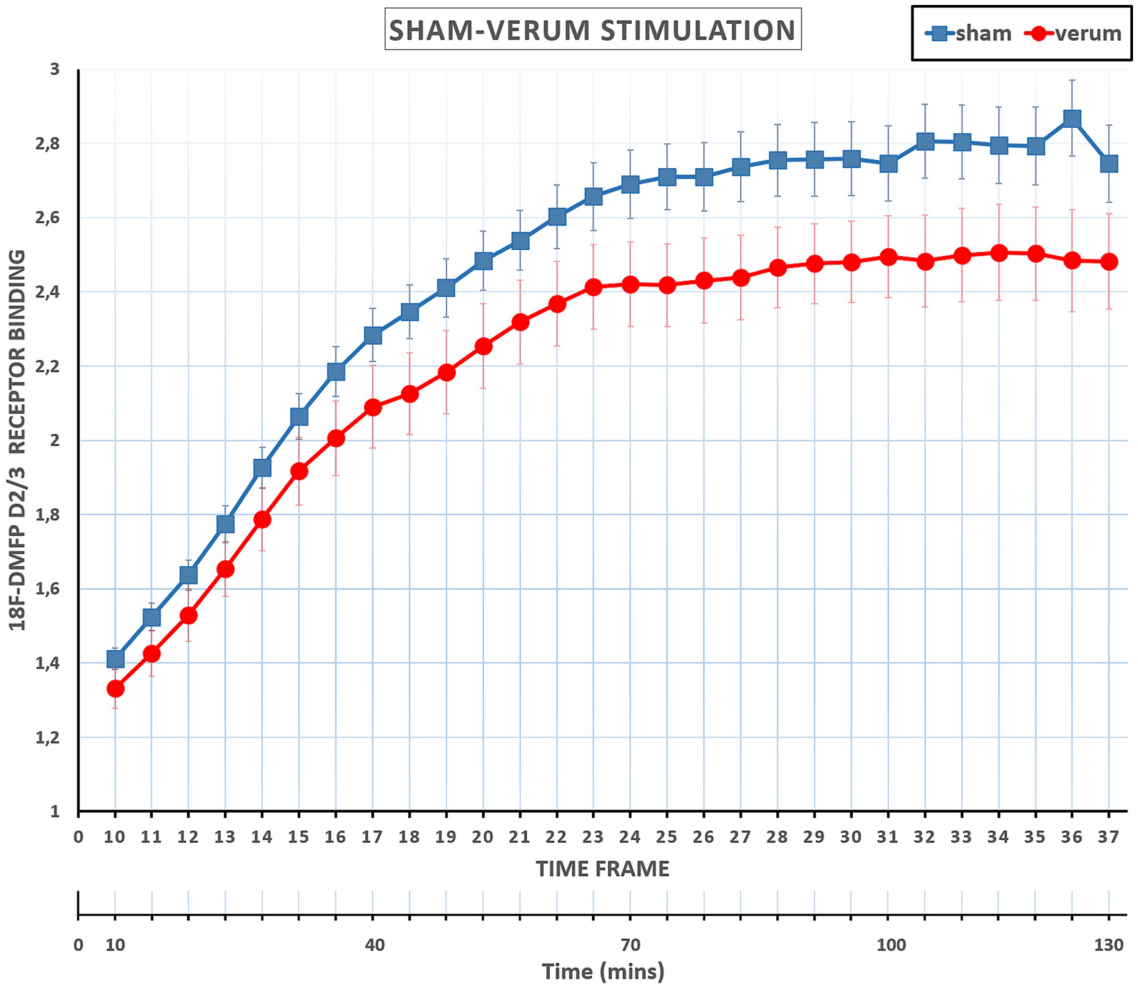

FIGURE 3
Mean Receptor Binding ratios at sham and verum TMSs across time frames 10 to 37. Receptor Binding ratios in the verum condition showed a progressive decrease from time frame 10 to time frame 28 (about 85 min) and then essentially stabilized until the end of the session, frame 37. Error bars represents the standard errors. PET scan included 37 frames (Total scan time of 130 min): the initial 9 frames (frame 1–9, total 10 min) were reserved for radiotracer uptake, and the remaining 28 frames (frame 10–37, total 120 min) were allocated for the experiment and also utilized for the interventions.

(approximately 85 min after the start of the session and after three iTBS bouts), and then essentially stabilized until the end of the session. In summary, our data show that repeated blocks of iTBS resulted in dose-dependent effects on the dopaminergic level with the enhancement of dopaminergic fronto-striatal connectivity. These results are in accordance with a previous study by Nettekoven et al. (2014), in which iTBS dose-dependent enhancement of brain connectivity was observed after stimulations of the Primary Motor Cortex.

The physiological mechanism behind the iTBS induced connectivity is that excitatory cortico-striatal projections can promote dopamine release by a local effect of glutamate on adjacent nigrostriatal nerve terminals (Chéramy et al., 1986). Such an effect may be mediated by glutamate receptors in the striatum, perhaps acting on dopamine nerve terminals (Hanbauer et al., 1992). These various observations from human (Strafella, 2003), primate studies (Ohnishi et al., 2004) and also between healthy subjects and patient groups (Pogarell et al., 2006, 2007) strongly emphasize how underlying neurochemical changes and the functional state of neuronal circuits along with different stimulation parameters may influence rTMS effects on striatal dopamine release.

The most important factor for the success of our study was the use of the radiotracer 18F-DMFP, which has a different data acquisition protocol in comparison to the previously used 11C-Raclopride tracer. The best direct comparison of the two ligands was performed by Siessmeier and colleagues (Siessmeier et al., 2005). It was demonstrated that the 18F-DMFP had a longer scan time as compared to the 11C-Raclopride. The use of DMFP allowed for a single injection followed by a dynamic acquisition of the effects of the repeated iTBS. Also important for our study was, that this tracer is not dependent on an onsite production due to the long half-life.

The findings of this study have not only significant theoretical, but also clinical implications.

Our study further supports the modulatory effects of TMS on dopaminergic circuits (Badgaiyan, 2010). The observation of increased dopaminergic activity in the Striatum is consistent with previous

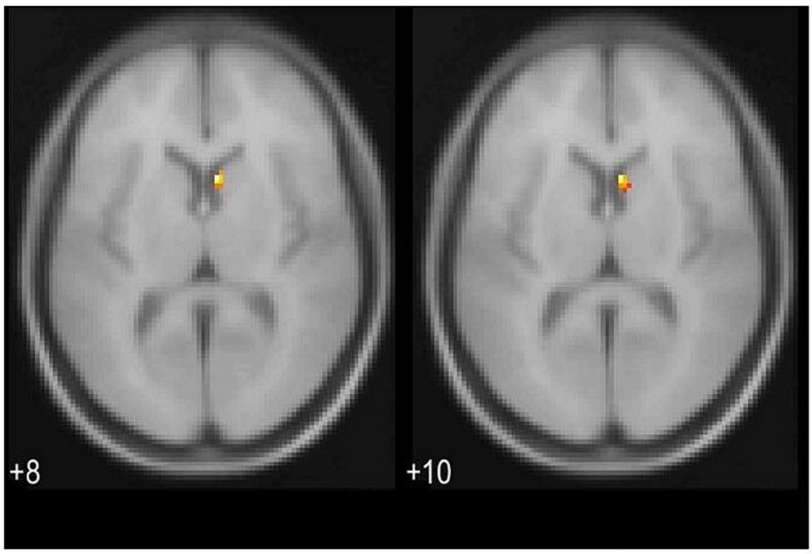

Statistics: ***p-values adjusted for search volume***

set-level		cluster-level				peak-level					coordinates (MNI)		
p	c	$p_{FWE\text{-}corr}$	$q_{FDR\text{-}corr}$	k_E	p_{uncorr}	$p_{FWE\text{-}corr}$	$q_{FDR\text{-}corr}$	T	(Z_E)	p_{uncorr}	x	y	z
0.000	3	0.001	0.017	46	0.011	0.000	0.000	8.85	Inf	0.000	4	14	6

FIGURE 4
TMS sham vs. verum contrast (difference between the images) analysis for time frames 17 to 37 (2nd, 3rd, and 4th TMS blocks). The statistical parametric map (axial section) of the change in 18F-DMFP Receptor Binding is overlaid on the MNI stereotaxic space. The color scale represents the *T*-statistic. The parameters for displaying the image are as following, threshold $T = 3.926$ and value of $p < 0.05$ (FWE). Release of dopamine is assessed using PET following four bouts of iTBS to the left DLPF cortex. Release is demonstrated by a reduction in 18F-DMFP binding. The results showed a separate cluster in the striatum region, the largest one having its peak at the coordiantes of $x = 4$, $y = 14$, $z = 6$ (Caudate Nucleus), and a size of 46 voxels. This observation shows that the prefrontal-striatal fibers can modulate the release of dopamine.

structural and functional studies that have implicated these areas as a consequence of TMS (Strafella et al., 2001; Strafella, 2003; Ko et al., 2008).

In patients with major depression, Pogarell and others (Pogarell et al., 2006) showed a reduction of 123I-IBZM Binding Potential (9.6%) in the striatum after left prefrontal stimulation. Using 11C-Raclopride PET, Kim et al. (2008) investigated the therapeutic effect of rTMS on motor cortex in PD patients. On two consecutive days, two sessions of rTMS induced a significant decrease of Binding Potential in the contralateral Caudate Nucleus (12.1%, but not ipsilateral to the stimulated hemisphere), while providing significant clinical benefits, as measured by the motor section of the Unified Parkinson's Disease Rating Scale (UPDRS III). In fact, studies into synaptic plasticity have not only been an important driving force in neuroscience research but they are also contributing to the understanding of brain activity responses related to stimuli and finding new solutions to treat diseases.

Recently, comparison studies came with some striking observations of higher iTBS efficiency with respect to conventional rTMS protocols (Paus and Barrett, 2004; Cristancho et al., 2020). In patients with treatment-resistant depression, positive effects of iTBS were non-inferior to those obtained with 10 Hz rTMS. To note, the duration of a iTBS protocol is significantly reduced to a few minutes, compared to a rTMS protocol which normally lasts not less than 30 min. Furthermore, from a practical-operational point of view, by use of shorter iTBS protocols, either the number of stimulations within one session can be increased or the number of patients treated per day can be kept significantly higher without compromising clinical effectiveness (Blumberger et al., 2018).

TMS has been shown to normalize abnormal functional connectivity of cortico-cortical circuits in depression. Interestingly, Avissar and his group (Avissar et al., 2017), applied daily and over a 5 weeks period 10 Hz excitatory TMS on the left DLPFC. This protocol established higher functional connectivity between the DLPFC and striatum, which predicted better treatment response. Our study has shown comparable results and supports the use of TMS in clinical trials. More reliably, our findings suggest that three blocks of stimulation (spaced by 30 min interval) within one session are practicable and have a dose dependent additive effect on the dopamine activity in the striatum. This may plausibly correspond to increased therapeutic effectiveness of single therapeutic sessions.

5 Limitations

In the clinical application, it would be relevant to explore the effects on Dopamine also in patients. For the cumulative effects, it cannot be stated for sure that the increasing effects during the time

course is solely due to repeated stimulation, i.e., it cannot be excluded completely that one bout alone results in delayed increasing effects. To test this, separate sessions with one, two, three and four bouts would have been required.

Considering the large age population (18–65) in the study, the effects might not be equivalent for the younger and older subjects. Also, here we have a mixture of men and women, the neuromechanisms for the effects of non-invasive brain stimulation might depend on the biological sex, see Rudroff et al. (2020) for an example in tDCS and Inghilleri et al. (2004) for example with rTMS.

Further research, incorporating a sample size with only men or women, with different combinations of stimulation protocols (e.g., continuous vs. intermittent theta burst), should be carried out. Furthermore, studies comparing healthy subjects and patients with depression and parkinson's disease could lead to further understanding of the frontal-striatal network, and its effectiveness using with TMS as a possible treatment.

6 Conclusion

The repeated bouts of iTBS over the prefrontal cortex induced a dose dependent increase of regional prefrontal excitation and led to a modulation of the fronto-striatal network. These results provide an important contribution to the understanding of the mechanisms of cortically controlled dopamine release in the striatum.

This study also proposes a novel experimental approach – repeated blocks of iTBS – that allows to detect changes in radioligand binding during the uptake phase. Mapping of increased dopamine release was demonstrated in contralateral striatum in healthy subjects. For what concerns potential therapeutic applications, it is worth of mentioning that a three times repetition of iTBS can increase the effectiveness of the intervention, whereas further repetitions seem not to provide any additional benefit.

Data availability statement

The raw data supporting the conclusions of this article will be made available by the authors, without undue reservation.

Ethics statement

The studies involving humans were approved by Ethical committee, faculty of medicine, RWTH Aachen University (protocol number: 003/15). The studies were conducted in accordance with the local legislation and institutional requirements. The participants provided their written informed consent to participate in this study.

Author contributions

US: Writing – original draft, Writing – review & editing, Conceptualization, Formal analysis, Investigation, Methodology, Software, Visualization. AP: Formal analysis, Investigation, Methodology, Software, Validation, Writing – review & editing. AS: Resources, Software, Visualization, Writing – review & editing. AH: Resources, Writing – review & editing. OW: Resources, Software, Visualization, Writing – review & editing. HH: Methodology, Validation, Writing – review & editing. FM: Conceptualization, Funding acquisition, Methodology, Project administration, Supervision, Writing – review & editing. FB: Conceptualization, Funding acquisition, Methodology, Project administration, Supervision, Writing – review & editing.

Funding

The author(s) declare financial support was received for the research, authorship, and/or publication of this article. This work was supported by the Brain Imaging Facility of the Interdisciplinary Center for Clinical Research (IZKF) Aachen within the Faculty of Medicine at RWTH Aachen University.

Acknowledgments

We would like to thank Ruben Scholle and Anna Simanek for their support in the recruitment of the participants, and the conduction of the experiment, and Giorgio Papitto for his support in the conduction of the experiment.

Conflict of interest

The authors declare that the research was conducted in the absence of any commercial or financial relationships that could be construed as a potential conflict of interest.

Publisher's note

References

Alkhasli, I., Sakreida, K., Mottaghy, F. M., and Binkofski, F. (2019). Modulation of Fronto-striatal functional connectivity using transcranial magnetic stimulation. *Front. Hum. Neurosci.* 13:190. doi: 10.3389/fnhum.2019.00190

Avissar, M., Powell, F., Ilieva, I., Respino, M., Gunning, F. M., Liston, C., et al. (2017). Functional connectivity of the left DLPFC to striatum predicts treatment response of depression to TMS. *Brain Stimul.* 10, 919–925. doi: 10.1016/j.brs.2017.07.002

Badgaiyan, R. D. (2010). Dopamine is released in the striatum during human emotional processing. *Neuroreport* 21, 1172–1176. doi: 10.1097/WNR.0b013e3283410955

Badgaiyan, R. D., Fischman, A. J., and Alpert, N. M. (2009). Dopamine release during human emotional processing. *NeuroImage* 47, 2041–2045. doi: 10.1016/j.neuroimage.2009.06.008

Bean, A. J., During, M. J., and Roth, R. H. (1989). Stimulation-induced release of coexistent transmitters in the prefrontal cortex: an in vivo microdialysis study of dopamine and neurotensin release. *J. Neurochem.* 53, 655–657. doi: 10.1111/j.1471-4159.1989.tb07384.x

Beste, C., Ness, V., Lukas, C., Hoffmann, R., Stüwe, S., Falkenstein, M., et al. (2012). Mechanisms mediating parallel action monitoring in fronto-striatal circuits. *NeuroImage* 62, 137–146. doi: 10.1016/j.neuroimage.2012.05.019

Blumberger, D. M., Vila-Rodriguez, F., Thorpe, K. E., Feffer, K., Noda, Y., Giacobbe, P., et al. (2018). Effectiveness of theta burst versus high-frequency repetitive transcranial magnetic stimulation in patients with depression (THREE-D): a randomised non-inferiority trial. *Lancet* 391, 1683–1692. doi: 10.1016/S0140-6736(18)30295-2

Bulteau, S., Beynel, L., Marendaz, C., DallIgna, G., Peré, M., Harquel, S., et al. (2019). Twice-daily neuronavigated intermittent theta burst stimulation for bipolar depression: a randomized sham-controlled pilot study. *Neurophysiol. Clin.* 49, 371–375. doi: 10.1016/j.neucli.2019.10.002

Cachope, R., and Cheer, J. F. (2014). Local control of striatal dopamine release. *Front. Behav. Neurosci.* 8:188. doi: 10.3389/fnbeh.2014.00188

Carlsson, M., and Carlsson, A. (1990). Interactions between glutamatergic and monoaminergic systems within the basal ganglia--implications for schizophrenia and Parkinson's disease. *Trends Neurosci.* 13, 272–276. doi: 10.1016/0166-2236(90)90108-m

Chéramy, A., Romo, R., Godeheu, G., Baruch, P., and Glowinski, J. (1986). In vivo presynaptic control of dopamine release in the cat caudate nucleus—II. Facilitatory or inhibitory influence ofl-glutamate. *Neuroscience* 19, 1081–1090. doi: 10.1016/0306-4522(86)90124-7

Cho, S. S., and Strafella, A. P. (2009). rTMS of the left dorsolateral prefrontal cortex modulates dopamine release in the ipsilateral anterior cingulate cortex and orbitofrontal cortex. *PLoS One* 4:e6725. doi: 10.1371/journal.pone.0006725

Chouinard, P. A., Van Der Werf, Y. D., Leonard, G., and Paus, T. (2003). Modulating neural networks with transcranial magnetic stimulation applied over the dorsal premotor and primary motor cortices. *J. Neurophysiol.* 90, 1071–1083. doi: 10.1152/jn.01105.2002

Cole, E. J., Stimpson, K. H., Bentzley, B. S., Gulser, M., Cherian, K., Tischler, C., et al. (2020). Stanford accelerated intelligent neuromodulation therapy for treatment-resistant depression. *Am. J. Psychiatr.* 177, 716–726. doi: 10.1176/appi.ajp.2019.19070720

Cristancho, P., Kamel, L., Araque, M., Berger, J., Blumberger, D. M., Miller, J. P., et al. (2020). iTBS to relieve depression and executive dysfunction in older adults: an open label study. *Am. J. Geriatr. Psychiatry* 28, 1195–1199. doi: 10.1016/j.jagp.2020.03.001

Cropley, V. L., Fujita, M., Bara-Jimenez, W., Brown, A. K., Zhang, X.-Y., Sangare, J., et al. (2008). Pre- and post-synaptic dopamine imaging and its relation with frontostriatal cognitive function in Parkinson disease: PET studies with [11C]NNC 112 and [18F]FDOPA. *Psychiatry Res.* 163, 171–182. doi: 10.1016/j.pscychresns.2007.11.003

Dowdle, L. T., Brown, T. R., George, M. S., and Hanlon, C. A. (2018). Single pulse TMS to the DLPFC, compared to a matched sham control, induces a direct, causal increase in caudate, cingulate, and thalamic BOLD signal. *Brain Stimul.* 11, 789–796. doi: 10.1016/j.brs.2018.02.014

Duprat, R., Desmyter, S., Rudi, D. R., van Heeringen, K., Van den Abbeele, D., Tandt, H., et al. (2016). Accelerated intermittent theta burst stimulation treatment in medication-resistant major depression: a fast road to remission? *J. Affect. Disord.* 200, 6–14. doi: 10.1016/j.jad.2016.04.015

Endres, C. J., Kolachana, B. S., Saunders, R. C., Su, T., Weinberger, D., Breier, A., et al. (1997). Kinetic modeling of [11C]raclopride: combined PET-microdialysis studies. *J. Cereb. Blood Flow Metab.* 17, 932–942. doi: 10.1097/00004647-199709000-00002

Fitzgerald, P. B., Maller, J. J., Hoy, K. E., Thomson, R., and Daskalakis, Z. J. (2009). Exploring the optimal site for the localization of dorsolateral prefrontal cortex in brain stimulation experiments. *Brain Stimul.* 2, 234–237. doi: 10.1016/j.brs.2009.03.002

Fried, P. J., Santarnecchi, E., Antal, A., Bartres-Faz, D., Bestmann, S., Carpenter, L. L., et al. (2021). Training in the practice of noninvasive brain stimulation: recommendations from an IFCN committee. *Clin. Neurophysiol.* 132, 819–837. doi: 10.1016/j.clinph.2020.11.018

Furman, D. J., Hamilton, J. P., and Gotlib, I. H. (2011). Frontostriatal functional connectivity in major depressive disorder. *Biol. Mood Anxiety Disord.* 1:11. doi: 10.1186/2045-5380-1-11

Grace, A. A. (1991). Phasic versus tonic dopamine release and the modulation of dopamine system responsivity: a hypothesis for the etiology of schizophrenia. *Neuroscience* 41, 1–24. doi: 10.1016/0306-4522(91)90196-u

Gründer, G., Siessmeier, T., Piel, M., Vernaleken, I., Buchholz, H.-G., Zhou, Y., et al. (2003). Quantification of D2-like dopamine receptors in the human brain with 18F-desmethoxyfallypride. *J. Nucl. Med.* 44, 109–116.

Haber, S. N., and Knutson, B. (2010). The reward circuit: linking primate anatomy and human imaging. *Neuropsychopharmacology* 35, 4–26. doi: 10.1038/npp.2009.129

Hallett, M., Di Iorio, R., Rossini, P. M., Park, J. E., Chen, R., Celnik, P., et al. (2017). Contribution of transcranial magnetic stimulation to assessment of brain connectivity and networks. *Clin. Neurophysiol.* 128, 2125–2139. doi: 10.1016/j.clinph.2017.08.007

Hanbauer, I., Wink, D., Osawa, Y., Edelman, G. M., and Gaily, J. A. (1992). Role of nitric oxide in NMDA-evoked release of [3H]-dopamine from striatal slices. *Neuroreport* 3, 409–412. doi: 10.1097/00001756-199205000-00008

Hanlon, C. A., Dowdle, L. T., Correia, B., Mithoefer, O., Kearney-Ramos, T., Lench, D., et al. (2017). Left frontal pole theta burst stimulation decreases orbitofrontal and insula activity in cocaine users and alcohol users. *Drug Alcohol Depend.* 178, 310–317. doi: 10.1016/j.drugalcdep.2017.03.039

Huang, Y.-Z., Edwards, M. J., Rounis, E., Bhatia, K. P., and Rothwell, J. C. (2005). Theta burst stimulation of the human motor cortex. *Neuron* 45, 201–206. doi: 10.1016/j.neuron.2004.12.033

Inghilleri, M., Conte, A., Currà, A., Frasca, V., Lorenzano, C., and Berardelli, A. (2004). Ovarian hormones and cortical excitability. An rTMS study in humans. *Clin. Neurophysiol.* 115, 1063–1068. doi: 10.1016/J.CLINPH.2003.12.003

Ishida, T., Dierks, T., Strik, W., and Morishima, Y. (2020). Converging resting state networks unravels potential remote effects of transcranial magnetic stimulation for major depression. *Front. Psych.* 11:836. doi: 10.3389/fpsyt.2020.00836

Janicak, P., and Dokucu, M. E. (2015). Transcranial magnetic stimulation for the treatment of major depression. *Neuropsychiatr. Dis. Treat.* 11, 1549–1560. doi: 10.2147/NDT.S67477

Johnson, K. A., Baig, M., Ramsey, D., Lisanby, S. H., Avery, D., McDonald, W. M., et al. (2013). Prefrontal rTMS for treating depression: location and intensity results from the OPT-TMS multi-site clinical trial. *Brain Stimul.* 6, 108–117. doi: 10.1016/j.brs.2012.02.003

Kaiser, R. H., Treadway, M. T., Wooten, D. W., Kumar, P., Goer, F., Murray, L., et al. (2018). Frontostriatal and dopamine markers of individual differences in reinforcement learning: a multi-modal investigation. *Cereb. Cortex* 28, 4281–4290. doi: 10.1093/cercor/bhx281

Kanno, M., Matsumoto, M., Togashi, H., Yoshioka, M., and Mano, Y. (2004). Effects of acute repetitive transcranial magnetic stimulation on dopamine release in the rat dorsolateral striatum. *J. Neurol. Sci.* 217, 73–81. doi: 10.1016/j.jns.2003.08.013

Karreman, M., and Moghaddam, B. (2002). The prefrontal cortex regulates the basal release of dopamine in the limbic striatum: an effect mediated by ventral tegmental area. *J. Neurochem.* 66, 589–598. doi: 10.1046/j.1471-4159.1996.66020589.x

Keck, M. E., Welt, T., Müller, M. B., Erhardt, A., Ohl, F., Toschi, N., et al. (2002). Repetitive transcranial magnetic stimulation increases the release of dopamine in the mesolimbic and mesostriatal system. *Neuropharmacology* 43, 101–109. doi: 10.1016/S0028-3908(02)00069-2

Kim, J. Y., Chung, E. J., Lee, W. Y., Shin, H. Y., Lee, G. H., Choe, Y.-S., et al. (2008). Therapeutic effect of repetitive transcranial magnetic stimulation in Parkinson's disease: analysis of [11C] raclopride PET study. *Mov. Disord.* 23, 207–211. doi: 10.1002/mds.21787

Kish, S. J., Shannak, K., and Hornykiewicz, O. (1988). Uneven pattern of dopamine loss in the striatum of patients with idiopathic Parkinson's disease. Pathophysiologic and clinical implications. *N. Engl. J. Med.* 318, 876–880. doi: 10.1056/NEJM198804073181402

Klostermann, E. C., Braskie, M. N., Landau, S. M., O'Neil, J. P., and Jagust, W. J. (2012). Dopamine and frontostriatal networks in cognitive aging. *Neurobiol. Aging* 33, 623.e15–623.e24. doi: 10.1016/j.neurobiolaging.2011.03.002

Ko, J. H., Monchi, O., Ptito, A., Bloomfield, P., Houle, S., and Strafella, A. P. (2008). Theta burst stimulation-induced inhibition of dorsolateral prefrontal cortex reveals hemispheric asymmetry in striatal dopamine release during a set-shifting task: a TMS-[(11)C]raclopride PET study. *Eur. J. Neurosci.* 28, 2147–2155. doi: 10.1111/j.1460-9568.2008.06501.x

Laruelle, M. D. M. (1997). Imaging D2 receptor occupancy by endogenous dopamine in humans. *Neuropsychopharmacology* 17, 162–174. doi: 10.1016/S0893-133X(97)00043-2

Li, C.-T., Chen, M.-H., Juan, C.-H., Huang, H.-H., Chen, L.-F., Hsieh, J.-C., et al. (2014). Efficacy of prefrontal theta-burst stimulation in refractory depression: a randomized sham-controlled study. *Brain* 137, 2088–2098. doi: 10.1093/brain/awu109

Li, Z., He, Y., Tang, J., Zong, X., Hu, M., and Chen, X. (2015). Molecular imaging of striatal dopamine transporters in major depression--a meta-analysis. *J. Affect. Disord.* 174, 137–143. doi: 10.1016/j.jad.2014.11.045

Lin, P., Wang, X., Zhang, B., Kirkpatrick, B., Öngür, D., Levitt, J. J., et al. (2018). Functional dysconnectivity of the limbic loop of frontostriatal circuits in first-episode, treatment-naive schizophrenia. *Hum. Brain Mapp.* 39, 747–757. doi: 10.1002/hbm.23879

Lotze, M., Reimold, M., Heymans, U., Laihinen, A., Patt, M., and Halsband, U. (2009). Reduced ventrolateral fMRI response during observation of emotional gestures related to the degree of dopaminergic impairment in Parkinson disease. *J. Cogn. Neurosci.* 21, 1321–1331. doi: 10.1162/jocn.2009.21087

Masina, F., Tarantino, V., Vallesi, A., and Mapelli, D. (2019). Repetitive TMS over the left dorsolateral prefrontal cortex modulates the error positivity: an ERP study. *Neuropsychologia* 133:107153. doi: 10.1016/j.neuropsychologia.2019.107153

McGirr, A., Vila-Rodriguez, F., Cole, J., Torres, I. J., Arumugham, S. S., Keramatian, K., et al. (2021). Efficacy of active vs sham intermittent Theta burst transcranial magnetic stimulation for patients with bipolar depression. *JAMA Netw. Open* 4:e210963. doi: 10.1001/jamanetworkopen.2021.0963

Mendlowitz, A. B., Shanbour, A., Downar, J., Vila-Rodriguez, F., Daskalakis, Z. J., Isaranuwatchai, W., et al. (2019). Implementation of intermittent theta burst stimulation compared to conventional repetitive transcranial magnetic stimulation in patients with

treatment resistant depression: a cost analysis. *PLoS One* 14:e0222546. doi: 10.1371/journal.pone.0222546

Mukherjee, J., Christian, B. T., Dunigan, K. A., Shi, B., Narayanan, T. K., Satter, M., et al. (2002). Brain imaging of18F-fallypride in normal volunteers: blood analysis, distribution, test-retest studies, and preliminary assessment of sensitivity to aging effects on dopamine D-2/D-3 receptors. *Synapse* 46, 170–188. doi: 10.1002/syn.10128

Mukherjee, J., Yang, Z.-Y., Brown, T., Roemer, J., and Cooper, M. (1996). 18F-desmethoxyfallypride: a fluorine-18 labeled radiotracer with properties similar to carbon-11 raclopride for pet imaging studies of dopamine D2 receptors. *Life Sci.* 59, 669–678. doi: 10.1016/0024-3205(96)00348-7

Murase, S., Grenhoff, J., Chouvet, G., Gonon, F. G., and Svensson, T. H. (1993). Prefrontal cortex regulates burst firing and transmitter release in rat mesolimbic dopamine neurons studied in vivo. *Neurosci. Lett.* 157, 53–56. doi: 10.1016/0304-3940(93)90641-W

Nettekoven, C., Volz, L. J., Kutscha, M., Pool, E.-M., Rehme, A. K., Eickhoff, S. B., et al. (2014). Dose-dependent effects of Theta burst rTMS on cortical excitability and resting-state connectivity of the human motor system. *J. Neurosci.* 34, 6849–6859. doi: 10.1523/JNEUROSCI.4993-13.2014

Ohnishi, T., Hayashi, T., Okabe, S., Nonaka, I., Matsuda, H., Iida, H., et al. (2004). Endogenous dopamine release induced by repetitive transcranial magnetic stimulation over the primary motor cortex: an [11C]raclopride positron emission tomography study in anesthetized macaque monkeys. *Biol. Psychiatry* 55, 484–489. doi: 10.1016/j.biopsych.2003.09.016

Oldfield, R. C.. (1971). The assessment and analysis of handedness: the Edinburgh inventory. *Neuropsychologia.* 9:97–113. doi: 10.1016/0028-3932(71)90067-4

Parr, A. C., Calabro, F., Larsen, B., Tervo-Clemmens, B., Elliot, S., Foran, W., et al. (2021). Dopamine-related striatal neurophysiology is associated with specialization of frontostriatal reward circuitry through adolescence. *Prog. Neurobiol.* 201:101997. doi: 10.1016/j.pneurobio.2021.101997

Paus, T., and Barrett, J. (2004). Transcranial magnetic stimulation (TMS) of the human frontal cortex: implications for repetitive TMS treatment of depression. *J. Psychiatry Neurosci.* 29, 268–279.

Paus, T., Castro-Alamancos, M. A., and Petrides, M. (2001). Cortico-cortical connectivity of the human mid-dorsolateral frontal cortex and its modulation by repetitive transcranial magnetic stimulation. *Eur. J. Neurosci.* 14, 1405–1411. doi: 10.1046/j.0953-816x.2001.01757.x

Paus, T., Jech, R., Thompson, C. J., Comeau, R., Peters, T., and Evans, A. C. (1997). Transcranial magnetic stimulation during positron emission tomography: a new method for studying connectivity of the human cerebral cortex. *J. Neurosci.* 17, 3178–3184. doi: 10.1523/JNEUROSCI.17-09-03178.1997

Philip, N. S., Barredo, J., Aiken, E., Larson, V., Jones, R. N., Shea, M. T., et al. (2019). Theta-burst transcranial magnetic stimulation for posttraumatic stress disorder. *Am. J. Psychiatr.* 176, 939–948. doi: 10.1176/appi.ajp.2019.18101160

Pogarell, O., Koch, W., Pöpperl, G., Tatsch, K., Jakob, F., Mulert, C., et al. (2007). Acute prefrontal rTMS increases striatal dopamine to a similar degree as D-amphetamine. *Psychiatry Res.* 156, 251–255. doi: 10.1016/j.pscychresns.2007.05.002

Pogarell, O., Koch, W., Pöpperl, G., Tatsch, K., Jakob, F., Zwanzger, P., et al. (2006). Striatal dopamine release after prefrontal repetitive transcranial magnetic stimulation in major depression: preliminary results of a dynamic [123I] IBZM SPECT study. *J. Psychiatr. Res.* 40, 307–314. doi: 10.1016/j.jpsychires.2005.09.001

Rossi, S., Antal, A., Bestmann, S., Bikson, M., Brewer, C., Brockmöller, J., et al. (2021). Safety and recommendations for TMS use in healthy subjects and patient populations, with updates on training, ethical and regulatory issues: expert guidelines. *Clin. Neurophysiol.* 132, 269–306. doi: 10.1016/j.clinph.2020.10.003

Rudroff, T., Workman, C. D., Fietsam, A. C., and Kamholz, J. (2020). Response variability in transcranial direct current stimulation: why sex matters. *Front. Psych.* 11:585. doi: 10.3389/fpsyt.2020.00585

Schreckenberger, M., Hägele, S., Siessmeier, T., Buchholz, H.-G., Armbrust-Henrich, H., Rösch, F., et al. (2004). The dopamine D2 receptor ligand 18F-desmethoxyfallypride: an appropriate fluorinated PET tracer for the differential diagnosis of parkinsonism. *Eur. J. Nucl. Med. Mol. Imaging* 31, 1128–1135. doi: 10.1007/s00259-004-1465-5

Sibon, I., Strafella, A. P., Gravel, P., Ko, J. H., Booij, L., Soucy, J. P., et al. (2007). Acute prefrontal cortex TMS in healthy volunteers: effects on brain 11C-αMtrp trapping. *NeuroImage* 34, 1658–1664. doi: 10.1016/j.neuroimage.2006.08.059

Siessmeier, T., Zhou, Y., Buchholz, H.-G., Landvogt, C., Vernaleken, I., Piel, M., et al. (2005). Parametric mapping of binding in human brain of D2 receptor ligands of different affinities. *J. Nucl. Med.* 46, 964–972.

Strafella, A. P. (2003). Striatal dopamine release induced by repetitive transcranial magnetic stimulation of the human motor cortex. *Brain* 126, 2609–2615. doi: 10.1093/brain/awg268

Strafella, A. P., Paus, T., Barrett, J., and Dagher, A. (2001). Repetitive transcranial magnetic stimulation of the human prefrontal cortex induces dopamine release in the caudate nucleus. *J. Neurosci.* 21:RC157. doi: 10.1523/JNEUROSCI.21-15-j0003.2001

Tik, M., Hoffmann, A., Sladky, R., Tomova, L., Hummer, A., Navarro de Lara, L., et al. (2017). Towards understanding rTMS mechanism of action: stimulation of the DLPFC causes network-specific increase in functional connectivity. *NeuroImage* 162, 289–296. doi: 10.1016/j.neuroimage.2017.09.022

Tremblay, S., Tuominen, L., Zayed, V., Pascual-Leone, A., and Joutsa, J. (2020). The study of noninvasive brain stimulation using molecular brain imaging: a systematic review. *NeuroImage* 219:117023. doi: 10.1016/j.neuroimage.2020.117023

Willner, P. (1983). Dopamine and depression: a review of recent evidence. I. Empirical studies. *Brain Res.* 6, 211–224. doi: 10.1016/0165-0173(83)90005-x

Zgaljardic, D. J., Borod, J. C., Foldi, N. S., and Mattis, P. (2003). A review of the cognitive and behavioral sequelae of Parkinson's disease: relationship to frontostriatal circuitry. *Cogn. Behav. Neurol.* 16, 193–210. doi: 10.1097/00146965-200312000-00001

Zrenner, B., Zrenner, C., Gordon, P. C., Belardinelli, P., McDermott, E. J., Soekadar, S. R., et al. (2020). Brain oscillation-synchronized stimulation of the left dorsolateral prefrontal cortex in depression using real-time EEG-triggered TMS. *Brain Stimul.* 13, 197–205. doi: 10.1016/j.brs.2019.10.007

frontiers | Frontiers in Neuroscience

TYPE Original Research
PUBLISHED 19 March 2024
DOI 10.3389/fnins.2024.1354523

OPEN ACCESS

EDITED BY
Chang-Hoon Choi,
Helmholtz Association of German Research Centres (HZ), Germany

REVIEWED BY
Ghazaleh Soleimani,
University of Minnesota Twin Cities, United States
Gerald Cooray,
Karolinska Institutet (KI), Sweden

*CORRESPONDENCE
David W. Carmichael
✉ david.carmichael@kcl.ac.uk

†These authors have contributed equally to this work

RECEIVED 12 December 2023
ACCEPTED 13 February 2024
PUBLISHED 19 March 2024

CITATION
Cohen Z, Steinbrenner M, Piper RJ, Tangwiriyasakul C, Richardson MP, Sharp DJ, Violante IR and Carmichael DW (2024) Transcranial electrical stimulation during functional magnetic resonance imaging in patients with genetic generalized epilepsy: a pilot and feasibility study.
Front. Neurosci. 18:1354523.
doi: 10.3389/fnins.2024.1354523

Transcranial electrical stimulation during functional magnetic resonance imaging in patients with genetic generalized epilepsy: a pilot and feasibility study

Zachary Cohen[1†], Mirja Steinbrenner[1,2†], Rory J. Piper[1,3], Chayanin Tangwiriyasakul[1], Mark P. Richardson[4], David J. Sharp[5], Ines R. Violante[6†] and David W. Carmichael[1*†]

[1]Department of Biomedical Engineering, School of Biomedical Engineering and Imaging Sciences, King's College London, London, United Kingdom, [2]Department of Neurology, Charité – Universitätsmedizin Berlin, Berlin, Germany, [3]University College London Great Ormond Street Institute of Child Health, University College London, London, United Kingdom, [4]Department of Basic and Clinical Neuroscience, Institute of Psychiatry, Psychology, and Neuroscience, King's College London, London, United Kingdom, [5]The Computational, Cognitive and Clinical Neuroimaging Laboratory, Department of Medicine, Imperial College London, London, United Kingdom, [6]School of Psychology, Faculty of Health and Medical Sciences, University of Surrey, Guildford, United Kingdom

Objective: A third of patients with epilepsy continue to have seizures despite receiving adequate antiseizure medication. Transcranial direct current stimulation (tDCS) might be a viable adjunct treatment option, having been shown to reduce epileptic seizures in patients with focal epilepsy. Evidence for the use of tDCS in genetic generalized epilepsy (GGE) is scarce. We aimed to establish the feasibility of applying tDCS during fMRI in patients with GGE to study the acute neuromodulatory effects of tDCS, particularly on sensorimotor network activity.

Methods: Seven healthy controls and three patients with GGE received tDCS with simultaneous fMRI acquisition while watching a movie. Three tDCS conditions were applied: anodal, cathodal and sham. Periods of 60 s without stimulation were applied between each stimulation condition. Changes in sensorimotor cortex connectivity were evaluated by calculating the mean degree centrality across eight nodes of the sensorimotor cortex defined by the Automated Anatomical Labeling atlas (primary motor cortex (precentral left and right), supplementary motor area (left and right), mid-cingulum (left and right), postcentral gyrus (left and right)), across each of the conditions, for each participant.

Results: Simultaneous tDCS-fMRI was well tolerated in both healthy controls and patients without adverse effects. Anodal and cathodal stimulation reduced mean degree centrality of the sensorimotor network (Friedman's ANOVA with Dunn's multiple comparisons test; adjusted $p = 0.02$ and $p = 0.03$ respectively). Mean degree connectivity of the sensorimotor network during the sham condition was not different to the rest condition (adjusted $p = 0.94$).

Conclusion: Applying tDCS during fMRI was shown to be feasible and safe in a small group of patients with GGE. Anodal and cathodal stimulation caused a significant reduction in network connectivity of the sensorimotor cortex across participants. This initial research supports the feasibility of using fMRI to guide

and understand network modulation by tDCS that might facilitate its clinical application in GGE in the future.

KEYWORDS

epilepsy, Juvenile Myoclonic Epilepsy, transcranial electrical stimulation, functional MRI, neuromodulation, sensorimotor

Introduction

Epilepsy is a neurological disorder that affects approximately 70 million people worldwide and is common in both children and adults (Ngugi et al., 2010). Despite the availability of anti-seizure medications, around one-third of patients have seizures that cannot be adequately controlled by medication alone. Recent drug development has not yielded many new solutions, with the rate of drug-resistant epilepsy remaining relatively stable for the past 30 years (Brodie, 2017). Even in cases where anti-seizure medication is effective, up to 17% of individuals experience limiting side effects from the medication (Chen et al., 2017). While epilepsy surgery is a good option for some patients with focal epilepsy, a third continue to have seizures despite surgery and it is generally not an option for those with genetic generalized epilepsy (GGE) (Baud et al., 2018). As a result, a significant portion of patients, particularly those with GGE, are left without effective treatment. Novel, and preferably non-invasive treatments, are urgently needed.

Transcranial electrical stimulation (tES) is a promising novel therapeutic approach for drug-resistant epilepsy (Yang et al., 2020; Simula et al., 2022). tES involves the application of a low-intensity electric current (typically <2 mA) to the brain via scalp electrodes. tES can be delivered using different waveforms, the most common being: (1) Direct current stimulation (tDCS), which is applied with a uniform, unidirectional current flowing from the anode to the cathode. While being an over-simplification, from results obtained from motor cortex stimulation, if the region of interest is under the anode (i.e., during anodal tDCS) it is broadly believed that this will result in a local increase of neuronal activity. Conversely, if it is under the cathode (i.e., during cathodal tDCS) it will lead to a decrease in neuronal activity (Bestmann and Walsh, 2017). Sham stimulation, in which the current is ramped up at the same rate as tDCS but then quickly turned off, is typically used as the control condition in investigations (Bestmann and Walsh, 2017).

Previous pre-clinical and clinical studies have shown that tDCS can be effective in reducing interictal epileptiform discharges (IEDs) and seizures in individuals affected by epilepsy (San-Juan et al., 2017; Simula et al., 2022). A recent systematic review of the use of tDCS in epilepsy demonstrated that tDCS in epilepsy is safe and led to a relevant seizure reduction in most clinical studies, though results varied greatly due to different stimulation paradigms (Simula et al., 2022). So far there exists only one double-blind, randomized, sham-controlled trial and almost all studies have been done in patients with focal epilepsy (Yang et al., 2020). Data on the application of tES in GGE is very limited, and to date it has been found to be ineffective (San-Juan et al., 2016). A recent meta-analysis of clinically established neurostimulation techniques such as vagus nerve and deep brain stimulation has shown a significant effect on seizure frequency in GGE (Haneef and Skrehot, 2023). While the underlying mechanisms of these techniques differ, they provide encouraging evidence to further investigate the use of tES in GGE. Current evidence from *in-vitro* and human studies assessing functional connectivity and using computational models indicate that the effects of tES are mainly achieved through the modulation of large brain networks, instead of focal brain activity (Simula et al., 2022). One possible target in patients with GGE may be the sensorimotor network, which has been shown to have greater network synchrony in the minute before epileptiform discharge onset (Tangwiriyasakul et al., 2018), in comparison to their healthy relatives (Tangwiriyasakul et al., 2019). This network has also been a frequent target of tES in studies outside of epilepsy, which provide existing protocols to build from (Violante et al., 2017; Mencarelli et al., 2020).

The primary objective of this study was to establish the feasibility and safety of using tDCS during fMRI in both healthy participants and patients with Juvenile Myoclonic Epilepsy (JME), a subtype of GGE (Hirsch et al., 2022). The secondary objective was to investigate the acute changes in brain connectivity within the sensorimotor network in both groups. Our hypotheses were that tES would (a) be low-risk and tolerable in both groups and (b) lead to altered connectivity in the sensorimotor network. To test these hypotheses, we applied an established protocol and analyzed network connectivity using measures of degree centrality to determine if network modulation might be feasibly measured via this approach.

Materials and methods

Participants

Seven healthy control participants were recruited via email adverts. One healthy control was later excluded due to diagnosis of a neurological disease while the study was ongoing. Ethical approval to study our healthy participants was granted through the local ethics boards Research Ethics Committee (London – West London and GTAC). Three patients with JME being treated at King's College Hospital were recruited. Ethical approval to study our patient group was granted by the Health Research Authority and Health and Care Research Wales (HCRW): REC reference: 19/LO/1668. All participants signed an informed consent form.

Transcranial electrical stimulation

All participants received transcranial electric stimulation (tES) from MR-conditional battery-driven stimulators (NeuroConn GmbH, Ilmenau, Germany). Electrode positions were marked on the scalp

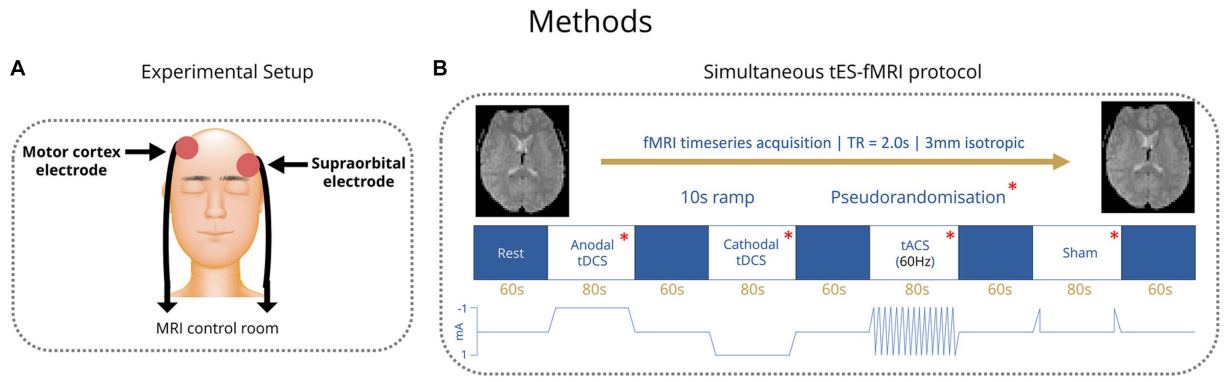

FIGURE 1
(A) Placement of tES electrodes over the right motor cortex and the left supraorbital region. **(B)** TES stimulation paradigm blocks. Order of conditions pseudorandomized.

using an EEG cap. Stimulation electrodes were placed over the right motor cortex, with the middle of the electrode positioned over FC6, and the left supraorbital region with the middle of the electrode positioned over AF7 (Figure 1A) (Wolf and Goosses, 1986). Electrodes were rectangular 5x7cm and placed on the participant's heads using an evenly spread conductive paste, approximately half a centimeter in thickness, the exact amount was not measured (Ten20, D.O. Weaver, Aurora, CO, USA). The tES setup was in place throughout the MRI session (including structural imaging). Impedances were kept below 10 kΩ and checked in each individual before they went into the scanner and again before starting stimulation. Participants were first exposed to short blocks of stimulation (with current increasing from 0.2 mA to 1 mA) before entering the scanner to ensure they were comfortable with it. Overall, we followed the hardware arrangement as previously described by Violante et al. (2017): In summary, the stimulators were placed outside the shielded MR room. The current from the stimulators was delivered into the scanner room after being filtered from RF noise by two filter boxes, one placed in the operator room and another inside the scanner bore connected via a waveguide. The second box was connected to the stimulation electrodes via MR-conditional cables. The wire routing pattern was out the back of the bore and around the control room, wires were connected to the patient shortly before the scan and positioned as straight as possible to not create loops. The filter box and wires were secured with tape. The stimulator was controlled and monitored using an in-house written Matlab code (by IRV) via a NI USB-6216 BNC data acquisition unit (National Instruments, Austin, USA). The beginning and end of each stimulation block was controlled via an external trigger sent to the NI USB-6216 BNC from the computer running the experimental paradigm (which received TTL triggers from the MR scanner). The setup used to route stimulation through the participant inside the scanner did not introduce artifacts in the fMRI signal (Li et al., 2019; Violante et al., 2023).

In healthy control subjects, four different tES conditions were applied: Anodal transcranial direct current stimulation (tDCS), cathodal tDCS, transcranial alternating current stimulation (tACS) with 60 Hz and a sham condition, where current was ramped up to test levels and then stopped. Anodal and cathodal tDCS were applied with 1 mA current intensity and tACS 1 mA peak to peak. Conditions were applied in blocks of 80 s with 60 s rest periods between them (Figure 1B). Healthy control participants completed four runs of these four conditions. The order of the conditions within each run was pseudorandomized to allow trends to be measured irrespective of the order of conditions. After the scan, healthy controls were asked to fill in a short form about the effects they experienced during tES. Patients received the same number of conditions within each run but with the tACS condition replaced by another condition (sham, anodal tDCS or cathodal tDCS) that was altered in each run such that over four runs, conditions were balanced. Stimulation parameters (i.e current intensity and montage) in patients matched those of controls. The tACS condition was found to commonly elicit a flickering visual disturbance (phosphenes) in the healthy control group from the survey. Among patients with genetic generalized epilepsies and especially in those with JME, there is a reported high prevalence of photosensitivity of up to 30.5%, which means that flickering lights can elicit seizures in those individuals (Wolf and Goosses, 1986; Fisher et al., 2005). Therefore, in the patient group, the tACS condition was removed due to potential health risks that could be associated with seizure induction.

Functional magnetic resonance imaging (fMRI)

Image acquisition

Three hundred and sixteen echo-planar images were acquired per run. Healthy participants were scanned on a Siemens Verio 3 T at the Clinical Imaging Facility at Imperial College London (3 mm isotropic voxels, repetition time [TR] = 2 s, echo time = 30 ms, flip angle 80°). Patients were scanned on GE 3 T at King's College London (3 mm isotropic voxels, repetition time [TR] = 2 s, echo time = 30 ms, flip angle 80°). During scanning we applied a movie paradigm, participants watched a cartoon (Gulliver's Travels), chosen to better control attention levels, preventing them from falling asleep. This approach was selected because isolated brain state dynamics in fMRI using a movie paradigm could be more reliably attributed to a disease state or progression change (van der Meer et al., 2020).

Image pre-processing

Pre-processing of fMRI data was performed with Statistical Parametric Mapping (SPM 12) using MATLAB (R2021a; MathWorks). The first five volumes of each fMRI run were removed to account for T1-related signal fluctuations. Following realignment to correct for head motion across each run, the Functional Image Artifact Correction Heuristic (FIACH) tool for R was used to remove biophysically implausible signal jumps and provide a noise model from signal time courses in brain regions with high noise levels (Tierney et al., 2016). Images were then normalized to a standard MNI space with an isotropic resolution of 2 mm and smoothing was applied using a Gaussian function of 8 mm full width at half-maximum. A second-order Butterworth filter for the fMRI time series was then applied to limit the signal to a low pass frequency of 0.2 Hz, and a high pass frequency of 0.1 Hz, with the signal passed forwards and backwards to avoid phase shifts (Cabral et al., 2017). We also compared the temporal signal-to-noise ratio between our rest, anodal, cathodal and sham conditions confirming no significant differences.

Sensorimotor connectivity analysis

The mean denoised fMRI time-series was calculated across the voxels in each of the 90 cerebral regions in the Automated Anatomical Labeling (AAL) atlas (Tzourio-Mazoyer et al., 2002). This time series was then partitioned according to the timings of the onset of each condition. A session-specific regressor (consisting of ones and zeros) was included to account for any difference in mean signal between rest epochs. For each condition, across each run, for every participant, whole brain connectivity was assessed using Pearson's correlation coefficient to generate a 90 by 90 adjacency matrix. The top 1% of the strongest connections for the whole adjacency matrix were determined and the remaining 99% were omitted. A submatrix of the nodes from the 90 by 90 matrix lying in the sensorimotor cortex was created, using the same regions from previous research (Tangwiriyasakul et al., 2019) specifically the primary motor area (left and right), supplementary motor area (left and right), mid-cingulum (left and right), postcentral gyrus (left and right). The degree centrality was calculated for each node within the sensorimotor cortex using the Brain Connectivity Toolbox (Rubinov and Sporns, 2010) and the mean degree of connectivity was calculated across all the nodes. Next, the mean degree of connectivity was computed for the sensorimotor cortex across each of the conditions and runs for each participant (Figure 2). This was performed to provide a single index of local motor network connectivity (Zuo et al., 2012). Degree centrality has been used before in genetic generalized epilepsies as a way to measure alterations in functional connectivity (Wang et al., 2017; Tangwiriyasakul et al., 2018).

Statistical analysis

The mean degree of connectivity per run was not normally distributed based on the results of the Shapiro–Wilk Test ($W = 0.93$, $p = 0.0002$). Therefore, a non-parametric statistical test, the Friedman's ANOVA, was used to compare the mean degree of connectivity of the rest condition to that of the anodal, cathodal, and sham stimulation conditions. To correct for multiple comparisons, a Dunn's test was applied. Statistics were performed using Prism 9.5.0 (Dotmatics, GraphPad Software, Boston, USA).

Results

Feasibility assessment

TES-fMRI data of six healthy controls was included in this study, the mean age was 30.5 years (±7.87 years), and 4/6 were female. The tES paradigm lasted approximately 1.5 h and was well tolerated in both healthy controls and patients, only one scan had to be briefly interrupted due to participant anxiety but could afterwards be completed. No serious adverse events were encountered. This includes seizure induction, cognitive changes, or allergic reactions. Additionally, skin irritation, headaches, nausea or allergic reactions were also not reported by participants for anodal and cathodal stimulation. Healthy participants reported a tingling sensation on their scalp for anodal and cathodal stimulation, but no pain or dizziness. During tACS, all healthy participants reported phosphenes in their visual field. Phosphenes stopped completely when tACS was stopped, but because phosphenes could plausibly induce seizures in patients with photosensitive epilepsy, this condition was not applied to patients. One healthy control experienced a feeling of panic during the first stimulation condition, after being immediately removed from the scanner they were able to re-enter and finish the paradigm without

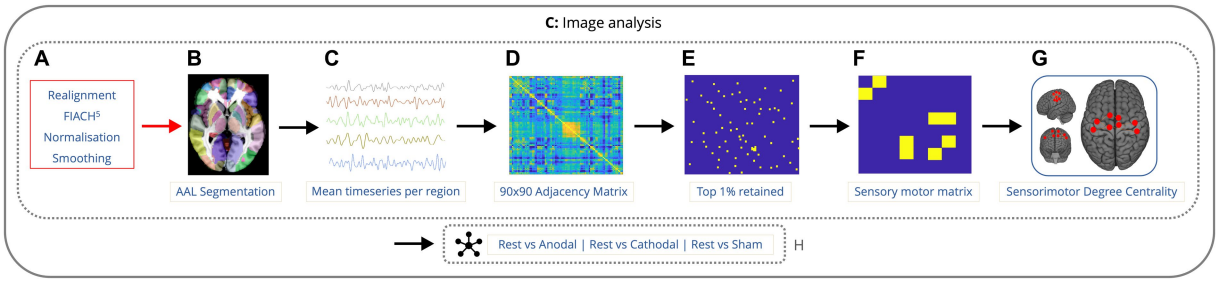

FIGURE 2
Imaging analysis pipeline showing the order of data processing. Data is preprocessed with realignment, FIACH, normalization to standard space, and smoothing **(A)**. fMRI time-series calculated across voxels in 90 cerebral regions **(B,C)**. 90×90 correlation matrix for each condition, across each run, for every participant **(D)**. Top 1% of the strongest connections were determined and the remaining 99% were omitted **(E)**. Submatrix of the 8 nodes from the 90 by 90 matrix lying in the sensorimotor cortex was created **(F)**. The degree centrality was calculated for each node within the sensorimotor cortex along with the mean degree of connectivity for all the nodes **(G)**. Next, the mean degree of connectivity was computed for the sensorimotor cortex comparing rest to each condition **(H)**.

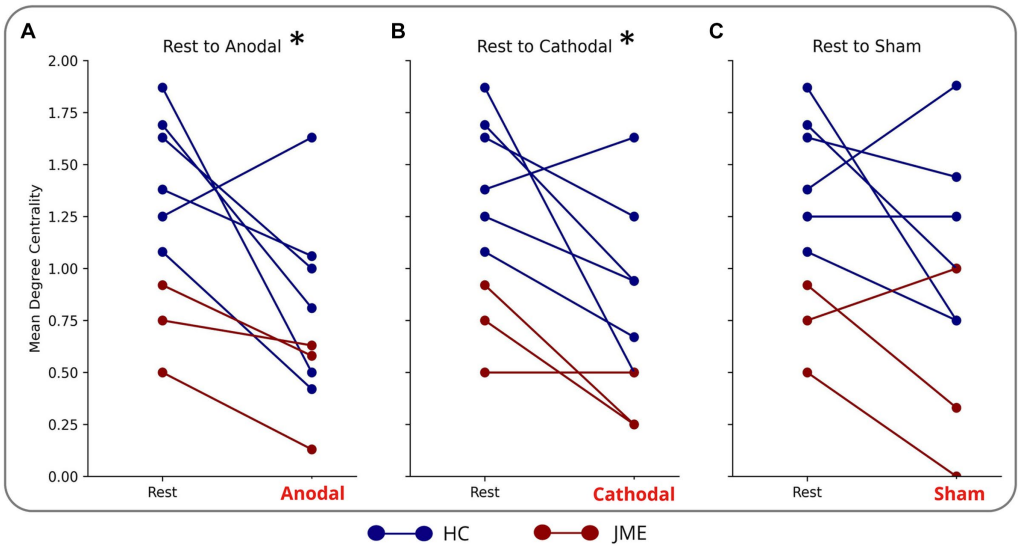

FIGURE 3
Reduction in mean degree centrality of sensorimotor nodes during **(A)** anodal **(B)** cathodal and **(C)** sham tDCS. Each blue line is a different HC. Each red line is a different patient with JME. *indicates significance: adjusted (p = 0.02 for anodal and p = 0.03 cathodal).

further incident. Two of the three patients had received a routine EEG prior to tES. This was reviewed by a neurologist trained in EEG interpretation (MS). No epileptiform discharges were detected in patients before the tES-MRI.

Sensorimotor connectivity

Anodal stimulation caused a reduction in mean degree centrality of the sensorimotor cortex (comprised of left and right precentral, postcentral, supplementary motor area and cingulum) in 8/9 subjects and cathodal stimulation had the same effect in 7/9 subjects. This culminated in anodal and cathodal stimulation reducing the mean degree centrality of the nodes of the sensorimotor network compared to rest (adjusted $p = 0.02$ and $p = 0.03$ respectively) (Figures 3A,B). There was not a statistically different mean degree centrality of the nodes of the sensorimotor network between rest and sham (Figure 3C).

Discussion

We have met our primary objective regarding feasibility and tolerability: Anodal and cathodal tDCS were applied in healthy controls and three patients with GGE during fMRI without adverse events and were well tolerated by the subjects. In contrast to our results, a case study suggested a potential health risk of using tES in patients with GGE (San-Juan et al., 2016). We have found that phosphenes were routinely reported during tACS in our healthy controls. Computational head models of similar montages to the one used in our study have been reported in the literature and shown that the electric fields pass through the eye (Iacono et al., 2015). The electrode in the supraorbital area in our montage was close enough to the eye to allow for current to reach the retinas and induce phosphenes. Even montages with electrodes placed only on the occipital cortices are known to induce phosphenes (Lorenz et al., 2019). As explained in the Methods section we decided against using tACS in our patient group due to the potential health risks. Although tACS was not applied in the patient group in this study, owing to the potential risk of inducing seizures in photosensitive epilepsy patients, it has been shown to be an effective means to alter connectivity (Lang et al., 2019; Klink et al., 2020). In this context further investigation of tACS for this purpose should be considered further, utilizing a stimulation montage that can better target the motor network while avoiding stimulation of the visual cortex. Establishing the feasibility of applying tES simultaneously with fMRI in patients with GGE enables the investigation of changes in network connectivity caused by tDCS. This could have a potential therapeutic impact since network changes have been shown to reduce markers of epileptogenicity (Simula et al., 2022). At the same time data from recent years has strengthened the hypothesis that epilepsy is a network disorder (Bartolomei et al., 2017). tES has demonstrated the potential to reduce IEDs and seizures in patients with drug-resistant epilepsy through modulating large-scale brain networks (Simula et al., 2022). In our small sample, no IEDs were present in the EEG recordings prior to tDCS.

Regarding our secondary objective, we have shown that all healthy controls and patients had a significant decrease in degree centrality through anodal and cathodal tDCS. Patients with GGE had an overall lower degree centrality in the sensorimotor cortex than controls, though this could not be statistically assessed in such a small sample, and may be confounded by inter-scanner variability. Two recent systematic reviews on the use of tES in epilepsy reported only one case report in patients with GGE (Sudbrack-Oliveira et al., 2021), it is therefore difficult to compare our findings to preexisting literature. Studies using tES in other types of epilepsy with diffuse onset like Lennox–Gastaut or Rassmussen encephalitis have shown a significant seizure reduction (Auvichayapat et al., 2013; Tekturk et al., 2016). Currently, available studies using tES in epilepsy are overall highly

heterogeneous regarding sample characteristics and methodology. For this reason, it is argued that conducting a meta-analysis would create biased effect sizes and estimations (Sudbrack-Oliveira et al., 2021), to date no meta-analysis exists.

Studies investigating tES during fMRI on brain networks of healthy controls lack consensus regarding its efficacy in modulating network function (Ghobadi-Azbari et al., 2021). Looking at individual studies, one study targeting the sensorimotor network in healthy controls through applying cathodal tDCS of 1 mA for 5 min, using the same montage as in our study, resulted in decreased activation in the sensorimotor cortex (Baudewig et al., 2001), concurring with our finding. A study investigating numerous brain networks including the sensorimotor network after the application of 5-min stimulation periods at 2 mA, found connectivity near the applied field and also with remote nodes decreased during tDCS (Leaver et al., 2022). In our research, a similar finding was achieved in patients despite potential differences owing to pathology and medication. This demonstrates network modulation with tES is feasible. Conversely, it has been shown that stimulation for 20 s at 1 mA did not produce a detectable BOLD signal change (Antal et al., 2011). These variable results can among other factors be explained by differences in anatomy (i.e., scalp and skull thickness), placement of electrodes and current intensity (Liu et al., 2018) and analysis approaches. The network effects of tDCS are also dependent on brain state, with cathodal tDCS having greater effects during a task while anodal tDCS has greater effects during rest (Li et al., 2019). Epileptic brain activity, both seizures and IEDs, are often more prevalent during certain states of arousal such as sleep in both focal epilepsy and in GGE (Bernard et al., 2023). This shows that the probability of epileptic activity is modulated by the global state of the brain which relates to cortical excitability.

There is evidence for significant clinical benefit in GGE from the use of VNS and DBS (Haneef and Skrehot, 2023), but a downside of these techniques is their invasiveness, both needing surgery, making non-invasive approaches like tES attractive alternatives if efficacy can be established. Additionally, electric stimulation-driven, non-invasive approaches such as temporal interference have also been shown to reduce epileptiform activity in mouse models and it would be beneficial to analyse how temporal interference affects sensorimotor connectivity with a paradigm like ours (Acerbo et al., 2022). Our preliminary evidence of reduced mean degree centrality of the sensorimotor network supports previous literature about the modulatory effect of tES on the brain. Further confirming our hypothesis, the sham condition was not significantly different from the rest condition and cathodal stimulation significantly reduced the mean degree centrality of the nodes of the sensorimotor network, indicating reduced excitability. In line with previous studies anodal tDCS showed the same results as cathodal tDCS in reducing synchrony (Li et al., 2019; Kurtin et al., 2021).

One key limitation of our research is the sample size of participants. Recruiting patients with JME was cut short by the global COVID-19 pandemic, though the effects of tES on this small group were still powerful enough to produce statistically significant results. While there is a statistically significant difference between the stimulation conditions, a larger group size would add further power and validity to these findings. A further limitation is that the healthy controls were scanned in a different location to the patients, though both were scanned at 3 T. The small sample size and different scanner types precluded conducting a meaningful group comparison because the differences in baseline might be due to either scanner or population. Parameters were matched, however, and the same overall main trend of reduced sensorimotor cortex connectivity was observed within subjects between stimulation conditions in both healthy controls and patients which is not affected by scanner type. Another potential limitation is the effect on SNR. TES has been shown to affect image quality only minimally, with a minor effect on image SNR (Antal et al., 2011). One further limitation is the intake of different anti-seizure medications (ASM) by the patients. Due to the small number included here we could not perform a statistical analysis to account for possible pharmacological effects. Again, although this factor might change overall network connectivity in individuals, the directional reduction in sensorimotor degree centrality between conditions is likely to exist regardless of medication.

Conclusion

This study provides initial evidence that tES can be safely applied during fMRI in patients with JME. Here, we have also demonstrated sensorimotor network alterations in mean degree centrality that was used as a measure of network connectivity related to overall network synchrony. This preliminary finding appeared to be unrelated to the polarity of the applied stimulation. Further work is required to determine the reliability of this finding in a larger cohort, understand the interaction between current distribution and individual brain structures and establish if the modulation of motor network synchrony can modulate epileptogenicity.

Data availability statement

The raw data supporting the conclusions of this article will be made available by the authors, without undue reservation.

Ethics statement

The studies involving humans were approved by London – West London and GTAC & Health Research Authority and Health and Care Research Wales (HCRW): REC reference: 19/LO/1668. The studies were conducted in accordance with the local legislation and institutional requirements. The participants provided their written informed consent to participate in this study.

Author contributions

ZC: Formal analysis, Writing – original draft. MS: Data curation, Formal analysis, Funding acquisition, Investigation, Methodology, Project administration, Writing – original draft. RP: Formal analysis, Writing – review & editing. CT: Writing – review & editing. MR: Conceptualization, Writing – review & editing. DS: Writing – review & editing. IV: Conceptualization, Data curation, Funding acquisition,

Methodology, Project administration, Writing – review & editing. DC: Conceptualization, Data curation, Formal analysis, Funding acquisition, Investigation, Methodology, Project administration, Writing – review & editing.

Funding

The author(s) declare financial support was received for the research, authorship, and/or publication of this article. This work was supported by funding from Epilepsy Research UK (ERUK PGE1802). ZC was funded by the Engineering and Physical Sciences Research Council (EP/R513064/1). IV was funded by the Wellcome Trust (103045/Z/13/Z) and BBSRC (BB/S008314/1). This study represents independent research supported by the National Institute for Health Research (NIHR) / Wellcome Trust King's Clinical Research Facility and the NIHR Biomedical Research Centre and Dementia Unit at South London and Maudsley NHS Foundation Trust and King's College London and by the National Institute for Health Research (NIHR) Biomedical Research Centre based at Guy's and St Thomas' NHS Foundation Trust and King's College London and/or the NIHR Clinical Research Facility. This study was also supported by core funding from the Wellcome/EPSRC Centre for Medical Engineering [WT203148/Z/16/Z]. The views expressed are those of the author(s) and not necessarily those of the NHS, the NIHR or the Department of Health and Social Care.

Conflict of interest

The authors declare that the research was conducted in the absence of any commercial or financial relationships that could be construed as a potential conflict of interest.

Publisher's note

References

Acerbo, E., Jegou, A., Luff, C., Dzialecka, P., Botzanowski, B., Missey, F., et al. (2022). Focal non-invasive deep-brain stimulation with temporal interference for the suppression of epileptic biomarkers. *Front. Neurosci.* 16:945221. doi: 10.3389/fnins.2022.945221

Antal, A., Polania, R., Schmidt-Samoa, C., Dechent, P., and Paulus, W. (2011). Transcranial direct current stimulation over the primary motor cortex during fMRI. *NeuroImage* 55, 590–596. doi: 10.1016/j.neuroimage.2010.11.085

Auvichayapat, N., Rotenberg, A., Gersner, R., Ngodklang, S., Tiamkao, S., Tassaneeyakul, W., et al. (2013). Transcranial direct current stimulation for treatment of refractory childhood focal epilepsy. *Brain Stimul.* 6, 696–700. doi: 10.1016/j.brs.2013.01.009

Bartolomei, F., Lagarde, S., Wendling, F., McGonigal, A., Jirsa, V., Guye, M., et al. (2017). Defining epileptogenic networks: contribution of SEEG and signal analysis. *Epilepsia* 58, 1131–1147. doi: 10.1111/epi.13791

Baud, M. O., Perneger, T., Rácz, A., Pensel, M. C., Elger, C., Rydenhag, B., et al. (2018). European trends in epilepsy surgery. *Neurology* 91:2. doi: 10.1212/WNL.0000000000005776

Baudewig, J., Nitsche, M. A., Paulus, W., and Frahm, J. (2001). Regional modulation of BOLD MRI responses to human sensorimotor activation by transcranial direct current stimulation. *Magn. Reson. Med.* 45, 196–201. doi: 10.1002/1522-2594(200102)45:2<196::AID-MRM1026>3.0.CO;2-1

Bernard, C., Frauscher, B., Gelinas, J., and Timofeev, I. (2023). Sleep, oscillations, and epilepsy. *Epilepsia* 64, S3–S12. doi: 10.1111/epi.17664

Bestmann, S., and Walsh, V. (2017). Transcranial electrical stimulation. *Curr. Biol.* 27, R1258–R1262. doi: 10.1016/j.cub.2017.11.001

Brodie, M. J. (2017). Outcomes in newly diagnosed epilepsy in adolescents and adults: insights across a generation in Scotland. *Seizure* 44, 206–210. doi: 10.1016/j.seizure.2016.08.010

Cabral, J., Vidaurre, D., Marques, P., Magalhães, R., Silva Moreira, P., Miguel Soares, J., et al. (2017). Cognitive performance in healthy older adults relates to spontaneous switching between states of functional connectivity during rest. *Sci. Rep.* 7:5135. doi: 10.1038/s41598-017-05425-7

Chen, B., Choi, H., Hirsch, L. J., Katz, A., Legge, A., Buchsbaum, R., et al. (2017). Psychiatric and behavioral side effects of antiepileptic drugs in adults with epilepsy. *Epilepsy Behav.* 76, 24–31. doi: 10.1016/j.yebeh.2017.08.039

Fisher, R. S., Harding, G., Erba, G., Barkley, G. L., and Wilkins, A. (2005). Photic-and pattern-induced seizures: a review for the epilepsy foundation of america working group. *Epilepsia* 46, 1426–1441. doi: 10.1111/j.1528-1167.2005.31405.x

Ghobadi-Azbari, P., Jamil, A., Yavari, F., Esmaeilpour, Z., Malmir, N., Mahdavifar-Khayati, R., et al. (2021). fMRI and transcranial electrical stimulation (tES): a systematic review of parameter space and outcomes. *Prog. Neuro-Psychopharmacol. Biol. Psychiatry* 107:110149. doi: 10.1016/j.pnpbp.2020.110149

Haneef, Z., and Skrehot, H. C. (2023). Neurostimulation in generalized epilepsy: a systematic review and meta-analysis. *Epilepsia* 64, 811–820. doi: 10.1111/epi.17524

Hirsch, E., French, J., Scheffer, I. E., Bogacz, A., Alsaadi, T., Sperling, M. R., et al. (2022). ILAE definition of the idiopathic generalized epilepsy syndromes: position statement by the ILAE task force on nosology and definitions. *Epilepsia* 63, 1475–1499. doi: 10.1111/epi.17236

Iacono, M. I., Neufeld, E., Akinnagbe, E., Bower, K., Wolf, J., Oikonomidis, I. V., et al. (2015). MIDA: a multimodal imaging-based detailed anatomical model of the human head and neck. *PLoS One* 10:e0124126. doi: 10.1371/journal.pone.0124126

Klink, K., Peter, J., Wyss, P., and Klöppel, S. (2020). Transcranial electric current stimulation during associative memory encoding: comparing tACS and tDCS effects in healthy aging. *Front. Aging Neurosci.* 12:66. doi: 10.3389/fnagi.2020.00066

Kurtin, D. L., Violante, I. R., Zimmerman, K., Leech, R., Hampshire, A., Patel, M. C., et al. (2021). Investigating the interaction between white matter and brain state on tDCS-induced changes in brain network activity. *Brain Stimul.* 14, 1261–1270. doi: 10.1016/j.brs.2021.08.004

Lang, S., Gan, L. S., Alrazi, T., and Monchi, O. (2019). Theta band high definition transcranial alternating current stimulation, but not transcranial direct current stimulation, improves associative memory performance. *Sci. Rep.* 9:8562. doi: 10.1038/s41598-019-44680-8

Leaver, A. M., Gonzalez, S., Vasavada, M., Kubicki, A., Jog, M., Wang, D. J. J., et al. (2022). Modulation of brain networks during MR-compatible transcranial direct current stimulation. *NeuroImage* 250:118874. doi: 10.1016/j.neuroimage.2022.118874

Li, L. M., Violante, I. R., Leech, R., Ross, E., Hampshire, A., Opitz, A., et al. (2019). Brain state and polarity dependent modulation of brain networks by transcranial direct current stimulation. *Hum. Brain Mapp.* 40, 904–915. doi: 10.1002/hbm.24420

Liu, A., Vöröslakos, M., Kronberg, G., Henin, S., Krause, M. R., Huang, Y., et al. (2018). Immediate neurophysiological effects of transcranial electrical stimulation. *Nat. Commun.* 9:5092. doi: 10.1038/s41467-018-07233-7

Lorenz, R., Simmons, L. E., Monti, R. P., Arthur, J. L., Limal, S., Laakso, I., et al. (2019). Efficiently searching through large tACS parameter spaces using closed-loop Bayesian optimization. *Brain Stimul.* 12, 1484–1489. doi: 10.1016/j.brs.2019.07.003

Mencarelli, L., Menardi, A., Neri, F., Monti, L., Ruffini, G., Salvador, R., et al. (2020). Impact of network-targeted multichannel transcranial direct current stimulation on intrinsic and network-to-network functional connectivity. *J. Neurosci. Res.* 98, 1843–1856. doi: 10.1002/jnr.24690

Ngugi, A. K., Bottomley, C., Kleinschmidt, I., Sander, J. W., and Newton, C. R. (2010). Estimation of the burden of active and life-time epilepsy: a meta-analytic approach. *Epilepsia* 51, 883–890. doi: 10.1111/j.1528-1167.2009.02481.x

Rubinov, M., and Sporns, O. (2010). Complex network measures of brain connectivity: uses and interpretations. *NeuroImage* 52, 1059–1069. doi: 10.1016/j.neuroimage.2009.10.003

San-Juan, D., Espinoza López, D. A., Vázquez Gregorio, R., Trenado, C., Fernández-González Aragón, M., Morales-Quezada, L., et al. (2017). Transcranial direct current stimulation in mesial temporal lobe epilepsy and hippocampal sclerosis. *Brain Stimul.* 10, 28–35. doi: 10.1016/j.brs.2016.08.013

San-Juan, D., Sarmiento, C. I., Hernandez-Ruiz, A., Elizondo-Zepeda, E., Santos-Vázquez, G., Reyes-Acevedo, G., et al. (2016). Transcranial alternating current stimulation: a potential risk for genetic generalized epilepsy patients (study case). *Front. Neurol.* 7:7(NOV). doi: 10.3389/fneur.2016.00213

Simula, S., Daoud, M., Ruffini, G., Biagi, M. C., Bénar, C. G., Benquet, P., et al. (2022). Transcranial current stimulation in epilepsy: a systematic review of the fundamental and clinical aspects. *Front. Neurosci.* 16:909421. doi: 10.3389/fnins.2022.909421

Statistical parametric mapping. Available at: https://www.fil.ion.ucl.ac.uk/spm/

Sudbrack-Oliveira, P., Barbosa, M. Z., Thome-Souza, S., Razza, L. B., Gallucci-Neto, J., Da Costa Lane Valiengo, L., et al. (2021). Transcranial direct current stimulation (tDCS) in the management of epilepsy: a systematic review. *Seizure* 86, 85–95. doi: 10.1016/j.seizure.2021.01.020

Tangwiriyasakul, C., Perani, S., Abela, E., Carmichael, D. W., and Richardson, M. P. (2019). Sensorimotor network hypersynchrony as an endophenotype in families with genetic generalized epilepsy: a resting-state functional magnetic resonance imaging study. *Epilepsia* 60, e14–e19. doi: 10.1111/epi.14663

Tangwiriyasakul, C., Perani, S., Centeno, M., Yaakub, S. N., Abela, E., Carmichael, D. W., et al. (2018). Dynamic brain network states in human generalized spike-wave discharges. *Brain* 141, 2981–2994. doi: 10.1093/brain/awy223

Tekturk, P., Erdogan, E. T., Kurt, A., Kocagoncu, E., Kucuk, Z., Kinay, D., et al. (2016). Transcranial direct current stimulation improves seizure control in patients with Rasmussen encephalitis. *Epileptic Disord.* 18, 58–66. doi: 10.1684/epd.2016.0796

Tierney, T. M., Weiss-Croft, L. J., Centeno, M., Shamshiri, E. A., Perani, S., Baldeweg, T., et al. (2016). FIACH: a biophysical model for automatic retrospective noise control in fMRI. *NeuroImage* 124, 1009–1020. doi: 10.1016/j.neuroimage.2015.09.034

Tzourio-Mazoyer, N., Landeau, B., Papathanassiou, D., Crivello, F., Etard, O., Delcroix, N., et al. (2002). Automated anatomical labeling of activations in SPM using a macroscopic anatomical parcellation of the MNI MRI single-subject brain. *NeuroImage* 15, 273–289. doi: 10.1006/nimg.2001.0978

van der Meer, J. N., Breakspear, M., Chang, L. J., Sonkusare, S., and Cocchi, L. (2020). Movie viewing elicits rich and reliable brain state dynamics. *Nat. Commun.* 11:5004. doi: 10.1038/s41467-020-18717-w

Violante, I., Alania, K., Cassarà, A., Neufeld, E., Acerbo, E., Williamson, A., et al. (2023). Non-invasive temporal interference electrical stimulation of the human hippocampus. *Brain Stimul.* 16:408. doi: 10.1016/j.brs.2023.01.833

Violante, I. R., Li, L. M., Carmichael, D. W., Lorenz, R., Leech, R., Hampshire, A., et al. (2017). Externally induced frontoparietal synchronization modulates network dynamics and enhances working memory performance. *elife* 6:6. doi: 10.7554/eLife.22001

Wang, X., Jiao, D., Zhang, X., and Lin, X. (2017). Altered degree centrality in childhood absence epilepsy: a resting-state fMRI study. *J. Neurol. Sci.* 373, 274–279. doi: 10.1016/j.jns.2016.12.054

Wolf, P., and Goosses, R. (1986). Relation of photosensitivity to epileptic syndromes. *J. Neurol. Neurosurg. Psychiatry* 49, 1386–1391. doi: 10.1136/jnnp.49.12.1386

Yang, D., Wang, Q., Xu, C., Fang, F., Fan, J., Li, L., et al. (2020). Transcranial direct current stimulation reduces seizure frequency in patients with refractory focal epilepsy: a randomized, double-blind, sham-controlled, and three-arm parallel multicenter study. *Brain Stimul.* 13, 109–116. doi: 10.1016/j.brs.2019.09.006

Zuo, X. N., Ehmke, R., Mennes, M., Imperati, D., Castellanos, F. X., Sporns, O., et al. (2012). Network centrality in the human functional connectome. *Cereb. Cortex* 22, 1862–1875. doi: 10.1093/cercor/bhr269

frontiers | Frontiers in Neuroscience

TYPE Review
PUBLISHED 18 June 2024
DOI 10.3389/fnins.2024.1389651

OPEN ACCESS

EDITED BY
Chang-Hoon Choi,
Helmholtz Association of German Research Centres (HZ), Germany

REVIEWED BY
Satoshi Tanaka,
Hamamatsu University School of Medicine, Japan
Bruce Michael Luber,
National Institute of Mental Health (NIH), United States

*CORRESPONDENCE
Marcus Meinzer
✉ marcus.meinzer@med.uni-greifswald.de
Alireza Shahbabaie
✉ Alireza.Shahbabaie@med.uni-greifswald.de

†These authors have contributed equally to this work

RECEIVED 21 February 2024
ACCEPTED 15 May 2024
PUBLISHED 18 June 2024

CITATION
Meinzer M, Shahbabaie A, Antonenko D, Blankenburg F, Fischer R, Hartwigsen G, Nitsche MA, Li S-C, Thielscher A, Timmann D, Waltemath D, Abdelmotaleb M, Kocataş H, Caisachana Guevara LM, Batsikadze G, Grundei M, Cunha T, Hayek D, Turker S, Schlitt F, Shi Y, Khan A, Burke M, Riemann S, Niemann F and Flöel A (2024) Investigating the neural mechanisms of transcranial direct current stimulation effects on human cognition: current issues and potential solutions.
Front. Neurosci. 18:1389651.
doi: 10.3389/fnins.2024.1389651

Investigating the neural mechanisms of transcranial direct current stimulation effects on human cognition: current issues and potential solutions

Marcus Meinzer[1*†], Alireza Shahbabaie[1*†], Daria Antonenko[1], Felix Blankenburg[2], Rico Fischer[3], Gesa Hartwigsen[4,5], Michael A. Nitsche[6,7,8], Shu-Chen Li[9], Axel Thielscher[10,11], Dagmar Timmann[12], Dagmar Waltemath[13], Mohamed Abdelmotaleb[1], Harun Kocataş[1], Leonardo M. Caisachana Guevara[3], Giorgi Batsikadze[12], Miro Grundei[2], Teresa Cunha[10], Dayana Hayek[1], Sabrina Turker[4,5], Frederik Schlitt[12], Yiquan Shi[9], Asad Khan[6], Michael Burke[6], Steffen Riemann[1], Filip Niemann[1] and Agnes Flöel[1,14]

[1]Department of Neurology, University Medicine Greifswald, Greifswald, Germany, [2]Neurocomputation and Neuroimaging Unit, Department of Education and Psychology, Freie Universität Berlin, Berlin, Germany, [3]Department of Psychology, University of Greifswald, Greifswald, Germany, [4]Max Planck Institute for Human Cognitive and Brain Sciences, Leipzig, Germany, [5]Wilhelm Wundt Institute for Psychology, Leipzig University, Leipzig, Germany, [6]Department of Psychology and Neurosciences, Leibniz Research Centre for Working Environment and Human Factors at TU Dortmund, Dortmund, Germany, [7]German Center for Mental Health (DZPG), Bochum, Germany, [8]Bielefeld University, University Hospital OWL, Protestant Hospital of Bethel Foundation, University Clinic of Psychiatry and Psychotherapy, Bielefeld, Germany, [9]Chair of Lifespan Developmental Neuroscience, Faculty of Psychology, Technische Universität Dresden, Dresden, Germany, [10]Section for Magnetic Resonance, Department of Health Technology, Technical University of Denmark, Kongens Lyngby, Denmark, [11]Danish Research Centre for Magnetic Resonance, Centre for Functional and Diagnostic Imaging and Research, Copenhagen University Hospital Amager and Hvidovre, Copenhagen, Denmark, [12]Department of Neurology and Center for Translational Neuro- and Behavioral Sciences (C-TNBS), Essen University Hospital, University of Duisburg-Essen, Essen, Germany, [13]Core Unit Data Integration Center, University Medicine Greifswald, Greifswald, Germany, [14]German Center for Neurodegenerative Diseases (DZNE Site Greifswald), Greifswald, Germany

Transcranial direct current stimulation (tDCS) has been studied extensively for its potential to enhance human cognitive functions in healthy individuals and to treat cognitive impairment in various clinical populations. However, little is known about how tDCS modulates the neural networks supporting cognition and the complex interplay with mediating factors that may explain the frequently observed variability of stimulation effects within and between studies. Moreover, research in this field has been characterized by substantial methodological variability, frequent lack of rigorous experimental control and small sample sizes, thereby limiting the generalizability of findings and translational potential of tDCS. The present manuscript aims to delineate how these important issues can be addressed within a neuroimaging context, to reveal the neural underpinnings, predictors and mediators of tDCS-induced behavioral modulation. We will focus on functional magnetic resonance imaging (fMRI), because it allows the investigation of tDCS effects with excellent spatial precision and sufficient temporal resolution across the entire brain. Moreover, high resolution structural imaging data can be acquired for precise localization of stimulation effects, verification of electrode positions on the scalp and realistic

current modeling based on individual head and brain anatomy. However, the general principles outlined in this review will also be applicable to other imaging modalities. Following an introduction to the overall state-of-the-art in this field, we will discuss in more detail the underlying causes of variability in previous tDCS studies. Moreover, we will elaborate on design considerations for tDCS-fMRI studies, optimization of tDCS and imaging protocols and how to assure high-level experimental control. Two additional sections address the pressing need for more systematic investigation of tDCS effects across the healthy human lifespan and implications for tDCS studies in age-associated disease, and potential benefits of establishing large-scale, multidisciplinary consortia for more coordinated tDCS research in the future. We hope that this review will contribute to more coordinated, methodologically sound, transparent and reproducible research in this field. Ultimately, our aim is to facilitate a better understanding of the underlying mechanisms by which tDCS modulates human cognitive functions and more effective and individually tailored translational and clinical applications of this technique in the future.

KEYWORDS

tES, tDCS-fMRI, cognition, variability, experimental control, lifespan, design optimization, consortia

1 Introduction

Non-invasive brain stimulation (NIBS) techniques apply electric fields to the brain using currents injected via scalp electrodes (tES, transcranial electric simulation) or electromagnetic induction (TMS, transcranial magnetic stimulation). They aim to modulate the excitability of the human brain and induce neuroplasticity. NIBS has been ascribed great promise for allowing targeted modulation of specific brain regions or large-scale brain networks relevant for higher cognitive functions. In particular, transcranial direct current stimulation (tDCS) has recently sparked considerable scientific, clinical, and public interest (Dubljević et al., 2014; Riggall et al., 2015). Compared to other types of NIBS (e.g., transcranial magnetic stimulation, TMS), tDCS is relatively low-cost and easy to administer, has no significant adverse effects, and offers a relatively effective mode for placebo (sham) stimulation (Antal et al., 2017a).

The underlying neurophysiological mechanisms of tDCS have been studied extensively in the motor system by utilizing neuropharmacological interventions and TMS, to explore the modulation of cortico-cortical and cortico-spinal excitability (Cirillo et al., 2017). These studies have revealed that the applied current does not induce action potentials. Rather, it is suggested that tDCS transiently shifts the neuronal resting membrane potential toward either de- or hyperpolarization, resulting in enhanced or reduced neural excitability at the macroscale level with standard protocols (Sandrini et al., 2011; Stagg et al., 2018). Moreover, with regard to tDCS effects involving synaptic plasticity, animal and human studies have indicated that tDCS also introduces a secondary mechanism (in addition to alterations of the resting-membrane potential) that involves the induction of long-term potentiation and depression (LTP and LTD)-like processes (Stagg et al., 2018). Repeated stimulation sessions can enhance training-induced adaptive neuroplasticity and induce long-lasting behavioral improvements (Allman et al., 2016; Perceval et al., 2020).

TDCS has also been studied extensively with regard to its potential to enhance cognitive functions in healthy individuals and to treat cognitive impairment in various neurological and psychiatric diseases. However, recent reviews have noted substantial methodological variability, frequent lack of rigorous experimental control and overall, highly variable outcomes within and between studies (Galli et al., 2019; Lee et al., 2021; Lavezzi et al., 2022). Moreover, several recent registered reports have reported weak effects of tDCS, limited intra-individual reliability of tDCS responses or failed to replicate previous studies (Boayue et al., 2020; Alexandersen et al., 2022; Willmot et al., 2024). Nonetheless, a substantial body of research has demonstrated potential positive effects of tDCS on behavior and brain function, but the aforementioned issues also suggest that the current "state-of-the-art" may not yet be suited for translational applications. This would require systematic and coordinated evaluation of the parameter space, clarification of the underlying neural mechanisms, and likely individual adaptation of interventions based on this knowledge. Here, we review and critically discuss recent efforts that aim to address these important issues to improve the effectiveness of tDCS in experimental and clinical settings, as well as transparency and reproducibility of research outcomes in this field. We also aim to provide recommendations for future research investigating the neural mechanisms underlying tDCS effects on higher cognitive functions using neuroimaging technology (see Table 1 for a summary of the recommendations).

2 Functional imaging to study effects of tDCS on higher-order human brain functions

Approximately 80% of the published tDCS studies target the primary motor cortex (M1), and it is currently unclear if results from these studies generalize to other cortical regions and brain networks, in particular those enabling higher cognitive functions (Stagg et al., 2018). Moreover, while neurophysiological effects of tDCS on local cortical excitability in the motor system can be assessed directly via

TABLE 1 Summary of key recommendations for imaging cognitive tDCS effects.

Planning stage	**Technologically challenging tDCS-imaging studies require careful planning** • Assemble necessary expertise from relevant fields (e.g., physics, imaging, tDCS, data analysis and management) • Consult relevant technical guidelines for tDCS and combined tDCS-imaging • Address specific issues arising from combining tDCS with specific imaging approaches (e.g., safety, artifacts, distortions)
Imaging and task paradigms	(1) **Consider the specific strengths and limitations of specific imaging approaches to answer the research question** • e.g., spatial vs. temporal resolution, is structural MRI required (modeling) (2) **Ensure compatibility of planned behavioral tasks with the imaging approach** • Consider that task modifications may be required by specific imaging techniques and that changing behavioral tasks can affect tDCS effects • Use robust and simple (few conditions) designs; maximize trial numbers • Establish test–retest reliability of (adapted) designs • Establish behavioral stimulation effects for (adapted) designs in the target population of the planned imaging study
tDCS	(1) **Targeting** • Neuronavigated targeting is preferred over scalp-based approaches, especially for focal set-ups • Implement methods to minimize electrode displacement and verification of positioning accuracy relative to intended target regions (see Figure 1) (2) **Stimulation** • Individually optimized tDCS are preferable over uniform approaches in contexts that aim to maximize effectiveness • Optimization can be enhanced by considering multiple sources (e.g., anatomy, modeling, fMRI) • Focal tDCS is recommended for establishing causal brain-behavior relationships; conventional tDCS may have advantages in specific contexts (e.g., clinical populations)
Control	(1) **Blinding** • Triple blinding and use of optimized methods for participant blinding and assessment are recommended • Reporting of blinding success and adverse effects is essential (2) **Experimental design** • Carefully consider the required level of experimental control (e.g., task, regional, timing, polarity or a combination of them) to answer specific research questions (3) **Meta-control** • Pre-registered reports are the best option to reduce bias and to enhance transparency (Note: early planning for protocol development and peer review is required) • Pre-register methods, hypotheses and analytical approaches and clear statement of exploratory analyses are minimum requirements • Implement open science principles, including FAIRification • Adhere to relevant field specific (i.e., imaging, tDCS) guidelines for data analysis, sharing and reporting

modulation of TMS-induced motor evoked potentials (MEPs), this approach cannot be used to quantify neural effects of tDCS on cognition. Contemporary systems neuroscience research has also highlighted that cognitive functions are enabled by large-scale functional brain networks relying on coordinated processing across various regions (Breakspear, 2017; Pang et al., 2023). To date, however, there is still relatively little knowledge about how tDCS impacts these complex human brain networks, which can be addressed by combining tDCS with modern brain imaging techniques.

In principle, tDCS can be combined with different functional imaging techniques, including electroencephalography (EEG, Polanía et al., 2011; Okazaki et al., 2023), magnetoencephalography (MEG, Jang et al., 2017; Matsushita et al., 2021), functional near-infrared spectroscopy (fNIRS, McKendrick et al., 2015; Dutta, 2021) or functional magnetic resonance imaging (fMRI, Esmaeilpour et al., 2020; Jamil et al., 2020). However, combining tDCS with imaging technology requires careful consideration of appropriate designs and also decisions about which approach is best suited to answer specific research questions.

For example, imaging can be conducted either sequentially (before and after tDCS) or concurrently with tDCS. Sequential imaging allows the investigation of potential after-effects of the stimulation on brain function (Keeser et al., 2011; Shahbabaie et al., 2018) or can be used to interrogate the neural consequences of behavioral add-on effects when tDCS is administered during multiday training sessions or therapeutic interventions (Allman et al., 2016; Antonenko et al., 2023). In contrast, concurrent imaging and tDCS allows investigation of immediate tDCS effects on brain function (Esmaeilpour et al., 2020).

With regard to imaging modalities, EEG and MEG allow mapping of brain dynamics with excellent temporal resolution, which renders them optimal for investigating modulation of fast neural oscillations (Rossi et al., 2022). MEG and fNIRS are most sensitive to modulation of cortical regions (Attal et al., 2012; Li et al., 2023), and therefore less suited to investigate potential subcortical stimulation effects. In this review, we will focus on fMRI, because it allows investigating tDCS effects on brain dynamics with high spatial precision and sufficient temporal resolution across the entire brain. In addition, high resolution structural imaging data can be acquired in the same imaging session, allowing precise localization of potential stimulation effects, verification of correct electrode positions on the scalp and realistic current modeling based on individual head and brain anatomy (Hunold et al., 2023). These advantages have turned fMRI into the most widely used imaging technique to investigate the neural mechanisms underlying tDCS (Esmaeilpour et al., 2020), including pioneering intrascanner work that demonstrated acute modulation of ongoing brain activity at the stimulation site and large-scale neural

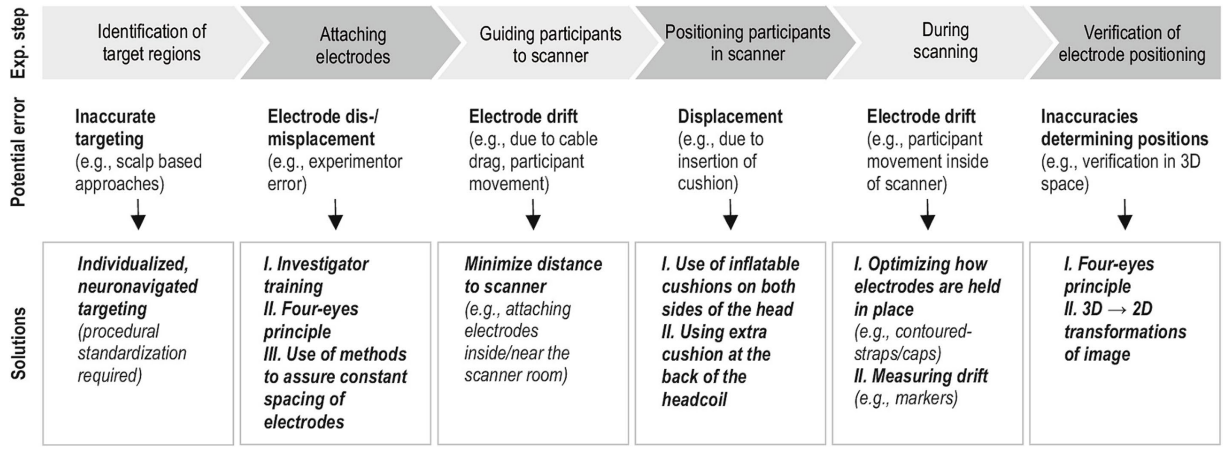

FIGURE 1
Illustrates factors that can affect electrode position accuracy during concurrent fMRI-tDCS experiments and subsequent verification. Suggestions are based on our own experience during an ongoing multicenter, intrascanner tDCS-fMRI project (www.memoslap.de/). The upper panel shows the different phases of a concurrent tDCS-fMRI study and subsequent identification of electrode positions based on structural images of individual participants. Below, examples for potential sources of errors (middle panel) and possible solutions (bottom panel) are described. An example for a method to assure constant spacing of electrodes for a 3 × 1 focal montage that uses a 3D printed spacer can be found in Niemann et al. (2024). Because verification of electrode positions based on 3D structural images can be challenging, transformation into a 2D "pancake view" of the reconstructed scalp may be suited to facilitate identification of actual scalp positions of tDCS electrodes (De Munck et al., 2013; Fleury et al., 2019). Fully automated methods based on neural network models are currently being developed by our group.

networks (Meinzer et al., 2013; Antonenko et al., 2017; Jamil et al., 2020).

3 Investigating the underlying causes of variability in tDCS-fMRI studies

Since the reintroduction of tDCS at the turn of the 20th century (Priori et al., 1998; Nitsche and Paulus, 2000), numerous publications have reported promising effects of tDCS on motor and cognitive functions in health and disease, but also substantial intra- and interindividual variability of stimulation effects. This has prompted increased interest in investigating the underlying sources of variable tDCS responses, that are thought to be multifactorial and can broadly be classified as participant- and stimulation-dependent factors (Fertonani and Miniussi, 2017). In addition, developing optimal designs for either tDCS and fMRI studies can be challenging in itself. This is further complicated when both techniques are combined and design optimization may require creative solutions and specialist input from different fields. This will be discussed in the following sections.

3.1 Participant- and stimulation-dependent factors

Participant-dependent factors include trait- and state-dependent characteristics of the participants, including baseline behavioral performance, microstructural, metabolic and functional brain network variations between participants or intraindividual differences in intrinsic brain states of each participant at different stimulation sessions (Hordacre et al., 2017; Aberra et al., 2018; Antonenko et al., 2019a). The importance to account for these factors has been emphasized by studies showing that the tDCS response can be associated with demographic, behavioral, or neurofunctional characteristics of participants, including sex, age, education levels, genetics, cultural background, baseline task performance and neural network organization (Kuo et al., 2006; Berryhill and Jones, 2012; Martin et al., 2017b, 2019b; Antonenko et al., 2018; Fridriksson et al., 2019; Perceval et al., 2020; Ghasemian-Shirvan et al., 2022). Moreover, electric field modeling studies that considered individual head and brain anatomy have demonstrated associations between regional electric field strength and modulation of behavior, neurophysiological parameters, fMRI-derived brain networks, regional cerebral blood flow and neurochemical parameters (Kim et al., 2014; Cabral-Calderin et al., 2016; Antonenko et al., 2017, 2023; Jamil et al., 2020). These studies have highlighted the contribution of various participant characteristics to variable tDCS responses that require more systematic investigation in the future.

On the other hand, many stimulation-dependent factors, like the timing, intensity or duration of tDCS are determined by a given experiment. Yet, even minor modifications to experimental protocols can alter the outcomes (e.g., Gauvin et al., 2017), thereby contributing to differences between studies. However, many of these factors can also interact directly with participant characteristics. For example, while the intensity of the induced current was held constant in the majority of previous tDCS studies, it has been convincingly suggested that individual skull (Datta et al., 2009; Bikson et al., 2012; Hanley and Tales, 2019; Sun et al., 2021), or brain anatomy (Suh et al., 2012; Dahnke et al., 2013; Filmer et al., 2019), critically determine how much current reaches the target regions for tDCS, resulting in variable current dose in the target regions. Moreover, accurate positioning of the electrodes on the participants' scalp, one of the most critical stimulation dependent factors, can be affected by experimenter error (i.e., electrode misplacement) or incremental drift over the course of the experiment, resulting in current flow variations between participants (Woods et al., 2016; Indahlastari et al., 2023). This issue

might be even more relevant for focal tDCS set-ups, that constrain the current flow to circumscribed brain regions (Villamar et al., 2013; Gbadeyan et al., 2016b), because the regional specificity of the administered current renders these setups particularly vulnerable for deviations from intended electrode positions, resulting in reduced current dose in target regions for tDCS (Niemann et al., 2024).

Of note, complex intrascanner tDCS-fMRI studies that require participants to walk to and be positioned inside the scanner with electrodes attached, are at high risk for electrode displacement and this effect may vary depending on target sites (e.g., electrodes positioned underneath the cushions that are used to stabilize the head may be more likely to move). Specific problems pertaining to mis- and displacement of electrodes during tDCS-fMRI studies and subsequent verification of correct electrode positions are illustrated in Figure 1, along with suggestions how to minimize them. Therefore, future research in this field should routinely implement appropriate methods not only for improving electrode positioning prior to scanning (e.g., electrode placement guided by neuronavigation) (De Witte et al., 2018), but also implement methods to minimize electrode displacement and drift, verify electrode positions before and/or after functional imaging, and consider empirically determined actual electrode positions when dose–response relationships are investigated (Woods et al., 2015; Knotkova et al., 2019; Antonenko et al., 2019b; Albizu et al., 2023; Niemann et al., 2024).

3.2 Design considerations for tDCS-fMRI studies

Investigating and controlling for variability in tDCS-fMRI studies can be challenging because stimulation effects are not assessed by a direct marker of brain physiology (i.e., MEPs), but rely on proxy measures of brain function (i.e., variable behavioral performance in task-related fMRI and indirect measures of neural activity, like the blood oxygenation-dependent response). Behavioral performance parameters can be significantly influenced by numerous internal and external factors. For example, improvements in performance across repeated sessions have been linked to familiarization and training effects, or the development of cognitive strategies (Bell et al., 2018). These confounds are particularly relevant for cross-over designs frequently used in tDCS-fMRI studies and can result in reduced effect sizes, even when the stimulation conditions are appropriately balanced across participants (Falleti et al., 2006; Hausknecht et al., 2007; Bartels et al., 2010). While these confounds can be mitigated to some degree by choosing robust designs and implementation of parallel task versions, it is advisable to formally establish test–retest reliability of experimental paradigms in the specific target populations (e.g., young vs. older individuals, clinical populations of interest) prior to implementation in costly tDCS-fMRI studies and to consider the outcomes when interpreting effect sizes of behavioral and neural modulation.

Moreover, specific paradigms or populations are particularly challenging for tDCS-fMRI studies. For example, learning paradigms are typically associated with performance increases across time, therefore the number of correct responses and errors vary depending on learning stage. Inclusion of both response types in the analysis can be problematic, because the neural signatures differ (Postman-Caucheteux et al., 2010). Moreover, restricting the analysis to correct trials reduces statistical power to detect learning specific neural activation in early stages or in different tDCS conditions. One possible solution for this problem was suggested by Sliwinska et al. (2017), who used an associative picture-word learning paradigm and provided feedback about correct associations after each trial. This feedback-based design assured that "learning" was possible even following incorrect responses, thereby allowing to investigate a common neural process across all trials. Moreover, behavioral responses can be highly variable *per se* in certain populations, which can mask potential neural tDCS effects. This was addressed by Darkow and Flöel (2016), who investigated tDCS effects during a picture naming task in patients with chronic language impairment (aphasia). In this study, only object pictures that could be named consistently by the patients across several baseline naming assessments were used. This maximized the number of correct responses during a subsequent cross-over tDCS-fMRI study and allowed imaging of the neural effects of tDCS on residual language networks, independent of performance.

Another important aspect specific to imaging of tDCS effects pertains to the robustness of the imaging procedure itself, that can be affected by a number of different factors including physiological noise due to cardiac and respiratory cycles, head motion artifacts, magnetic field inhomogeneities, and fMRI signal drift. These factors can contribute to variability in cross-over and longitudinal tDCS-fMRI studies and need to be monitored and considered in data analysis (Esmaeilpour et al., 2020). However, certain aspects of tDCS-fMRI studies can also be addressed at the design level. For example, fMRI signal drift depends on gradual heating of the MRI scanner and can be controlled for to some extent by scanning participants at the same time of day or by "warming up" the scanner prior to each session. However, this does not address within-session effects, i.e., signal changes from the early to later stages of a paradigm. An elegant solution to this problem was suggested by Sliwinska et al. (2017) in their picture-word association learning paradigm. The authors grouped learning trials in a way that different stages of the learning process (i.e., low vs. higher proficiency) were achieved repeatedly across consecutive micro-blocks, thereby minimizing the effect of signal drift on fMRI activity for each learning stage. Notably, numerous other factors have been shown to reduce reliability in task-related imaging protocols, including participant characteristics (e.g., advanced age, clinical populations > young healthy participants), design (e.g., long > short retest intervals; event-related > block designs) or specifics of data analysis (e.g., univariate or region-of-interest > multivariate analyses, complex > simple contrasts; for review see Noble et al., 2021). Because these factors can also increase variability in tDCS-fMRI studies, they require careful consideration at the design stage, to minimize the risk of masking potential tDCS effects on behavior and brain functions.

Additional consideration pertains to imaging artifacts that are induced by conventional and focal set-ups. While image distortions are typically limited to the scalp and skull, signal-to-noise (SNR) reductions in the functional images, that are most pronounced underneath the location of the electrodes, have been reported (Saiote et al., 2013). SNR reductions are most pronounced for the comparison between images acquired with and without electrodes (Gbadeyan et al., 2016b), but occur to a lesser degree also for the comparison of active vs. sham conditions and may vary between brain regions (Antal et al., 2011; Holland et al., 2011). Therefore, careful quantification of potential imaging artifacts and SNR reductions associated with

specific equipment and target regions is necessary, and the outcomes should be considered in the design of the study. For example, when effects of different active stimulation sites are of interest, the between site effect needs to be controlled by comparison with its own sham condition with a similar regional SNR profile.

In sum, investigating the variability underlying tDCS effects using fMRI requires careful consideration of generic issues relevant for each individual approach (e.g., robustness of designs, accurate placement of electrodes), but also those that are specific to their combined use (e.g., imaging artifacts induced by the tDCS set-up, drift of electrodes during imaging, design optimization for imaging and tDCS), which can be challenging. However, tDCS-fMRI approaches also offer unique opportunities to tease apart the contribution of participant-, stimulation- and design-dependent factors on the variability of tDCS effects (e.g., structural MRI allows to estimate effects of anatomical variability on current flow patterns; comparison of tDCS administered during task performance or rest investigate neural stimulation effects on a constrained vs. unconstrained set of brain regions), thereby contributing to the development of future individualized tDCS approaches with potential to enhance the effectiveness of this technique in experimental and translational human neuroscience.

4 Optimization of tDCS protocols

The specific montages used to administer tDCS (e.g., conventional vs. focal set-ups, size and positioning of electrodes) affect the intensity and distribution of the induced current. Conventional set-ups use relatively large electrodes (e.g., 5 × 7 cm, up to 10 × 10 cm) that are typically attached over cortical regions in different hemispheres and induce a relatively wide-spread current flow affecting multiple neural networks. This lack of focality renders them less desirable for revealing regionally specific, causal brain-behavior relationships compared to focal montages. Those use smaller and often concentrically arranged electrodes in the same hemisphere to constrain the current to circumscribed brain regions (Kuo et al., 2013; Bortoletto et al., 2016). Notably, conventional setups may be more resilient to positioning errors and electrode drift compared to focal set-ups and electrode displacement has been shown to result in physiologically significant reductions in current dosage specifically within the immediate target regions (Niemann et al., 2024). This is particularly relevant for tDCS-fMRI studies, that are at high risk for electrode displacement, e.g., due to positioning of participants in the scanner after electrode attachment (see discussion above). Conventional set-ups may also have advantages in contexts where experimenter error is more likely to occur (e.g., routine clinical care, multicenter intervention studies) or specific clinical populations with variable lesion patterns and functional reorganization (Darkow et al., 2017). Therefore, the choice of montage in tDCS-fMRI studies strongly depends on the specific research question and population.

Furthermore, the majority of tDCS research has relied on the 10–20 (or 10–10) EEG system to identify target brain regions (Thair et al., 2017). This approach involves manual or automatic identification of anatomical markers (e.g., nasion, inion, preauricular points) and additional measurements (e.g., head circumference, calculation of intersections between landmarks) to determine the intended scalp positions of electrodes. Depending on which system is used, 25 or 74 reference points are available and placement is often guided by electrode caps (Tsuzuki et al., 2016). While this approach considers head size of individual participants to some degree, other properties of brain and skull morphology are neglected, resulting in a loss of precision (Herwig et al., 2003; De Witte et al., 2018). Structural MRI-guided neuro-navigation is a more individualized localization technique, which has mainly been used in experimental and clinical TMS studies, but more recently also for positioning of tDCS electrodes (De Witte et al., 2018; Lioumis and Rosanova, 2022). This approach requires a high-resolution structural T1-weighted image of individual participants that can be acquired prior to a tDCS-fMRI study. By co-registration of the structural image with a three-dimensional brain model and use of specific soft- and hardware for identifying the target brain regions, electrode positioning accuracy relative to individual brain anatomy can be improved (De Witte et al., 2018). Because of significant variations in brain anatomy and head shape, individualized neuronavigation-based electrode placement is currently the best option to improve positioning of electrodes at the intended scalp positions in tDCS-fMRI studies and scalp-based approaches are discouraged, especially for focal set-ups.

Individual differences in brain anatomy are crucial not only for precise placement of electrodes but also for optimizing the distribution of tDCS-induced electric fields within individual brains (Kim et al., 2014; Bikson et al., 2015; Antonenko et al., 2021). Previous studies have also highlighted the importance of investigating fundamental aspects of the induced electric field, such as current strength, focality, and its dependency on anatomical features of the head (Edwards et al., 2013; Opitz et al., 2015; Saturnino et al., 2015). In this context, computational models are frequently used to estimate the strength of the cortical electric field, since direct measurement in the human brain is not feasible except in highly selected patient populations (e.g., tumor resection, brain surgery for epilepsy treatment; e.g., Huang et al., 2017).

Recently, individualized electric field calculations have allowed investigating correlations between the individually received physical stimulation dose and the physiological impact of tDCS (for review see Hunold et al., 2023), known as cortical dose–response relationship. Moreover, manufacturers of brain stimulation devices are increasingly interested in updating their devices' capabilities to estimate the electric field via computer modeling techniques, which rely on electrode positioning and stimulation current intensity. For instance, Soterix HD-Explore[1] is a commercial, stand-alone software that models the current flow using the finite element method to estimate the electric field distribution for complex tDCS set-ups. However, it is essential to note that computer simulations estimate the electric field based on assumptions about electrical conductivity of different tissue classes and that they depend on the anatomical accuracy of the (semi-)automatic tissue segmentations obtained from the MR images. Therefore, validation of these assumptions and assessment of the segmentation accuracy is critical to improve the accuracy of computational models, and simulation errors may obscure potential associations between estimated fields and the recorded behavioral or neural response. In this context, Magnetic Resonance Current Density Imaging (MRCDI) and Magnetic Resonance Electrical Impedance Tomography (MREIT) are emerging

1 https://soterixmedical.com/research/software/hd-explore

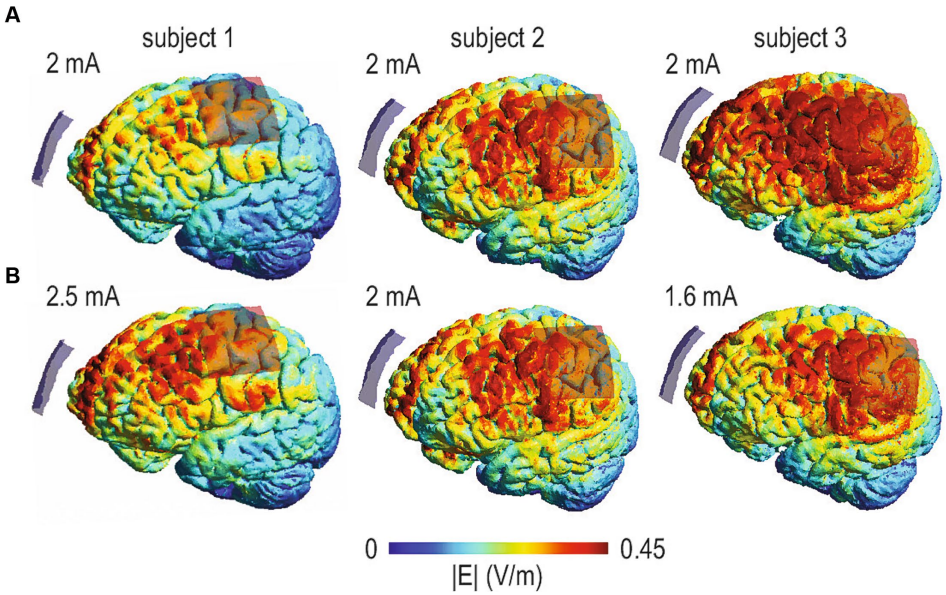

FIGURE 2
Computational models of tDCS-induced electrical current flow based on structural MRI data of three participants and a conventional montage targeting the left primary motor cortex (anode). Cathodes are positioned over the contralateral supraorbital region. Colors illustrate the distribution and intensity of the current (electric field strength, V/m). Only the left side of the brain is shown. **(A)** When individual head and brain anatomy is considered in computational models of current flow, the same intensity (i.e., tDCS administered with 2 mA) can result in highly variable current flow in individual participants. **(B)** Provides a simple example of dose control. Simulations were conducted with different intensities (i.e., 2.6, 2.0, and 1.5 mA) to minimize differences between participants.

techniques to investigate tDCS-induced current flow conductivity of brain tissue during concurrent tDCS-MRI measurements, respectively (Göksu et al., 2018, 2019). These modalities have potential for validating tDCS electric field simulations and optimizing individualized current dose calculations in both healthy participants and patients.

Another issue that has recently gained substantial attention in tDCS studies is dose control. In this context it is important to note that even when the same current intensity is applied, participant-specific factors like skull and brain anatomy and others are major determinants of the actual current dose arriving in the target regions (Evans et al., 2020; Antonenko et al., 2021). This is illustrated in Figure 2. Hence, recent studies have used computational current modeling approaches to optimize stimulation intensity across participants. For example, Caulfield et al. (2020) acquired structural MRI data of individual participants to compute a "reverse-calculated tDCS dose" of tDCS applied at the scalp required to induce a uniform E-field (arbitrarily set at 1.00 V/m and not yet empirically tested in a prospective stimulation study) in a region-of-interest in the primary motor cortex. Notably, the minimum current intensity threshold for physiological modulation in different brain regions is unknown and may vary between stimulation sites and individuals. Moreover, increasing intensity does not necessarily increase neurophysiological effects and even changes in polarity have been observed. For example, while cathodal tDCS with 1 mA and 3 mA induced inhibitory effects, 2 mA may result in enhanced excitability (Batsikadze et al., 2013; Mosayebi Samani et al., 2019).

Therefore, currently little is known about objective optimization criteria for field intensity (Lee et al., 2021). Moreover, reaching a pre-determined criterion may require intensities beyond accepted safety thresholds in individual participants (Antal et al., 2017a) and in the study above, the required current intensity across participants ranged from 3.75–9.74 mA (Caulfield et al., 2020). Therefore, alternative approaches are currently being developed that use a combination of individual electric field modeling and anatomical information to enhance regional precision (Rasmussen et al., 2021) or the development of prospective dosing strategies aimed at matching the average field dose in different target regions at the group level, while maintaining dose variability for each region to enable systematic tests of dose–response relationships (Saturnino et al., 2021). However, in order to be valuable, optimization approaches should be informed by multiple sources (e.g., underlying anatomy, computational estimation of field magnitude, focality or functional task-dependent activity for optimization of stimulation targets) rather than being unidimensional.

5 High-level control

Achieving high-level experimental control is crucial not only to ensure reliable and valid results, but also to establish causal relationships in tDCS studies. In this context, we will discuss two major aspects relevant to tDCS-fMRI studies: (a) blinding of participants and research staff and (b) design-related issues pertaining the establishment of valid assumptions about the relationship between brain stimulation and behavioral and neural modulation. A separate section, we will discuss "control" from a broader perspective, i.e., in the context of open science practices and recent efforts to increase the validity, reproducibility and transparency of empirical research, which is highly relevant for tDCS-fMRI studies.

5.1 Blinding

The majority of previous tDCS studies have relied on placebo ("sham") tDCS conditions to control for placebo effects. Sham-tDCS typically involves gradually increasing the current to the target intensity (e.g., over 10 s), followed by an immediate or briefly delayed fade-out period, during which the current intensity is decreased to zero (Huey et al., 2007; Axelrod et al., 2015; Jaberzadeh et al., 2019). Sham-tDCS protocols intend to elicit a transient physical sensation on the scalp (e.g., tingling, itching) that closely resembles the sensation experienced during active stimulation, but without inducing physiologically relevant effects on brain function due to the short duration of the stimulation. Sham protocols have been suggested to allow for effective blinding of participants (Gandiga et al., 2006) without modulating corticospinal excitability, CSE (Dissanayaka et al., 2018). However, several recent studies have also questioned blinding efficacy of specific sham-tDCS protocols (O'Connell et al., 2012; Wallace et al., 2016; Greinacher et al., 2019; Turi et al., 2019). For instance, Greinacher et al. (2019) probed blinding integrity every 30 s during a low-intensity active or sham tDCS protocol (30 s ramp-up/down, 600 vs. 20 s active 1 mA M1-tDCS) and demonstrated that participants could identify active tDCS in approx. 60% of the probes with high confidence.

These findings have recently led to the development of novel sham protocols that minimize differences between active and sham conditions in tDCS studies. For example, Neri et al. (2020) introduced a new sham-tDCS approach for multi-electrode tDCS that used computational current modeling to optimize electrode positions during sham in a way that zero or very low magnitude electric fields are delivered to the brain, while medium to high intensity currents are maintained in at least some scalp electrodes. Notably, participant blinding for this new approach was superior compared a conventional bifocal montage and the desired blinding effect was achieved without eliciting a significant effect on CSE (Neri et al., 2020). These findings suggest that blinding efficacy reported for conventional sham protocols may need to be interpreted with caution (O'Connell et al., 2012) and alternative protocols that minimize differences between active and sham-tDCS may be more appropriate for achieving participant blinding.

In addition, rigorous staff blinding is crucial for preventing experimenter effects, such as the introduction of selection bias, observer bias, or inadvertent effects on experimental outcomes or during data analysis (Grimes and Schulz, 2002; Holman et al., 2015). Blinding of experimenters conducting the experiment and interacting with participants can be difficult with some commercially available stimulators (e.g., with indicator lights or sounds indicating on vs. off conditions), unless a two-experimenter approach is adopted: one administering the stimulation, while the second remains blinded while interacting with the participant (Reinhart et al., 2017). However, the majority of modern stimulators can now be equipped with advanced study modes, enabling easy customization for various stimulation conditions and parameters that can be triggered by pre-assigned codes. These new developments minimize the risk of unintentional unblinding of the experimenter and it is highly advisable to use such approaches in tDCS-fMRI studies. In addition, blinding of staff during data analysis is also advised and can be achieved by masking the stimulation conditions (i.e., by using participant codes that do not reveal active and control conditions).

The final issue pertains to how blinding is assessed. Here, a common practice involves a post-stimulation questionnaire, serving two key purposes: (a) directly valuating participants' capacity to differentiate between stimulation conditions, which is frequently complemented by (b) self-reported assessment of potential side effects (e.g., tingling or burning, changes in mood or concentration levels) experienced during the stimulation (Ambrus et al., 2012; Turi et al., 2019). Although end-of-study questionnaires have been considered valid measures for evaluating the effectiveness of blinding (Antal et al., 2017b), a recent study by Turner et al. (2021) reported that the accuracy of end-of-study guesses was not more reliable than chance in predicting participants' ability to distinguish between active or sham tDCS. Hence, it was suggested to incorporate additional online probe questions during the stimulation process for more accurate evaluation of blinding efficacy if possible. In any case, careful documentation of methods and results of participant and staff blinding is essential in all tDCS studies (Ekhtiari et al., 2022).

5.2 Establishing causality in tDCS studies

Another aspect particularly relevant for tDCS-fMRI studies pertains to establishing causal relationships between stimulation effects and behavioral and neural modulation. This cannot be achieved by comparing the effects of active vs. sham tDCS alone, because the latter only controls for potential placebo effects. In principle, stronger causal assumptions for the relevance of a given brain region to specific behavioral outcomes are potentially possible by additional direct comparison of anodal-excitation and cathodal-inhibition effects (AeCi). However, AeCi effects have rarely been demonstrated for cognitive tasks, mainly due to relatively weak or variable inhibitory effects of cathodal tDCS on cognition, which may be explained by redundancy within the neural networks supporting higher-order cognitive functions (Jacobson et al., 2012). Moreover, cathodal tDCS has also been shown to enhance performance during specific tasks, presumably by enhancing signal-to-noise during cognitive tasks (Antal et al., 2004).

However, several other approaches to achieve high-level experimental control in tDCS-fMRI studies are suitable and depend on the specific research question. For example, regional specificity of tDCS effects can be investigated by including one or more additional active control stimulation sites, specifically targeting cortical regions outside of the neural network(s) involved in processing of the task of interest. This approach not only allows to investigate unspecific (placebo) effects, but also the specificity of neural network modulation relative to the respective task. For example, Gbadeyan et al. (2016a) investigated behavioral effects of focal tDCS administered to either the left or right dorsolateral prefrontal cortex (dlPFC) and M1 during a visual Flanker task. Prefrontal active vs. sham tDCS improved adaptive cognitive control, thereby confirming involvement of both left and right dlPFC in this specific process. The absence of stimulation effects after left or right M1 tDCS demonstrated regional specificity. Notably, higher-order cognitive functions are often supported by multiple brain regions that are organized in partially overlapping neural networks. Therefore, selecting suitable and meaningful active control sites can be challenging.

Regional specificity can be complemented by the investigation of task specificity of tDCS effects. At the lowest level of control, the latter involves two or more different tasks, that are completed while the same cortical region is stimulated. This allows controlling for unspecific effects of the stimulation and demonstration that a given

region or network is involved in task A, but not B. For instance, Martin et al. (2017a) demonstrated improved performance in a visual perspective taking task when focal anodal tDCS was administered over the dorsomedial frontal cortex (dmPFC). No significant change was observed in a source memory task with the same tDCS intervention, which illustrates a simple case of task-specificity of tDCS effects. Another highly specific aspect of task specificity pertains to activity selective stimulation effects (Bikson et al., 2013). This implies that even though several brain regions may be affected by the current, only those activated by a specific task are susceptible to the effects of tDCS. To the best of our knowledge, this assumption has not yet been tested with functional imaging. In principle, this could be investigated with a conventional montage that induces relevant current in neighboring brain areas that are differentially activated by two tasks. In this context, it would be predicted that the same montage preferentially modulates activity in the respective task-relevant regions and networks.

Moreover, one of the highest levels of experimental control at the design stage can be achieved by the combined investigation of regional and task specificity. This requires a minimum of two stimulation sites targeting processes or neural networks relevant for different tasks. For example, Martin et al. (2019a) investigated effects of focal tDCS administered to either the right TPJ or dmPFC on social cognition, including visual perspective taking tasks requiring line-of-sight and mental rotation judgments. Using this approach, the authors demonstrated a double dissociation of behavioral tDCS effects, indexed by specific facilitation of embodied mental rotation of the self into an alternate perspective by rTPJ tDCS, while dmPFC tDCS facilitated integration of social information relevant to self-directed processes.

Finally, analysis of specificity is not limited to tasks and regions, but also applies to the timing of the stimulation relative to a given task (temporal specificity). The majority of previous studies have employed single tasks and investigated behavioral effects of tDCS administered at different time points (i.e., prior to, during or after the task). These studies have highlighted that maximal tDCS effects may be achieved with varying timing across different functional domains, including visuomotor and visuospatial skills (Reis et al., 2015; Oldrati et al., 2018), motor network modulation (Calzolari et al., 2023) and language processing (Cao and Liu, 2018). Moreover, timing specific neurophysiological or behavioral modulation have been reported in different populations (i.e., young vs. older adults, for review see Perceval et al., 2016). Hence, these factors also need to be considered in the design phase of future tDCS-fMRI studies, e.g., by establishing optimal stimulation time windows in prior behavioral studies.

5.3 Scientific rigor and integrity beyond the experimental context

From a broader perspective, high-level control also includes the promotion of open and transparent research practices (Munro and Prendergast, 2019). For example, fMRI data analysis is a complex process that can be accomplished using a variety of platforms and analytical approaches that frequently comprise custom code. This was highlighted by Botvinik-Nezer et al. (2020), who demonstrated that of 70 labs that were asked to analyze the same fMRI dataset, all used different workflows. In the context of the ongoing replication crisis in science (Open Science Collaboration, 2015), appropriate documentation of data analysis procedures, code, and optimally pre-registration of analytical steps is highly desirable when investigating tDCS effects using imaging. This will facilitate the interpretation of the results and enhance the validity of research in this field (Esmaeilpour et al., 2020). Transparency, reproducibility and availability of data and analytical approaches can be further enhanced by adhering to relevant guidelines for data analysis and sharing (e.g., Gorgolewski and Poldrack, 2016; Nichols et al., 2017) and the FAIR (Findable, Accessible, Interoperable, Reusable) guiding principles for scientific data management and stewardship (Wilkinson et al., 2016).

Another important issue pertains to publication bias favoring positive outcomes, either because researchers do not attempt to disseminate negative results, or are discouraged by publishers to submit even valid negative findings. A particularly powerful approach to prevent publication bias are registered reports, where a study is accepted for publication based on its merit to answer a specific research question, irrespective of the eventual outcomes (that will be published alongside the protocol after study completion). Unlike pre-registration, the methodology and hypotheses of the planned study undergoes peer review, which helps to prevent publication of negative results based on methodological flaws (Chambers and Tzavella, 2021). Pre-registered reports are particularly relevant in the context of recent meta-analyses and systematic reviews of tDCS effects on human cognition (Galli et al., 2019; Yan et al., 2020; Figeys et al., 2021; Majdi et al., 2022), that have discussed not only limited reproducibility and small sample sizes in this field, but also the risk of p-hacking or HARKing (i.e., Hypothesizing After the Results are Known). Pre-registrated reports effectively address these biases and also provide a robust foundation for hypothesis-driven research and confirmatory replication. Notably, several hundred of journals now offer this option, including high profile neuroscience and neuroimaging outlets that are of interest for tDCS-fMRI studies (e.g., Nature Communications, NeuroImage, Cortex). Nevertheless, we would also like to emphasize the importance of data-driven and exploratory analyses. This particularly relevant in a relatively novel and evolving fields of science like tDCS-fMRI and the multitude of parameters that can influence stimulation success. In this context, clearly stated exploratory analyses can generate new hypotheses and serve as starting points for subsequent confirmatory studies.

6 Systematic assessment of tDCS effects across the human lifespan

Translational tDCS research that aims at counteracting age-associated decline or impairment of cognitive functions has yielded promising but mixed results so far (e.g., Perceval et al., 2016). For example, studies that directly compared tDCS effects in young and older adults have demonstrated larger behavioral effects in younger (Ross et al., 2011; Manenti et al., 2013), while others revealed larger effects in older adults (Zimerman et al., 2014; Cespón et al., 2017; Perceval et al., 2020). Moreover, while some studies have suggested that tDCS can improve (impaired) performance in older adults to the level of younger adults (Meinzer et al., 2013), others found detrimental effects in older adults when using the same montage that improved behavioral functions in young adults (Boggio et al., 2010; Fertonani et al., 2014). These findings are not surprising, because the neural substrates that support cognition and motor function in young and older adults can differ substantially and therefore, positive results

obtained in tDCS studies involving young individuals cannot automatically be translated to older populations (Perceval et al., 2016). This needs to be investigated more systematically in the future across functional domains and the entire human lifespan.

Furthermore, neural aging, which for most cognitive domains becomes apparent by the end of the third decade of life (e.g., Hedden and Gabrieli, 2004), is not a uniform process and the degree of functional and structural brain reorganization is influenced by a number of intra-individual, environmental and life-style factors (Gutchess, 2014). In addition, age-related changes in brain structure, cerebrospinal fluid/brain ratio or skull thickness may affect the degree or distribution of the induced current itself (Opitz et al., 2015; Indahlastari et al., 2020; Antonenko et al., 2021). These aging-related factors may explain differences in stimulation response between young and older individuals, but also variability of stimulation effects within older population. To date, however, it has not yet been systematically investigated how potential differences in current flow due to brain atrophy or other factors, reported to significantly impact current flow based on simulation studies (Indahlastari et al., 2020), and interactions with age-associated functional network reorganization, affect behavioral and neural tDCS effects. TDCS-fMRI approaches are particularly suited to investigate these important issues, because they can provide information on both baseline neural network organization and functional changes due to the stimulation. Moreover, structural imaging data can be acquired in the same session and subsequently be used for individualized current modeling. Consideration of these variables in data analysis has great potential to reveal the underlying mechanisms and predictors of stimulation response across the human lifespan.

Finally, many neurological conditions (e.g., stroke-induced motor or cognitive impairment, dementia and precursors) primarily occur in elderly individuals, thereby a pathological process is superimposed on "normal" age-associated structural and functional brain reorganization. Hence, a better understanding of how these age-associated brain changes interact with tDCS also has direct implications for enhancing the clinical application of this technique in the future (Crosson et al., 2015).

7 Establishing large-scale consortia for coordination of tDCS research

Developing research consortia has yielded unprecedented insights and facilitated discovery research in many fields of basic and translational neuroscience (e.g., Human Brain Project[2]; ENIGMA[3]), by strengthening of research capacity through pooling of resources and expertise and generating standardized outcomes and solutions for a common set of questions (Tagoe et al., 2019).

To date, however, a significant proportion of tDCS studies have been limited by small sample sizes and highly variable methodological approaches (Minarik et al., 2016; Hiew et al., 2022). Given the vast parameter space of tDCS experiments (e.g., montage, current intensity, target region, polarity, control condition; Sergiou et al., 2020; Kurtin et al., 2021), there are rarely comparable studies with similar protocols, precluding definitive conclusions regarding the effects of tDCS on cognition or establishing optimal protocols for specific research questions. Consortia can effectively address these issues by facilitating participant recruitment from multiple contributors using coordinated methodology and outcome measures. The increased diversity of the sample can in turn increase the generalizability of research findings and concurrent recruitment of participants expedites data acquisition, thereby accelerating the research process. This is currently being addressed for the first time by a recently funded project in Germany, that employs highly coordinated tDCS-fMRI and computational approaches to systematically investigate the underlying neural mechanisms and predictors of tDCS effects on learning and memory across different functional domains and the human lifespan. This consortium will also play an important educational role by providing training opportunities for junior scientists and researchers through high-quality brain stimulation workshops and conferences, to foster knowledge exchange, skill development, and networking. Notably, a similar global approach has been initiated by the International Network of Neuroimaging Neuromodulation (INNN), a group comprising experts and early-mid career researchers, that conducts regular workshops and education seminars that are publicly available via a YouTube channel.[4]

Furthermore, consortia play a vital role in monitoring and standardizing the execution and reporting of tDCS interventions. Importantly, combining tDCS with fMRI requires specific equipment, poses multiple technological challenges (e.g., safety assurance and management of potential imaging artifacts introduced by the equipment). Consequently, research consortia should aim to bring together expertise not only from brain stimulation, but also invite collaborators from additional relevant fields with specific expertise in neurophysics, engineering, neuroimaging methodology and data analysis and also data management, to further strengthen this field. These approaches will be highly relevant, because development of large-scale coordinated tDCS-fMRI datasets will require advanced and automated analytical procedures like machine learning and other data-driven approaches. For example, machine learning algorithms have shown great promise in predicting tDCS response in small scale studies based on a variety of factors, including current intensity and direction (e.g., Albizu et al., 2020). Adapting and fine-tuning these methods for the use in large-scale samples will likely be the next frontier in increasing our understanding of the neural mechanisms and predictors of tDCS response.

Finally, the lack of sufficient methodological and procedural information frequently hinders reproducibility and further advances in this field (Esmaeilpour et al., 2020). This was recently addressed by an international consortium (The International Network of Transcranial Electrical Stimulation-fMRI, tES-fMRI) by establishing a consensus-based standard for reporting essential details in concurrent tES-fMRI studies (Ekhtiari et al., 2022). The checklist comprises 17 items across three broad categories, namely technological factors (e.g., details of equipment, electrode positioning), safety and noise tests (e.g., reporting of incidents, noise quantification) and methodological factors (e.g., reporting of set-up schematics or the

2 https://www.humanbrainproject.eu/en/

3 https://enigma.ini.usc.edu/

4 https://www.youtube.com/@INNN_Network

tES-fMRI timing). These critical elements represent suggestions for the minimum required information to ensure reproducibility and to enhance the technical and scientific quality and interpretability of future concurrent fMRI-tDCS studies. Importantly, the checklist is suited to facilitate development of similar guidelines for other imaging modalities.

8 Conclusion

To date, there is limited knowledge on how tDCS modulates the complex neural networks supporting higher human cognitive functions in health and disease. Combining neuroimaging technology with tDCS has great potential to reveal the neural mechanisms and predictors underlying behavioral modulation and to identify sources of variability in stimulation response. The present manuscript aimed to discuss the underlying causes of variability in tDCS studies, elaborate on design-related considerations for tDCS-fMRI research, optimization of tDCS and imaging protocols and how to assure high-level experimental control at the level of individual experiments and from a meta-perspective. We also addressed variable tDCS effects across the healthy human lifespan, implications for tDCS studies in age-associated disease, and potential benefits of establishing large-scale, multidisciplinary consortia for more coordinated tDCS research in the future.

We hope that this manuscript will contribute to more coordinated, methodologically sound, transparent and reproducible research in this field, thereby fostering a better understanding of the underlying mechanisms by which tDCS modulates human cognitive functions and ultimately more effective and individually tailored translational and clinical applications of this technique in the future. Ultimately, this will yield information if and how tDCS can modulate human brain functions in a meaningful way.

Author contributions

MM: Conceptualization, Writing – original draft, Writing – review & editing, Investigation, Methodology, Supervision, Funding acquisition, Resources. AS: Conceptualization, Investigation, Methodology, Supervision, Writing – original draft, Writing – review & editing, Visualization. DA: Writing – review & editing. FB: Writing – review & editing. RF: Writing – review & editing. GH: Writing – review & editing. MAN: Writing – review & editing. S-CL: Writing – review & editing. AT: Writing – review & editing. DT: Writing – review & editing. MA: Writing – original draft, Writing – review & editing. HK: Writing – review & editing. LC: Writing – review & editing. GB: Writing – review & editing. MG: Writing – review & editing. TC: Writing – review & editing. DH: Writing – review & editing. ST: Writing – review & editing. FS: Writing – review & editing. YS: Writing – review & editing. AK: Writing – review & editing. MB: Writing – review & editing. AF: Writing – review & editing, Funding acquisition, Supervision, Writing – original draft. DW: Writing – review & editing. SR: Writing – review & editing. FN: Writing – review & editing.

Funding

The author(s) declare that financial support was received for the research, authorship, and/or publication of this article. This research was funded by the German Research Foundation (project grants: ME 3161/3-1; FL 379/26-1; CRC INST 276/741-2 and 292/155-1, Research Unit 5429/1 (467143400), FL 379/34-1, FL 379/35-1, Fl 379/37-1, Fl 379/22-1, Fl 379/26-1, ME 3161/5-1, ME 3161/6-1, AN 1103/5-1, TH 1330/6-1, TH 1330/7-1, NI 683/17-1, HA 6314/10-1, TI 239/23-1, BL 977/4-1, LI 879/24-1). AT was supported by the Lundbeck foundation (grant R313-2019-622). GH was supported by Lise Meitner Excellence funding from the Max Planck Society, and by the European Research Council (ERC-2021-COG 101043747).

Conflict of interest

MAN is in the scientific advisory board of Neuroelectrics and Précis's.

The remaining authors declare that the research was conducted in the absence of any commercial or financial relationships that could be construed as a potential conflict of interest.

The reviewer BL declared a past co-authorship with the authors AF and MAN to the handling editor.

Publisher's note

References

Aberra, A. S., Peterchev, A. V., and Grill, W. M. (2018). Biophysically realistic neuron models for simulation of cortical stimulation. *J. Neural Eng.* 15:066023. doi: 10.1088/1741-2552/aadbb1

Albizu, A., Fang, R., Indahlastari, A., O'Shea, A., Stolte, S. E., See, K. B., et al. (2020). Machine learning and individual variability in electric field characteristics predict tDCS treatment response. *Brain Stimul.* 13, 1753–1764. doi: 10.1016/j.brs.2020.10.001

Albizu, A., Indahlastari, A., Huang, Z., Waner, J., Stolte, S. E., Fang, R., et al. (2023). Machine-learning defined precision tDCS for improving cognitive function. *Brain Stimul.* 16, 969–974. doi: 10.1016/j.brs.2023.05.020

Alexandersen, A., Csifcsák, G., Groot, J., and Mittner, M. (2022). The effect of transcranial direct current stimulation on the interplay between executive control, behavioral variability and mind wandering: a registered report. *Neuroimage: Reports* 2:100109. doi: 10.1016/j.ynirp.2022.100109

Allman, C., Amadi, U., Winkler, A. M., Wilkins, L., Filippini, N., Kischka, U., et al. (2016). Ipsilesional anodal tDCS enhances the functional benefits of rehabilitation in patients after stroke. *Sci. Transl. Med.* 8:330re1. doi: 10.1126/scitranslmed.aad5651

Ambrus, G. G., Al-Moyed, H., Chaieb, L., Sarp, L., Antal, A., and Paulus, W. (2012). The fade-in – short stimulation – fade out approach to sham tDCS – reliable at 1 mA for naïve and experienced subjects, but not investigators. *Brain Stimul.* 5, 499–504. doi: 10.1016/j.brs.2011.12.001

Antal, A., Alekseichuk, I., Bikson, M., Brockmöller, J., Brunoni, A. R., Chen, R., et al. (2017). Low intensity transcranial electric stimulation: safety, ethical, legal regulatory and application guidelines. *Clin. Neurophysiol.* 128, 1774–1809. doi: 10.1016/j.clinph.2017.06.001

Antal, A., Nitsche, M. A., Kruse, W., Kincses, T. Z., Hoffmann, K.-P., and Paulus, W. (2004). Direct current stimulation over V5 enhances Visuomotor coordination by improving motion perception in humans. *J. Cogn. Neurosci.* 16, 521–527. doi: 10.1162/089892904323057263

Antal, A., Polania, R., Schmidt-Samoa, C., Dechent, P., and Paulus, W. (2011). Transcranial direct current stimulation over the primary motor cortex during fMRI. *NeuroImage* 55, 590–596. doi: 10.1016/j.neuroimage.2010.11.085

Antonenko, D., Fromm, A. E., Thams, F., Grittner, U., Meinzer, M., and Flöel, A. (2023). Microstructural and functional plasticity following repeated brain stimulation during cognitive training in older adults. *Nat. Commun.* 14:3184. doi: 10.1038/s41467-023-38910-x

Antonenko, D., Grittner, U., Saturnino, G., Nierhaus, T., Thielscher, A., and Flöel, A. (2021). Inter-individual and age-dependent variability in simulated electric fields induced by conventional transcranial electrical stimulation. *NeuroImage* 224:117413. doi: 10.1016/j.neuroimage.2020.117413

Antonenko, D., Hayek, D., Netzband, J., Grittner, U., and Flöel, A. (2019a). tDCS-induced episodic memory enhancement and its association with functional network coupling in older adults. *Sci. Rep.* 9:2273. doi: 10.1038/s41598-019-38630-7

Antonenko, D., Nierhaus, T., Meinzer, M., Prehn, K., Thielscher, A., Ittermann, B., et al. (2018). Age-dependent effects of brain stimulation on network centrality. *NeuroImage* 176, 71–82. doi: 10.1016/j.neuroimage.2018.04.038

Antonenko, D., Schubert, F., Bohm, F., Ittermann, B., Aydin, S., Hayek, D., et al. (2017). tDCS-induced modulation of GABA levels and resting-state functional connectivity in older adults. *J. Neurosci.* 37, 4065–4073. doi: 10.1523/JNEUROSCI.0079-17.2017

Antonenko, D., Thielscher, A., Saturnino, G. B., Aydin, S., Ittermann, B., Grittner, U., et al. (2019b). Towards precise brain stimulation: is electric field simulation related to neuromodulation? *Brain Stimul.* 12, 1159–1168. doi: 10.1016/j.brs.2019.03.072

Attal, Y., Maess, B., Friederici, A., and David, O. (2012). Head models and dynamic causal modeling of subcortical activity using magnetoencephalographic/electroencephalographic data. *Rev. Neurosci.* 23, 85–95. doi: 10.1515/rns.2011.056

Axelrod, V., Rees, G., Lavidor, M., and Bar, M. (2015). Increasing propensity to mind-wander with transcranial direct current stimulation. *Proc. Natl. Acad. Sci. USA* 112, 3314–3319. doi: 10.1073/pnas.1421435112

Bartels, C., Wegrzyn, M., Wiedl, A., Ackermann, V., and Ehrenreich, H. (2010). Practice effects in healthy adults: a longitudinal study on frequent repetitive cognitive testing. *BMC Neurosci.* 11:118. doi: 10.1186/1471-2202-11-118

Batsikadze, G., Moliadze, V., Paulus, W., Kuo, M. -F., and Nitsche, M. A. (2013). Partially non-linear stimulation intensity-dependent effects of direct current stimulation on motor cortex excitability in humans. *J. Physiol.* 591, 1987–2000. doi: 10.1113/jphysiol.2012.249730

Bell, L., Lamport, D. J., Field, D. T., Butler, L. T., and Williams, C. M. (2018). Practice effects in nutrition intervention studies with repeated cognitive testing. *NHA* 4, 309–322. doi: 10.3233/NHA-170038

Berryhill, M. E., and Jones, K. T. (2012). tDCS selectively improves working memory in older adults with more education. *Neurosci. Lett.* 521, 148–151. doi: 10.1016/j.neulet.2012.05.074

Bikson, M., Name, A., and Rahman, A. (2013). Origins of specificity during tDCS: anatomical, activity-selective, and input-bias mechanisms. *Front. Hum. Neurosci.* 7:688. doi: 10.3389/fnhum.2013.00688

Bikson, M., Rahman, A., and Datta, A. (2012). Computational models of transcranial direct current stimulation. *Clin. EEG Neurosci.* 43, 176–183. doi: 10.1177/1550059412445138

Bikson, M., Truong, D. Q., Mourdoukoutas, A. P., Aboseria, M., Khadka, N., Adair, D., et al. (2015). Modeling sequence and quasi-uniform assumption in computational neurostimulation. *Prog. Brain Res.* 222, 1–23. doi: 10.1016/bs.pbr.2015.08.005

Boayue, N. M., Csifcsák, G., Aslaksen, P., Turi, Z., Antal, A., Groot, J., et al. (2020). Increasing propensity to mind-wander by transcranial direct current stimulation? A registered report. *Eur. J. Neurosci.* 51, 755–780. doi: 10.1111/ejn.14347

Boggio, P. S., Campanhã, C., Valasek, C. A., Fecteau, S., Pascual-Leone, A., and Fregni, F. (2010). Modulation of decision-making in a gambling task in older adults with transcranial direct current stimulation. *Eur. J. Neurosci.* 31, 593–597. doi: 10.1111/j.1460-9568.2010.07080.x

Bortoletto, M., Rodella, C., Salvador, R., Miranda, P. C., and Miniussi, C. (2016). Reduced current spread by concentric electrodes in transcranial electrical stimulation (tES). *Brain Stimul.* 9, 525–528. doi: 10.1016/j.brs.2016.03.001

Botvinik-Nezer, R., Holzmeister, F., Camerer, C. F., Dreber, A., Huber, J., Johannesson, M., et al. (2020). Variability in the analysis of a single neuroimaging dataset by many teams. *Nature* 582, 84–88. doi: 10.1038/s41586-020-2314-9

Breakspear, M. (2017). Dynamic models of large-scale brain activity. *Nat. Neurosci.* 20, 340–352. doi: 10.1038/nn.4497

Cabral-Calderin, Y., Anne Weinrich, C., Schmidt-Samoa, C., Poland, E., Dechent, P., Bähr, M., et al. (2016). Transcranial alternating current stimulation affects the BOLD signal in a frequency and task-dependent manner. *Hum. Brain Mapp.* 37, 94–121. doi: 10.1002/hbm.23016

Calzolari, S., Jalali, R., and Fernández-Espejo, D. (2023). Characterising stationary and dynamic effective connectivity changes in the motor network during and after tDCS. *NeuroImage* 269:119915. doi: 10.1016/j.neuroimage.2023.119915

Cao, J., and Liu, H. (2018). Modulating the resting-state functional connectivity patterns of language processing areas in the human brain with anodal transcranial direct current stimulation applied over the Broca's area. *Neurophoton* 5:1. doi: 10.1117/1.NPh.5.2.025002

Caulfield, K. A., Badran, B. W., Li, X., Bikson, M., and George, M. S. (2020). Can transcranial electrical stimulation motor threshold estimate individualized tDCS doses over the prefrontal cortex? Evidence from reverse-calculation electric field modeling. *Brain Stimul.* 13, 1150–1152. doi: 10.1016/j.brs.2020.05.012

Cespón, J., Rodella, C., Rossini, P. M., Miniussi, C., and Pellicciari, M. C. (2017). Anodal transcranial direct current stimulation promotes frontal compensatory mechanisms in healthy elderly subjects. *Front. Aging Neurosci.* 9:420. doi: 10.3389/fnagi.2017.00420

Chambers, C. D., and Tzavella, L. (2021). The past, present and future of registered reports. *Nat. Hum. Behav.* 6, 29–42. doi: 10.1038/s41562-021-01193-7

Cirillo, G., Di Pino, G., Capone, F., Ranieri, F., Florio, L., Todisco, V., et al. (2017). Neurobiological after-effects of non-invasive brain stimulation. *Brain Stimul.* 10, 1–18. doi: 10.1016/j.brs.2016.11.009

Crosson, B., McGregor, K. M., Nocera, J. R., Drucker, J. H., Tran, S. M., and Butler, A. J. (2015). The relevance of aging-related changes in brain function to rehabilitation in aging-related disease. *Front. Hum. Neurosci.* 9:307. doi: 10.3389/fnhum.2015.00307

Dahnke, R., Yotter, R. A., and Gaser, C. (2013). Cortical thickness and central surface estimation. *NeuroImage* 65, 336–348. doi: 10.1016/j.neuroimage.2012.09.050

Darkow, R., and Flöel, A. (2016). Aphasie: evidenzbasierte Therapieansätze. *Nervenarzt* 87, 1051–1056. doi: 10.1007/s00115-016-0213-y

Darkow, R., Martin, A., Würtz, A., Flöel, A., and Meinzer, M. (2017). Transcranial direct current stimulation effects on neural processing in post-stroke aphasia. *Hum. Brain Mapp.* 38, 1518–1531. doi: 10.1002/hbm.23469

Datta, A., Bansal, V., Diaz, J., Patel, J., Reato, D., and Bikson, M. (2009). Gyri-precise head model of transcranial direct current stimulation: improved spatial focality using a ring electrode versus conventional rectangular pad. *Brain Stimul.* 2, 201–207.e1. doi: 10.1016/j.brs.2009.03.005

De Munck, J. C., Van Houdt, P. J., Gonçalves, S. I., Van Wegen, E., and Ossenblok, P. P. W. (2013). Novel artefact removal algorithms for co-registered EEG/fMRI based on selective averaging and subtraction. *NeuroImage* 64, 407–415. doi: 10.1016/j.neuroimage.2012.09.022

De Witte, S., Klooster, D., Dedoncker, J., Duprat, R., Remue, J., and Baeken, C. (2018). Left prefrontal neuronavigated electrode localization in tDCS: 10–20 EEG system versus MRI-guided neuronavigation. *Psychiatry Res. Neuroimaging* 274, 1–6. doi: 10.1016/j.pscychresns.2018.02.001

Dissanayaka, T. D., Zoghi, M., Farrell, M., Egan, G. F., and Jaberzadeh, S. (2018). Sham transcranial electrical stimulation and its effects on corticospinal excitability: a systematic review and meta-analysis. *Rev. Neurosci.* 29, 223–232. doi: 10.1515/revneuro-2017-0026

Dubljević, V., Saigle, V., and Racine, E. (2014). The rising tide of tDCS in the media and academic literature. *Neuron* 82, 731–736. doi: 10.1016/j.neuron.2014.05.003

Dutta, A. (2021). Simultaneous functional near-infrared spectroscopy (fNIRS) and electroencephalogram (EEG) to elucidate neurovascular modulation by transcranial electrical stimulation (tES). *Brain Stimul.* 14, 1093–1094. doi: 10.1016/j.brs.2021.07.019

Edwards, D., Cortes, M., Datta, A., Minhas, P., Wassermann, E. M., and Bikson, M. (2013). Physiological and modeling evidence for focal transcranial electrical brain stimulation in humans: a basis for high-definition tDCS. *NeuroImage* 74, 266–275. doi: 10.1016/j.neuroimage.2013.01.042

Ekhtiari, H., Ghobadi-Azbari, P., Thielscher, A., Antal, A., Li, L. M., Shereen, A. D., et al. (2022). A checklist for assessing the methodological quality of concurrent tES-fMRI studies (ConTES checklist): a consensus study and statement. *Nat. Protoc.* 17, 596–617. doi: 10.1038/s41596-021-00664-5

Esmaeilpour, Z., Shereen, A. D., Ghobadi-Azbari, P., Datta, A., Woods, A. J., Ironside, M., et al. (2020). Methodology for tDCS integration with fMRI. *Hum. Brain Mapp.* 41, 1950–1967. doi: 10.1002/hbm.24908

Evans, C., Bachmann, C., Lee, J. S. A., Gregoriou, E., Ward, N., and Bestmann, S. (2020). Dose-controlled tDCS reduces electric field intensity variability at a cortical target site. *Brain Stimul.* 13, 125–136. doi: 10.1016/j.brs.2019.10.004

Falleti, M. G., Maruff, P., Collie, A., and Darby, D. G. (2006). Practice effects associated with the repeated assessment of cognitive function using the CogState battery at 10-minute, one week and one month test-retest intervals. *J. Clin. Exp. Neuropsychol.* 28, 1095–1112. doi: 10.1080/13803390500205718

Fertonani, A., Brambilla, M., Cotelli, M., and Miniussi, C. (2014). The timing of cognitive plasticity in physiological aging: a tDCS study of naming. *Front. Aging Neurosci.* 6:131. doi: 10.3389/fnagi.2014.00131

Fertonani, A., and Miniussi, C. (2017). Transcranial electrical stimulation: what we know and do not know about mechanisms. *Neuroscientist* 23, 109–123. doi: 10.1177/1073858416631966

Figeys, M., Zeeman, M., and Kim, E. S. (2021). Effects of transcranial direct current stimulation (tDCS) on cognitive performance and cerebral oxygen hemodynamics: a systematic review. *Front. Hum. Neurosci.* 15:623315. doi: 10.3389/fnhum.2021.623315

Filmer, H. L., Ehrhardt, S. E., Shaw, T. B., Mattingley, J. B., and Dux, P. E. (2019). The efficacy of transcranial direct current stimulation to prefrontal areas is related to underlying cortical morphology. *NeuroImage* 196, 41–48. doi: 10.1016/j.neuroimage.2019.04.026

Fleury, M., Barillot, C., Mano, M., Bannier, E., and Maurel, P. (2019). Automated electrodes detection during simultaneous EEG/fMRI. *Front. ICT* 5:31. doi: 10.3389/fict.2018.00031

Fridriksson, J., Basilakos, A., Stark, B. C., Rorden, C., Elm, J., Gottfried, M., et al. (2019). Transcranial direct current stimulation to treat aphasia: longitudinal analysis of a randomized controlled trial. *Brain Stimul.* 12, 190–191. doi: 10.1016/j.brs.2018.09.016

Galli, G., Vadillo, M. A., Sirota, M., Feurra, M., and Medvedeva, A. (2019). A systematic review and meta-analysis of the effects of transcranial direct current stimulation (tDCS) on episodic memory. *Brain Stimul.* 12, 231–241. doi: 10.1016/j.brs.2018.11.008

Gandiga, P. C., Hummel, F. C., and Cohen, L. G. (2006). Transcranial DC stimulation (tDCS): a tool for double-blind sham-controlled clinical studies in brain stimulation. *Clin. Neurophysiol.* 117, 845–850. doi: 10.1016/j.clinph.2005.12.003

Gauvin, H. S., Meinzer, M., and De Zubicaray, G. I. (2017). tDCS effects on word production: limited by design? Comment on Westwood et al. (2017). *Cortex* 96, 137–142. doi: 10.1016/j.cortex.2017.06.017

Gbadeyan, O., McMahon, K., Steinhauser, M., and Meinzer, M. (2016a). Stimulation of dorsolateral prefrontal cortex enhances adaptive cognitive control: a high-definition transcranial direct current stimulation study. *J. Neurosci.* 36, 12530–12536. doi: 10.1523/JNEUROSCI.2450-16.2016

Gbadeyan, O., Steinhauser, M., McMahon, K., and Meinzer, M. (2016b). Safety, tolerability, blinding efficacy and Behavioural effects of a novel MRI-compatible, high-definition tDCS set-up. *Brain Stimul.* 9, 545–552. doi: 10.1016/j.brs.2016.03.018

Ghasemian-Shirvan, E., Mosayebi-Samani, M., Farnad, L., Kuo, M.-F., Meesen, R. L. J., and Nitsche, M. A. (2022). Age-dependent non-linear neuroplastic effects of cathodal tDCS in the elderly population: a titration study. *Brain Stimul.* 15, 296–305. doi: 10.1016/j.brs.2022.01.011

Göksu, C., Hanson, L. G., Siebner, H. R., Ehses, P., Scheffler, K., and Thielscher, A. (2018). Human *in-vivo* brain magnetic resonance current density imaging (MRCDI). *NeuroImage* 171, 26–39. doi: 10.1016/j.neuroimage.2017.12.075

Göksu, C., Scheffler, K., Siebner, H. R., Thielscher, A., and Hanson, L. G. (2019). The stray magnetic fields in magnetic resonance current density imaging (MRCDI). *Phys. Med.* 59, 142–150. doi: 10.1016/j.ejmp.2019.02.022

Gorgolewski, K. J., and Poldrack, R. A. (2016). A practical guide for improving transparency and reproducibility in neuroimaging research. *PLoS Biol.* 14:e1002506. doi: 10.1371/journal.pbio.1002506

Greinacher, R., Buhôt, L., Möller, L., and Learmonth, G. (2019). The time course of ineffective sham-blinding during low-intensity (1 mA) transcranial direct current stimulation. *Eur. J. Neurosci.* 50, 3380–3388. doi: 10.1111/ejn.14497

Grimes, D. A., and Schulz, K. F. (2002). An overview of clinical research: the lay of the land. *Lancet* 359, 57–61. doi: 10.1016/S0140-6736(02)07283-5

Gutchess, A. (2014). Plasticity of the aging brain: new directions in cognitive neuroscience. *Science* 346, 579–582. doi: 10.1126/science.1254604

Hanley, C. J., and Tales, A. (2019). Anodal tDCS improves attentional control in older adults. *Exp. Gerontol.* 115, 88–95. doi: 10.1016/j.exger.2018.11.019

Hausknecht, J. P., Halpert, J. A., Di Paolo, N. T., and Moriarty Gerrard, M. O. (2007). Retesting in selection: a meta-analysis of coaching and practice effects for tests of cognitive ability. *J. Appl. Psychol.* 92, 373–385. doi: 10.1037/0021-9010.92.2.373

Hedden, T., and Gabrieli, J. D. E. (2004). Insights into the ageing mind: a view from cognitive neuroscience. *Nat. Rev. Neurosci.* 5, 87–96. doi: 10.1038/nrn1323

Herwig, U., Satrapi, P., and Schönfeldt-Lecuona, C. (2003). Using the international 10-20 EEG system for positioning of transcranial magnetic stimulation. *Brain Topogr.* 16, 95–99. doi: 10.1023/B:BRAT.0000006333.93597.9d

Hiew, S., Nguemeni, C., and Zeller, D. (2022). Efficacy of transcranial direct current stimulation in people with multiple sclerosis: a review. *Eur. J. Neurol.* 29, 648–664. doi: 10.1111/ene.15163

Holland, R., Leff, A. P., Josephs, O., Galea, J. M., Desikan, M., Price, C. J., et al. (2011). Speech facilitation by left inferior frontal cortex stimulation. *Curr. Biol.* 21, 1403–1407. doi: 10.1016/j.cub.2011.07.021

Holman, L., Head, M. L., Lanfear, R., and Jennions, M. D. (2015). Evidence of experimental Bias in the life sciences: why we need blind data recording. *PLoS Biol.* 13:e1002190. doi: 10.1371/journal.pbio.1002190

Hordacre, B., Moezzi, B., Goldsworthy, M. R., Rogasch, N. C., Graetz, L. J., and Ridding, M. C. (2017). Resting state functional connectivity measures correlate with the response to anodal transcranial direct current stimulation. *Eur. J. Neurosci.* 45, 837–845. doi: 10.1111/ejn.13508

Huang, A. Y., Yu, D., Davis, L. K., Sul, J. H., Tsetsos, F., Ramensky, V., et al. (2017). Rare copy number variants in NRXN1 and CNTN6 increase risk for Tourette syndrome. *Neuron* 94, 1101–1111.e7. doi: 10.1016/j.neuron.2017.06.010

Huey, E. D., Probasco, J. C., Moll, J., Stocking, J., Ko, M.-H., Grafman, J., et al. (2007). No effect of DC brain polarization on verbal fluency in patients with advanced frontotemporal dementia. *Clin. Neurophysiol.* 118, 1417–1418. doi: 10.1016/j.clinph.2007.02.026

Hunold, A., Haueisen, J., Nees, F., and Moliadze, V. (2023). Review of individualized current flow modeling studies for transcranial electrical stimulation. *J. Neurosci. Res.* 101, 405–423. doi: 10.1002/jnr.25154

Indahlastari, A., Albizu, A., O'Shea, A., Forbes, M. A., Nissim, N. R., Kraft, J. N., et al. (2020). Modeling transcranial electrical stimulation in the aging brain. *Brain Stimul.* 13, 664–674. doi: 10.1016/j.brs.2020.02.007

Indahlastari, A., Dunn, A. L., Pedersen, S., Kraft, J. N., Someya, S., Albizu, A., et al. (2023). The importance of accurately representing electrode position in transcranial direct current stimulation computational models. *Brain Stimul.* 16, 930–932. doi: 10.1016/j.brs.2023.05.010

Jaberzadeh, S., Martin, D., Knotkova, H., and Woods, A. J. (2019). "Methodological considerations for selection of transcranial direct current stimulation approach, protocols and devices" in *Practical guide to transcranial direct current stimulation*. eds. H. Knotkova, M. A. Nitsche, M. Bikson and A. J. Woods (Cham: Springer International Publishing), 199–223.

Jacobson, L., Koslowsky, M., and Lavidor, M. (2012). tDCS polarity effects in motor and cognitive domains: a meta-analytical review. *Exp. Brain Res.* 216, 1–10. doi: 10.1007/s00221-011-2891-9

Jamil, A., Batsikadze, G., Kuo, H., Meesen, R. L. J., Dechent, P., Paulus, W., et al. (2020). Current intensity- and polarity-specific online and aftereffects of transcranial direct current stimulation: an fMRI study. *Hum. Brain Mapp.* 41, 1644–1666. doi: 10.1002/hbm.24901

Jang, S., Kim, D., Cho, H., Kwon, M., and Jun, S. C. (2017). Assessing stimulation effects induced by tDCS using MEG. *Brain Stimul.* 10:526. doi: 10.1016/j.brs.2017.01.536

Keeser, D., Meindl, T., Bor, J., Palm, U., Pogarell, O., Mulert, C., et al. (2011). Prefrontal transcranial direct current stimulation changes connectivity of resting-state networks during fMRI. *J. Neurosci.* 31, 15284–15293. doi: 10.1523/JNEUROSCI.0542-11.2011

Kim, J.-H., Kim, D.-W., Chang, W. H., Kim, Y.-H., Kim, K., and Im, C.-H. (2014). Inconsistent outcomes of transcranial direct current stimulation may originate from anatomical differences among individuals: electric field simulation using individual MRI data. *Neurosci. Lett.* 564, 6–10. doi: 10.1016/j.neulet.2014.01.054

Knotkova, H., Riggs, A., Berisha, D., Borges, H., Bernstein, H., Patel, V., et al. (2019). Automatic M1-SO montage headgear for transcranial direct current stimulation (TDCS) suitable for home and high-throughput in-clinic applications. *Neuromodulation* 22, 904–910. doi: 10.1111/ner.12786

Kuo, H.-I., Bikson, M., Datta, A., Minhas, P., Paulus, W., Kuo, M.-F., et al. (2013). Comparing cortical plasticity induced by conventional and high-definition 4 × 1 ring tDCS: a neurophysiological study. *Brain Stimul.* 6, 644–648. doi: 10.1016/j.brs.2012.09.010

Kuo, M.-F., Paulus, W., and Nitsche, M. A. (2006). Sex differences in cortical neuroplasticity in humans. *Neuroreport* 17, 1703–1707. doi: 10.1097/01.wnr.0000239955.68319.c2

Kurtin, D. L., Violante, I. R., Zimmerman, K., Leech, R., Hampshire, A., Patel, M. C., et al. (2021). Investigating the interaction between white matter and brain state on tDCS-induced changes in brain network activity. *Brain Stimul.* 14, 1261–1270. doi: 10.1016/j.brs.2021.08.004

Lavezzi, G. D., Sanz Galan, S., Andersen, H., Tomer, D., and Cacciamani, L. (2022). The effects of tDCS on object perception: a systematic review and meta-analysis. *Behav. Brain Res.* 430:113927. doi: 10.1016/j.bbr.2022.113927

Lee, J.-H., Jeun, Y.-J., Park, H. Y., and Jung, Y.-J. (2021). Effect of transcranial direct current stimulation combined with rehabilitation on arm and hand function in stroke patients: a systematic review and Meta-analysis. *Healthcare* 9:1705. doi: 10.3390/healthcare9121705

Li, R., Hosseini, H., Saggar, M., Balters, S. C., and Reiss, A. L. (2023). Current opinions on the present and future use of functional near-infrared spectroscopy in psychiatry. *Neurophoton* 10:013505. doi: 10.1117/1.NPh.10.1.013505

Lioumis, P., and Rosanova, M. (2022). The role of neuronavigation in TMS–EEG studies: current applications and future perspectives. *J. Neurosci. Methods* 380:109677. doi: 10.1016/j.jneumeth.2022.109677

Majdi, A., Van Boekholdt, L., Sadigh-Eteghad, S., and Mc Laughlin, M. (2022). A systematic review and meta-analysis of transcranial direct-current stimulation effects on cognitive function in patients with Alzheimer's disease. *Mol. Psychiatry* 27, 2000–2009. doi: 10.1038/s41380-022-01444-7

Manenti, R., Brambilla, M., Petesi, M., Ferrari, C., and Cotelli, M. (2013). Enhancing verbal episodic memory in older and young subjects after non-invasive brain stimulation. *Front. Aging Neurosci.* 5:49. doi: 10.3389/fnagi.2013.00049

Martin, A. K., Dzafic, I., Ramdave, S., and Meinzer, M. (2017a). Causal evidence for task-specific involvement of the dorsomedial prefrontal cortex in human social cognition. *Soc. Cogn. Affect. Neurosci.* 12, 1209–1218. doi: 10.1093/scan/nsx063

Martin, A. K., Huang, J., Hunold, A., and Meinzer, M. (2017b). Sex mediates the effects of high-definition transcranial direct current stimulation on "mind-Reading". *Neuroscience* 366, 84–94. doi: 10.1016/j.neuroscience.2017.10.005

Martin, A. K., Huang, J., Hunold, A., and Meinzer, M. (2019a). Dissociable roles within the social brain for self–other processing: a HD-tDCS study. *Cereb. Cortex* 29, 3642–3654. doi: 10.1093/cercor/bhy238

Martin, A. K., Su, P., and Meinzer, M. (2019b). Common and unique effects of HD-tDCS to the social brain across cultural groups. *Neuropsychologia* 133:107170. doi: 10.1016/j.neuropsychologia.2019.107170

Matsushita, R., Puschmann, S., Baillet, S., and Zatorre, R. J. (2021). Inhibitory effect of tDCS on auditory evoked response: simultaneous MEG-tDCS reveals causal role of right auditory cortex in pitch learning. *NeuroImage* 233:117915. doi: 10.1016/j.neuroimage.2021.117915

McKendrick, R., Parasuraman, R., and Ayaz, H. (2015). Wearable functional near infrared spectroscopy (fNIRS) and transcranial direct current stimulation (tDCS): expanding vistas for neurocognitive augmentation. *Front. Syst. Neurosci.* 9:27. doi: 10.3389/fnsys.2015.00027

Meinzer, M., Lindenberg, R., Antonenko, D., Flaisch, T., and Floel, A. (2013). Anodal transcranial direct current stimulation temporarily reverses age-associated cognitive decline and functional brain activity changes. *J. Neurosci.* 33, 12470–12478. doi: 10.1523/JNEUROSCI.5743-12.2013

Minarik, T., Berger, B., Althaus, L., Bader, V., Biebl, B., Brotzeller, F., et al. (2016). The importance of sample size for reproducibility of tDCS effects. *Front. Hum. Neurosci.* 10:453. doi: 10.3389/fnhum.2016.00453

Mosayebi Samani, M., Agboada, D., Jamil, A., Kuo, M.-F., and Nitsche, M. A. (2019). Titrating the neuroplastic effects of cathodal transcranial direct current stimulation (tDCS) over the primary motor cortex. *Cortex* 119, 350–361. doi: 10.1016/j.cortex.2019.04.016

Munro, K. J., and Prendergast, G. (2019). Encouraging pre-registration of research studies. *Int. J. Audiol.* 58, 123–124. doi: 10.1080/14992027.2019.1574405

Neri, F., Mencarelli, L., Menardi, A., Giovannelli, F., Rossi, S., Sprugnoli, G., et al. (2020). A novel tDCS sham approach based on model-driven controlled shunting. *Brain Stimul.* 13, 507–516. doi: 10.1016/j.brs.2019.11.004

Nichols, T. E., Das, S., Eickhoff, S. B., Evans, A. C., Glatard, T., Hanke, M., et al. (2017). Best practices in data analysis and sharing in neuroimaging using MRI. *Nat. Neurosci.* 20, 299–303. doi: 10.1038/nn.4500

Niemann, F., Riemann, S., Hubert, A.-K., Antonenko, D., Thielscher, A., Martin, A. K., et al. (2024). Electrode positioning errors reduce current dose for focal tDCS set-ups: evidence from individualized electric field mapping. *Clin. Neurophysiol.* 162, 201–209. doi: 10.1016/j.clinph.2024.03.031

Nitsche, M. A., and Paulus, W. (2000). Excitability changes induced in the human motor cortex by weak transcranial direct current stimulation. *J. Physiol.* 527, 633–639. doi: 10.1111/j.1469-7793.2000.t01-1-00633.x

Noble, S., Scheinost, D., and Constable, R. T. (2021). A guide to the measurement and interpretation of fMRI test-retest reliability. *Curr. Opin. Behav. Sci.* 40, 27–32. doi: 10.1016/j.cobeha.2020.12.012

O'Connell, N. E., Cossar, J., Marston, L., Wand, B. M., Bunce, D., Moseley, G. L., et al. (2012). Rethinking clinical trials of transcranial direct current stimulation: participant and Assessor blinding is inadequate at intensities of 2mA. *PLoS One* 7:e47514. doi: 10.1371/journal.pone.0047514

Okazaki, Y., Izumiya, M., Hagihara, M., and Kitajo, K. (2023). An HD-tDCS–EEG study to reveal current polarity-dependent effects on attentional fluctuations. *Brain Stimul.* 16:381. doi: 10.1016/j.brs.2023.01.759

Oldrati, V., Colombo, B., and Antonietti, A. (2018). Combination of a short cognitive training and tDCS to enhance visuospatial skills: a comparison between online and offline neuromodulation. *Brain Res.* 1678, 32–39. doi: 10.1016/j.brainres.2017.10.002

Open Science Collaboration (2015). Estimating the reproducibility of psychological science. *Science* 349:aac4716. doi: 10.1126/science.aac4716

Opitz, A., Paulus, W., Will, S., Antunes, A., and Thielscher, A. (2015). Determinants of the electric field during transcranial direct current stimulation. *NeuroImage* 109, 140–150. doi: 10.1016/j.neuroimage.2015.01.033

Pang, J. C., Aquino, K. M., Oldehinkel, M., Robinson, P. A., Fulcher, B. D., Breakspear, M., et al. (2023). Geometric constraints on human brain function. *Nature* 618, 566–574. doi: 10.1038/s41586-023-06098-1

Perceval, G., Flöel, A., and Meinzer, M. (2016). Can transcranial direct current stimulation counteract age-associated functional impairment? *Neurosci. Biobehav. Rev.* 65, 157–172. doi: 10.1016/j.neubiorev.2016.03.028

Perceval, G., Martin, A. K., Copland, D. A., Laine, M., and Meinzer, M. (2020). Multisession transcranial direct current stimulation facilitates verbal learning and memory consolidation in young and older adults. *Brain Lang.* 205:104788. doi: 10.1016/j.bandl.2020.104788

Polanía, R., Nitsche, M. A., and Paulus, W. (2011). Modulating functional connectivity patterns and topological functional organization of the human brain with transcranial direct current stimulation. *Hum. Brain Mapp.* 32, 1236–1249. doi: 10.1002/hbm.21104

Postman-Caucheteux, W. A., Birn, R. M., Pursley, R. H., Butman, J. A., Solomon, J. M., Picchioni, D., et al. (2010). Single-trial fMRI shows Contralesional activity linked to overt naming errors in chronic aphasic patients. *J. Cogn. Neurosci.* 22, 1299–1318. doi: 10.1162/jocn.2009.21261

Priori, A., Berardelli, A., Rona, S., Accornero, N., and Manfredi, M. (1998). Polarization of the human motor cortex through the scalp. *Neuroreport* 9, 2257–2260. doi: 10.1097/00001756-199807130-00020

Rasmussen, I. D., Boayue, N. M., Mittner, M., Bystad, M., Grønli, O. K., Vangberg, T. R., et al. (2021). High-definition transcranial direct current stimulation improves delayed memory in Alzheimer's disease patients: a pilot study using computational modeling to optimize electrode position. *JAD* 83, 753–769. doi: 10.3233/JAD-210378

Reinhart, R. M. G., Cosman, J. D., Fukuda, K., and Woodman, G. F. (2017). Using transcranial direct-current stimulation (tDCS) to understand cognitive processing. *Atten. Percept. Psychophys.* 79, 3–23. doi: 10.3758/s13414-016-1224-2

Reis, J., Fischer, J. T., Prichard, G., Weiller, C., Cohen, L. G., and Fritsch, B. (2015). Time- but not sleep-dependent consolidation of tDCS-enhanced Visuomotor skills. *Cereb. Cortex* 25, 109–117. doi: 10.1093/cercor/bht208

Riggall, K., Forlini, C., Carter, A., Hall, W., Weier, M., Partridge, B., et al. (2015). Researchers' perspectives on scientific and ethical issues with transcranial direct current stimulation: an international survey. *Sci. Rep.* 5:10618. doi: 10.1038/srep10618

Ross, L. A., McCoy, D., Coslett, H. B., Olson, I. R., and Wolk, D. A. (2011). Improved proper Name recall in aging after electrical stimulation of the anterior temporal lobes. *Front. Aging Neurosci.* 3:16. doi: 10.3389/fnagi.2011.00016

Rossi, S., Santarnecchi, E., and Feurra, M. (2022). "Noninvasive brain stimulation and brain oscillations" in *Handbook of Clinical Neurology* (United States: Elsevier), 239–247.

Saiote, C., Turi, Z., Paulus, W., and Antal, A. (2013). Combining functional magnetic resonance imaging with transcranial electrical stimulation. *Front. Hum. Neurosci.* 7:435. doi: 10.3389/fnhum.2013.00435

Sandrini, M., Umiltà, C., and Rusconi, E. (2011). The use of transcranial magnetic stimulation in cognitive neuroscience: a new synthesis of methodological issues. *Neurosci. Biobehav. Rev.* 35, 516–536. doi: 10.1016/j.neubiorev.2010.06.005

Saturnino, G. B., Antunes, A., and Thielscher, A. (2015). On the importance of electrode parameters for shaping electric field patterns generated by tDCS. *NeuroImage* 120, 25–35. doi: 10.1016/j.neuroimage.2015.06.067

Saturnino, G. B., Madsen, K. H., and Thielscher, A. (2021). Optimizing the electric field strength in multiple targets for multichannel transcranial electric stimulation. *J. Neural Eng.* 18:014001. doi: 10.1088/1741-2552/abca15

Sergiou, C. S., Santarnecchi, E., Franken, I. H. A., and Van Dongen, J. D. M. (2020). The effectiveness of transcranial direct current stimulation as an intervention to improve empathic abilities and reduce violent behavior: a literature review. *Aggress. Violent Behav.* 55:101463. doi: 10.1016/j.avb.2020.101463

Shahbabaie, A., Ebrahimpoor, M., Hariri, A., Nitsche, M. A., Hatami, J., Fatemizadeh, E., et al. (2018). Transcranial DC stimulation modifies functional connectivity of large-scale brain networks in abstinent methamphetamine users. *Brain Behav.* 8:e00922. doi: 10.1002/brb3.922

Sliwinska, M. W., Violante, I. R., Wise, R. J. S., Leech, R., Devlin, J. T., Geranmayeh, F., et al. (2017). Stimulating multiple-demand cortex enhances vocabulary learning. *J. Neurosci.* 37, 7606–7618. doi: 10.1523/JNEUROSCI.3857-16.2017

Stagg, C. J., Antal, A., and Nitsche, M. A. (2018). Physiology of transcranial direct current stimulation. *J. ECT* 34, 144–152. doi: 10.1097/YCT.0000000000000510

Suh, H. S., Lee, W. H., and Kim, T.-S. (2012). Influence of anisotropic conductivity in the skull and white matter on transcranial direct current stimulation via an anatomically realistic finite element head model. *Phys. Med. Biol.* 57, 6961–6980. doi: 10.1088/0031-9155/57/21/6961

Sun, W., Wang, H., Zhang, J., Yan, T., and Pei, G. (2021). Multi-layer skull modeling and importance for tDCS simulation. In Proceedings of the 2021 International Conference on Bioinformatics and Intelligent Computing, (Harbin: ACM), 250–256.

Tagoe, N., Molyneux, S., Pulford, J., Murunga, V. I., and Kinyanjui, S. (2019). Managing health research capacity strengthening consortia: a systematised review of the published literature. *BMJ Glob. Health* 4:e001318. doi: 10.1136/bmjgh-2018-001318

Thair, H., Holloway, A. L., Newport, R., and Smith, A. D. (2017). Transcranial direct current stimulation (tDCS): a Beginner's guide for design and implementation. *Front. Neurosci.* 11:641. doi: 10.3389/fnins.2017.00641

Tsuzuki, D., Watanabe, H., Dan, I., and Taga, G. (2016). MinR 10/20 system: quantitative and reproducible cranial landmark setting method for MRI based on minimum initial reference points. *J. Neurosci. Methods* 264, 86–93. doi: 10.1016/j.jneumeth.2016.02.024

Turi, Z., Csifcsák, G., Boayue, N. M., Aslaksen, P., Antal, A., Paulus, W., et al. (2019). Blinding is compromised for transcranial direct current stimulation at 1 mA for 20 min in young healthy adults. *Eur. J. Neurosci.* 50, 3261–3268. doi: 10.1111/ejn.14403

Turner, C., Jackson, C., and Learmonth, G. (2021). Is the "end-of-study guess" a valid measure of sham blinding during transcranial direct current stimulation? *Eur. J. Neurosci.* 53, 1592–1604. doi: 10.1111/ejn.15018

Villamar, M. F., Volz, M. S., Bikson, M., Datta, A., DaSilva, A. F., and Fregni, F. (2013). Technique and considerations in the use of 4x1 ring high-definition transcranial direct current stimulation (HD-tDCS). *JoVE* 50309:e50309. doi: 10.3791/50309

Wallace, D., Cooper, N. R., Paulmann, S., Fitzgerald, P. B., and Russo, R. (2016). Perceived comfort and blinding efficacy in randomised sham-controlled transcranial direct current stimulation (tDCS) trials at 2 mA in young and older healthy adults. *PLoS One* 11:e0149703. doi: 10.1371/journal.pone.0149703

Wilkinson, M. D., Dumontier, M., Aalbersberg, I. J., Appleton, G., Axton, M., Baak, A., et al. (2016). The FAIR guiding principles for scientific data management and stewardship. *Sci. Data* 3:160018. doi: 10.1038/sdata.2016.18

Willmot, N., Leow, L.-A., Filmer, H. L., and Dux, P. E. (2024). Exploring the intra-individual reliability of tDCS: a registered report. *Cortex* 173, 61–79. doi: 10.1016/j.cortex.2023.12.015

Woods, A. J., Antal, A., Bikson, M., Boggio, P. S., Brunoni, A. R., Celnik, P., et al. (2016). A technical guide to tDCS, and related non-invasive brain stimulation tools. *Clin. Neurophysiol.* 127, 1031–1048. doi: 10.1016/j.clinph.2015.11.012

Woods, A. J., Bryant, V., Sacchetti, D., Gervits, F., and Hamilton, R. (2015). Effects of electrode drift in transcranial direct current stimulation. *Brain Stimul.* 8, 515–519. doi: 10.1016/j.brs.2014.12.007

Yan, R., Zhang, X., Li, Y., Hou, J., Chen, H., and Liu, H. (2020). Effect of transcranial direct-current stimulation on cognitive function in stroke patients: a systematic review and meta-analysis. *PLoS One* 15:e0233903. doi: 10.1371/journal.pone.0233903

Zimerman, M., Heise, K.-F., Gerloff, C., Cohen, L. G., and Hummel, F. C. (2014). Disrupting the ipsilateral motor cortex interferes with training of a complex motor task in older adults. *Cereb. Cortex* 24, 1030–1036. doi: 10.1093/cercor/bhs385

frontiers | Frontiers in Neuroscience

TYPE Original Research
PUBLISHED 01 July 2024
DOI 10.3389/fnins.2024.1362607

OPEN ACCESS

EDITED BY
Chang-Hoon Choi,
Helmholtz Association of German Research Centres (HZ), Germany

REVIEWED BY
Xiaogai Li,
Royal Institute of Technology, Sweden
Panteleimon Chriskos,
Aristotle University of Thessaloniki, Greece

*CORRESPONDENCE
Tomofumi Yamaguchi
✉ yamaguchi.tomofumi.3i@kyoto-u.ac.jp

RECEIVED 28 December 2023
ACCEPTED 18 June 2024
PUBLISHED 01 July 2024

CITATION
Sato T, Katagiri N, Suganuma S, Laakso I, Tanabe S, Osu R, Tanaka S and Yamaguchi T (2024) Simulating tDCS electrode placement to stimulate both M1 and SMA enhances motor performance and modulates cortical excitability depending on current flow direction.
Front. Neurosci. 18:1362607.
doi: 10.3389/fnins.2024.1362607

Simulating tDCS electrode placement to stimulate both M1 and SMA enhances motor performance and modulates cortical excitability depending on current flow direction

Takatsugu Sato[1,2], Natsuki Katagiri[2,3], Saki Suganuma[1], Ilkka Laakso[4], Shigeo Tanabe[5], Rieko Osu[6], Satoshi Tanaka[7] and Tomofumi Yamaguchi[1,8,9]*

[1]Department of Physical Therapy, Yamagata Prefectural University of Health Sciences, Yamagata, Japan, [2]Department of Rehabilitation Medicine, Tokyo Bay Rehabilitation Hospital, Narashino, Japan, [3]Graduate School of Health Sciences, Yamagata Prefectural University of Health Sciences, Yamagata, Japan, [4]Department of Electrical Engineering and Automation, Aalto University, Espoo, Finland, [5]Faculty of Rehabilitation, School of Health Sciences, Fujita Health University, Toyoake, Japan, [6]Faculty of Human Sciences, Waseda University, Tokorozawa, Japan, [7]Laboratory of Psychology, Hamamatsu University School of Medicine, Hamamatsu, Japan, [8]Department of Physical Therapy, Faculty of Health Science, Juntendo University, Tokyo, Japan, [9]Department of Physical Therapy, Human Health Sciences, Graduate School of Medicine, Kyoto University, Kyoto, Japan

Introduction: The conventional method of placing transcranial direct current stimulation (tDCS) electrodes is just above the target brain area. However, this strategy for electrode placement often fails to improve motor function and modulate cortical excitability. We investigated the effects of optimized electrode placement to induce maximum electrical fields in the leg regions of both M1 and SMA, estimated by electric field simulations in the T1 and T2-weighted MRI-based anatomical models, on motor performance and cortical excitability in healthy individuals.

Methods: A total of 36 healthy volunteers participated in this randomized, triple-blind, sham-controlled experiment. They were stratified by sex and were randomly assigned to one of three groups according to the stimulation paradigm, including tDCS with (1) anodal and cathodal electrodes positioned over FCz and POz, respectively, (A-P tDCS), (2) anodal and cathodal electrodes positioned over POz and FCz, respectively, (P-A tDCS), and (3) sham tDCS. The sit-to-stand training following tDCS (2 mA, 10 min) was conducted every 3 or 4 days over 3 weeks (5 sessions total).

Results: Compared to sham tDCS, A-P tDCS led to significant increases in the number of sit-to-stands after 3 weeks training, whereas P-A tDCS significantly increased knee flexor peak torques after 3 weeks training, and decreased short-interval intracortical inhibition (SICI) immediately after the first session of training and maintained it post-training.

Discussion: These results suggest that optimized electrode placement of the maximal EF estimated by electric field simulation enhances motor performance and modulates cortical excitability depending on the direction of current flow.

KEYWORDS

primary motor cortex, supplementary motor area, non-invasive brain stimulation, lower limb, muscle strength, rehabilitation

1 Introduction

Transcranial direct current stimulation (tDCS) is a non-invasive cortical stimulation procedure in which weak direct currents polarize target brain regions (Nitsche and Paulus, 2000). The application of tDCS to motor-related cortical areas transiently alters cortical excitability and improves motor performance in healthy individuals and patients with stroke (Jeffery et al., 2007; Tanaka et al., 2009, 2011; Madhavan et al., 2011; Tatemoto et al., 2013; Sriraman et al., 2014; Chang et al., 2015; Vitor-Costa et al., 2015; Angius et al., 2016, 2018; Montenegro et al., 2016; Washabaugh et al., 2016). However, the conventional method of placing tDCS electrodes just above the target brain area often fails to modulate excitability within the target cortex or improve motor performance, frequently limited by significant inter-individual variability (López-Alonso et al., 2014, 2015; Wiethoff et al., 2014; Chew et al., 2015; Yamaguchi et al., 2016; Maeda et al., 2017).

One possible source of this inter-individual variability is the variability of tDCS-generated electrical fields (EFs) (Laakso et al., 2019). The EFs in the brain depend on the electrical resistance of the tissues, i.e., scalp, skull, meninges, and cerebrospinal fluid (CSF), between the electrode and the brain (Truong et al., 2013; Laakso et al., 2015; Opitz et al., 2015). To reduce inter-individual variability in tDCS-induced effects, Laakso et al. (2015, 2016) proposed a systematic way to estimate EFs induced by tDCS at the population level by registering calculated EFs with structural brain magnetic resonance imaging (MRI). Electric field simulation provides information that is useful for optimizing tDCS settings (intensity, electrode size, electrode placement), which in turn may generate EFs with minimized variation among individuals (Evans et al., 2020; Mikkonen et al., 2020). Previous studies speculated that motor-evoked potential (MEP) and cerebral blood flow changes induced by tDCS were related to EF values in the target brain area (Mosayebi-Samani et al., 2021). However, conventional tDCS electrode placement in healthy controls and stroke patients often fails to induce sufficient EFs to achieve the desired effects within the targeted area (van der Cruijsen et al., 2022; Yoon et al., 2024), making the use of electrical field simulations to optimize electrode placement a novel approach for modulating cortical excitability and enhancing motor performance in stroke patients (van der Cruijsen et al., 2022).

Another possible factor of variability is the tDCS-induced current flow. One study reported that tDCS over primary motor cortex (M1) with posterior to anterior (P-A) current flow decreased corticospinal excitability (Rawji et al., 2018). Another group studying motor task learning under tDCS over M1 reported that using anterior to posterior (A-P) current flow disturbed the retention of learned skills (Hannah et al., 2019). These studies suggest that the tDCS-induced current flow plays an important role in mediating changes in corticospinal excitability and motor learning. However, to the best of our knowledge, the effects of current flow direction on motor performance and cortical excitability under tDCS using optimized electrode placement have not been investigated. New insights obtained by such investigation may help enhance tDCS effects, which in turn could benefit patients with neurological disorders in neurorehabilitation with increased cortical excitability and improve motor performance.

The sit-to-stand movement, a typical daily activity (Alexander et al., 2000), relies on the lower limb fields of M1 for essential motor signaling to induce muscle contraction during this action (Pearson, 2000). The supplementary motor area (SMA) is integral for the coordination and execution of motor programs, particularly in skilled movements and postural control (Mihara et al., 2008, 2012; Fujimoto et al., 2014). Considering this, we selected FCz and POz electrode placements in our study to induce the maximal average EFs in M1 and SMA on both sides, as revealed by electric field simulations. These simulations demonstrated that conventional electrode placements above the target brain area do not achieve maximal EFs in these regions (Table 1). Moreover, the extent of EFs induced in the target area correlates with the cortical excitability changes induced by tDCS (Mosayebi-Samani et al., 2021), leading to our decision not to include a conventional tDCS group in this study.

We hypothesized that the jointly optimal tDCS for SMA and M1, as estimated by electric field simulation, would positively influence motor performance in the sit-to-stand movement, as assessed by muscle strength and neurophysiological assessments; MEPs and short-inter-cortical inhibition (SICI). To address this hypothesis, we used electric field simulation to determine the electrode placement that maximized EFs in SMA and M1 and then examined how tDCS influenced sit-to-stand performance, muscle strength, and cortical excitability in healthy individuals.

2 Materials and methods

2.1 Participants

The study involved 36 healthy young college student volunteers (18 women; aged 21 ± 1 year) (Table 2). Out of 37 initial participants, one was excluded due to medication affecting the central nervous system. The sample size, set at 12 per group, was determined by a power analysis referencing Tanaka et al. (2009), and aligns with the recommended minimum for pilot studies (Julious, 2005).

Participants had no history of orthopedic or neurological diseases and were not treated with medications that would affect the central nervous system. To control factors that could influence the effectiveness of non-invasive brain stimulation, participants were asked to avoid vigorous physical activity and consumption of alcohol and caffeine during the experiment period and to ensure adequate sleep the night before the experiment to avoid sleep deprivation (Guerra et al., 2020).

All participants gave written informed consent before participating in the experiment. This study was approved by the Ethics Committee of Yamagata Prefectural University of Health Sciences (approval number: 1806–06) and was performed according to the ethical standards of the Declaration of Helsinki.

Abbreviations: aMT, active motor threshold; ANOVA, analysis of variance; A-P, anterior to posterior; CSF, cerebrospinal fluid; EFs, electric fields; EMG, electromyography; FEM, finite element method; GABAergic, gamma-aminobutyric acidergic; MEP, motor evoked potential; MNI, montreal neurological institute; MRI, magnetic resonance imaging; M1, primary motor cortex; P-A, posterior to anterior; RF, rectus femoris; rMT, resting motor threshold; SICI, short-interval intracortical inhibition; SMA, supplementary motor area; tDCS, transcranial direct current stimulation; TMS, transcranial magnetic stimulation; T1- and T2-weighted, T1w and T2w.

TABLE 1 Electric field simulation of each electrode montage.

		Electric field strength (V/m)				
		M1		SMA		
Electrode 1	Electrode 2	Left	Right	Left	Right	Average
Fz	Extracephalic	0.29 ± 0.04	0.29 ± 0.04	0.43 ± 0.07	0.43 ± 0.08	0.36 ± 0.05
FCz	Extracephalic	0.40 ± 0.06	0.40 ± 0.06	0.58 ± 0.10	0.57 ± 0.11	0.49 ± 0.07
Cz	Extracephalic	0.50 ± 0.07	0.51 ± 0.08	0.63 ± 0.11	0.63 ± 0.11	0.57 ± 0.09
CPz	Extracephalic	0.54 ± 0.09	0.55 ± 0.09	0.52 ± 0.09	0.52 ± 0.09	0.53 ± 0.08
Pz	Extracephalic	0.50 ± 0.09	0.51 ± 0.08	0.37 ± 0.06	0.38 ± 0.06	0.44 ± 0.07
Fz	Iz	0.41 ± 0.05	0.42 ± 0.05	0.52 ± 0.08	0.52 ± 0.09	0.47 ± 0.06
FCz	Iz	0.50 ± 0.06	0.51 ± 0.07	0.62 ± 0.10	0.62 ± 0.11	0.56 ± 0.08
Cz	Iz	0.58 ± 0.07	0.58 ± 0.08	0.61 ± 0.11	0.61 ± 0.11	0.60 ± 0.08
CPz	Iz	0.55 ± 0.09	0.56 ± 0.09	0.45 ± 0.08	0.46 ± 0.08	0.50 ± 0.08
Pz	Iz	0.43 ± 0.08	0.44 ± 0.07	0.28 ± 0.05	0.28 ± 0.05	0.36 ± 0.06
Fz	Fpz	0.11 ± 0.02	0.12 ± 0.03	0.22 ± 0.05	0.22 ± 0.06	0.17 ± 0.03
FCz	Fpz	0.24 ± 0.05	0.24 ± 0.05	0.46 ± 0.10	0.46 ± 0.10	0.35 ± 0.07
Cz	Fpz	0.39 ± 0.07	0.40 ± 0.08	0.65 ± 0.12	0.65 ± 0.11	0.52 ± 0.09
CPz	Fpz	0.51 ± 0.09	0.53 ± 0.10	0.65 ± 0.10	0.65 ± 0.10	0.59 ± 0.09
Pz	Fpz	0.56 ± 0.09	0.58 ± 0.08	0.56 ± 0.08	0.56 ± 0.08	0.56 ± 0.07
POz	Fpz	0.51 ± 0.07	0.52 ± 0.06	0.47 ± 0.06	0.47 ± 0.06	0.49 ± 0.05
Fz	POz	0.58 ± 0.07	0.59 ± 0.07	0.63 ± 0.09	0.62 ± 0.10	0.61 ± 0.07
FCz	POz	0.63 ± 0.07	0.64 ± 0.07	0.66 ± 0.11	0.66 ± 0.11	0.65 ± 0.08
Cz	POz	0.62 ± 0.08	0.62 ± 0.08	0.55 ± 0.10	0.55 ± 0.10	0.59 ± 0.08
CPz	POz	0.44 ± 0.07	0.44 ± 0.07	0.30 ± 0.06	0.30 ± 0.06	0.37 ± 0.06
Fz	Pz	0.59 ± 0.08	0.61 ± 0.08	0.68 ± 0.10	0.68 ± 0.11	0.64 ± 0.08
FCz	Pz	0.60 ± 0.08	0.61 ± 0.08	0.67 ± 0.11	0.67 ± 0.12	0.63 ± 0.08
Cz	Pz	0.49 ± 0.07	0.50 ± 0.06	0.45 ± 0.09	0.45 ± 0.09	0.48 ± 0.07

Data are represented as mean ± standard deviation over 62 head models.

TABLE 2 Participant characteristics.

	A-P tDCS group (n = 12)	P-A tDCS group (n = 12)	Sham tDCS group (n = 12)	p-value
Age (years)	21 (1)	21 (1)	22 (1)	0.09
Sex, male/female (number)	6/6	6/6	6/6	–
Height (cm)	164.6 (9.8)	166.3 (8.2)	163.5 (6.4)	0.72
Weight (kg)	56.5 (8.2)	62.9 (13.5)	56.9 (6.5)	0.68

Data are presented as the mean (standard deviation). After confirmation of the normality of each dataset, one-way analysis of variance was utilized for normally distributed data, and Kruskal–Wallis test was employed for non-normally distributed data. To specify the effect of group difference, a p-value was conducted. tDCS, transcranial direct current stimulation; A-P tDCS, anterior-to-posterior current flow tDCS; P-A tDCS, posterior-to-anterior current flow tDCS.

2.2 Experimental procedure

The study was a randomized, triple-blind, sham-controlled trial. Intervention conditions were concealed from participants, outcome assessors, and data analysts. Participants were stratified by sex and randomly assigned to groups using float numbers between 0 and 1 from a continuous uniform distribution. Assignment was based on whether the number drawn is smaller or equal in value compared to 0.5 or larger than 0.5. These numbers were generated by a third party unrelated to evaluation or intervention (Microsoft, Washington, United States).

To induce the maximal EFs in both SMA and M1, the optimal electrode configuration was determined through computer simulations (see "Electric field simulation"). These simulations indicated that the field maximizing electrode-pair positions were at FCz and POz (Figure 1). Participants received tDCS with one of the following three different electrode placements: (1) anodal and cathodal electrodes positioned over FCz and POz, respectively, resulting in anterior-to-posterior current flow (A-P tDCS); (2) the reverse arrangement, where anodal and cathodal electrodes were positioned over POz and FCz, respectively, resulting in the reverse (posterior to anterior) currents (P-A tDCS), and (3) no current passed (sham tDCS) (Figure 2).

Participants were stratified by sex and were randomly assigned to one of the above three groups. All participants underwent the sit-to-stand training following tDCS intervention. The sit-to-stand training was conducted once every 3 or 4 days for 3 weeks (a total of 5 sessions). Exercise performance, measured by the number of

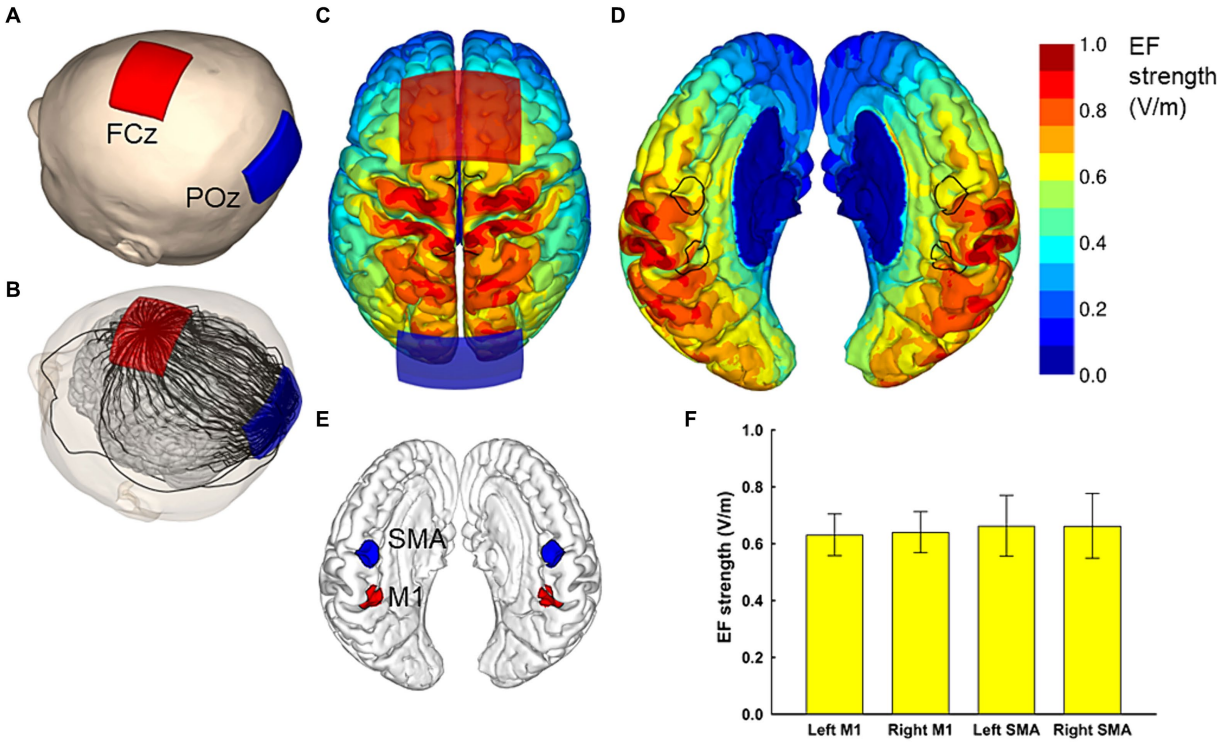

FIGURE 1
Electric field simulations. The optimal electrode locations were at FCz and POz **(A)**, which produced a current flow in the anterior–posterior or posterior–anterior direction, depending on the polarity of the electrodes. A streamline plot visualizes the current direction between the electrodes in a representative head model **(B)**. The Electric field (EF) strengths averaged over 62 head models and registered to a common template brain are shown from the superior direction at a depth of 1 mm below the surface of the grey matter **(C,D)**. In **(D)**, the hemispheres have been separated to visualize the EF strength along the interhemispheric fissure, with the black outlines showing the regions of interest (ROI) that correspond to the left and right SMA and M1 **(E)**. The average EF strengths over each ROI are presented as mean ± standard deviation **(F)**.

sit-to-stands executed in a minute, was assessed pre-training, during each training session, and post-training. Muscle strength (knee extension and flexion peak torques) was measured pre- and post-training. Cortical excitability was measured pre-training, immediately after the first training session, and post-training. Pre-training assessments were conducted between 48 and 72 h before the first training session. Post-training assessments were conducted between 48 and 72 h after the final training session.

2.3 tDCS setting

tDCS was administered using a DC-Stimulator-Plus (neuroConn, GmbH, Germany) connected to a pair of sponge surface electrodes, each with a surface area of 35 cm^2, soaked in a 0.9% NaCl saline solution. With the electrodes placed on the scalp of the participant, a direct current of 2 mA was applied for 10 min. Skin pre-treatment agents and alcohol swabs were used to reduce scalp skin resistance at the electrode contact area. The electrode placement was consistently maintained at the same positions, determined by measuring the length of the participant's head with a tape measure during each session. For the sham condition, the same procedure was performed; however, the current was turned off after the first 15 s to mimic the transient skin sensation felt at the beginning of the direct current. Intervention condition was masked to participants, outcome assessors, and data analysts.

2.4 Electric field simulation

In order to induce the maximal EF strength in both SMA and M1, the optimal electrode montage was determined based on computer simulation of the EFs, similarly to our previous studies (Laakso et al., 2016; Fujimoto et al., 2017).

For the computer simulations of the EF, we utilized 62 individual MRI-based anatomical models, consistent with those used in our previous studies (Laakso et al., 2016; Fujimoto et al., 2017). Each model, with an isotropic resolution of 0.5 mm, was constructed from the segmentation of T1- and T2-weighted (T1w and T2w) MRI data. FreeSurfer image analysis software was employed to segment the brain, including gray and white matter (Dale et al., 1999; Fischl et al., 1999; Fischl and Dale, 2000). Other tissue compartments were segmented as follows: The inner and outer boundaries of the skull, along with the outer surface of the scalp, were identified from the MRI data. An experienced investigator utilized semi-automatic image processing techniques, including thresholding, opening/closing, smoothing, and region growing on the T1w and T2w data, with the parameter values chosen on a per-subject basis. The spaces between the brain, inner skull surface, outer skull surface, and the scalp surface were automatically segmented into multiple tissue types using both MRI data and geometrical operations. The space between the skull and brain was segmented into CSF (large T2w), blood (small T2w), and dura (outer 1.5 mm which is not CSF or a large dural vein). The space between the inner and outer boundaries of the skull was segmented

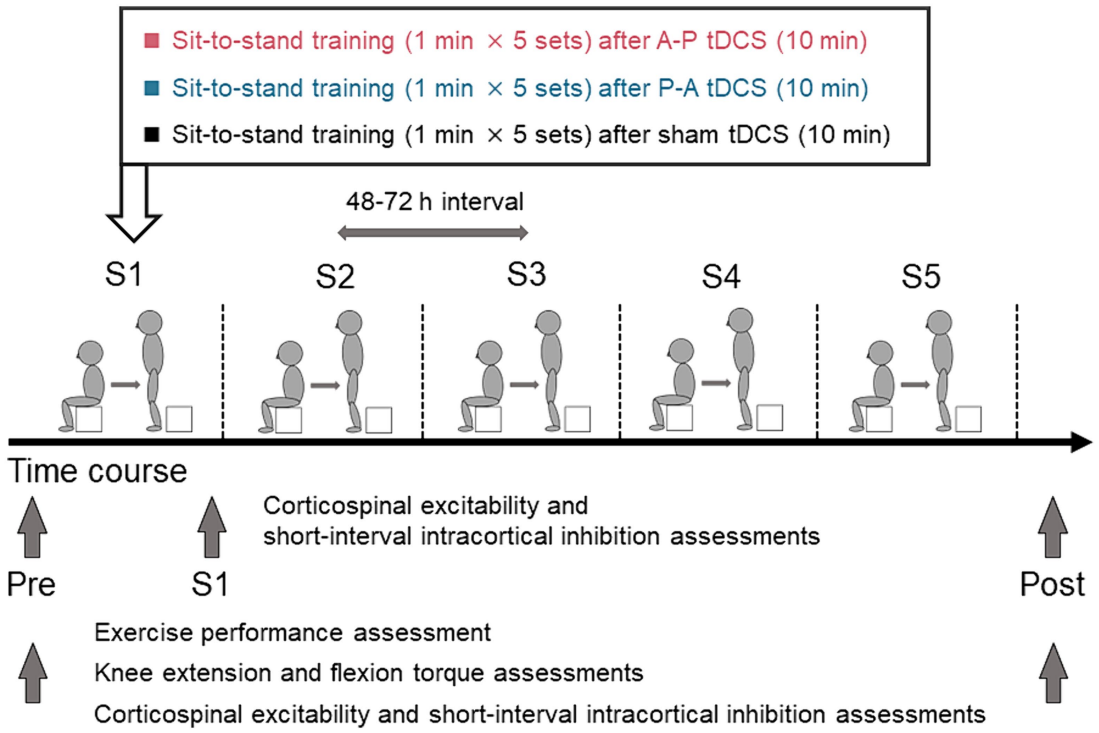

FIGURE 2
Schematics and timeline of the experimental procedures. Healthy participants were randomly assigned to one of three groups in which sit-to-stand training followed tDCS using different current flow paradigms: (i) anterior–posterior (A-P tDCS), (ii) posterior–anterior (P-A tDCS), and (iii) no current (sham tDCS). A single training session consisted of 5 sets of 1 min sit-to-stand with a 180-s rest period between sets. The training was conducted in 5 sessions over 3 weeks, with 48 to 72 h between sessions. Sit-to-stand were assessed before tDCS intervention (Pre), at each of the five sessions (S1, S2, S3, S4, S5), and after training sessions (Post). The single- and paired-pulse TMS were assessed at Pre, S1, and Post and knee extensor and flexor peak torques were assessed at Pre and Post.

into compact bone (small T2w but having at least a 1-mm-thick inner layer and 1.5-mm-thick outer layer) and spongy bone (large T2w). Lastly, the space between the outer boundary of the skull and the surface of the scalp was stratified into fat (large T1w), muscle (small T1w), and skin (small T1w, at least 2-mm thick, at most 1-cm thick including subcutaneous fat) The quality of each model was verified by two independent examiners (Laakso et al., 2016). The electrical conductivities assigned to each tissue were (Laakso et al., 2016): gray matter (0.2 S/m), white matter (0.14 S/m), blood (0.7 S/m), compact bone (0.008 S/m), spongy bone (0.027 S/m), dura (0.16 S/m), CSF (1.8 S/m), muscle (0.16 S/m), skin and fat (0.08 S/m), and eye (1.5 S/m). The sensitivity of the EF to conductivity values was assessed by varying bone conductivity by ±50% and the CSF conductivity by ±10% and repeating all calculations.

The EF was determined as the gradient of the electric scalar potential (ϕ), which was obtained by numerically solving $\nabla\cdot\sigma\nabla\phi = i$ with homogeneous Neumann boundary conditions, where σ is the conductivity (S/m) and i is the current source/sink (A/m^3). The finite element method (FEM) with 0.5 mm cubical first-order elements was employed for numerical solution (Laakso and Hirata, 2012; available at https://version.aalto.fi/gitlab/ilaakso/vgm-fem). The stimulation electrodes were modeled identically to our previous studies (Laakso et al., 2016; Fujimoto et al., 2017), as a 1 mm thick rubber sheet embedded in a saline-soaked sponge (1.6 S/m), with size, shape, and current intensity identical to those in the actual experiment (Figure 1). After obtaining the EF, it was interpolated to a polygonal surface reconstruction of the brain at 1 mm depth below the gray matter surface. As detailed in Laakso et al. (2016), the individual surface EFs were then registered with each other and mapped to the Montreal Neurological Institute (MNI) ICBM 2009a nonlinear asymmetric template (Fonov et al., 2009, 2011) using FreeSurfer and the spherical demons algorithm (Yeo et al., 2010). This process enabled determination of the population-average EFs of the bilateral SMA and M1 in the MNI space.

For the optimization of the electrode montage, we considered four regions of interest. The regions of interest for M1 and SMA had a radius of 1 cm and were centered at [± 9, − 39, 54] and [± 3, − 9, 60] in the standard brain space, respectively. Our aim was to find a montage of two electrodes that produces symmetric bilateral stimulation and maximizes the average EF strength over the four regions of interest. To achieve symmetric stimulation, both the anode and cathode needed to be placed on the midline of the head. For practical applicability, the electrode locations were selected using the International 10–10 system: The first electrode was placed at Fz, FCz, Cz, CPz, or Pz, and the second electrode at an extracephalic location, frontally (Fpz), posteriorly (Iz), or close to the stimulated areas (POz or Pz). The electrodes were oriented so that the long edges of the electrodes were perpendicular to the posterior–anterior direction. Any locations which would have caused the electrodes to overlap were excluded, leaving 23 electrode montages, listed in the first two columns of Table 1.

The EF produced by each montage were calculated for all 62 head models, and the EF strength averaged over each/all regions of interest was determined. Finally, the mean and standard deviation of these average values were calculated over the 62 head models. The results for each studied electrode montage are provided in Table 1. It was found that the FCz-POz configuration induced the largest mean value of the average EF strength over the four regions of interests, closely followed by the Fz-Pz montage. At the individual level, FCz-POz was the optimal montage in 32/62 models and Fz-Pz in 22/62 models (Supplementary Table S1). Repeating the EF analyses for altered bone and CSF conductivities indicated that either the FCz-POz or the Fz-Pz montage was the optimal configuration regardless of the choice of the conductivity values (Supplementary Table S1). Thus, the FCz-POz configuration, visualized in Figure 1, was used in the experiment.

2.5 Sit-to-stand training

The participants performed the sit-to-stand task starting from a seated position on a 20 cm box. They were instructed to perform the sit-to-stand task by standing up straight from the box as quickly as possible with fully extended trunk, hip joints, and knee joints, then sit down. The training protocol of a single session consisted of 5 sets of 1 min sit-to-stand task with a 180-s rest period between sets (Figure 2). While monitoring the participant's performance to ensure proper form (fully extend the trunk, hip joints, and knee joints) examiners counted the completion of each correctly executed sit-to-stand. The counts were averaged over the 5 sets. The sit-to-stand training was conducted a total of 5 sessions. The 48 to 72 h interval between sessions was used to avoid the effect of fatigue on the performance. Before training session, participants warmed up on a bicycle for 5 min, then performed a set of stretches focused on the knee extensor and flexor muscles. They repeated the same routine to warm down after each session.

2.6 Muscle strength assessment

Knee extensor and flexor peak torques were assessed using an isokinetic dynamometer (Multi-Joint 3, Biodex Medical Systems Inc., Shirley, NY, United States) with the same procedure as Maeda et al. (2017). Participants were instructed to extend the knee with maximal effort while the dynamometer flexed the knee at a speed of 30°/s from the initial 20° to the 90° eccentric contraction of the knee extensors. For the measurement of the knee flexors torques, participants flexed the knee while the dynamometer extended the knee at 30°/s from 90° to 20°. The maximal knee extensor and flexor torques were evaluated for 3 sets (5 repetitions/set) under eccentric (30°/s) conditions. The maximal knee extensor and flexor torques obtained in 5 repetitions were taken as the peak torque, and the average of the peak torque for each set was calculated.

2.7 Electromyography

The participants were comfortably seated in a chair with their arms resting on a cushion. The electromyography (EMG) was recorded via Ag/AgCl-plated surface electrodes (1 cm diameter) placed 2 cm apart over the right rectus femoris (RF) muscle. Responses were acquired using a Neuropack MEB-2200 system (Nihon Kohden, Tokyo, JPN) filtered in the 10 Hz to 1 kHz pass-band. EMG signals were sampled at 5 kHz and stored on the computer for off-line analysis using the LabVIEW software (National Instruments Inc., Austin, Texas, United States).

2.8 Transcranial magnetic stimulation

To assess changes in motor cortex excitability, single-pulse transcranial magnetic stimulation (TMS) was applied to the leg area of the left M1 using a magnetic stimulator (Magstim200, Magstim, Dyfed, UK) connected to a double-cone coil of 110-mm diameter. The hotspot of the M1 was confirmed based on induction of the largest MEP amplitude in the right RF muscle during tonic voluntary contraction. The stimulation intensity was adjusted to 120% of the active motor threshold (aMT). The aMT was defined as the lowest stimulus intensity needed to produce MEPs greater than 200 μV in at least 5 out of 10 consecutive trials during the maintenance of 100 μV of RF voluntary isometric contraction (Rossini et al., 2015; Temesi et al., 2017). The time between stimulus pulses was varied between 5 and 7 s. The stimulus timing was automatically controlled using LabVIEW.

In order to induce SICI we used a subthreshold conditioning paired-pulse paradigm (Kujirai et al., 1993). We used stimulus intensities of 80% aMT for the conditioning stimulus and 120% resting motor threshold (rMT) for the test stimulus. Throughout the experiment, the test stimulus was adjusted to maintain the MEP amplitude equal to the RF MEP amplitude at baseline. The interstimulus interval was set at 2.5 ms, and 15 MEPs were recorded from the RF muscle (Fisher et al., 2002). The conditioned MEP amplitudes were expressed as percentages of the mean test MEP amplitudes.

2.9 Statistical analysis

The primary outcome measures included the sit-to-stand counts and muscle strength measured pre-training and post-training. We used the 2-way mixed-model analysis of variance (ANOVA) to evaluate the differences in outcome with group (A-P tDCS, P-A tDCS, sham tDCS) and time (pre-training and post-training) used as within-subject factors. Muscle strength was tested separately for the left and right knee flexors and extensors. Similarly, for the sit-to-stand counts during training sessions, we used a 2-way mixed-model ANOVA with the group (A-P tDCS, P-A tDCS, sham tDCS) and time (pre-training, session 1, session 2, session 3, session 4, and session 5) as factors. A t-test with Bonferroni adjustment for multiple comparisons was performed to compare training effects for the group and time factor. For MEP amplitudes and SICI, we applied a 2-way mixed-model ANOVA with the group (A-P tDCS, P-A tDCS, sham tDCS) and time (pre-training, immediately after a first session of training, post-training) as factors. A t-test with Bonferroni adjustment for multiple comparisons was performed to compare changes in cortical excitability pre-training, immediately after the first session of training, post-training for the group and time factor. p values <0.05 were considered statistically significant for all analyses. Statistical analyses were performed using SPSS 28.0 (IBM, Armonk, NY, United States).

3 Results

All participants successfully completed the 3-week training. There were no reports of adverse events related to the training or tDCS. However, data for one participant in the P-A tDCS group was lost due to a device malfunction during the post-training test MEP and SICI measurements. Despite this, the percentage of correct responses in the condition remained below the chance level, indicating that, blinding in the intervention condition was maintained. The results of the motor performance and physiological factors for each group are illustrated in Tables 3, 4.

3.1 The sit-to-stand counts

The sit-to-stand counts continued to increase throughout the 5 sessions and were greater after than before training in all groups. At post-training assessment, the sit-to-stand counts for the A-P tDCS group were significantly higher than the sham tDCS group, indicating that A-P tDCS promoted sit-to-stand performance (Figure 3). These observations were supported by primary outcome results of the 2-way mixed-model ANOVA, which revealed significant interactions ($F_{(2, 33)} = 3.652$, $p < 0.05$), with a significant main effect of time ($F_{(1, 33)} = 88.990$, $p < 0.01$). No significant main effect of the intervention was observed ($F_{(2, 33)} = 0.398$, $p = 0.675$). Similarly, the multiple comparison test revealed that the sit-to-stand counts were significantly increased at post-training for all groups compared to the pre-training ($p < 0.01$). When the sit-to-stand counts were compared between the groups, the counts were significantly greater in the A-P tDCS group compared to the sham tDCS group ($p < 0.05$) at post-training. However, 2-way mixed-model ANOVA found no significant differences in the counts among the groups during training session ($F_{(10, 165)} = 1.879$, $p = 0.051$). The main effects of time were significant ($F_{(5, 165)} = 25.685$, $p < 0.01$), but no significant main effect of the intervention was observed ($F_{(2, 33)} = 0.777$, $p = 0.468$).

3.2 Muscle strength

The peak torque in right and left knee flexors were increased in the P-A tDCS group, and only in that group, following 3 weeks of training (Figure 4). In contrast, no changes were observed for peak torque in the knee extensors in any of the groups. Statistical analyses supported these observations. For knee flexor torques, 2-way mixed-model ANOVA showed significant interactions between intervention and time (Right: $F_{(2, 33)} = 8.099$, $p < 0.01$, Left: $F_{(2, 33)} = 10.917$, $p < 0.01$). The main effects of time were significant (Right: $F_{(1, 33)} = 9.425$, $p < 0.01$, Left: $F_{(1, 33)} = 8.436$, $p < 0.01$). No significant main effects of the intervention were observed ($p > 0.1$ for both right and left). For knee extensor torques, there was also no interaction between intervention and time, and the main effects of both time and intervention were not significant ($p > 0.1$ for each test, for both right and left).

Multiple comparison test revealed that the left and right knee flexor peak torques in the P-A tDCS group were significantly increased at post-training above their pre-training levels ($p < 0.01$). The left knee flexor peak torques in the P-A tDCS group, in particular, were significantly increased over levels in the sham tDCS group at post-training ($p < 0.05$).

3.3 MEP amplitudes

There was no significant interaction between intervention and time ($F_{(4, 66)} = 0.655$, $p = 0.626$), and the main effects of both time and intervention were not significant ($p > 0.3$ for both). These results confirmed that MEP amplitudes remained stable at pre-training levels during and after training.

3.3.1 SICI

SICI was suppressed in the P-A tDCS group immediately after the first session of training and remained so post-training. Moreover, compared to other groups, the suppression seen in the P-A tDCS group was marked (Figure 5), suggesting that P-A tDCS-induced plastic changes of SICI in the primary motor cortex.

This result were borne out by a 2-way mixed-model ANOVA, showing significant interactions ($F_{(4, 65)} = 3.261$, $p < 0.05$) between intervention and time, and main effects of session times ($F_{(2, 65)} = 3.796$, $p < 0.05$) and intervention ($F_{(2, 33)} = 3.678$, $p < 0.05$). Multiple comparison showed that SICI in P-A tDCS group was significantly decreased immediately after the first session of training and remained so post-training below the pre-training values (both, $p < 0.05$). Furthermore, the SICI was significantly decreased in the P-A tDCS

TABLE 3 Motor performance.

	A-P tDCS group (n = 12)		P-A tDCS group (n = 12)		sham tDCS group (n = 12)	
	Pre	Post	Pre	Post	Pre	Post
SIT-to-stand counts						
	43 (9)	60 (4)	44 (11)	55 (6)	45 (7)	54 (6)
KNEE extensor torque (Nm)						
Right side	99.9 (19.8)	95.9 (25.0)	102.4 (31.9)	107.9 (28.1)	97.2 (25.9)	98.7 (28.5)
Left side	87.0 (26.0)	87.4 (24.5)	95.0 (32.6)	100.3 (30.6)	89.8 (24.5)	86.3 (21.7)
KNEE flexor torque (Nm)						
Right side	128.3 (22.2)	124.8 (20.4)	124.2 (20.3)	144.2 (19.9)	117.6 (26.2)	123.1 (28.9)
Left side	123.0 (24.3)	121.8 (24.7)	122.5 (18.7)	145.3 (20.5)	117.0 (16.0)	116.3 (24.8)

Data are presented as the mean (standard deviation). The data demonstrate the sit-to-stand counts and muscle strength before training (Pre) and after 3 weeks training (Post). tDCS, transcranial direct current stimulation; A-P tDCS, anterior-to-posterior current flow tDCS; P-A tDCS, posterior-to-anterior current flow tDCS.

TABLE 4 Physiological factors.

A-P tDCS group ($n = 12$)			P-A tDCS group ($n = 12$)			sham tDCS group ($n = 12$)		
Pre	S1	Post	Pre	S1	Post	Pre	S1	Post
SICI (% of test MEP)								
46.2 (14.5)	41.3 (16.7)	47.5 (18.7)	45.5 (11.2)	69.9 (10.4)	62.3 (18.4)	46.6 (19.4)	52.9 (14.7)	50.5 (26.1)
MEP AMPLITUDES (mV)								
1.44 (0.86)	0.96 (0.83)	1.15 (0.79)	1.49 (0.76)	1.30 (0.83)	1.70 (1.51)	1.42 (0.72)	1.53 (0.87)	1.63 (0.66)

Data are presented as the mean (standard deviation). The data show the short-interval intracortical inhibition (SICI) and motor-evoked potential (MEP) before training (Pre), after session 1 (S1), and after 3 weeks training (Post). tDCS, transcranial direct current stimulation; A-P tDCS, anterior-to-posterior current flow tDCS; P-A tDCS, posterior-to-anterior current flow tDCS.

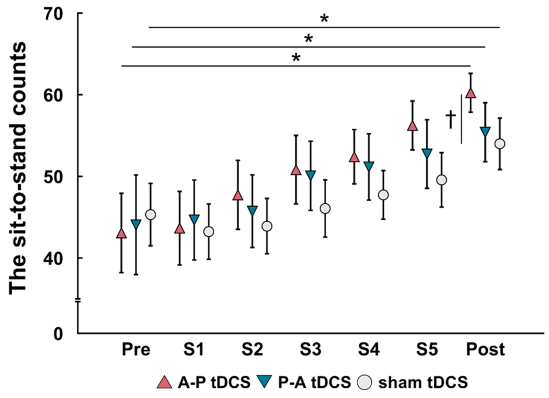

FIGURE 3
Changes in the sit-to-stand counts following tDCS combined with sit-to-stand training. Data are presented as mean (symbols) ± the confidence interval (whiskers). Data for the three groups are shown in different symbols: A-P tDCS (red triangles); P-A tDCS (blue inverted triangles); and sham tDCS (gray circles). The sit-to-stand counts were assessed before training (Pre), session 1 (S1), session 2 (S2), session 3 (S3), session 4 (S4), session 5 (S5) and after 3 weeks training (Post). Significant ($p < 0.05$) pairwise differences within group between the pre and another time point (asterisk) and between groups at a fixed time point (dagger) are indicated.

group compared to the A-P and sham tDCS groups immediately after the first session of training (both, $p < 0.05$).

4 Discussion

This is the first study to investigate the effects of different current flows with electrode placement optimized for tDCS to produce maximum EFs in SMA and M1. Our primary findings are as follows: (1) A-P tDCS enhanced sit-to-stand counts after 3 weeks of training; (2) P-A tDCS increased the right and left knee flexor peak torques after 3 weeks of training; and (3) P-A tDCS decreased SICI immediately after the first session of training held it decreased until post-training. These results indicate that optimized electrode placement of tDCS can promote motor performances and modulate cortical excitability depending on the current flow. Moreover, all participants completed the training without adverse effects, making applying our method in healthy controls a valuable step toward enhancing current neurorehabilitation practices.

The conventional method of placing tDCS electrodes is just above the target brain area where researchers expected to modulate cortical excitability (Nitsche and Paulus, 2000; Tanaka et al., 2009, 2011). However, this strategy for electrodes placement was unable to induce optimal EFs in the target cortical areas (Laakso et al., 2016), and it often fails to improve motor function and modulate cortical excitability in healthy individuals and patients with stroke (Kan et al., 2013; Muthalib et al., 2013; Maeda et al., 2017; Klomjai et al., 2018; Alix-Fages et al., 2020; Katagiri et al., 2021). Therefore, we adopted FCz and POz for the placement of the two electrodes because these loci were identified, by simulated EFs in MRI-based model brains, as those leading to the inducing of maximum EFs to the SMA and M1. The conventional method of placing the stimulation electrode just above the target brain area (i.e., Cz plus a reference electrode at a distant location) was not optimal for inducing EF to the target brain area (Table 1). The results of these simulations indicated that unconventional electrode placement (i.e., where the target brain area is between the two electrodes) may modulate the brain area. However, to the best of our knowledge, no studies have examined changes in motor performance with optimized electrode placement tDCS by electric field simulation. A previous study reported a positive correlation between the EF values induced in the target brain areas and changes in cortical excitability caused by tDCS (Mosayebi-Samani et al., 2021). Therefore, use of electrical field simulations for electrode placement tDCS may modulate cortical excitability and enhance motor performance. In addition, studies have reported that the conventional tDCS targeting M1 combined with long-term muscle strength training did not improve muscle strength or motor performance (Hendy and Kidgell, 2013; Maeda et al., 2017; Marcos-Frutos et al., 2023; Jung et al., 2024). On the other hand, we found that optimized electrode placement by electric field simulation enhances muscle strength and motor performance. Therefore, optimized electrode placement tDCS might elicit improvements in muscle strength and motor performance that could not be achieved with conventional methods. These results suggest that the determination of tDCS electrode placement by electric field simulation for standard brain models may provide important findings for future neurorehabilitation studies.

Surprisingly, we found that motor cortex excitability and motor performance improved when currents flowed in opposite directions. The tDCS effect depends on the relationship between the EF vector and the morphology and orientation of the neurons and individual neuronal compartments, which determines the polarization state of neurons (Liu et al., 2018). Indeed, it has been reported that corticospinal excitability and motor task learning are affected by

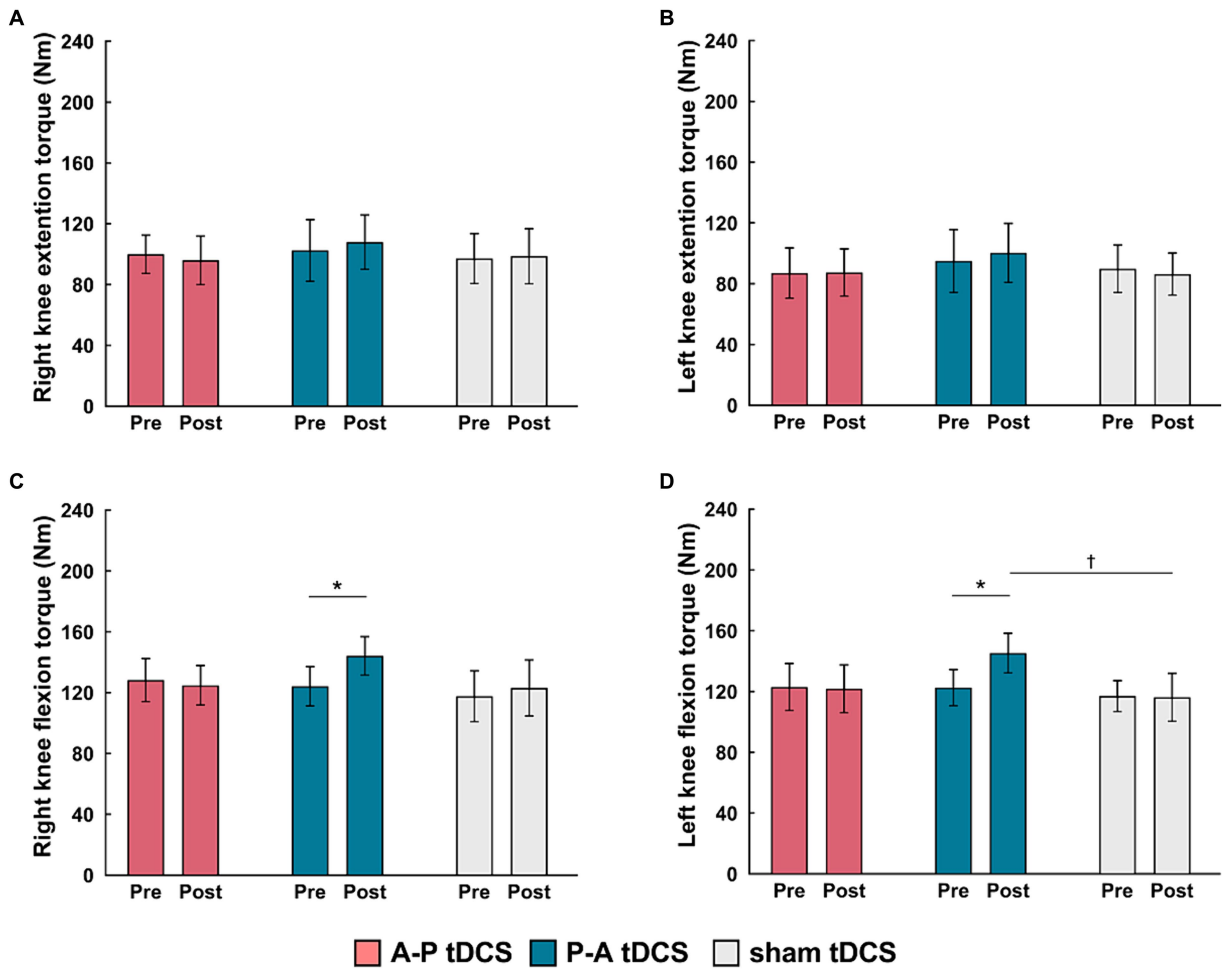

FIGURE 4
Changes in muscle strength following tDCS combined with sit-to-stand training. Muscle torque (Nm) measurements are presented as mean (bar) ± the confidence interval (whiskers) for the **(A)** right knee extension, **(B)** left knee extension, **(C)** right knee flexion, and **(D)** left knee flexion. Data for the three groups are labeled by color: A-P tDCS (red), P-A tDCS (blue), sham tDCS (gray). Muscle torque were assessed before training (Pre) and after 3 weeks training (Post). Significant ($p < 0.05$) pairwise differences within group between the Pre and Post (asterisks) and between groups at a fixed time point (daggers) are indicated.

current flow between the tDCS electrodes (Rawji et al., 2018; Hannah et al., 2019). Our tDCS electrode placement produced a similarly strong EFs in SMA and M1. Therefore, different populations of neurons in SMA and M1 may have depolarized or hyperpolarized depending on the direction of the current flow. A-P tDCS in our experiments induced current flows from SMA to M1, which is expected to effectively depolarize in the SMA area. This in turn is thought to facilitate the coordination and execution of motor programs during skilled movement and postural control, which are functions of the SMA (Mihara et al., 2008, 2012; Fujimoto et al., 2014). Investigators using a similar electrode placement to ours have reported that body weight-supported treadmill training and tDCS with anode in front of Cz and cathode over inion improved the balance and gait function after stroke, but paradoxically without changes in leg motor function (Manji et al., 2018). Conversely, P-A tDCS induces current from M1 to SMA, which is expected to effectively depolarize in the M1 area. In the previous studies, posterior to anterior current flow from M1 to the opposite supraorbital improved muscle strength in the upper and lower limbs (Tanaka et al., 2009; Hazime et al., 2017; Vargas et al., 2018). Therefore, posterior to anterior current flow targeting M1 and SMA in the P-A tDCS group may have led to the increased peak torque of knee flexion after the 3 weeks of training.

Interestingly, we found that the peak torque was improved in knee flexors, but not in the knee extensor. During the sit-to-standing exercise, knee flexor muscles are required for the smooth extension of the knee joint via eccentric muscle contraction, whereas knee extensor muscles are activated to extend the knee joint via concentric muscle contraction (Bryanton and Bilodeau, 2017). The effectiveness of muscle training depends on the mode of muscle contraction being evaluated (Higbie et al., 1996). Based on these earlier studies, the muscle strength increases we detected in the assessment of eccentric contraction of the knee flexor muscles was not unexpected.

A decrease in SICI was observed in the P-A tDCS group alone, while SICI did not change in the other groups. This result may also support the hypothesis that different populations of neurons in SMA and M1 may have depolarized or hyperpolarized depending on current flow. It has been reported that conventional non-optimized anodal tDCS over M1 reduced SICI there (Nitsche et al., 2005;

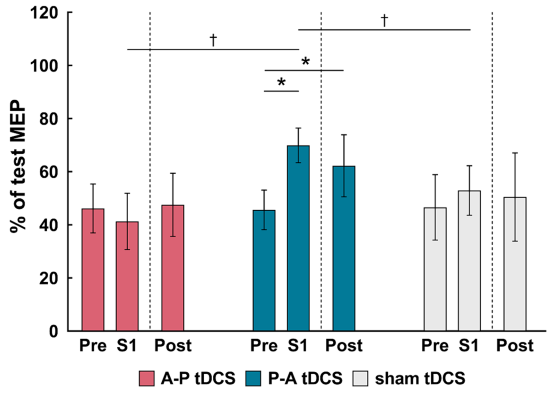

FIGURE 5
Changes in the short-interval intracortical inhibition (SICI) following tDCS combined with sit-to-stand training. The relative changes in SICI, as a % of the reference (test MEP), are shown as the mean (bars) and confidence intervals (whiskers) for three time points (pre, S1 and Post) in different colors for the three groups: A-P tDCS (red), P-A tDCS (blue), sham tDCS (gray). SICI were assessed before training (Pre), after session 1 (S1) and after 3 weeks training (Post). Significant ($p < 0.05$) pairwise differences within group between the pre and another time point (asterisks) and between groups at a fixed time point (dagger) are indicated.

Biabani et al., 2018). Others have shown that changes in SICI probably reflect the activity of $GABA_A$-ergic intracortical inhibitory connections in cortical layer 1 since the inhibition is evoked by conditioning stimulus below motor threshold (Di Lazzaro et al., 2006; Di Lazzaro and Rothwell, 2014). In addition, previous studies suggested that the current of tDCS will preferentially polarize neural components that are aligned with the direction of current flow (Bikson et al., 2004; Jackson et al., 2016; Hannah et al., 2019). Therefore, the neural elements involved in the change in SICI were more likely to be selectively modulated according to the direction of the applied EFs because they were specific to our task and located in a shallow layer. This is speculation that change in SICI might be associated with increasing the efficiency of transmission of the descending drive of M1, resulting in stronger muscle contraction (Hendy and Kidgell, 2014; Hendy et al., 2015). In contrast, the effects of the different tDCS conditions on corticospinal excitability were not observed in the present study. An earlier review reported for conventional anodal tDCS an increase in corticospinal excitability along with the reduction in SICI (McNeil et al., 2009). One possible factor is fatigue after training. It is known that fatigue after muscle contractions inhibits the corticospinal response at the spinal level (McNeil et al., 2009, 2011; Carroll et al., 2017). Thus, a negative effect on corticospinal rather than intracortical excitability may have been at play.

Relearning the sit-to-stand movement is essential to rehabilitation after a stroke (Alexander et al., 2000). Conventional rehabilitation, combined with anodal tDCS over M1, improved sit-to-stand performance in patients following stroke (Andrade et al., 2017). Therefore, tDCS with optimized electrode placement may assist with stroke rehabilitation. Furthermore, our results indicate that different effects are observed relative to tDCS current flow direction. These findings provide new insights into current neurorehabilitation paradigms. Specifically, the A-P tDCS could be adapted for stroke patients needing to improve their sit-to-stand performance. Additionally, P-A tDCS could be adapted for stroke patients requiring enhanced muscle strengthening. Therefore, the optimized electrode placement for tDCS can be determined based on patient-specific treatment objectives.

However, this study has several limitations. First, we have not compared the effects of the optimized electrode placement with those of the conventional tDCS electrode placement. A single session of conventional tDCS combined with exercise has been shown to enhance muscle strength and modulate corticospinal tract excitability (Kim and Ko, 2013; Washabaugh et al., 2016). In contrast, the effects of repetitive sessions remain unclear (Wang et al., 2021; Marcos-Frutos et al., 2023). Therefore, further studies are necessary to compare the effects of optimized electrode placement tDCS to conventional tDCS in repetitive sessions. Second, the cortical EFs were calculated numerically through the FEM in an anatomical model in accordance with the 62 MRIs, not the participants that were recruited. Third, the SMA activity changes were not evaluated following the training. Fourth, this study was conducted on healthy individuals. Therefore, in the future, EFs need to be calculated for each subject to reduce inter-individual variability in tDCS-induced effects. Additionally, SMA activity changes after training should be evaluated through postural control tasks. Finally, further research is required to examine whether tDCS with an optimized electrode placement can improve motor performance and brain function more than the conventional tDCS method in patients with stroke. In conclusion, we showed that electrode placement of the maximal EFs in SAM and M1 estimated by electric field simulation enhances sit-to-stand performance, lower limb muscle strength, and modulates motor cortical excitability depending on the direction of current flow in young healthy individuals.

Data availability statement

The original contributions presented in the study are included in the article/Supplementary material, further inquiries can be directed to the corresponding author.

Ethics statement

The studies involving humans were approved by Yamagata Prefectural University of Health Sciences (approval number: 1806-06). The studies were conducted in accordance with the local legislation and institutional requirements. The participants provided their written informed consent to participate in this study.

Author contributions

TS: Conceptualization, Data curation, Investigation, Writing – original draft. NK: Data curation, Investigation, Writing – original draft. SS: Conceptualization, Data curation, Investigation, Writing – original draft. IL: Formal analysis, Writing – review & editing. ShT: Software, Writing – review & editing. RO: Formal analysis, Writing – review & editing. SaT: Conceptualization, Funding acquisition, Writing – review & editing. TY: Conceptualization, Data curation, Formal analysis, Funding acquisition, Methodology, Supervision, Writing – original draft, Writing – review & editing.

Funding

The author(s) declare that financial support was received for the research, authorship, and/or publication of this article. This work was supported by a Japan Society for the Promotion of Science (JSPS) Grants-in-Aid for Scientific Research (B) [grant numbers 23K27943, 20H04050] to TY and SaT.

Conflict of interest

The authors declare that the research was conducted in the absence of any commercial or financial relationships that could be construed as a potential conflict of interest.

Publisher's note

Supplementary material

The Supplementary material for this article can be found online at: https://www.frontiersin.org/articles/10.3389/fnins.2024.1362607/full#supplementary-material

References

Alexander, N. B., Galecki, A. T., Nyquist, L. V., Hofmeyer, M. R., Grunawalt, J. C., Grenier, M. L., et al. (2000). Chair and bed rise performance in ADL-impaired congregate housing residents. *J. Am. Geriatr. Soc.* 48, 526–533. doi: 10.1111/j.1532-5415.2000.tb04999.x

Alix-Fages, C., García-Ramos, A., Calderón-Nadal, G., Colomer-Poveda, D., Romero-Arenas, S., Fernández-Del-Olmo, M., et al. (2020). Anodal transcranial direct current stimulation enhances strength training volume but not the force-velocity profile. *Eur. J. Appl. Physiol.* 120, 1881–1891. doi: 10.1007/s00421-020-04417-2

Andrade, S. M., Ferreira, J. J. A., Rufino, T. S., Medeiros, G., Brito, J. D., da Silva, M. A., et al. (2017). Effects of different montages of transcranial direct current stimulation on the risk of falls and lower limb function after stroke. *Neurol. Res.* 39, 1037–1043. doi: 10.1080/01616412.2017.1371473

Angius, L., Mauger, A. R., Hopker, J., Pascual-Leone, A., Santarnecchi, E., and Marcora, S. M. (2018). Bilateral extracephalic transcranial direct current stimulation improves endurance performance in healthy individuals. *Brain Stimul.* 11, 108–117. doi: 10.1016/j.brs.2017.09.017

Angius, L., Pageaux, B., Hopker, J., Marcora, S. M., and Mauger, A. R. (2016). Transcranial direct current stimulation improves isometric time to exhaustion of the knee extensors. *Neuroscience* 339, 363–375. doi: 10.1016/j.neuroscience.2016.10.028

Biabani, M., Aminitehrani, M., Zoghi, M., Farrell, M., Egan, G., and Jaberzadeh, S. (2018). The effects of transcranial direct current stimulation on short-interval intracortical inhibition and intracortical facilitation: a systematic review and meta-analysis. *Rev. Neurosci.* 29, 99–114. doi: 10.1515/revneuro-2017-0023

Bikson, M., Inoue, M., Akiyama, H., Deans, J. K., Fox, J. E., Miyakawa, H., et al. (2004). Effects of uniform extracellular DC electric fields on excitability in rat hippocampal slices in vitro. *J. Physiol.* 557, 175–190. doi: 10.1113/jphysiol.2003.055772

Bryanton, M., and Bilodeau, M. (2017). The role of thigh muscular efforts in limiting sit-to-stand capacity in healthy young and older adults. *Aging Clin. Exp. Res.* 29, 1211–1219. doi: 10.1007/s40520-016-0702-7

Carroll, T. J., Taylor, J. L., and Gandevia, S. C. (2017). Recovery of central and peripheral neuromuscular fatigue after exercise. *J. Appl. Physiol.* 122, 1068–1076. doi: 10.1152/japplphysiol.00775.2016

Chang, M. C., Kim, D. Y., and Park, D. H. (2015). Enhancement of cortical excitability and lower limb motor function in patients with stroke by transcranial direct current stimulation. *Brain Stimul.* 8, 561–566. doi: 10.1016/j.brs.2015.01.411

Chew, T., Ho, K. A., and Loo, C. K. (2015). Inter- and intra-individual variability in response to transcranial direct current stimulation (tDCS) at varying current intensities. *Brain Stimul.* 8, 1130–1137. doi: 10.1016/j.brs.2015.07.031

Dale, A. M., Fischl, B., and Sereno, M. I. (1999). Cortical surface-based analysis I segmentation and surface reconstruction. *NeuroImage* 9, 179–194. doi: 10.1006/nimg.1998.0395

Di Lazzaro, V., Pilato, F., Dileone, M., Ranieri, F., Ricci, V., Profice, P., et al. (2006). GABAA receptor subtype specific enhancement of inhibition in human motor cortex. *J. Physiol.* 575, 721–726. doi: 10.1113/jphysiol.2006.114694

Di Lazzaro, V., and Rothwell, J. C. (2014). Corticospinal activity evoked and modulated by non-invasive stimulation of the intact human motor cortex. *J. Physiol.* 592, 4115–4128. doi: 10.1113/jphysiol.2014.274316

Evans, C., Bachmann, C., Lee, J. S. A., Gregoriou, E., Ward, N., and Bestmann, S. (2020). Dose-controlled tDCS reduces electric field intensity variability at a cortical target site. *Brain Stimul.* 13, 125–136. doi: 10.1016/j.brs.2019.10.004

Fischl, B., and Dale, A. M. (2000). Measuring the thickness of the human cerebral cortex from magnetic resonance images. *Proc. Natl. Acad. Sci. USA* 97, 11050–11055. doi: 10.1073/pnas.200033797

Fischl, B., Sereno, M. I., Tootell, R. B., and Dale, A. M. (1999). High-resolution intersubject averaging and a coordinate system for the cortical surface. *Hum. Brain Mapp.* 8, 272–284. doi: 10.1002/(sici)1097-0193(1999)8:4<272::aid-hbm10>3.0.co;2-4

Fisher, R. J., Nakamura, Y., Bestmann, S., Rothwell, J. C., and Bostock, H. (2002). Two phases of intracortical inhibition revealed by transcranial magnetic threshold tracking. *Exp. Brain Res.* 143, 240–248. doi: 10.1007/s00221-001-0988-2

Fonov, V., Evans, A. C., Botteron, K., Almli, C. R., McKinstry, R. C., Collins, D. L., et al. (2011). Unbiased average age-appropriate atlases for pediatric studies. *NeuroImage* 54, 313–327. doi: 10.1016/j.neuroimage.2010.07.033

Fonov, V., Evans, A. C., McKinstry, R. C., Almli, C. R., and Collins, D. L. (2009). Unbiased nonlinear average age-appropriate brain templates from birth to adulthood. *NeuroImage* 47:S102. doi: 10.1016/S1053-8119(09)70884-5

Fujimoto, H., Mihara, M., Hattori, N., Hatakenaka, M., Kawano, T., Yagura, H., et al. (2014). Cortical changes underlying balance recovery in patients with hemiplegic stroke. *NeuroImage* 85, 547–554. doi: 10.1016/j.neuroimage.2013.05.014

Fujimoto, S., Tanaka, S., Laakso, I., Yamaguchi, T., Kon, N., Nakayama, T., et al. (2017). The effect of dual-hemisphere transcranial direct current stimulation over the parietal operculum on tactile orientation discrimination. *Front. Behav. Neurosci.* 11:173. doi: 10.3389/fnbeh.2017.00173

Guerra, A., López-Alonso, V., Cheeran, B., and Suppa, A. (2020). Variability in non-invasive brain stimulation studies: reasons and results. *Neurosci. Lett.* 719:133330. doi: 10.1016/j.neulet.2017.12.058

Hannah, R., Iacovou, A., and Rothwell, J. C. (2019). Direction of TDCS current flow in human sensorimotor cortex influences behavioural learning. *Brain Stimul.* 12, 684–692. doi: 10.1016/j.brs.2019.01.016

Hazime, F. A., da Cunha, R. A., Soliaman, R. R., Romancini, A. C. B., Pochini, A. C., Ejnisman, B., et al. (2017). Anodal transcranial direct current stimulation (TDCS) increases isometric strength of shoulder rotators muscles in handball PLAYERS. *Int. J. Sports Phys. Ther.* 12, 402–407. Available at: https://ijspt.org/.

Hendy, A. M., and Kidgell, D. J. (2013). Anodal tDCS applied during strength training enhances motor cortical plasticity. *Med. Sci. Sports Exerc.* 45, 1721–1729. doi: 10.1249/MSS.0b013e31828d2923

Hendy, A. M., and Kidgell, D. J. (2014). Anodal-tDCS applied during unilateral strength training increases strength and corticospinal excitability in the untrained homologous muscle. *Exp. Brain Res.* 232, 3243–3252. doi: 10.1007/s00221-014-4016-8

Hendy, A. M., Teo, W. P., and Kidgell, D. J. (2015). Anodal transcranial direct current stimulation prolongs the cross-education of strength and Corticomotor plasticity. *Med. Sci. Sports Exerc.* 47, 1788–1797. doi: 10.1249/MSS.0000000000000600

Higbie, E. J., Cureton, K. J., Warren, G. L., and Prior, B. M. (1996). Effects of concentric and eccentric training on muscle strength, cross-sectional area, and neural activation. *J. Appl. Physiol.* 81, 2173–2181. doi: 10.1152/jappl.1996.81.5.2173

Jackson, M. P., Rahman, A., Lafon, B., Kronberg, G., Ling, D., Parra, L. C., et al. (2016). Animal models of transcranial direct current stimulation: methods and mechanisms. *Clin. Neurophysiol.* 127, 3425–3454. doi: 10.1016/j.clinph.2016.08.016

Jeffery, D. T., Norton, J. A., Roy, F. D., and Gorassini, M. A. (2007). Effects of transcranial direct current stimulation on the excitability of the leg motor cortex. *Exp. Brain Res.* 182, 281–287. doi: 10.1007/s00221-007-1093-y

Julious, S. A. (2005). Sample size of 12 per group rule of thumb for a pilot study. *Pharm. Stat.* 4, 287–291. doi: 10.1002/pst.185

Jung, J., Salazar Fajardo, J. C., Kim, S., Kim, B., Oh, S., and Yoon, B. (2024). Effect of tDCS combined with physical training on physical performance in a healthy population. *Res. Q. Exerc. Sport* 95, 149–156. doi: 10.1080/02701367.2023.2166894

Kan, B., Dundas, J. E., and Nosaka, K. (2013). Effect of transcranial direct current stimulation on elbow flexor maximal voluntary isometric strength and endurance. *Appl. Physiol. Nutr. Metab.* 38, 734–739. doi: 10.1139/apnm-2012-0412

Katagiri, N., Kawakami, S., Okuyama, S., Koseki, T., Kudo, D., Namba, S., et al. (2021). Single-session cerebellar transcranial direct current stimulation affects postural control learning and cerebellar brain inhibition in healthy individuals. *Cerebellum* 20, 203–211. doi: 10.1007/s12311-020-01208-5

Kim, G. W., and Ko, M. H. (2013). Facilitation of corticospinal tract excitability by transcranial direct current stimulation combined with voluntary grip exercise. *Neurosci. Lett.* 548, 181–184. doi: 10.1016/j.neulet.2013.05.037

Klomjai, W., Aneksan, B., Pheungphrarattanatrai, A., Chantanachai, T., Choowong, N., Bunleukhet, S., et al. (2018). Effect of single-session dual-tDCS before physical therapy on lower-limb performance in sub-acute stroke patients: a randomized sham-controlled crossover study. *Ann. Phys. Rehabil. Med.* 61, 286–291. doi: 10.1016/j.rehab.2018.04.005

Kujirai, T., Caramia, M. D., Rothwell, J. C., Day, B. L., Thompson, P. D., Ferbert, A., et al. (1993). Corticocortical inhibition in human motor cortex. *J. Physiol.* 471, 501–519. doi: 10.1113/jphysiol.1993.sp019912

Laakso, I., and Hirata, A. (2012). Fast multigrid-based computation of the induced electric field for transcranial magnetic stimulation. *Phys. Med. Biol.* 57, 7753–7765. doi: 10.1088/0031-9155/57/23/7753

Laakso, I., Mikkonen, M., Koyama, S., Hirata, A., and Tanaka, S. (2019). Can electric fields explain inter-individual variability in transcranial direct current stimulation of the motor cortex? *Sci. Rep.* 9:626. doi: 10.1038/s41598-018-37226-x

Laakso, I., Tanaka, S., Koyama, S., De Santis, V., and Hirata, A. (2015). Inter-subject variability in electric fields of motor cortical tDCS. *Brain Stimul.* 8, 906–913. doi: 10.1016/j.brs.2015.05.002

Laakso, I., Tanaka, S., Mikkonen, M., Koyama, S., Sadato, N., and Hirata, A. (2016). Electric fields of motor and frontal tDCS in a standard brain space: a computer simulation study. *NeuroImage* 137, 140–151. doi: 10.1016/j.neuroimage.2016.05.032

Liu, A., Vöröslakos, M., Kronberg, G., Henin, S., Krause, M. R., Huang, Y., et al. (2018). Immediate neurophysiological effects of transcranial electrical stimulation. *Nat. Commun.* 9:5092. doi: 10.1038/s41467-018-07233-7

López-Alonso, V., Cheeran, B., Río-Rodríguez, D., and Fernández-Del-Olmo, M. (2014). Inter-individual variability in response to non-invasive brain stimulation paradigms. *Brain Stimul.* 7, 372–380. doi: 10.1016/j.brs.2014.02.004

López-Alonso, V., Fernández-Del-Olmo, M., Costantini, A., Gonzalez-Henriquez, J. J., and Cheeran, B. (2015). Intra-individual variability in the response to anodal transcranial direct current stimulation. *Clin. Neurophysiol.* 126, 2342–2347. doi: 10.1016/j.clinph.2015.03.022

Madhavan, S., Weber, K. A., and Stinear, J. W. (2011). Non-invasive brain stimulation enhances fine motor control of the hemiparetic ankle: implications for rehabilitation. *Exp. Brain Res.* 209, 9–17. doi: 10.1007/s00221-010-2511-0

Maeda, K., Yamaguchi, T., Tatemoto, T., Kondo, K., Otaka, Y., and Tanaka, S. (2017). Transcranial direct current stimulation does not affect lower extremity muscle strength training in healthy individuals: a triple-blind Sham-Controlled Study. *Front. Neurosci.* 11:179. doi: 10.3389/fnins.2017.00179

Manji, A., Amimoto, K., Matsuda, T., Wada, Y., Inaba, A., and Ko, S. (2018). Effects of transcranial direct current stimulation over the supplementary motor area body weight-supported treadmill gait training in hemiparetic patients after stroke. *Neurosci. Lett.* 662, 302–305. doi: 10.1016/j.neulet.2017.10.049

Marcos-Frutos, D., López-Alonso, V., Mera-González, I., Sánchez-Molina, J. A., Colomer-Poveda, D., and Márquez, G. (2023). Chronic functional adaptations induced by the application of transcranial direct current stimulation combined with exercise programs: a systematic review of randomized controlled trials. *J. Clin. Med.* 12:6724. doi: 10.3390/jcm12216724

McNeil, C. J., Giesebrecht, S., Gandevia, S. C., and Taylor, J. L. (2011). Behaviour of the motoneurone pool in a fatiguing submaximal contraction. *J. Physiol.* 589, 3533–3544. doi: 10.1113/jphysiol.2011.207191

McNeil, C. J., Martin, P. G., Gandevia, S. C., and Taylor, J. L. (2009). The response to paired motor cortical stimuli is abolished at a spinal level during human muscle fatigue. *J. Physiol.* 587, 5601–5612. doi: 10.1113/jphysiol.2009.180968

Mihara, M., Miyai, I., Hatakenaka, M., Kubota, K., and Sakoda, S. (2008). Role of the prefrontal cortex in human balance control. *NeuroImage* 43, 329–336. doi: 10.1016/j.neuroimage.2008.07.029

Mihara, M., Miyai, I., Hattori, N., Hatakenaka, M., Yagura, H., Kawano, T., et al. (2012). Cortical control of postural balance in patients with hemiplegic stroke. *Neuroreport* 23, 314–319. doi: 10.1097/WNR.0b013e328351757b

Mikkonen, M., Laakso, I., Tanaka, S., and Hirata, A. (2020). Cost of focality in TDCS: Interindividual variability in electric fields. *Brain Stimul.* 13, 117–124. doi: 10.1016/j.brs.2019.09.017

Montenegro, R. A., Midgley, A., Massaferri, R., Bernardes, W., Okano, A. H., and Farinatti, P. (2016). Bihemispheric motor cortex transcranial direct current stimulation improves force steadiness in post-stroke Hemiparetic patients: a randomized crossover controlled trial. *Front. Hum. Neurosci.* 10:426. doi: 10.3389/fnhum.2016.00426

Mosayebi-Samani, M., Jamil, A., Salvador, R., Ruffini, G., Haueisen, J., and Nitsche, M. A. (2021). The impact of individual electrical fields and anatomical factors on the neurophysiological outcomes of tDCS: a TMS-MEP and MRI study. *Brain Stimul.* 14, 316–326. doi: 10.1016/j.brs.2021.01.016

Muthalib, M., Kan, B., Nosaka, K., and Perrey, S. (2013). Effects of transcranial direct current stimulation of the motor cortex on prefrontal cortex activation during a neuromuscular fatigue task: an fNIRS study. *Adv. Exp. Med. Biol.* 789, 73–79. doi: 10.1007/978-1-4614-7411-1_11

Nitsche, M. A., and Paulus, W. (2000). Excitability changes induced in the human motor cortex by weak transcranial direct current stimulation. *J. Physiol.* 527, 633–639. doi: 10.1111/j.1469-7793.2000.t01-1-00633.x

Nitsche, M. A., Seeber, A., Frommann, K., Klein, C. C., Rochford, C., Nitsche, M. S., et al. (2005). Modulating parameters of excitability during and after transcranial direct current stimulation of the human motor cortex. *J. Physiol.* 568, 291–303. doi: 10.1113/jphysiol.2005.092429

Opitz, A., Paulus, W., Will, S., Antunes, A., and Thielscher, A. (2015). Determinants of the electric field during transcranial direct current stimulation. *NeuroImage* 109, 140–150. doi: 10.1016/j.neuroimage.2015.01.033

Pearson, K. (2000). Motor systems. *Curr. Opin. Neurobiol.* 10, 649–654. doi: 10.1016/s0959-4388(00)00130-6

Rawji, V., Ciocca, M., Zacharia, A., Soares, D., Truong, D., Bikson, M., et al. (2018). tDCS changes in motor excitability are specific to orientation of current flow. *Brain Stimul.* 11, 289–298. doi: 10.1016/j.brs.2017.11.001

Rossini, P. M., Burke, D., Chen, R., Cohen, L. G., Daskalakis, Z., Di Iorio, R., et al. (2015). Non-invasive electrical and magnetic stimulation of the brain, spinal cord, roots and peripheral nerves: basic principles and procedures for routine clinical and research application. An updated report from an I.F.C.N Committee. *Clin. Neurophysiol.* 126, 1071–1107. doi: 10.1016/j.clinph.2015.02.001

Sriraman, A., Oishi, T., and Madhavan, S. (2014). Timing-dependent priming effects of tDCS on ankle motor skill learning. *Brain Res.* 1581, 23–29. doi: 10.1016/j.brainres.2014.07.021

Tanaka, S., Hanakawa, T., Honda, M., and Watanabe, K. (2009). Enhancement of pinch force in the lower leg by anodal transcranial direct current stimulation. *Exp. Brain Res.* 196, 459–465. doi: 10.1007/s00221-009-1863-9

Tanaka, S., Takeda, K., Otaka, Y., Kita, K., Osu, R., Honda, M., et al. (2011). Single session of transcranial direct current stimulation transiently increases knee extensor force in patients with hemiparetic stroke. *Neurorehabil. Neural Repair* 25, 565–569. doi: 10.1177/1545968311402091

Tatemoto, T., Yamaguchi, T., Otaka, Y., Kondo, K., and Tanaka, S. (2013). Anodal transcranial direct current stimulation over the lower limb motor cortex increases the cortical excitability with Extracephalic reference electrodes. *Conv. Clin. Eng. Res. Neurorehabil.* 1:135. doi: 10.1007/978-3-642-34546-3_135

Temesi, J., Ly, S. N., and Millet, G. Y. (2017). Reliability of single- and paired-pulse transcranial magnetic stimulation for the assessment of knee extensor muscle function. *J. Neurol. Sci.* 375, 442–449. doi: 10.1016/j.jns.2017.02.037

Truong, D. Q., Magerowski, G., Blackburn, G. L., Bikson, M., and Alonso-Alonso, M. (2013). Computational modeling of transcranial direct current stimulation (tDCS) in obesity: impact of head fat and dose guidelines. *NeuroImage Clin.* 2, 759–766. doi: 10.1016/j.nicl.2013.05.011

van der Cruijsen, J., Dooren, R. F., Schouten, A. C., Oostendorp, T. F., Frens, M. A., Ribbers, G. M., et al. (2022). Addressing the inconsistent electric fields of tDCS by using patient-tailored configurations in chronic stroke: implications for treatment. *NeuroImage Clin.* 36:103178. doi: 10.1016/j.nicl.2022.103178

Vargas, V. Z., Baptista, A. F., Pereira, G. O. C., Pochini, A. C., Ejnisman, B., Santos, M. B., et al. (2018). Modulation of isometric quadriceps strength in soccer Players with transcranial direct current stimulation: a crossover study. *J. Strength Cond. Res.* 32, 1336–1341. doi: 10.1519/JSC.0000000000001985

Vitor-Costa, M., Okuno, N. M., Bortolotti, H., Bertollo, M., Boggio, P. S., Fregni, F., et al. (2015). Improving cycling performance: transcranial direct current stimulation increases time to exhaustion in cycling. *PLoS One* 10:e0144916. doi: 10.1371/journal.pone.0144916

Wang, B., Xiao, S., Yu, C., Zhou, J., and Fu, W. (2021). Effects of transcranial direct current stimulation combined with physical training on the excitability of the motor cortex, physical performance, and motor learning: a systematic review. *Front. Neurosci.* 15:648354. doi: 10.3389/fnins.2021.648354

Washabaugh, E. P., Santos, L., Claflin, E. S., and Krishnan, C. (2016). Low-level intermittent quadriceps activity during transcranial direct current stimulation facilitates knee extensor force-generating capacity. *Neuroscience* 329, 93–97. doi: 10.1016/j.neuroscience.2016.04.037

Wiethoff, S., Hamada, M., and Rothwell, J. C. (2014). Variability in response to transcranial direct current stimulation of the motor cortex. *Brain Stimul.* 7, 468–475. doi: 10.1016/j.brs.2014.02.003

Yamaguchi, T., Fujiwara, T., Tsai, Y. A., Tang, S. C., Kawakami, M., Mizuno, K., et al. (2016). The effects of anodal transcranial direct current stimulation and patterned electrical stimulation on spinal inhibitory interneurons and motor function in patients with spinal cord injury. *Exp. Brain Res.* 234, 1469–1478. doi: 10.1007/s00221-016-4561-4

Yeo, B. T., Sabuncu, M. R., Vercauteren, T., Ayache, N., Fischl, B., and Golland, P. (2010). Spherical demons: fast diffeomorphic landmark-free surface registration. *IEEE Trans. Med. Imaging* 29, 650–668. doi: 10.1109/TMI.2009.2030797

Yoon, M. J., Park, H. J., Yoo, Y. J., Oh, H. M., Im, S., Kim, T. W., et al. (2024). Electric field simulation and appropriate electrode positioning for optimized transcranial direct current stimulation of stroke patients: an in silico model. *Sci. Rep.* 14:2850. doi: 10.1038/s41598-024-52874-y

frontiers | Frontiers in Human Neuroscience

TYPE Original Research
PUBLISHED 13 December 2024
DOI 10.3389/fnhum.2024.1461417

OPEN ACCESS

EDITED BY
Samar S. Ayache,
Hôpitaux Universitaires Henri Mondor, France

REVIEWED BY
Yuhei Takado,
National Institutes for Quantum and Radiological Science and Technology (Japan), Japan
Carlos Andrés Mugruza Vassallo,
San Juan Bautista Private University, Peru

*CORRESPONDENCE
Ferdinand Binkofski
✉ fbinkofski@ukaachen.de

RECEIVED 08 July 2024
ACCEPTED 02 December 2024
PUBLISHED 13 December 2024

CITATION
Patel HJ, Stollberg L-S, Choi C-H, Nitsche MA, Shah NJ and Binkofski F (2024) A study of long-term GABA and high-energy phosphate alterations in the primary motor cortex using anodal tDCS and $^{1}H/^{31}P$ MR spectroscopy. *Front. Hum. Neurosci.* 18:1461417. doi: 10.3389/fnhum.2024.1461417

A study of long-term GABA and high-energy phosphate alterations in the primary motor cortex using anodal tDCS and $^{1}H/^{31}P$ MR spectroscopy

Harshal Jayeshkumar Patel[1], Lea-Sophie Stollberg[1], Chang-Hoon Choi[2], Michael A. Nitsche[3], N. Jon Shah[2,4,5,6] and Ferdinand Binkofski[1,2,4]*

[1]Division of Clinical Cognitive Sciences, Department of Neurology, RWTH Aachen University Hospital, Aachen, Germany, [2]Institute of Neuroscience and Medicine-4, Forschungszentrum Jülich GmbH, Jülich, Germany, [3]Leibniz Research Centre for Working Environment and Human Factors, Department of Psychology and Neurosciences, Dortmund, Germany, [4]JARA-BRAIN-Translational Medicine, Jülich-Aachen-Research-Alliance (JARA), Aachen, Germany, [5]Department of Neurology, RWTH Aachen University Hospital, Aachen, Germany, [6]Institute of Neuroscience and Medicine-11, Forschungszentrum Juelich, Jülich, Germany

Introduction: Anodal transcranial direct current stimulation (tDCS) has been reported to modulate gamma-aminobutyric acid levels and cerebral energy consumption in the brain. This study aims to investigate long-term GABA and cerebral energy modulation following anodal tDCS over the primary motor cortex.

Method: To assess GABA and energy level changes, proton and phosphorus magnetic resonance spectroscopy data were acquired before and after anodal or sham tDCS. In anodal stimulation, a 1 mA current was applied for 20 min, and the duration of ramping the current up/down at the start and end of the intervention was 10 s. In the sham-stimulation condition, the current was first ramped up over a period of 10 s, then immediately ramped down, and the condition was maintained for the next 20 min.

Results: The GABA concentration increased significantly following anodal stimulation in the first and second post-stimulation measurements. Likewise, both ATP/Pi and PCr/Pi ratios increased after anodal stimulation in the first and second post-stimulation measurements.

Conclusion: The approach employed in this study shows the feasibility of measuring long-term modulation of GABA and high-energy phosphates following anodal tDCS targeting the left M1, offering valuable insights into the mechanisms of neuroplasticity and energy metabolism, which may have implications for applications of this intervention in clinical populations.

KEYWORDS

tDCS, GABA, ^{31}PMRS , ^{1}HMRS, primary motor cortex, neuroplasticity, energy metabolism

Introduction

Several studies have demonstrated molecular and neurophysiological evidence linking altered neuronal plasticity to neurological disorders (Di Lazzaro et al., 2010) and altered energy metabolism to metabolic disorders (Soares et al., 2011) in brain areas. It has been suggested that metabolic disorders are associated with neurological disorders (Crabtree and Gogos, 2014; Penninx and Lange, 2018). For instance, abnormal neuroplasticity mediated by altered neurotransmission (Harrison, 1999) has been observed in the prefrontal cortex in schizophrenia patients (Hulshoff Pol and Kahn, 2008). One suggested explanation is that hypofunction of the NMDA-type glutamate receptor cause a decrease in the excitation of GABAergic interneurons, resulting in glutamatergic neurons disinhibition (Kondziella et al., 2007; Moghaddam et al., 1997; Olney et al., 1999; Stone et al., 2009). This disinhibition of glutamatergic neurons may result in excessive glutamate stimulation, which may cause neuronal damage or death via excitotoxicity leading to a hyperdopaminergic state and psychosis. In an EEG study comparing healthy subjects with schizophrenia, variation in the P3a distribution was found which shows differences in the attention system activity (Mugruza-Vassallo and Potter, 2019). Functional imaging studies that assess regional cerebral blood flow (rCBF) can help identify cerebral activity associated with schizophrenia (Tamminga, 1999). For example, Liddle et al. (1992a) and Liddle et al. (1992b) found a negative correlation between the psychomotor poverty symptoms of schizophrenia and rCBF in the lateral prefrontal cortex and overactivity in the striatum.

Pharmacological studies have discovered genes involved in the pathophysiology of schizophrenia (De Jong et al., 2016; Gaspar and Breen, 2017; Rodriguez-Lopez et al., 2020; Ruby et al., 2014), such as GRM3 expression in astrocytic cells, which is required to protect neurons against NMDA induced neurotoxicity (Hikmah et al., 2023). This suggests that diminished GRM3 functionality, which may result in hyper-glutamatergic signalling, may cause more damage to the neurons as a result of the abnormal signaling exhibited in schizophrenia (Saini et al., 2017). In schizoaffective disorder, both schizophrenic and affective occur at the same time (Werner and Covenas, 2016). The mesolimbic system (the hippocampus and prefrontal cortex) plays an important role in the symptoms, which involves alteration in a multi-neurotransmitter system such as dopamine, serotonin, GABA and glutamate (Kulkarni et al., 2022) due to susceptibility genes such as neuregulin-1 dysbindin-1, GAD67 catechol-O-methyl transferase and monoamine oxidase (Haller et al., 2014; Ruby et al., 2014; Werner and Coveñas, 2013).

Several studies using magnetic resonance spectroscopy (MRS) have indicated that major depressive disorder (MDD) individuals have lower GABA concentrations in occipital cortex than healthy controls (Sanacora et al., 2004; Sanacora et al., 1999; Sanacora et al., 2003). MDD, along with GABA, is also related to altered serotonin activity. In many research studies, the binding potential of serotonin receptor, 5-hydroxytryptamine or (5-HT) was found to be lower in patients with MDD than in control subjects (Bhagwagar et al., 2004; Drevets et al., 1999; Hirvonen et al., 2008; Sargent et al., 2000). Selective serotonin reuptake inhibitors (SSRI) are most widely used to treat MDD and have shown significant change in the dorsolateral prefrontal cortex (DLPFC) volume and resting-state functionality (Lee et al., 2023).

Altered neurotransmission as seen in MDD is multifaceted and has been associated with the risk of developing severe medical disorders. i.e. it increases the risk of cardiovascular disorders by 1.5–2 fold (Van der Kooy et al., 2007) for stroke 1.8 fold (Ramasubbu and Patten, 2003) for Alzheimer's disease by 2.1 fold (Green et al., 2003) and diabetes by 60% (Mezuk et al., 2008). The relationship between metabolic disorder and other psychiatric disorders is evident in the above-mentioned studies. Moreover psychiatric disorders are often accompanied by cognitive impairment in various domains, such as attention, executive functions, memory, and processing speed, as highlighted in studies (Grundman et al., 2004; McIntyre et al., 2015; Millan et al., 2012; Reichenberg, 2010). GABA neurotransmitter plays an important role in cognition and several studies have shown a link between dorsolateral prefrontal cortex GABA to working memory (Duncan et al., 2014; Yoon et al., 2016) and supplementary motor area GABA levels to motor distraction (Duncan et al., 2014; Mullins et al., 2014) and to alterations in cognitive processing with age (Harris et al., 2017; Porges et al., 2017). The interaction between altered neuroplasticity and metabolism has implications on cognitive functions or impairment. Therefore, simultaneously studying the neurochemical mechanisms behind neuronal plasticity and energy metabolism may offer significant breakthroughs for therapeutic interventions. With the advanced assessment of high-energy phosphate and neurotransmitters like gamma amino butyric acid (GABA) we can get a deeper insight into the mechanism of such changes in the brain of patients suffering from psychiatric and metabolic disorders.

A well-established approach for modulating neuronal plasticity and energy in humans is a non-invasive brain stimulation technique known as transcranial direct current stimulation (tDCS). By targeting specific brain regions, tDCS can be used to modulate brain energy metabolism and neuronal plasticity. Human *in vivo* studies have demonstrated that the application of anodal tDCS in the primary motor cortex can lead to spontaneous firing rates of cortical neurons, inducing neuronal excitation and altering energy consumption (Binkofski et al., 2011; Nitsche and Paulus, 2000). This modulation in excitability and energy is likely mediated by an altered concentration of the inhibitory neurotransmitter GABA (Stagg et al., 2009) and high-energy phosphates, e.g., adenosine triphosphate (ATP) and phosphocreatine (PCr).

Owing to ongoing advancements in magnetic resonance (MR) techniques (Choi et al., 2021; Henning, 2018; Wilson et al., 2019), changes in GABA and high-energy phosphates in M1 following tDCS can be monitored using MR spectroscopy (MRS). Specifically, it has been shown that proton (^{1}H)-MRS (Patel et al., 2019) and phosphorus (^{31}P)-MRS can be used to measure changes in GABA and energy phosphates in the M1, for example, following anodal tDCS as compared to sham tDCS. The time courses of separately measured concentrations of GABA and ATP/PCr in the aforementioned studies indicated that GABAergic activity and bioenergetics inside the M1 might work together to modulate neuronal excitability and energy. Consecutive measurement of both ^{1}H- and ^{31}P-MRS, before and after tDCS, could offer a promising approach to yield information related to plastic adaptation and energy consumption in both healthy and diseased brains.

In this study, we hypothesize that the application of anodal tDCS to the M1 region modulates GABA concentration and brain energy consumption. Notably, this work presents a measurement approach

that integrates one pre-tDCS, ^{1}H- and ^{31}P-MRS measurement and two consecutive post-anodal tDCS, ^{1}H- and ^{31}P-MRS measurements to demonstrate the viability of using MRI and MRS to measure the long-term modulation of GABA and high-energy phosphates following anodal tDCS targeting the left M1 for the first time.

Materials and methods

Forty-four healthy subjects (22 anodal and 22 sham) with no history of neurological or psychiatric diseases were recruited for this single-blind, randomized control pilot study. The subjects (Mean age: 28 ± 7; Gender: 26 Female and 18 Male) were all right-handed, as evaluated by the Edinburgh Handedness Inventory (Oldfield, 1971). All examinations were conducted at the Division of Clinical Cognitive Sciences of the RWTH Aachen University, Germany, and subjects provided their written informed consent for participation in this pilot study, which was agreed upon by the local ethics committee.

The non-invasive DC-Stimulator (neuroConn GmbH, Germany) used to stimulate the M1 region was programmed to deliver constant, direct current to the brain via two rubber electrodes (5 × 7 cm) covered by saline-soaked (0.9% NaCl) sponges, which modulate brain activity. One electrode was centered over the left M1 (5 cm lateral to Cz, C3) and the other over the contralateral supraorbital ridge using the conventional EEG 10/20 system. To accomplish the electrical contact between the electrodes and the scalp, 0.9% NaCl solution was used as a conducting medium. In anodal stimulation, a 1 mA current was applied for 20 min, and the duration of ramping the current up/down at the start and end of the intervention was 10 s. In the sham-stimulation condition, the current was first ramped up over a period of 10 s, then immediately ramped down, and the condition was maintained for the next 20 min.

All MR measurements were carried out on a 3 T PRISMA MRI scanner (Siemens Healthineers, Erlangen, Germany) with a dockable patient bed. A quadrature double-tuned head coil (RAPID Biomedical, Wuerzburg, Germany) was used to achieve both ^{1}H and ^{31}P acquisitions. Figure 1 shows a tabular representation of the overall experimental design. Each experimental session started with a localizer followed by the acquisition of whole-brain anatomical images using an MP-RAGE MRI sequence [parameters: voxel size = 1.5 × 1.5 × 1.5 mm^3, repetition time (TR) = 2,000 ms, echo time (TE) = 2.05 ms, inversion time (TI) = 900 ms, acquisition time (TA) = 4:32 min], with RF power and global static magnetic field (B_0) shimming calibrations. Figure 2 shows the 3D anatomical image used to locate a 30 × 30 × 30 mm^3 voxel-of-interest (VOI) within the hand-knob area of the left M1. Prior to the MRS measurements, an additional advanced shimming procedure was employed using a FASTEST map MRS sequence (Gruetter and Tkáč, 2000) to improve the B_0 homogeneity in the selected VOI. A full-width at half-maximum (FWHM) of the ^{1}H resonance peak in the VOI was achieved at approximately 15 Hz. A MEGA-PRESS MRS sequence (Mescher et al., 1998; parameters: voxel size = 30 × 30 × 30 mm^3, TR = 5,350 ms, TE = 68 ms, TA =17:53 min, averages = 96, vector size = 1,024, flip angle = 90°) and a 3D chemical shift imaging MRS sequence (Wenger et al., 2020; parameters: voxel size = 30 × 30 × 30 mm^3, TR = 3,730 ms, TE = 2.3 ms, TA = 14:33 min, averages = 6, vector size = 1,024, flip angle = 90°) were applied to acquire ^{1}H-GABA and ^{31}P spectra, respectively. A standard PRESS MRI sequence with eight averages was also included to record an unedited spectrum for the assessment of the creatine and N-acetylaspartate acid (NAA) linewidths. The nuclear Overhauser effect enhancement technique was employed to improve the quality of the spectra in the ^{31}P acquisition. Reference ^{1}H and ^{31}P spectra as shown in Figure 3 were attained before the application of tDCS (pre-stimulation measurements), which took approximately 35 min. After obtaining the baseline MRS scans, the whole patient table, including the subject and the coil, was undocked from the scanner and moved outside the magnet room for stimulation. The stimulation was delivered for 20 min, during which participants were asked to remain still. Following the stimulation, the patient table was docked back to the MR scanner for the subsequent measurements. Undocking and docking of the table procedure helped to mitigate subject movement between the pre- and post-stimulation MRS measurements. The same MP-RAGE MRI sequence was used post-stimulation to ensure that the location of the VOI was identical to the pre-stimulation position. Two consecutive post-stimulation ^{1}H and ^{31}P MRS measurements were conducted. The ^{1}H MRS measurement was conducted for 17:53 min, and then ^{31}P MRS was conducted for 14:33 min twice, in a constant order post-stimulation. All subjects were informed about the duration of the measurement and were asked to remain awake and not to move during the whole experimental procedure.

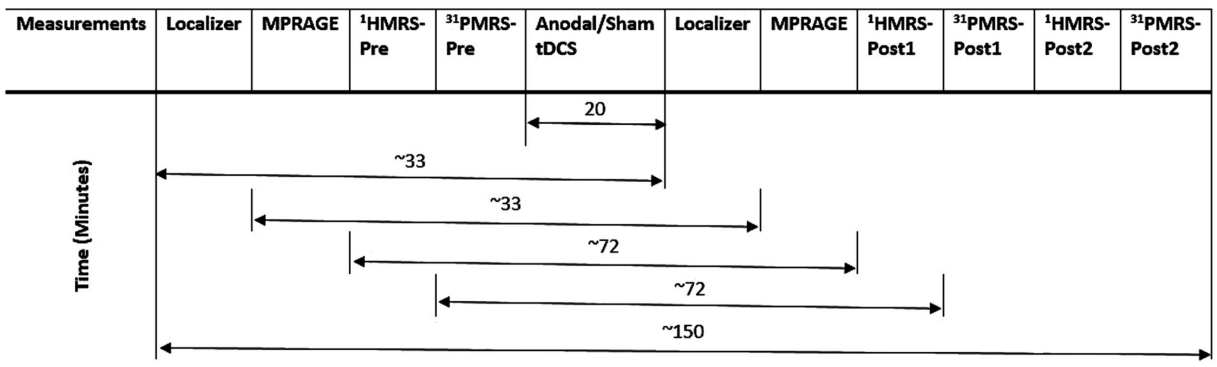

FIGURE 1
The table shows the ^{1}H GABA, ^{31}P MRS and other MR measurements performed before and after tDCS.

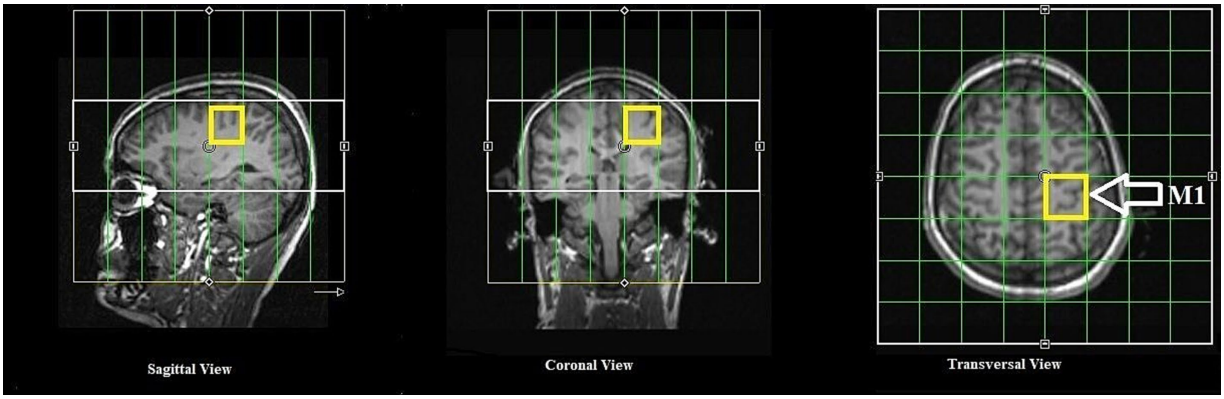

FIGURE 2
Anatomical MR images in axial, coronal and sagittal slices and the overlaid voxel of interest (in yellow) for ^{1}H and ^{31}P MRS.

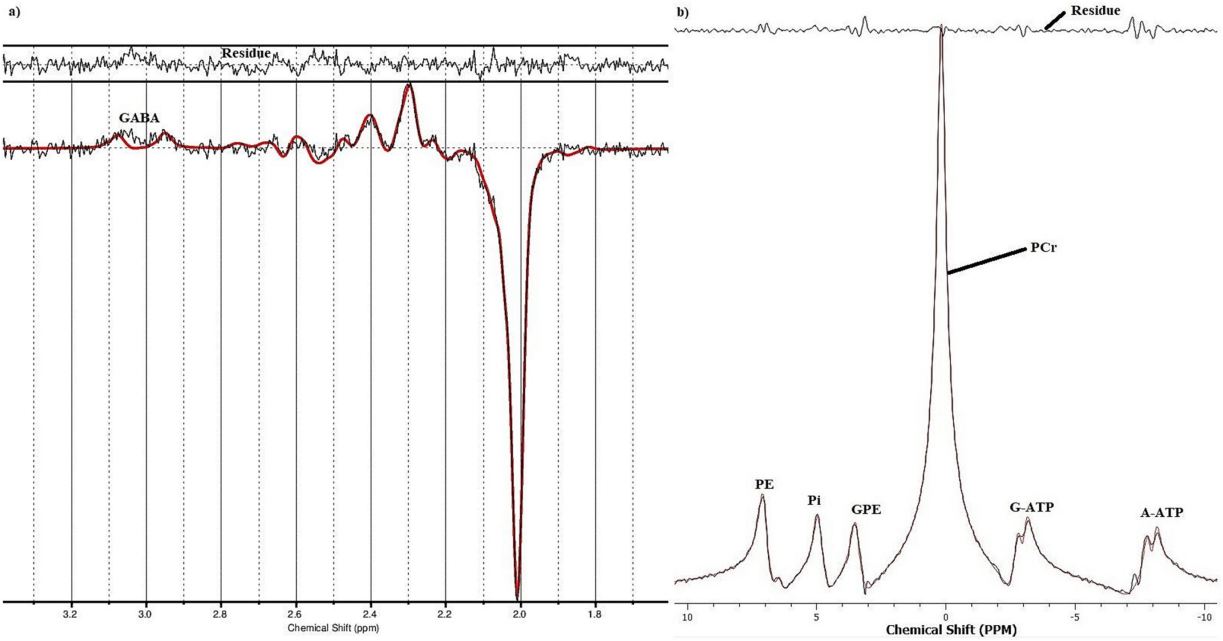

FIGURE 3
An example of a fitted **(A)** 1H GABA and **(B)** 31P spectrum from a healthy subject.

All ^{1}H-GABA-MRS data processing was performed using the LCModel (Provencher, 1993), a spectral quantification tool that fits each spectrum as a weighted linear combination of basis spectra from individual brain metabolites. The difference basis set included GABA, Glu, glutamine, glutathione, and NAA. Based on an 8 × 8 CSI grid, the ^{31}P MR spectra from one voxel were analyzed with TARQUIN 4.3.10(Wilson et al., 2011). All data underwent a Fourier transformation, as well as zero and first-order phase correction, and were fitted as linear combinations of the simulated metabolic basis set, including PCr, ATP, Pi, PE, GPC and GPE for ^{31}P-MRS. While PCr, Pi, PE, GPC and GPE are observed as singlet Lorentzian peaks, the signals from the α- and γ-ATP were modelled as doublets. However, the signal from ATP-ß was excluded from the analysis due to phasing instabilities (Novak et al., 2014). The quality of the final spectra was assessed using the Cramér-Rao-Lower-Bounds (Rao, 1947) minimum possible variance on a fit parameter. Only data that had Cramér-Rao-Lower-Bounds values of less than ≤20% were included in the analysis (Kreis, 2016; Öz et al., 2014; Peek et al., 2023; Wilson et al., 2019).

Statistical analysis

In order to investigate the effects of tDCS on the inhibitory neurotransmitter and energy metabolites in the left M1, changes in proton and phosphorus metabolites in pre- and post-stimulation scans were calculated separately to obtain the information about GABA, ATP/Pi and PCr/Pi. Each ratio was normalized (post1-tDCS/pre-tDCS & post2-tDCS/pre-tDCS) with its reference measurement (pre-tDCS). Statistical analysis was conducted with SPSS (version 29.0 Armonk, NY, USA), with $p = 0.05$ set as the significance threshold. A

mixed-design Analysis of variance was performed for GABA concentration, ATP/Pi and PCr/Pi metabolites. Stimulation (sham vs. anodal) was considered as the between-subjects factor, and measurement (three measurements: one pre-stimulation and two post-stimulation measurements [post1 and post2]) was considered as the within-subject factor. Paired sample t-test comparisons ($p > 0.05$) were performed in the cases of significant ANOVA results.

Results

Effect of tDCS on GABA

For GABA, the main effect of the stimulation was found to be significant [$F_{(1, 42)} = 4.742$, $p = 0.035$]; however, the main effect of the measurement was not significant [$F_{(2, 84)} = 2.855$, $p = 0.063$]. That being said, the stimulation × measurement interaction was significant [$F_{(2,84)} = 3.387$, $p = 0.038$]. Paired sample *t*-test comparisons show that concentration did not change significantly from pre-tDCS measurement to post1- and post2-tDCS measurements [$ts_{(21)} \leq 0.277$ $ps > 0.05$] for the sham group. Conversely, relative to the pre-tDCS, GABA concentration in the anodal tDCS group significantly increased after 14 min at the post1-tDCS measurement [$ts_{(21)} = 3.380$ $p = 0.001$], and also after 48 min at the post2-tDCS measurement [$ts_{(21)} = 1.893$ $p = 0.036$]. Thus, in the sham group, GABA concentration stayed at the pre-tDCS baseline level across all post-tDCS measurements. In contrast, data from the anodal group suggest an increase in GABA concentration across the two time points in the post-tDCS phase. Figure 4A shows the changes in normalized GABA concentration levels induced by tDCS at pre-tDCS, post1-tDCS and post2-tDCS spectroscopy measurements.

Effect of tDCS on energy phosphates (ATP/pi & PCr/pi)

For ATP/Pi ratios, neither the main effect of stimulation [$F_{(1,42)} = 1.573$, $p = 0.217$] nor the main effect of the measurement [$F_{(2,84)} = 0.259$, $p = 0.772$] was significant. Furthermore, the interaction stimulation × measurement was also not significant [$F_{(2,84)} = 0.887$, $p = 0.416$]. Figure 4B shows changes in normalized ATP/Pi ratios for pre-tDCS, post1-tDCS and post2-tDCS spectroscopy measurements. For PCr/Pi ratios, neither the main effect of stimulation [$F_{(1,42)} = 0.218$, $p = 0.643$] nor the main effect of the measurement [$F_{(2,84)} = 0.045$, $p = 0.956$] was significant. Additionally, the interaction stimulation × measurement was also not shown to be significant [$F_{(2,84)} = 852$, $p = 0.430$]. Figure 4C shows tDCS-induced effects on normalized PCr/Pi ratios for pre-tDCS, post1-tDCS and post2-tDCS spectroscopy measurements.

Discussion

The human brain functions as a dynamic system, continually adjusting its metabolic interactions to accommodate the activation status and energy requirements of the entire organism. Therefore, static MRS measurements obtained in single sessions necessarily deliver an incomplete picture of the state of the brain. To address this limitation, our feasibility study demonstrates the acquisition of combined measurements using ^{1}H-GABA-MRS, ^{31}P-MRS and anodal stimulation to provide unique information relating to adaptive plasticity and energy consumption in the human brain during extended time periods after plasticity-inducing brain stimulation.

Our results indicate a notable increase in GABA levels measured by ^{1}H-MRS following 20 min of anodal stimulation over the M1 at both the initial post-tDCS measurement and the second post-tDCS measurement, which contradicts previous reports showing a reduction in GABA levels at these time points (Agboada et al., 2019; Patel et al., 2019). Studies have shown that changes in cortical excitability due to tDCS are calcium-dependent (Grundey et al., 2018; Nitsche et al., 2003) and that calcium concentration within a specific range is required for LTP induction (Lisman, 2001). Therefore, it could be argued that previous studies (Patel et al., 2019; Stagg et al., 2009) utilizing relatively low tDCS intensities and/or short durations might have been operating at the lower limit of the calcium concentrations required for inducing the aforementioned neuroplastic changes. Within the range given in Lisman (2001), increasing calcium concentration should, theoretically, increase the efficacy of LTP induction. Hence, prolonging the duration of stimulation beyond a critical time point may lead to a saturation of the after-effects, possibly caused by calcium overflow (Monte-Silva et al., 2013). Consequently, higher calcium concentration might activate counteracting homeostatic mechanisms, such as the activation of potassium channels or the saturation of NMDA receptors, thereby limiting the amount of plasticity (An et al., 2000; Lau and Zukin, 2007; Misonou et al., 2004). These potential mechanisms require further exploration. To the best of our knowledge, there are very few studies investigating the mechanism underlying these non-linear effects (Batsikadze et al., 2013; Jamil et al., 2017; Monte-Silva et al., 2013). In line with this notion, studies using different non-invasive brain stimulation techniques have also reported non-linear cortical excitability effects post-tDCS (Batsikadze et al., 2013; Kuo et al., 2013) with respect to varying intensity (Moliadze et al., 2012) and duration (Choi et al., 2021; Heimrath et al., 2020; Monte-Silva et al., 2013).

In an apparent contradiction to the results obtained in our study, a study from Agboada et al. (2019) reported that, having applied anodal tDCS with 1 mA current for 20 min, cortical excitation could be subsequently monitored for two hours by measuring motor evoked potentials (MEPs) using TMS. However, the reason for these opposing results might be due to a difference in the study population. Furthermore, the amount of extracellular GABA measured by MRS might not correlate with TMS-induced activity in the GABAergic synapses. As neurotransmitters are active in intracellular and extracellular space (Belelli et al., 2009; Martin and Rimvall, 1993), and MRS is not sensitive enough to differentiate between these sources, it is only possible to speculate about mechanisms that are known to change GABA concentration. Moreover, animal studies conducted by Purpura and McMurtry (1965) have shown that direct stimulation in the deep cortical layers leads to the activation of neurons through cathodal stimulation and deactivation through anodal stimulation. Hence, the longer tDCS protocol used in the present study might have more significant effects on GABAergic neurons, which are less affected under the weaker electric field induced by a shorter stimulation duration. It is also possible that longer tDCS protocols may affect the target neurons as well as neighbouring non-target neurons, which might change the direction of plasticity in the target regions.

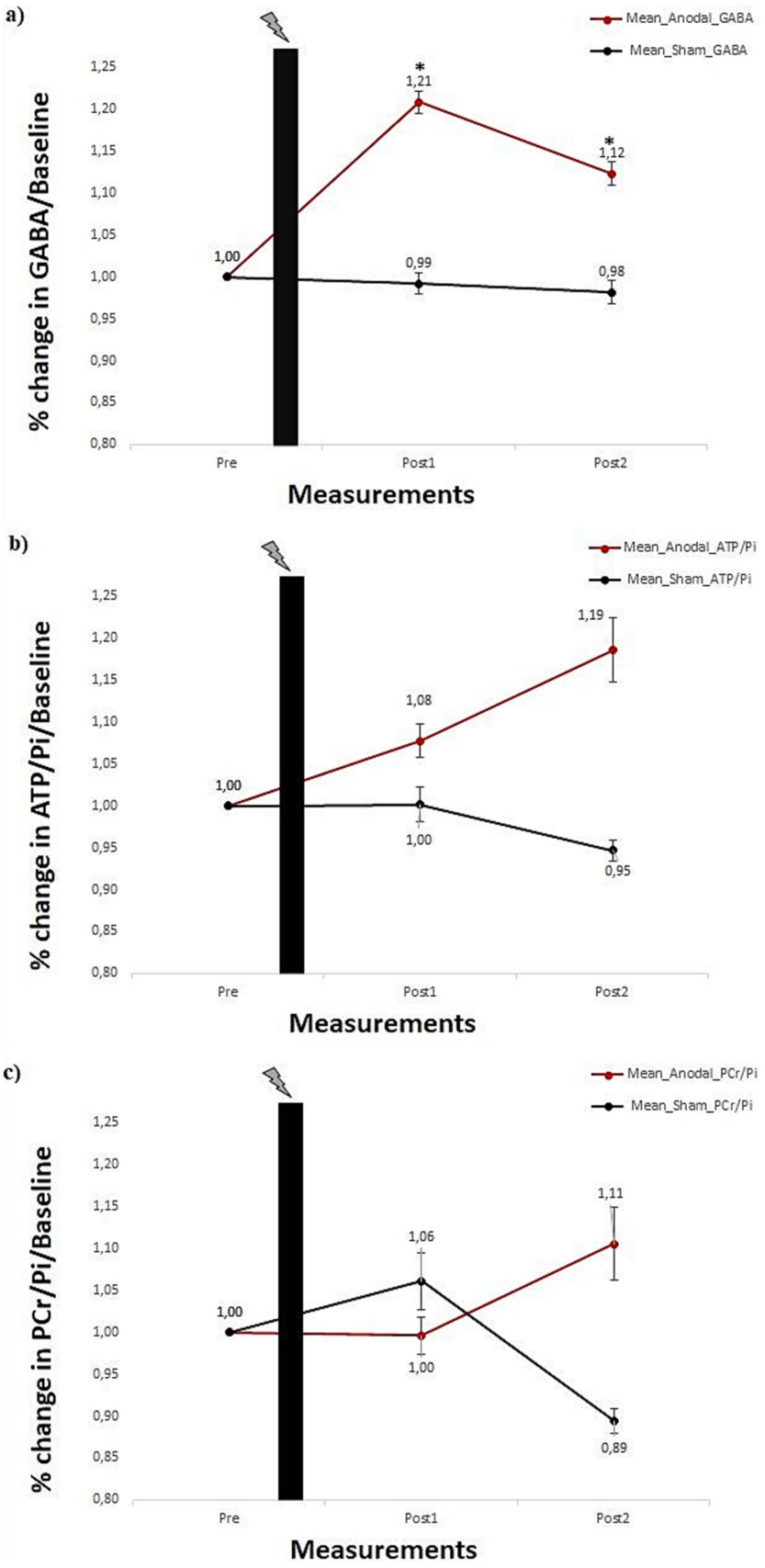

FIGURE 4
(A) Percentage change in mean GABA concentration. **(B)** ATP/Pi ratio, and **(C)** PCr/Pi ratio for anodal and sham stimulation groups, each comprising 22 subjects. Error bars reflect the standard error of the mean. Black plot: anodal/sham stimulation. *Show significances ($p < 0.05$) for a paired sample *t*-test.

The levels of MRS GABA have been linked to behavioural measures in M1, where higher GABA levels were associated with greater inhibition and slower reaction times (Stagg et al., 2011). Changes in GABA levels in the dorsolateral prefrontal cortex (DLPFC) have also been observed in studies on impulsivity, a personality trait associated with various psychiatric disorders in the DSM. Studies have indicated that higher GABA levels in the DLPFC are linked to lower urgency scores, suggesting a role in self-control for the GABA-mediated inhibitory mechanism (Boy et al., 2011). Additionally, research by Kühn et al. (2016) and Yoon et al. (2016) demonstrated that higher GABA levels in the DLPFC and anterior cingulate cortex (Rossini et al., 1994) are associated with less performance degradation under higher working memory load compared to subjects with lower GABA levels. Furthermore, elevated GABA levels in the visual cortex have been associated with improved cognitive and perceptual performance in visual discrimination tasks (Cook et al., 2016; Edden et al., 2009; Porges et al., 2017; Sumner et al., 2010). van Vugt et al. (2020) investigated the influence of GABA modulation on audio perception discrimination and mapping motor responses with perceived sounds. Elevated GABA levels in the left sensorimotor cortex (SM1) during training were associated with enhanced behavioural learning, highlighting the role of GABA modulation in forming unique audio-motor learning tasks. The elevated GABA levels in the ACC during situations involving conflict or uncertainty (Bezalel et al., 2019) contribute to decision-making by maintaining inhibition and preventing excessive excitement. A further study investigated the relationship between GABA levels within the sensorimotor cortex and measures of sensory discrimination and demonstrated that healthy subjects who had higher GABA levels showed greater frequency discrimination (Puts et al., 2011). Higher GABA levels were associated with improved performance in orientation discrimination task as seen in studies of the primary visual cortex (Edden et al., 2009). Similar relationships between a variety of task-specific behaviours and levels of GABAergic inhibition have also been demonstrated in a number of brain regions outside the sensorimotor cortex (Boy et al., 2010; Boy et al., 2011; Jocham et al., 2012; Sumner et al., 2010). This implies that MRS-derived measurements of GABA are behaviorally relevant in a variety of cortical areas, and not limited to M1.GABA modulation is not exclusive to learning and has been observed in memory consolidation as well. For an increase in GABA levels in the occipital lobes following a visual learning task helps in fast memory consolidation and protects against interference (Shibata et al., 2017). The use of Zolpidem, a GABAA agonist, during sleep has been shown to enhance episodic memories, indicating the role of GABA in memory consolidation. The Increased GABA activity during sleep supports memory consolidation (Mednick et al., 2013; Zhang et al., 2020).

Coxon and colleagues discovered that engaging in high-intensity interval exercise resulted in elevated GABA levels in SM1 (Coxon et al., 2018). In a study by Maddock, it was demonstrated that vigorous cycling increased GABA/Cr levels in the primary visual cortex post-exercise (Maddock et al., 2016). This suggests that physical exercise influences regional GABA levels beyond SM1, but the regional specificity of GABA changes due to exercise require further investigation.

It has been well reported that GABA and Glu interact along the same biochemical pathway, as Glu is the primary precursor for GABA synthesis (Petroff, 2002; Rae et al., 2003). Given that GABA is synthesized from the alpha decarboxylation of Glu by glutamic acid decarboxylase (GAD-67), the activity-driven expression of GAD-67 controls GABA synthesis and determines the concentration of GABA in interneurons (Lau and Murthy, 2012). It is possible that anodal tDCS may subtly interfere with GAD-67 activity and consequently affect this pathway, resulting in a change in the GABA concentration. However, we were only able to access the Glx information at 3 T, which combined glutamate and glutamine signals due to their close chemical shift range. A study, for example, using 7 T MRI, might help to investigate long-term glutamate modulation and allow further exploration of the mechanism of excitatory glutamatergic neurons in long-term plasticity.

The observed increase in ATP/Pi and PCr/Pi ratios shown in our study can be partially compared to findings from Binkofski et al. (2011), who reported their first non-significant post-tDCS measurement between the end of tDCS and before around 65th minute of MRS measurement, thus also showing an initial rise in energy followed by a subsequent decline after the 65th minute. The increase in ATP/Pi ratio and PCr/Pi ratio in our study could be attributed to a higher rate of energy phosphate synthesis compared to its consumption as a consequence of the longer tDCS duration. ATP concentration has been observed as a potential modulator of neurotransmission (Miller et al., 1980; Miller et al., 1977), and the neurotransmitter glutamate is a known precursor of GABA synthesis and uses glutamic acid decarboxylase (GAD) to synthesize GABA. At least 50% of GAD is present in the brain as apoenzyme (apoGAD), thereby providing a reservoir of inactive GAD that can be drawn on when additional GABA synthesis is required (Itoh and Uchimura, 1981; Miller et al., 1980; Miller et al., 1977). It seems that GAD plays an important role in regulating the transmitter pool of GABA. Studies indicate that the increase in the ATP/Pi ratio accelerates the formation of apoGAD (Meeley and Martin, 1983; Wu and Martin, 1984), inhibits its activation (Porter and Martin, 1988; Sze et al., 1983) and stabilizes apoGAD against thermal denaturation (Meeley and Martin, 1983; Porter and Martin, 1988). It appears that the activation of GAD is regulated by energy metabolism, and increased neural activity leads to a higher turnover of energy metabolites. Moreover, it is plausible that these energy metabolites play a vital role in linking GAD activity with neuronal activity. Thus, it is plausible that elevated levels of ATP might stimulate the activation of apoGAD, thereby promoting GABA synthesis.

GABA appears to have two major functions in nervous tissue, acting both as a neurotransmitter and as an intermediate in the energy metabolism of GABAergic neurons (Shelp et al., 2012). While much attention is given to the role of GABA as a neurotransmitter, its role as a metabolic intermediate is also important and may help to explain the link between neuronal plasticity and energy metabolism. This metabolic function of GABA arises from its relationship with the tricarboxylic acid (TCA) cycle (Baxter, 1970). The TCA cycle is a series of processes that produce high-energy phosphate, such as ATP, following glycolysis. Three enzymes of GABA pathways, GAD, GABA-a-oxoglutarate transaminase and succinic semialdehyde dehydrogenase, facilitate a bypass known as the GABA shunt. This bypass allows for the circumnavigation of two steps of the TCA cycle, leading to the production of glutamate for GABA synthesis. In this way, GABA is metabolized via the GABA shunt within the TCA cycle, thus emphasizing the role of GABA synthesis in maintaining adequate GABA levels. Based on this neurochemical mechanism, it

might be possible that the longer stimulation protocol demands higher energy phosphate synthesis and also higher GABA synthesis, which may work together to regulate the higher demand for energy phosphate and the corresponding GABA synthesis in the brain. Our study demonstrates that anodal tDCS leads to an increase in ATP resynthesis to meet the energy demand, which is similar to the energy regulation observed after physical exercise (Hargreaves and Spriet, 2020). Modulation of energy following physical activity has shown to improve memory, reasoning, planning, motor skill (Nanda et al., 2013; Statton et al., 2015) and promote cognitive functioning in both healthy as well as clinical populations such as stroke, multiple sclerosis and depression (Moriarty et al., 2019; Moriya et al., 2016; Sandroff et al., 2015; Sibley et al., 2006; Vasques et al., 2011; Wang et al., 2016). Physical activity boosts brain-derived neurotrophic factor (BDNF), promoting neuroplasticity (Loprinzi and Frith, 2019), and consequently enhancing memory and learning (Piepmeier and Etnier, 2015), while also offering protection against Alzheimer's and depression (Bjornebekk et al., 2005; Erickson et al., 2011; Liu and Nusslock, 2018). Elevated BDNF levels are associated with the survival and growth of neurons (McAllister et al., 1999). Lower BDNF levels are linked to ageing and neurodegenerative diseases (Holsinger et al., 2000). These findings reveal the usefulness of physical exercise or alteration of energy regulation as shown in our study can be employed as an auxiliary tool for rehabilitation because it appears to affect the neurological system for learning and skill acquisition.

The results of this study suggest that the new combined approach introduced here has strong implications for the measurement of energy and neural plasticity in both healthy subjects and neuropsychiatric patients (Gobel et al., 2013; Jauch-Chara et al., 2015; Stagg et al., 2011; Stagg and Johansen-Berg, 2013). For instance, psychiatric and metabolic diseases have been found to be interconnected, often acting as a precursor to each other (Estrov et al., 2000; Zuccoli et al., 2017). In this context, combined ^{1}H- and ^{31}P-MRS together with anodal tDCS may represent a two-pronged approach to better understand impaired glucose metabolism and psychiatric disorders without the need for pharmacological intervention. Furthermore, this approach can be employed in numerous additional experiments aiming to optimize the described experiment from a clinical perspective. For instance, improvements in terms of shortening acquisition time and increasing the signal-to-noise ratio can be achieved at ultra-high field strengths (Pradhan et al., 2015), particularly with the use of double-tuned, multi-channel array coils (Rowland et al., 2020). Additionally, further investigation of the intensity and duration of the stimulation in order to understand the neurochemical mechanisms involved could also extend the impact of the tDCS. Apart from tDCS, future research may explore other transcranial electrical stimulation options, including transcranial alternating current stimulation (tACS), transcranial pulsed current stimulation (tPCS) or transcranial random noise stimulation (tRNS), to investigate neurochemical pathways in the brain. This feasibility study serves as a potential tool for expanding our understanding of the neurochemistry underlying energy metabolism and neuronal plasticity. Moreover, our experimental approach represents an encouraging nonpharmacological alternative to investigate altered neuronal plasticity and energy metabolism in neurological and metabolic disorders.

Limitations of the study

The current study is limited by the relatively short duration of the post-tDCS measurements, i.e., 67 min following tDCS. This narrow timeframe could be one possible reason for the absence of late significant recovery of energy phosphates. To address this shortcoming and to capture the late energy effects following tDCS, as shown in the study by Binkofski et al. (2011), future studies should aim to measure energy metabolites over a longer time. The follow-up period may not be sufficient to assess the long-term effects of tDCS. Longer-term studies are necessary to determine the durability of the observed changes and their potential implications for clinical applications. Moreover, as this feasibility study is only based on the motor cortex, it cannot be generalized to other brain regions. More studies are needed to explore other brain areas with similar quantitative and statistical investigations.

As studies using identical tDCS protocols have demonstrated different effects in healthy young adults (Alexandersen et al., 2022; Boayue et al., 2020; Willmot et al., 2024), the results obtained from this study are not one-to-one transferable to different age populations or patient groups. However, investigating inter-individual variability was not the aim of the study, and hence, subtle differences between individuals may have been concealed due to the small sample size. For future studies that aim to study inter-individual variability, a larger sample size would be useful for detecting subtle differences. One-to-one comparison with other studies is not possible due to differences in the method, material, acquisition protocols, etc. Further research is needed to investigate the relevance of calcium dynamics at deeper cortical layers and neighbouring brain regions to evaluate the effects of prolonged stimulation protocols. While we have proposed some reasonable explanations and possible molecular mechanisms underlying the aftereffects of prolonged tDCS duration, the precise neurobiological framework regarding neuroplasticity and energy metabolism remains unclear and requires further study.

Conclusion

We have demonstrated that it is possible to induce long lasting effects by anodal tDCS and measure the corresponding GABA and energy phosphate change in left primary motor cortex using proton and phosphorus magnetic resonance spectroscopy. Hence, this new approach may help to better understand the neurochemical mechanism underlying neurological and metabolic disorders.

Data availability statement

The raw data supporting the conclusions of this article will be made available by the authors, without undue reservation.

Ethics statement

The studies involving humans were approved by the Ethical committee of the Faculty of medicine, RWTH Aachen University. The studies were conducted in accordance with the local legislation and

institutional requirements. The participants provided written informed consent to participate in this study.

Author contributions

HP: Writing – original draft, Writing – review & editing, Conceptualization, Data curation, Formal analysis, Investigation, Methodology, Project administration, Software. L-SS: Data curation, Writing – review & editing. C-HC: Data curation, Resources, Writing – review & editing. MN: Writing – review & editing. NS: Resources, Supervision, Writing – review & editing. FB: Conceptualization, Methodology, Resources, Supervision, Writing – review & editing.

Funding

The author(s) declare that no financial support was received for the research, authorship, and/or publication of this article.

Acknowledgments

The authors would like to thank Edward J. Auerbach and Małgorzata Marjańska from University of Minnesota for providing the CMRR (Center for Magnetic Resonance Research) spectroscopy package to run MEGA-PRESS and FASTMAP sequence. We also thank Ms. Claire Rick for English proofreading and Ms. Elene Iordanishvili for assisting in data collection.

Conflict of interest

Michael A. Nitsche is Scientific Advisory Boards of Neuroelectrics and Precisis.

The remaining authors declare that the research was conducted in the absence of any commercial or financial relationships that could be construed as a potential conflict of interest.

The author(s) declared that they were an editorial board member of Frontiers, at the time of submission. This had no impact on the peer review process and the final decision.

Publisher's note

References

Agboada, D., Mosayebi Samani, M., Jamil, A., Kuo, M. F., and Nitsche, M. A. (2019). Expanding the parameter space of anodal transcranial direct current stimulation of the primary motor cortex. *Sci. Rep.* 9:18185. doi: 10.1038/s41598-019-54621-0

Alexandersen, A., Csifcsák, G., Groot, J., and Mittner, M. (2022). The effect of transcranial direct current stimulation on the interplay between executive control, behavioral variability and mind wandering: a registered report. *Neuroimage Rep.* 2:100109. doi: 10.1016/j.ynirp.2022.100109

An, W. F., Bowlby, M. R., Betty, M., Cao, J., Ling, H. P., Mendoza, G., et al. (2000). Modulation of A-type potassium channels by a family of calcium sensors. *Nature* 403, 553–556. doi: 10.1038/35000592

Batsikadze, G., Moliadze, V., Paulus, W., Kuo, M. F., and Nitsche, M. A. (2013). Partially non-linear stimulation intensity-dependent effects of direct current stimulation on motor cortex excitability in humans. *J. Physiol.* 591, 1987–2000. doi: 10.1113/jphysiol.2012.249730

Baxter, C. F. (1970). "The nature of γ-aminobutyric acid" in Metabolic reactions in the nervous system. ed. A. Lajtha (Boston, MA: Springer US), 289–353.

Belelli, D., Harrison, N. L., Maguire, J., Macdonald, R. L., Walker, M. C., and Cope, D. W. (2009). Extrasynaptic GABAA receptors: form, pharmacology, and function. *J. Neurosci.* 29, 12757–12763. doi: 10.1523/JNEUROSCI.3340-09.2009

Bezalel, V., Paz, R., and Tal, A. (2019). Inhibitory and excitatory mechanisms in the human cingulate-cortex support reinforcement learning: a functional proton magnetic resonance spectroscopy study. *NeuroImage* 184, 25–35. doi: 10.1016/j.neuroimage.2018.09.016

Bhagwagar, Z., Rabiner, E. A., Sargent, P. A., Grasby, P. M., and Cowen, P. J. (2004). Persistent reduction in brain serotonin1A receptor binding in recovered depressed men measured by positron emission tomography with [11C]WAY-100635. *Mol. Psychiatry* 9, 386–392. doi: 10.1038/sj.mp.4001401

Binkofski, F., Loebig, M., Jauch-Chara, K., Bergmann, S., Melchert, U. H., Scholand-Engler, H. G., et al. (2011). Brain energy consumption induced by electrical stimulation promotes systemic glucose uptake. *Biol. Psychiatry* 70, 690–695. doi: 10.1016/j.biopsych.2011.05.009

Bjornebekk, A., Mathe, A. A., and Brene, S. (2005). The antidepressant effect of running is associated with increased hippocampal cell proliferation. *Int. J. Neuropsychopharmacol.* 8, 357–368. doi: 10.1017/S1461145705005122

Boayue, N. M., Csifcsak, G., Aslaksen, P., Turi, Z., Antal, A., Groot, J., et al. (2020). Increasing propensity to mind-wander by transcranial direct current stimulation? A registered report. *Eur. J. Neurosci.* 51, 755–780. doi: 10.1111/ejn.14347

Boy, E., Evans, C. J., Edden, R. A. E., Lawrence, A. D., Singh, K. D., Husain, M., et al. (2011). Dorsolateral prefrontal gamma-aminobutyric acid in men predicts individual differences in rash impulsivity. *Biol. Psychiatry* 70, 866–872. doi: 10.1016/j.biopsych.2011.05.030

Boy, E., Evans, C. J., Edden, R. A. E., Singh, K. D., Husain, M., and Sumner, P. (2010). Individual differences in subconscious motor control predicted by GABA concentration in SMA. *Curr. Biol.* 20, 1779–1785. doi: 10.1016/j.cub.2010.09.003

Choi, C. H., Iordanishvili, E., Shah, N. J., and Binkofski, F. (2021). Magnetic resonance spectroscopy with transcranial direct current stimulation to explore the underlying biochemical and physiological mechanism of the human brain: a systematic review. *Hum. Brain Mapp.* 42, 2642–2671. doi: 10.1002/hbm.25388

Cook, E., Hammett, S. T., and Larsson, J. (2016). GABA predicts visual intelligence. *Neurosci. Lett.* 632, 50–54. doi: 10.1016/j.neulet.2016.07.053

Coxon, J. P., Cash, R. F. H., Hendrikse, J. J., Rogasch, N. C., Stavrinos, E., Suo, C., et al. (2018). GABA concentration in sensorimotor cortex following high-intensity exercise and relationship to lactate levels. *J. Physiol.* 596, 691–702. doi: 10.1113/JP274660

Crabtree, G. W., and Gogos, J. A. (2014). Synaptic plasticity, neural circuits, and the emerging role of altered short-term information processing in schizophrenia. *Front. Synaptic Neurosci.* 6:28. doi: 10.3389/fnsyn.2014.00028

De Jong, S., Vidler, L. R., Mokrab, Y., Collier, D. A., and Breen, G. (2016). Gene-set analysis based on the pharmacological profiles of drugs to identify repurposing opportunities in schizophrenia. *J. Psychopharmacol.* 30, 826–830. doi: 10.1177/0269881116653109

Di Lazzaro, V., Profice, P., Pilato, F., Capone, F., Ranieri, F., Pasqualetti, P., et al. (2010). Motor cortex plasticity predicts recovery in acute stroke. *Cereb. Cortex* 20, 1523–1528. doi: 10.1093/cercor/bhp216

Drevets, W. C., Frank, E., Price, J. C., Kupfer, D. J., Holt, D., Greer, P. J., et al. (1999). PET imaging of serotonin 1A receptor binding in depression. *Biol. Psychiatry* 46, 1375–1387. doi: 10.1016/S0006-3223(99)00189-4

Duncan, N. W., Wiebking, C., and Northoff, G. (2014). Associations of regional GABA and glutamate with intrinsic and extrinsic neural activity in humans-a review of

multimodal imaging studies. *Neurosci. Biobehav. Rev.* 47, 36–52. doi: 10.1016/j.neubiorev.2014.07.016

Edden, R. A., Muthukumaraswamy, S. D., Freeman, T. C., and Singh, K. D. (2009). Orientation discrimination performance is predicted by GABA concentration and gamma oscillation frequency in human primary visual cortex. *J. Neurosci.* 29, 15721–15726. doi: 10.1523/JNEUROSCI.4426-09.2009

Erickson, K. I., Voss, M. W., Prakash, R. S., Basak, C., Szabo, A., Chaddock, L., et al. (2011). Exercise training increases size of hippocampus and improves memory. *Proc. Natl. Acad. Sci. USA* 108, 3017–3022. doi: 10.1073/pnas.1015950108

Estrov, Y., Scaglia, F., and Bodamer, O. A. (2000). Psychiatric symptoms of inherited metabolic disease. *J. Inherit. Metab. Dis.* 23, 2–6. doi: 10.1023/A:1005685010766

Gaspar, H., and Breen, G. (2017). Drug enrichment and discovery from schizophrenia genome-wide association results: an analysis and visualisation approach. *Sci. Rep.* 7:12460. doi: 10.1038/s41598-017-12325-3

Gobel, B., Oltmanns, K. M., and Chung, M. (2013). Linking neuronal brain activity to the glucose metabolism. *Theor. Biol. Med. Model.* 10:50. doi: 10.1186/1742-4682-10-50

Green, R. C., Cupples, L. A., Kurz, A., Auerbach, S., Go, R., Sadovnick, D., et al. (2003). Depression as a risk factor for Alzheimer disease - the MIRAGE study. *Arch. Neurol.* 60, 753–759. doi: 10.1001/archneur.60.5.753

Gruetter, R., and Tkáč, I. (2000). Field mapping without reference scan using asymmetric echo-planar techniques. *Mag. Resonan. Med.* 43, 319–323. doi: 10.1002/(SICI)1522-2594(200002)43:2<319::AID-MRM22>3.0.CO;2-1

Grundey, J., Barlay, J., Batsikadze, G., Kuo, M. F., Paulus, W., and Nitsche, M. (2018). Nicotine modulates human brain plasticity via calcium-dependent mechanisms. *J. Physiol.* 596, 5429–5441. doi: 10.1113/JP276502

Grundman, M., Petersen, R. C., Ferris, S. H., Thomas, R. G., Aisen, P. S., Bennett, D. A., et al. (2004). Mild cognitive impairment can be distinguished from Alzheimer disease and normal aging for clinical trials. *Arch. Neurol.* 61, 59–66. doi: 10.1001/archneur.61.1.59

Haller, C. S., Padmanabhan, J. L., Lizano, P., Torous, J., and Keshavan, M. (2014). Recent advances in understanding schizophrenia. *F1000prime Rep.* 6:57. doi: 10.12703/P6-57

Hargreaves, M., and Spriet, L. L. (2020). Skeletal muscle energy metabolism during exercise. *Nat. Metab.* 2, 817–828. doi: 10.1038/s42255-020-0251-4

Harris, A. D., Saleh, M. G., and Edden, R. A. E. (2017). Edited H magnetic resonance spectroscopy in vivo: methods and metabolites. *Magn. Reson. Med.* 77, 1377–1389. doi: 10.1002/mrm.26619

Harrison, P. J. (1999). The neuropathology of schizophrenia - a critical review of the data and their interpretation. *Brain* 122, 593–624. doi: 10.1093/brain/122.4.593

Heimrath, K., Brechmann, A., Blobel-Luer, R., Stadler, J., Budinger, E., and Zaehle, T. (2020). Transcranial direct current stimulation (tDCS) over the auditory cortex modulates GABA and glutamate: a 7 T MR-spectroscopy study. *Sci. Rep.* 10:20111. doi: 10.1038/s41598-020-77111-0

Henning, A. (2018). Proton and multinuclear magnetic resonance spectroscopy in the human brain at ultra-high field strength: a review. *NeuroImage* 168, 181–198. doi: 10.1016/j.neuroimage.2017.07.017

Hikmah, D. N., Syarifuddin, A., Santoso, S. B., Wijayatri, R., and Hidayat, I. W. (2023). "The role of genetic mutation on schizophrenia: a basic review prior to pharmacogenomics." in Paper presented at the 4th Borobudur International Symposium on Humanities and Social Science 2022 (BIS-HSS 2022).

Hirvonen, J., Karlsson, H., Kajander, J., Lepola, A., Markkula, J., Rasi-Hakala, H., et al. (2008). Decreased brain serotonin 5-HT1A receptor availability in medication-naive patients with major depressive disorder: an in-vivo imaging study using PET and [carbonyl-11C]WAY-100635. *Int. J. Neuropsychopharmacol.* 11, 465–476. doi: 10.1017/S1461145707008140

Holsinger, R. M., Schnarr, J., Henry, P., Castelo, V. T., and Fahnestock, M. (2000). Quantitation of BDNF mRNA in human parietal cortex by competitive reverse transcription-polymerase chain reaction: decreased levels in Alzheimer's disease. *Brain Res. Mol. Brain Res.* 76, 347–354. doi: 10.1016/S0169-328X(00)00023-1

Hulshoff Pol, H. E., and Kahn, R. S. (2008). What happens after the first episode? A review of progressive brain changes in chronically ill patients with schizophrenia. *Schizophr. Bull.* 34, 354–366. doi: 10.1093/schbul/sbm168

Itoh, M., and Uchimura, H. (1981). Regional differences in cofactor saturation of glutamate decarboxylase (GAD) in discrete brain nuclei of the rat. Effect of repeated administration of haloperidol on GAD activity in the substantia nigra. *Neurochem. Res.* 6, 1283–1289. doi: 10.1007/BF00964349

Jamil, A., Batsikadze, G., Kuo, H. I., Labruna, L., Hasan, A., Paulus, W., et al. (2017). Systematic evaluation of the impact of stimulation intensity on neuroplastic after-effects induced by transcranial direct current stimulation. *J. Physiol.* 595, 1273–1288. doi: 10.1113/JP272738

Jauch-Chara, K., Binkofski, F., Loebig, M., Reetz, K., Jahn, G., Melchert, U. H., et al. (2015). Blunted brain energy consumption relates to insula atrophy and impaired glucose tolerance in obesity. *Diabetes* 64, 2082–2091. doi: 10.2337/db14-0421

Jocham, G., Hunt, L. T., Near, J., and Behrens, T. E. (2012). A mechanism for value-guided choice based on the excitation-inhibition balance in prefrontal cortex. *Nat. Neurosci.* 15, 960–961. doi: 10.1038/nn.3140

Kondziella, D., Brenner, E., Eyjolfsson, E. M., and Sonnewald, U. (2007). How do glial–neuronal interactions fit into current neurotransmitter hypotheses of schizophrenia? *Neurochem. Int.* 50, 291–301. doi: 10.1016/j.neuint.2006.09.006

Kreis, R. (2016). The trouble with quality filtering based on relative Cramér-Rao lower bounds. *Magn. Reson. Med.* 75, 15–18. doi: 10.1002/mrm.25568

Kühn, S., Schubert, F., Mekle, R., Wenger, E., Ittermann, B., Lindenberger, U., et al. (2016). Neurotransmitter changes during interference task in anterior cingulate cortex: evidence from fMRI-guided functional MRS at 3 T. *Brain Struct. Funct.* 221, 2541–2551. doi: 10.1007/s00429-015-1057-0

Kulkarni, G., Murala, S., and Bollu, P. C. (2022). History of serotonin. *Neurochem. Clin. Pract.* 25, 25–43. doi: 10.1007/978-3-031-07897-2_2

Kuo, H. I., Bikson, M., Datta, A., Minhas, P., Paulus, W., Kuo, M. F., et al. (2013). Comparing cortical plasticity induced by conventional and high-definition 4 x 1 ring tDCS: a neurophysiological study. *Brain Stimul.* 6, 644–648. doi: 10.1016/j.brs.2012.09.010

Lau, C. G., and Murthy, V. N. (2012). Activity-dependent regulation of inhibition via GAD67. *J. Neurosci.* 32, 8521–8531. doi: 10.1523/JNEUROSCI.1245-12.2012

Lau, C. G., and Zukin, R. S. (2007). NMDA receptor trafficking in synaptic plasticity and neuropsychiatric disorders. *Nat. Rev. Neurosci.* 8, 413–426. doi: 10.1038/nrn2153

Lee, K. H., Shin, J., Lee, J., Yoo, J. H., Kim, J.-W., and Brent, D. A. (2023). Measures of connectivity and dorsolateral prefrontal cortex volumes and depressive symptoms following treatment with selective serotonin reuptake inhibitors in adolescents. *JAMA Netw. Open* 6:e2327331. doi: 10.1001/jamanetworkopen.2023.27331

Liddle, P., Friston, K., Frith, C., and Frackowiak, R. (1992a). Cerebral blood flow and mental processes in schizophrenia. *J. R. Soc. Med.* 85, 224–227. doi: 10.1177/014107689208500415

Liddle, P., Friston, K., Frith, C., Hirsch, S., Jones, T., and Frackowiak, R. (1992b). Patterns of cerebral blood flow in schizophrenia. *Br. J. Psychiatry* 160, 179–186. doi: 10.1192/bjp.160.2.179

Lisman, J. E. (2001). Three Ca^{2+} levels affect plasticity differently: the LTP zone, the LTD zone and no man's land. *J. Physiol. London* 532:285. doi: 10.1111/j.1469-7793.2001.0285f.x

Liu, P. Z., and Nusslock, R. (2018). Exercise-mediated neurogenesis in the Hippocampus via BDNF. *Front. Neurosci.* 12:52. doi: 10.3389/fnins.2018.00052

Loprinzi, P. D., and Frith, E. (2019). A brief primer on the mediational role of BDNF in the exercise-memory link. *Clin. Physiol. Funct. Imaging* 39, 9–14. doi: 10.1111/cpf.12522

Maddock, R. J., Casazza, G. A., Fernandez, D. H., and Maddock, M. I. (2016). Acute modulation of cortical glutamate and GABA content by physical activity. *J. Neurosci.* 36, 2449–2457. doi: 10.1523/JNEUROSCI.3455-15.2016

Martin, D. L., and Rimvall, K. (1993). Regulation of gamma-aminobutyric acid synthesis in the brain. *J. Neurochem.* 60, 395–407. doi: 10.1111/j.1471-4159.1993.tb03165.x

McAllister, A. K., Katz, L. C., and Lo, D. C. (1999). Neurotrophins and synaptic plasticity. *Annu. Rev. Neurosci.* 22, 295–318. doi: 10.1146/annurev.neuro.22.1.295

McIntyre, R. S., Xiao, H. X., Syeda, K., Vinberg, M., Carvalho, A. F., Mansur, R. B., et al. (2015). The prevalence, measurement, and treatment of the cognitive dimension/domain in major depressive disorder. *CNS Drugs* 29, 577–589. doi: 10.1007/s40263-015-0263-x

Mednick, S. C., McDevitt, E. A., Walsh, J. K., Wamsley, E., Paulus, M., Kanady, J. C., et al. (2013). The critical role of sleep spindles in hippocampal-dependent memory: a pharmacology study. *J. Neurosci.* 33, 4494–4504. doi: 10.1523/JNEUROSCI.3127-12.2013

Meeley, M. P., and Martin, D. L. (1983). Inactivation of brain glutamate decarboxylase and the effects of adenosine 5′-triphosphate and inorganic phosphate. *Cell. Mol. Neurobiol.* 3, 39–54. doi: 10.1007/BF00734997

Mescher, M., Merkle, H., Kirsch, J., Garwood, M., and Gruetter, R. (1998). Simultaneous in vivo spectral editing and water suppression. *NMR Biomed.* 11, 266–272. doi: 10.1002/(SICI)1099-1492(199810)11:6<266::AID-NBM530>3.0.CO;2-J

Mezuk, B., Eaton, W. W., Albrecht, S., and Golden, S. H. (2008). Depression and type 2 diabetes over the lifespan: a meta-analysis. *Diabetes Care* 31, 2383–2390. doi: 10.2337/dc08-0985

Millan, M. J., Agid, Y., Brune, M., Bullmore, E. T., Carter, C. S., Clayton, N. S., et al. (2012). Cognitive dysfunction in psychiatric disorders: characteristics, causes and the quest for improved therapy. *Nat. Rev. Drug Discov.* 11, 141–168. doi: 10.1038/nrd3628

Miller, L. P., Walters, J. R., Eng, N., and Martin, D. L. (1980). Glutamate holodecarboxylase levels and the regulation of GABA synthesis. *Brain Res. Bull.* 5, 89–94. doi: 10.1016/0361-9230(80)90014-3

Miller, L. P., Walters, J. R., and Martin, D. L. (1977). Post-mortem changes implicate adenine nucleotides and pyridoxal-5′ -phosphate in regulation of brain glutamate decarboxylase. *Nature* 266, 847–848. doi: 10.1038/266847a0

Misonou, H., Mohapatra, D. P., Park, E. W., Leung, V., Zhen, D., Misonou, K., et al. (2004). Regulation of ion channel localization and phosphorylation by neuronal activity. *Nat. Neurosci.* 7, 711–718. doi: 10.1038/nn1260

Moghaddam, B., Adams, B., Verma, A., and Daly, D. (1997). Activation of glutamatergic neurotransmission by ketamine: a novel step in the pathway from NMDA receptor blockade to dopaminergic and cognitive disruptions associated with the prefrontal cortex. *J. Neurosci.* 17, 2921–2927. doi: 10.1523/JNEUROSCI.17-08-02921.1997

Moliadze, V., Atalay, D., Antal, A., and Paulus, W. (2012). Close to threshold transcranial electrical stimulation preferentially activates inhibitory networks before switching to excitation with higher intensities. *Brain Stimul.* 5, 505–511. doi: 10.1016/j.brs.2011.11.004

Monte-Silva, K., Kuo, M. F., Hessenthaler, S., Fresnoza, S., Liebetanz, D., Paulus, W., et al. (2013). Induction of late LTP-like plasticity in the human motor cortex by repeated non-invasive brain stimulation. *Brain Stimul.* 6, 424–432. doi: 10.1016/j.brs.2012.04.011

Moriarty, T., Bourbeau, K., Bellovary, B., and Zuhl, M. N. (2019). Exercise intensity influences prefrontal cortex oxygenation during cognitive testing. *Behav. Sci.* 9:83. doi: 10.3390/bs9080083

Moriya, M., Aoki, C., and Sakatani, K. (2016). "Effects of physical exercise on working memory and prefrontal cortex function in post-stroke patients." in Paper presented at the Oxygen Transport to Tissue XXXVIII.

Mugruza-Vassallo, C., and Potter, D. (2019). Context dependence signature, stimulus properties and stimulus probability as predictors of ERP amplitude variability. *Front. Hum. Neurosci.* 13:39. doi: 10.3389/fnhum.2019.00039

Mullins, P. G., McGonigle, D. J., O'Gorman, R. L., Puts, N. A., Vidyasagar, R., Evans, C. J., et al. (2014). Current practice in the use of MEGA-PRESS spectroscopy for the detection of GABA. *NeuroImage* 86, 43–52. doi: 10.1016/j.neuroimage.2012.12.004

Nanda, B., Balde, J., and Manjunatha, S. (2013). The acute effects of a single bout of moderate-intensity aerobic exercise on cognitive functions in healthy adult males. *J. Clin. Diagn. Res.* 7, 1883–1885. doi: 10.7860/JCDR/2013/5855.3341

Nitsche, M. A., Fricke, K., Henschke, U., Schlitterlau, A., Liebetanz, D., Lang, N., et al. (2003). Pharmacological modulation of cortical excitability shifts induced by transcranial direct current stimulation in humans. *J. Physiol.* 553, 293–301. doi: 10.1113/jphysiol.2003.049916

Nitsche, M. A., and Paulus, W. (2000). Excitability changes induced in the human motor cortex by weak transcranial direct current stimulation. *J. Physiol.* 527, 633–639. doi: 10.1111/j.1469-7793.2000.t01-1-00633.x

Novak, J., Wilson, M., MacPherson, L., Arvanitis, T. N., Davies, N. P., and Peet, A. C. (2014). Clinical protocols for 31P MRS of the brain and their use in evaluating optic pathway gliomas in children. *Eur. J. Radiol.* 83, e106–e112. doi: 10.1016/j.ejrad.2013.11.009

Oldfield, R. C. (1971). The assessment and analysis of handedness: the Edinburgh inventory. *Neuropsychologia*, 9, 97–113.

Olney, J. W., Newcomer, J. W., and Farber, N. B. (1999). NMDA receptor hypofunction model of schizophrenia. *J. Psychiatr. Res.* 33, 523–533. doi: 10.1016/S0022-3956(99)00029-1

Öz, G., Alger, J. R., Barker, P. B., Bartha, R., Bizzi, A., Boesch, C., et al. (2014). Clinical proton MR spectroscopy in central nervous system disorders. *Radiology* 270, 658–679. doi: 10.1148/radiol.13130531

Patel, H. J., Romanzetti, S., Pellicano, A., Nitsche, M. A., Reetz, K., and Binkofski, F. (2019). Proton magnetic resonance spectroscopy of the motor cortex reveals long term GABA change following anodal transcranial direct current stimulation. *Sci. Rep.* 9:2807. doi: 10.1038/s41598-019-39262-7

Peek, A. L., Rebbeck, T. J., Leaver, A. M., Foster, S. L., Refshauge, K. M., Puts, N. A., et al. (2023). A comprehensive guide to MEGA-PRESS for GABA measurement. *Anal. Biochem.* 669:115113. doi: 10.1016/j.ab.2023.115113

Penninx, B. W., and Lange, S. M. (2018). Metabolic syndrome in psychiatric patients: overview, mechanisms, and implications. *Dialogues Clin. Neurosci.* 20, 63–73. doi: 10.31887/DCNS.2018.20.1/bpenninx

Petroff, O. A. (2002). Book review: GABA and glutamate in the human brain. *Neuroscientist* 8, 562–573. doi: 10.1177/1073858402238515

Piepmeier, A. T., and Etnier, J. L. (2015). Brain-derived neurotrophic factor (BDNF) as a potential mechanism of the effects of acute exercise on cognitive performance. *J. Sport Health Sci.* 4, 14–23. doi: 10.1016/j.jshs.2014.11.001

Porges, E. C., Woods, A. J., Edden, R. A., Puts, N. A., Harris, A. D., Chen, H., et al. (2017). Frontal gamma-aminobutyric acid concentrations are associated with cognitive performance in older adults. *Biol. Psychiatry* 2, 38–44. doi: 10.1016/j.bpsc.2016.06.004

Porter, T. G., and Martin, D. L. (1988). Stability and activation of glutamate apodecarboxylase from pig brain. *J. Neurochem.* 51, 1886–1891. doi: 10.1111/j.1471-4159.1988.tb01173.x

Pradhan, S., Bonekamp, S., Gillen, J. S., Rowland, L. M., Wijtenburg, S. A., Edden, R. A., et al. (2015). Comparison of single voxel brain MRS AT 3 T and 7 T using 32-channel head coils. *Magn. Reson. Imaging* 33, 1013–1018. doi: 10.1016/j.mri.2015.06.003

Provencher, S. W. (1993). Estimation of metabolite concentrations from localized in vivo proton NMR spectra. *Magn. Reson. Med.* 30, 672–679. doi: 10.1002/mrm.1910300604

Purpura, D. P., and McMurtry, J. G. (1965). Intracellular activities and evoked potential changes during polarization of motor cortex. *J. Neurophysiol.* 28, 166–185. doi: 10.1152/jn.1965.28.1.166

Puts, N. A., Edden, R. A., Evans, C. J., McGlone, F., and McGonigle, D. J. (2011). Regionally specific human GABA concentration correlates with tactile discrimination thresholds. *J. Neurosci.* 31, 16556–16560. doi: 10.1523/JNEUROSCI.4489-11.2011

Rae, C., Hare, N., Bubb, W. A., McEwan, S. R., Bröer, A., McQuillan, J. A., et al. (2003). Inhibition of glutamine transport depletes glutamate and GABA neurotransmitter pools:: further evidence for metabolic compartmentation. *J. Neurochem.* 85, 503–514. doi: 10.1046/j.1471-4159.2003.01713.x

Ramasubbu, R., and Patten, S. B. (2003). Effect of depression on stroke morbidity and mortality. *Can. J. Psychiatr.* 48, 250–257. doi: 10.1177/070674370304800409

Rao, C. R. (1947). "Minimum variance and the estimation of several parameters." in Paper presented at the Mathematical Proceedings of the Cambridge Philosophical Society. 43, 280, 283.

Reichenberg, A. (2010). The assessment of neuropsychological functioning in schizophrenia. *Dialogues Clin. Neurosci.* 12, 383–392. doi: 10.31887/DCNS.2010.12.3/areichenberg

Rodriguez-Lopez, J., Arrojo, M., Paz, E., Paramo, M., and Costas, J. (2020). Identification of relevant hub genes for early intervention at gene coexpression modules with altered predicted expression in schizophrenia. *Prog. Neuro-Psychopharmacol. Biol. Psychiatry* 98:109815. doi: 10.1016/j.pnpbp.2019.109815

Rossini, P. M., Barker, A., Berardelli, A., Caramia, M., Caruso, G., Cracco, R., et al. (1994). Non-invasive electrical and magnetic stimulation of the brain, spinal cord and roots: basic principles and procedures for routine clinical application. Report of an IFCN committee. *Electroencephalogr. Clin. Neurophysiol.* 91, 79–92. doi: 10.1016/0013-4694(94)90029-9

Rowland, B. C., Driver, I. D., Tachrount, M., Klomp, D. W., Rivera, D., Forner, R., et al. (2020). Whole brain 31P MRSI at 7T with a dual-tuned receive array. *Magn. Reson. Med.* 83, 765–775. doi: 10.1002/mrm.27953

Ruby, E., Polito, S., McMahon, K., Gorovitz, M., Corcoran, C., and Malaspina, D. (2014). Pathways associating childhood trauma to the neurobiology of schizophrenia. *Front. Psychol. Behav. Sci.* 3, 1–17. Available at: https://pubmed.ncbi.nlm.nih.gov/25419548/

Saini, S., Mancuso, S., Mostaid, M. S., Liu, C., Pantelis, C., Everall, I., et al. (2017). Meta-analysis supports GWAS-implicated link between GRM3 and schizophrenia risk. *Transl. Psychiatry* 7:e1196. doi: 10.1038/tp.2017.172

Sanacora, G., Gueorguieva, R., Epperson, C. N., Wu, Y.-T., Appel, M., Rothman, D. L., et al. (2004). Subtype-specific alterations of γ-aminobutyric acid and glutamatein patients with major depression. *Arch. Gen. Psychiatry* 61, 705–713. doi: 10.1001/archpsyc.61.7.705

Sanacora, M., Mason, G. F., Rothman, D. L., Behar, K. L., Hyder, F., Petroff, O. A. C., et al. (1999). Reduced cortical gamma-aminobutyric acid levels in depressed patients determined by proton magnetic resonance spectroscopy. *Arch. Gen. Psychiatry* 56, 1043–1047. doi: 10.1001/archpsyc.56.11.1043

Sanacora, G., Rothman, D. L., Mason, G., and Krystal, J. H. (2003). Clinical studies implementing glutamate neurotransmission in mood disorders. *Ann. N. Y. Acad. Sci.* 1003, 292–308. doi: 10.1196/annals.1300.018

Sandroff, B. M., Hillman, C. H., Benedict, R. H., and Motl, R. W. (2015). Acute effects of walking, cycling, and yoga exercise on cognition in persons with relapsing-remitting multiple sclerosis without impaired cognitive processing speed. *J. Clin. Exp. Neuropsychol.* 37, 209–219. doi: 10.1080/13803395.2014.1001723

Sargent, P. A., Kjaer, K. H., Bench, C. J., Rabiner, E. A., Messa, C., Meyer, J., et al. (2000). Brain serotonin1A receptor binding measured by positron emission tomography with [11C]WAY-100635: effects of depression and antidepressant treatment. *Arch. Gen. Psychiatry* 57, 174–180. doi: 10.1001/archpsyc.57.2.174

Shelp, B. J., Mullen, R. T., and Waller, J. C. (2012). Compartmentation of GABA metabolism raises intriguing questions. *Trends Plant Sci.* 17, 57–59. doi: 10.1016/j.tplants.2011.12.006

Shibata, K., Sasaki, Y., Bang, J. W., Walsh, E. G., Machizawa, M. G., Tamaki, M., et al. (2017). Overlearning hyperstabilizes a skill by rapidly making neurochemical processing inhibitory-dominant. *Nat. Neurosci.* 20, 470–475. doi: 10.1038/nn.4490

Sibley, B. A., Etnier, J. L., and Le Masurier, G. C. (2006). Effects of an acute bout of exercise on cognitive aspects of Stroop performance. *J. Sport Exerc. Psychol.* 28, 285–299. doi: 10.1123/jsep.28.3.285

Soares, M. J., Cummings, N. K., and Ping-Delfos, W. L. C. S. (2011). Energy metabolism and the metabolic syndrome: does a lower basal metabolic rate signal recovery following weight loss? *Diabetes Metab. Syndr. Clin. Res. Rev.* 5, 98–101. doi: 10.1016/j.dsx.2012.03.003

Stagg, B., Bachtiar, V., and Johansen-Berg, H. (2011). The role of GABA in human motor learning. *Curr. Biol.* 21, 480–484. doi: 10.1016/j.cub.2011.01.069

Stagg, B., Best, J. G., Stephenson, M. C., O'Shea, J., Wylezinska, M., Kincses, Z. T., et al. (2009). Polarity-sensitive modulation of cortical neurotransmitters by transcranial stimulation. *J. Neurosci.* 29, 5202–5206. doi: 10.1523/JNEUROSCI.4432-08.2009

Stagg, C. J., and Johansen-Berg, H. (2013). Studying the effects of transcranial direct-current stimulation in stroke recovery using magnetic resonance imaging. *Front. Hum. Neurosci.* 7:857. doi: 10.3389/fnhum.2013.00857

Statton, M. A., Encarnacion, M., Celnik, P., and Bastian, A. J. (2015). A single bout of moderate aerobic exercise improves motor skill acquisition. *PLoS One* 10:e0141393. doi: 10.1371/journal.pone.0141393

Stone, J. M., Day, F., Tsagaraki, H., Valli, I., McLean, M. A., Lythgoe, D. J., et al. (2009). Glutamate dysfunction in people with prodromal symptoms of psychosis: relationship to gray matter volume. *Biol. Psychiatry* 66, 533–539. doi: 10.1016/j.biopsych.2009.05.006

Sumner, P., Edden, R. A., Bompas, A., Evans, C. J., and Singh, K. D. (2010). More GABA, less distraction: a neurochemical predictor of motor decision speed. *Nat. Neurosci.* 13, 825–827. doi: 10.1038/nn.2559

Sze, P. Y., Sullivan, P., Alderson, R. F., and Towle, A. C. (1983). ATP binding to brain l-glutamate decarboxylase: a study by affinity chromatography. *Neurochem. Int.* 5, 51–56. doi: 10.1016/0197-0186(83)90008-6

Tamminga, C. A. (1999). Schizophrenia in a molecular age. Washington, DC, USA: American Psychiatric Press, Inc.

Van der Kooy, K., van Hout, H., Marwijk, H., Marten, H., Stehouwer, C., and Beekman, A. (2007). Depression and the risk for cardiovascular diseases: systematic review and meta analysis. *Int. J. Geriatr. Psychiatry* 22, 613–626. doi: 10.1002/gps.1723

van Vugt, F. T., Near, J., Hennessy, T., Doyon, J., and Ostry, D. J. (2020). Early stages of sensorimotor map acquisition: neurochemical signature in primary motor cortex and its relation to functional connectivity. *J. Neurophysiol.* 124, 1615–1624. doi: 10.1152/jn.00285.2020

Vasques, P. E., Moraes, H., Silveira, H., Deslandes, A. C., and Laks, J. (2011). Acute exercise improves cognition in the depressed elderly: the effect of dual-tasks. *Clinics* 66, 1553–1557. doi: 10.1590/S1807-59322011000900008

Wang, J., D'Amato, A., Bambrough, J., Swartz, A. M., and Miller, N. E. (2016). A positive association between active lifestyle and hemispheric lateralization for motor control and learning in older adults. *Behav. Brain Res.* 314, 38–44. doi: 10.1016/j.bbr.2016.07.048

Wenger, K. J., Wagner, M., Harter, P. N., Franz, K., Bojunga, J., Fokas, E., et al. (2020). Maintenance of energy homeostasis during calorically restricted ketogenic diet and fasting-MR-spectroscopic insights from the ERGO2 trial. *Cancer* 12:3549. doi: 10.3390/cancers12123549

Werner, F.-M., and Coveñas, R. (2013). Classical neurotransmitters and neuropeptides involved in schizophrenia: how to choose the appropriate antipsychotic drug? *Curr. Drug Therapy* 8, 132–143. doi: 10.2174/15748855113089990003

Werner, F.-M., and Covenas, R. (2016). Classical neurotransmitters and neuropeptides involved in schizoaffective disorder: Focus on prophylactic medication. Saif Zone Sharjah, U.A.E: Bentham Science Publishers.

Willmot, N., Leow, L. A., Filmer, H. L., and Dux, P. E. (2024). Exploring the intra-individual reliability of tDCS: a registered report. *Cortex* 173, 61–79. doi: 10.1016/j.cortex.2023.12.015

Wilson, M., Andronesi, O., Barker, P. B., Bartha, R., Bizzi, A., Bolan, P. J., et al. (2019). Methodological consensus on clinical proton MRS of the brain: Review and recommendations. *Magn. Reson. Med.* 82, 527–550. doi: 10.1002/mrm.27742

Wilson, M., Reynolds, G., Kauppinen, R. A., Arvanitis, T. N., and Peet, A. C. (2011). A constrained least-squares approach to the automated quantitation of in vivo 1H magnetic resonance spectroscopy data. *Magn. Reson. Med.* 65, 1–12. doi: 10.1002/mrm.22579

Wu, S. J., and Martin, D. L. (1984). Binding of Atp to brain glutamate-decarboxylase as studied by affinity-chromatography. *J. Neurochem.* 42, 1607–1612. doi: 10.1111/j.1471-4159.1984.tb12749.x

Yoon, J. H., Grandelis, A., and Maddock, R. J. (2016). Dorsolateral prefrontal cortex GABA concentration in humans predicts working memory load processing capacity. *J. Neurosci.* 36, 11788–11794. doi: 10.1523/JNEUROSCI.1970-16.2016

Zhang, J., Yetton, B., Whitehurst, L. N., Naji, M., and Mednick, S. C. (2020). The effect of zolpidem on memory consolidation over a night of sleep. *Sleep* 43:zsaa084. doi: 10.1093/sleep/zsaa084

Zuccoli, G. S., Saia-Cereda, V. M., Nascimento, J. M., and Martins-de-Souza, D. (2017). The energy metabolism dysfunction in psychiatric disorders postmortem brains: focus on proteomic evidence. *Front. Neurosci.* 11:493. doi: 10.3389/fnins.2017.00493

10.3389/fnhum.2024.1461417

Glossary

ATP	Adenosine triphosphate
B_0	Static magnetic field
CSI	Chemical shift imaging
FWHM	Fullwidth half maximum
GABA	Gamma amino butyric acid
Glu	Glutamate
Glx	Glutamate-glutamine
GAD	Glutamic acid decarboxylase
LTD	Long-term depression
LTP	Long-term potentiation
M1	Primary motor cortex
MRI	Magnetic resonance imaging
MRS	Magnetic resonance spectroscopy
NAA	N-acetylaspartate acid
PCr	Phosphocreatine
Pi	Inorganic phosphate
GPC	Glycerophosphocholine
GPE	Glycerophosphoethanolamine
TCA	Tricarboxylic acid
tDCS	Transcranial direct current stimulation
TMS	Transcranial magnetic stimulation
MEP	Motor evoked potential
VOI	Volume of interest
TR	Repetition time
TE	Echo time
TA	Acquisition time
PRESS	Point resolved spectroscopy,
MEGAPRESS	Meshcher-garwood point resolved spectroscopy
MDD	Major depressive disorder
DLPFC	Dorsolateral prefrontal cortex
SM1	Sensorimotor cortex
ACC	Anterior cingulate cortex
tACS	Transcranial alternating current stimulation
tPCS	Transcranial pulsed current stimulation
tRNS	Transcranial random noise stimulation

Frontiers in Neuroscience

Provides a holistic understanding of brain function from genes to behavior

Part of the most cited neuroscience journal series which explores the brain - from the new eras of causation and anatomical neurosciences to neuroeconomics and neuroenergetics.

Discover the latest Research Topics

See more →

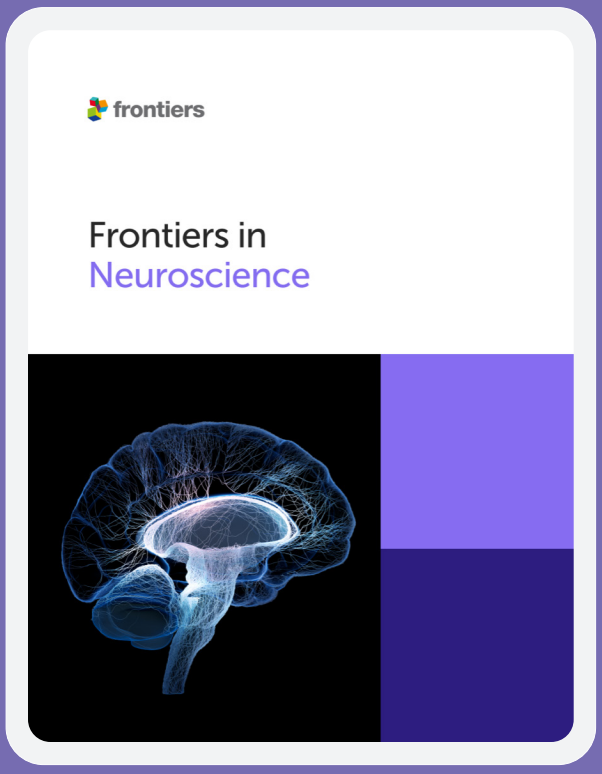

Frontiers

Avenue du Tribunal-Fédéral 34
1005 Lausanne, Switzerland
frontiersin.org

Contact us

+41 (0)21 510 17 00
frontiersin.org/about/contact